SPECTROMETER FOR ATMOSPHERIC IONS IN THEIR UPPERMOST RANGE OF MOBILITY

(Project: Measuring Ionic Mobilities in the Terrestrial Upper Stratosphere and Mesosphere--Phase I)

Prepared by

RESEARCH AND ADVANCED DEVELOPMENT DIVISION
AVCO CORPORATION
Wilmington, Massachusetts

Final Report--Avco RAD-TR-65-25

Contract DA-19-020-AMC-0058(X)
DASA-WEB No. 07.007
Ordnance OMC Code: OCMS 5010.21.83036
DASA PO 311-62

4 September 1965

Prepared for

COMMANDING GENERAL
HEADQUARTERS, ABERDEEN PROVING GROUNDS
Maryland

DISCLAIMER NOTICE

THIS DOCUMENT IS BEST QUALITY PRACTICABLE. THE COPY FURNISHED TO DTIC CONTAINED A SIGNIFICANT NUMBER OF PAGES WHICH DO NOT REPRODUCE LEGIBLY.

This document consists of 196 pages,
227 copies, Series A

SPECTROMETER FOR ATMOSPHERIC IONS IN THEIR UPPERMOST RANGE OF MOBILITY

(Project: Measuring Ionic Mobilities in the Terrestrial Upper Stratosphere and Mesosphere--Phase I)

Prepared by

RESEARCH AND ADVANCED DEVELOPMENT DIVISION
AVCO CORPORATION
Wilmington, Massachusetts

Final Report--Avco RAD-TR-65-25

Contract DA-19-020-AMC-0058(X)
DASA-WEB No. 07.007
Ordnance OMC Code: OCMS 5010.21.83036
DASA PO 311-62

by

H. Dolezalek
A. L. Oster

4 September 1965

APPROVED

R. Penndorf, Chief Geophysics Section, Project Manager

P. R. Swan, Manager
Space Science Department

Prepared for

COMMANDING GENERAL
HEADQUARTERS, ABERDEEN PROVING GROUNDS
Maryland

ABSTRACT

In the past, the mobility of atmospheric ions and the number density in different mobility ranges (ion spectrum) have been measured in the terrestrial atmosphere in the heights from gound to about 5 km. Electric conductivities of the atmosphere have been measured up to about 30 km and ion number densities to about 75 km. To extend the possibility of ion spectrum measurements up to the same height, a new method has been developed and tested in the laboratory. Its application in the free atmosphere is being prepared. The instrument may be used in planetarian atmospheres.

The method consists of a GERDIEN-type "differental ion counter of the second order," which provides a predetermined location of ion intake and a number of separate receiving electrodes for the ion impact. The driving voltage is ac; its amplitude is increasing downstream in the chamber.

A low-pressure wind tunnel for continuous operation, mostly in the subsonic range, has been developed and constructed for the laboratory experiments. This tunnel and its possible applications for other purposes are discussed.

An outline of the theory of the different GERDIEN type ion counters is communicated. The laboratory experiments are described, and ion spectrums obtained in the low-pressure wind tunnel are presented.

CONTENTS

CONTENTS (Concl'd)

ILLUSTRATIONS

ILLUSTRATIONS (Cont'd)

ILLUSTRATIONS (Cont'd)

ILLUSTRATIONS (Concl'd)

SYMBOLS

Following the recommendation (Paris, May 1965) of the "Joint Committee on Atmospheric and Space Electricity, of the International Association of Meteorology and Atmospheric Physics and the International Association of Geomagnetism and Aeronomy," the MKSA system of units is applied in this report. The symbols are written in the form suggested by the American Institute of Physics.

If not otherwise stated at the location where the symbols are used, the following general significance of symbols is applied:

Greek Letters:

α	recombination coefficient, general [$m^3\ sec^{-1}$]
γ	ratio of specific heats, [-]
ϵ	capacitivity, permittivity, dielectric constant, [$F\ m^{-1}$]
η	dynamic viscosity [$N\ sec\ m^{-2}$]
Λ	total conductivity [$\Omega^{-1}\ m^{-1}$]
λ	conductivity, general [$\Omega^{-1}\ m^{-1}$]
λ^+, λ^-	positive polar and negative polar conductivity, resp., [$\Omega^{-1}\ m^{-1}$]
ν	collision frequency [sec^{-1}]
ν	frequency of an ac voltage or current [Hz]
ν	kinematic viscosity [$m^2\ sec^{-1}$]
ρ	density [$kg\ m^{-3}$]
ρ	radius of ion location in cylindrical condenser [m]
τ	time constant ($= CR$) [sec]
τ	duration of pulse [sec]
ϕ	phase of sine wave [-]
ω	circular frequency of an ac voltage or current [sec^{-1}]

Latin Letters:

A	area [m^2]
a	acceleration [$m\ sec^{-2}$]
b	width (parallel to driving and receiving electrodes) of slit [m]
C	capacitance [F]
c	speed of sound [$m\ sec^{-1}$]
D	diffusion constant (indices indicate different natures) [$m^2\ sec^{-1}$]
d	distance between rings or electrodes [m]
E	electric field [$V\ m^{-1}$]
e	electric elementary charge [1.602×10^{-19} Cb]
F	force [N]
f(...)	function of....
I	current [A]
k	mobility [$m^2\ V^{-1}\ sec^{-1}$]
k_B	Boltzmann constant [1.38×10^{-23} W sec $degree^{-1}$]
L	overall length of GERDIEN condenser [m]
L_D	Debye shielding distance [m]
l	mean free path [m]
l	length of individual electrode or ring [m]
M_0	amount of air passing through whole Chamber [$m^3\ sec^{-1}$]
M_G	amount of air passing through ion gate [$m^3\ sec^{-1}$]
M	mass of neutral molecule or particle [amu]
M	velocity in MACH numbers (= v/c) [-]
m	mass of charged particle or ion [amu]

m_1	mass of ion [kg]
m_2	mass of neutral molecule [kg]
m^*	ratio $m_1/(m_1 + m_2)$ [-]
N	total number of ions [-]
n	number density of particles, general [m^{-3}]
n_1	number density of ions [m^{-3}]
n_2	number density of neutral molecules [m^{-3}]
n_e	number density of electrons [m^{-3}]
p	pressure [N m^{-2}] or [Torr]
Q	electric charge [Cb]
q	ionization rate [m^{-3} sec^{-1}]
R	radius of outer electrode in cylindrical condenser [m]
r	radius of inner electrode in cylindrical condenser [m]
T	temperature [°K]
T	duration of full period of ac voltage or current [sec]
t	time [sec]
U	voltage [V]
V	volume [m^3]
v	velocity [m sec^{-1}]
x	general coordinate parallel to the electrodes in a consenser, starting from upstream end of open space of chamber
x_1	distance to particular electrode [m]
Δx	length of individual receiving electrode [m]
Y	admittance [Ω^{-1}]

y	general coordinate perpendicular to the electrodes in a condenser, starting from point of intake for ions
y_1	distance between electrode and location of ion intake [m]
Δy	width of orifice for ion intake [m]

ACKNOWLEDGMENTS

Many helpful discussions during the course of the work have been held with the authors' colleagues. The design and construction of the laboratory instrumentation has been completed, in particular, by D. B. Norcia and L. Spadafora. Data reduction has been performed by Mrs. S. Darcy. M. R. Bernstein conducted, independently, supplementary investigations and made many calculations. The work was supervised by R. Penndorf, S. C. Coroniti, and M. E. Malin, and without some important decisions by the latter it would not have been completed. The design, engineering, and construction of the modified GERDIEN chambers, Models A and B1, was done by K. J. Coughlin, R. C. Reynolds, and S. A. Lippielo, and their colleagues under the supervision of R. E. Wetherby. Additional consulting services have been provided by R. H. Coleman, R. W. Freeman, R. P. John, J. R. Lambert, J. A. Morreal, P. J. Peggs, H. E. Schlosser, J. Shumsky, H. Weisblatt, and other employees of Avco RAD. For particular problems, the advice of Prof. Dr. H. Israël (Aachen, Germany), Dr. H. W. Kasemir (Neptune, N. J.), Mr. E. N. Willie and Dr. W. K. Volkers (both Port Washington, N. Y.), and of Prof. L. P. Kadanoff (Urbana, Ill.) was of great assistance. In particular, the contributions by fellow workers of the Applied Physics Branch, Ballistic Measurements Laboratory, U. S. Army Ballistic Research Laboratories must be mentioned. The assistance received from all of these, and from many other colleagues in this country and some others, is gratefully acknowledged.

PART 1

THEORY

1. 1 ATMOSPHERIC IONS

1. 1. 1 GENERATION, LIFE TIME, AND DESTRUCTION OF IONS

The existence of charged particles in the atmosphere -- aerosol, groups of molecules, molecules, atoms, subatomar particles -- is caused by several processes, the relative significance of which varies with altitude and in some cases with time.

Three main groups of ion generation in a volume under consideration may be distinguished: (1) the entrance of charged particles from outside the volume or even from outside the atmosphere (such as natural or anthropogeneous aerosol particles, blown up snow or sand, smoke, and the like, or penetrating subatomar particles, electrons, protons, alpha-rays, mesons); (2) the simultaneous generation of two (or more) charged particles of opposite sign by some superatomar "breaking-up process" (such as breaking of ice-crystals, splashing of raindrops, and so forth, within the atmosphere); and (3) the simultaneous generation of a free electron and a positive ion by a "subatomar breaking-up process" (the usual "ionization" by removing an electron from an atom or a group of atoms).

The average life times of these ions differ by many orders of magnitude. Generation, variation, and destruction of atmospheric ions is a dynamic process. The number of ions of a particular kind to be found depends on the time constant for that particular ion species, and this time constant depends on atmospheric density as well as on the number of the different partners with which the ion under consideration may react.

Free electrons close to the ground are attached within some 10^{-8} second to a neutral particle, thus forming a negative ion. In the tropopause, the time constant (i. e., the time in which 1/e of all freshly generated free electrons disappears) comes to about 10^{-7} second, in the stratopause it reaches about 10^{-2} second, and in the mesopause tenths or hundredths of seconds. In all these ranges, attachment is the dominant process for electron removal, but the combination with positive ions gains relative significance with increasing altitude. Positive and negative "small ions", i. e., the ions which carry the atmospheric electric current, have life time constants in the order of tenths to several hundredths of seconds close to ground, depending on the contamination of the atmosphere by aerosol particles. In greater heights, the average life time of negative ions first increases, then flattens off, and finally goes drastically down, reaching values of a few seconds in the altitude of the mesopause. The life time constant for positive ions generally increases with height. Charged aersol particles have, in general, a much longer life than smaller ions.

A typical pattern may be presented by showing the scheme of WAIT (1934) for the life of small ions in the troposphere (figure 1).

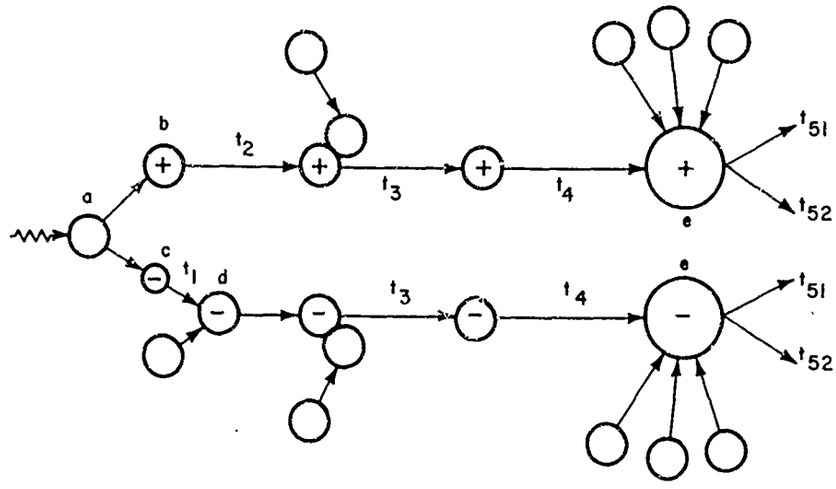

Figure 1 AN EXAMPLE FOR THE CREATION OF A PAIR OF "SMALL IONS" OR "CLUSTER IONS" IN THE LOWER ATMOSPHERE (AFTER WAIT 1934):
(A neutral molecule (a) is met by radiation, and one positive molecular ion (b) and one free electron (c) are formed. The free electron attaches to another neutral molecule and forms a negative molecular ion (d). Attachment of more neutral molecules brings cluster ions (e) into existence, which later may combine or attach to aerosol particles.)

The average total duration t_1 through t_4 is only about 10^{-6} second (ISRAEL (1957), p. 20). When one moves upwards in the atmosphere, the time durations t_1 through t_4 are enlarged, and chances that c and b or d and b (figure 1) meet and thus cancel each other are increased.

The life of a particular species of ions is terminated by several processes, which again depend in their relative significance on height. Three main possibilities may be distinguished here: two ions with opposite electric charges may disappear simultaneously with their electric charges by combination; an ion may switch over from one "group of ions" to another such as electrons to molecular, molecular to small, small to large ions, etc., by attachment or detachment; and an ion may remain within the same "group", but still change its nature. Attachment and detachment processes may involve one charged and one uncharged particle (free electron to neutral molecule, or liberation of an electron from an uncharged aerosol particle, and other cases) or two charged particles of the same sign (in this case at least one rather coarse aerosol particle which is able to hold more than one elementary charge is involved). Change of the nature of an ion may occur in many different ways: a charged raindrop may partially evaporate, a charged ice crystal may melt, a clustered ion may lose or attract one neutral molecule, a charged atom may combine with a neutral atom, charge transfer may occur, such as $O^+ + O_2 \rightarrow O + O_2^+$ and many others. The fact that we have differentiated between the two last possibilities is slightly arbitrary, depending on the denomination "group

of ions" as used above. It is justified by the habit of quoting differential equations for the variations in number densities without distinguishing between different ions of the same "group". However, for our later mobility discussions such differentiation is essential.

1.1.2 INDICATION TO THE DIFFERENTIAL EQUATIONS FOR ION EQUILIBRIUM

Analytical expressions for the variation of number densities of ions, dn/dt, have been proposed in great numbers. The attempt to write down a complete set of differential equations covering all ion generation, ion transfer, and ion decay processes for all heights and times would constitute a challenging task for a great computer program and is not made here. The simplest equation of them all, already used by THOMSON and RUTHERFORD (1896) and RUTHERFORD (1897), is still the most important one. It describes the ionic state in an environment in which only ions of one kind, but with two signs, exist:

$$dn/dt = q - \alpha n^2 \ ;$$

with

n the number density of ions of one sign (equal to that of ions with the

q the number of ions of one sign generated per unit volume and unit time

α the so-called "recombination" coefficient

For ion equilibrium, dn/dt must be zero.

v. SCHWEIDLER (1919, 1924) extended the discussion by including large ions with one elementary charge and uncharged aerosol particles, applying an additional "recombination coefficient," which in fact is a composed coefficient for true combination between ions of different sign and for attachment of small ions to uncharged particles. On this basis, much research work has been done to obtain quantitative values for the different coefficients and the discussions have been extended to intermediate ions (e. g., WAIT 1935), but only ions with one elementary charge have been considered. Using five different coefficients for ion production, four different combination coefficients, and two attachment coefficients

* The most important contributions: 1916: KENNEDY; 1918, 1919, 1924: v. SCHWEIDLER; 1925: NOLAN et al; 1927: HESS, NOLAN et al; 1928: HESS, 1929: NOLAN et al.; 1933: WHIPPLE, WRIGHT; 1934: HOGG; 1935: SCRASE, WAIT; 1936: WRIGHT; 1940: FLEMING, FISH & SHERMAN; 1941: v. SCHWEIDLER, THELLIER; 1944: NOLAN et al.; 1946: WAIT; 1949: BRICARD; and the different works of ISRAËL, reported in 1957; some more literature is given by GISH and SHERMAN 1940 and PARKINSON 1943.

ISRAEL (1957p. 189) gives a set of five differential equations, in which small ions and large ions and neutral aerosol particles are combined, but none has more than one elementary charge. Detachment coefficients are included in the ion production coefficients. No free electrons are discussed. For the inclusion of multiply-charged aerosol particles, PEDERSEN (1964) applies the plasma probe theory by LANGMUIR et al (1923 to 1939, in particular: MOTT-SMITH and LANGUIR, 1926, and LANGUIR and COMPTON, 1931) to a non-charged or charged aerosol particle, and he derives a set of equations in which the number of charges on an aerosol particle is included. Since he is concerned about the height range between 40 and 80 km, his equations also reflect the inclusion of attachment coefficients, detachment coefficients, and combination coefficients, which play a role in these heights. These have not been considered by the earlier workers mentioned in the footnote above, but have been added in the last decades.** In his equations PEDERSEN assumes that the aerosol particles have either no charge or a number of Z elementary charges; thus, he simplifies somewhat the given distribution of charges on the particles.

This fact, together with the already indicated situation that in all these proposed aeronomic reaction equations the possible differences between ions of one "kind" are not considered, has the consequence that most of the applied coefficients are related to a certain mixture of ions, and not to one species alone.

1.1.3 BRIEF DISCUSSION OF THE CHEMICAL NATURE OF IONS

On the other hand, chemical reaction equations, which may play a role in the atmosphere, have been listed in great numbers. The book by NAWROCKI and PAPA (1961, chapter 3) provides a selection. Number densities are not much considered here, although indications on the energy transfers and on probability are given. According to COLE and PIERCE (1965), the most important positive ions are probably NO^+ and O_2^+ but N_2^+ and complex ions, such as O_3^+ and N_4^+, may be present in significant quantities while negative ions are most probably O_2^- and, at greater heights, O^-. In lower altitudes, in particular, other ions have been considered as well, e.g., H_2O^+. There may still be found other ions in small numbers, such as H^-, OH^-, NO_2^-, O_3^-, and others, and large ions in addition to these. PEDERSEN (1964) discusses the existence of ions in the mesosphere which move but slowly under the influence of the electric fieled (heavy ions). NARCISI and BAILEY (1965), measuring with quadrupole massenfilter, moving with a velocity greater than that of sound, and after pumping down to reduce collisions within their instrument, observe, at altitudes between 64 and 82.5 km, ions of the species OH^+, N_2^+, NO^+, O_2^+, but also ions of mass 19 and 37 interpreted to be H_3O^+, and possibly $H_5O_2^+$. That ions of the last mentioned species may exist has been shown in the laboratory in the range from 40 to 80 N/m^2 (0.3.....6 torr) by KNEWSTUBB and TICKNER (1963).

** 1958: SMITH, BURCH and BRANSCOMB; 1959: CHANIN, PHELPS, and BIONDI; 1961: GUNTON et al., HOLT et al., Phelps and PACK; 1963: BIONDI (quoted after PEDERSEN).

NARCISI and BAILEY (1965) also observed, using another measuring mode, many positive ions of atomic mass greater than 45 in altitudes between 65 and 75 km, while the defined metallic ions such as Fe^+, Na^+, Ca^+, and Mg^+ have but small number densities below the mesopause. For the transition from the measured current to number densities, again only one charge per particle is assumed.

For all measurements made from rockets, the possibility must be investigated that species of ions found in the measuring results have been injected into the atmosphere by the rocket itself, and thus do not constitute genuine atmospheric ions.*

1.1.4 CONCLUSION

Considering the discussion of this chapter on atmospheric ions, one comes to the conclusion that a "measuring stick" for ions, which attaches one particular number to each ion species, is needed. The natural measuring stick for this purpose is mobility, as defined and discussed in the next chapter. For most cases, mobility provides a unanimous "label," but some ambiguity may appear in particular cases. This is rather probable in the case of large ions carrying more than one elementary charge. However, even in these cases, mobility is the most promising tool for the separation of different groups of ions from each other and for the separation of different ions within the same "group."

*Supplement made when proofreading: a recent paper by LINDZEN and GOODY (J. Atm. Sci. 22 (1965) 341) provides an impressive evidence for the complexity of the region between 30 and 70 km.

1.2 IONIC MOBILITY

1.2.1 DEFINITION OF THE PARAMETER MOBILITY

A generally applied formula for the relative motion of the two types of particles ("molecules") in a binary gas mixture follows:

$$\left.\begin{aligned} \vec{v}_{rel} = & -\frac{n_1 + n_2}{n_1\ n_2} D_{12} \text{ grad } n_1 \\ & - \frac{m_2 - m_1}{n_1 m_1 + n_2 m_2} \frac{D_{12}}{k_B T} \text{ grad } p \\ & + \frac{n_1 + n_2}{n_1 m_1 + n_2 m_2} \frac{D_{12}}{k_B T} m_1 m_2 (\vec{a}_1 - \vec{a}_2) \\ & - \frac{(n_1 + n_2)^2}{n_1 n_2} \frac{D_T}{T} \text{ grad } T \end{aligned}\right\} \qquad (1)$$

[Sydney CHAPMAN and COWLING, 1960, eq. (14.1/1), with substitutions according to eqs. (1.21/1), (2.5/2), (2.5/3), (2.5/4), (2.5/6), (2.5/12), and (8.3/5), and written in our own symbols], where:

v_{rel} is the average relative velocity between the two constituents of the gas [m/sec]

n_1 and n_2 are the number densities of the two constituents [m^{-3}]

D_{12} is the coefficient of mutual diffusion [m^2/sec]

m_1 and m_2 are the masses of the molecules of the two constituents [kg]

k_B is the BOLTZMANN constant, 1.38×10^{-23} [Newton-meter per degree or Watt-seconds per degree]

T is the temperature [degrees KELVIN]

p is the hydrostatic pressure [Newton/m^2]

$\vec{a}_1$ and $\vec{a}_2$ are the accelerations of the molecules of the two constituents, effected by external forces [m/sec^2]

D_T is the coefficient of thermal diffusion [m^2/sec].

For the significance of the second and the fourth term of eq. (1), refer to CHAPMAN and COWLING (1960), p. 143, lines 10 to 12 of the second, and all of the third, paragraph. If we consider local conditions in the atmosphere, confined to dimensions, in which grad p and grad T may be neglected, the second and the fourth term in eq. (1) vanish.

The first term represents the "gaskinetic" diffusion, which occurs if the two constituents are not evenly distributed throughout the gas (grad $n_1 \neq 0$), and the third term represents the motions of one of the constituents through the other one, if external forces act on this one constituent, and not, or not in the same amount, on the other one. We denote with the index 1 the ions, and with index 2 neutral molecules, and we restrict our discussion to only one kind of external force, an electric field (i. e., $a_2 = 0$). Then we may write for the motion of ions (of one kind) through a gas, constituted by only one type of neutral molecules, the following equation:

$$\vec{v}_{rel} = - \frac{n_1 + n_2}{n_1 n_2} D_{12} \text{ grad } n_1 + \frac{n_1 + n_2}{n_1 m_1 + n_2 m_2} \frac{D_{12}}{k_B T} m_1 \vec{a}_1 m_2 . \tag{2}$$

Replacing the external force acting on the ion with the electric charge e,

$$m_1 \vec{a}_1 = e \vec{E} \tag{3}$$

we get:

$$\vec{v}_{rel} = - \frac{n_1 + n_2}{n_1 n_2} D_{12} \text{ grad } n_1 + \frac{n_1 + n_2}{n_1 \frac{m_1}{m_2} + n_2} \frac{e D_{12}}{k_B T} \vec{E} \tag{4}$$

where $\vec{E}$ is the electric field strength. Thus, the average relative velocity between the two constituents of the binary gas in this case (grad T=grad p = 0) is composed of two components:

$$\vec{v}_{rel} = (\vec{v}_{rel})_D + (\vec{v}_{rel})_E \tag{5}$$

with

$$(\vec{v}_{rel})_D = - \frac{n_1 + n_2}{n_1 n_2} D_{12} \text{ grad } n_1 \tag{6}$$

and

$$(\vec{v}_{rel})_E = \frac{n_1 + n_2}{n_1 \frac{m_1}{m_2} + n_2} \frac{e D_{12}}{k_B T} \vec{E} . \tag{7}$$

We restrict out discussions in this section to eq. (7). The term with the diffusion coefficient may be substituted by the parameter "mobility" as follows:

$$k = \frac{eD_{12}}{k_B T} \quad . \tag{8}$$

Expression (8) is often referred to as the EINSTEIN relation. In MKSA-units, the mobility is given in $m^2 V^{-1} sec^{-1}$ (for the derivation, remember $1\ Nm \equiv 1\ Wsec$). With this parameter, eq. (7) comes to:

$$(\overrightarrow{v_{rel}})_E = \frac{n_1 + n_2}{n_1 \frac{m_1}{m_2} + n_2} \, k \vec{E} \; ; \tag{9}$$

and, if

$$n_1 << n_2 \quad \text{and} \quad n_1 \frac{m_1}{m_2} << n_2 \; , \tag{10}$$

$$(\overrightarrow{v_{rel}})_E = k \vec{E} \quad . \tag{11}$$

This expression leads to a definition of the parameter "mobility": In a slightly ionized gas (condition (10)), the mobility is the average velocity (drift velocity) of an ion under the influence of an electric field of unity strength.

If we measure the average velocity, or the field strength with an accuracy of 1 percent the term "slightly ionized" means that

$$\left| \frac{n_1 + n_2}{n_1 \frac{m_1}{m_2} + n_2} - 1 \right| < 0.01 \; . \tag{12}$$

In the free atmosphere, the lightest molecular or atomic ions may be hydrogen, and the heaviest radon; thus m_1/m_2 would vary from about 1/30 to about 8. If we include cluster ions (up to 20 neutral molecules fixed to one ionized molecule), the upper limit may shift to 20 or more, and if we include large and ultralarge ions, it may go up to about 1000. This means, that eq. (12) holds for molecular ions, cluster ions, and ultralarge ions up to:

Ion	n_1 less than	
Molecular ion	1.4×10^{-3}	
Cluster ion	5.2×10^{-4}	(13)
Ultralarge ion	10^{-5}	
		of n_2.

If we know that in the gas under consideration only ions with $m_1 \approx m_2$ exist, we may permit higher ionization ratios. However, we must be cautious so as not to hurt other limitations, e.g., the one mentioned in the next paragraph concerning the mutual influence between ions. For electrons, a ratio of even less than 10^{-5} applies. Furthermore, definition (11) is applicable only, where the CHAPMAN-COWLING equation (1) is valid. That means, at first, that we must consider the average behavior of the ion in a space large enough to allow the derivation of mean values from a great number of particles participating in a great number of collisions, and do not study the fact that between collisions the ions have an accelerated motion. Secondly, the number of ions must be "so small that their mutual influence on each other's mean velocities is negligible" (CHAPMAN and COWLING (1960), p. 321, valid not only for more than one species of ions).

Although eq. (1) is derived only for a binary gas, it is an established custom to speak of a mobility also in the case of gases composed of many different molecules, e.g., in the atmosphere. In this case, n_2 represents the number density of all neutral particles, and m_2 is the weighted average mass of them, in the terrestrial atmosphere up to more than hundreds of kilometers, approximately $29 \times 1.7 \times 10^{-27}$ kg.

1.2.2 GENERAL MACROSCOPIC DISCUSSION ON MOBILITY

In this section, we treat the gas in which the ion moves, as a continuum, while in the following section (microscopic discussion) the molecular structure of the gas is considered. Be definition, mobility is a "macroscopic" parameter.

If in a gas containing ions there is a difference of electric potential across some distance, there will be an electric "conduction" current; and if there is an electric current, there will be an electric field. In the gas mixture under consideration (slightly ionized, short mean free paths, many collisions), the parameter connecting electric fields and "conduction currents," conductivity, is composed of ion number density, electric charge of the ions, and ionic mobility. Be definition (eq. (11)), mobility is the ionic velocity in a unity field. Accordingly, the most direct method to measure mobility is to measure the velocity of the ion, i.e., to measure a current. In fact, this is the usual method.

There are two principal difficulties related to this measurement.

At first, with the usual ion (or electron) velocities, the current represented by the motion of a single elementary charge is too small to be measured with present methods. Thus, we measure the sum of the motions of a great number of ions which may be different kinds, having different mobilities (and different signs). Such a measurement would yield an "average mobility." For a more informative measurement, the ions must be separated into different ranges of mobility prior to the measurement of the current. If this is done successfully, we obtain a mobility spectrum, i.e., an information on the number of ions in each range

of mobility, or

$$\frac{dn}{dk} = f(k). \tag{14}$$

The separation must be done prior to the measurement, because in the usual methods the measurement destroys the ion. Also, in the case of the measurement of the ion spectrum, the current measured for each mobility range must be represented by a great number of ions moving, and moving through a great number of collisions.

This is not only required by the fact that we do not have methods to measure so small a current as the one representing the motion of just one or a few ions. More essentially, the integration over many ions and many collisions is required by the facts that ions of any mobility are constantly generated and destroyed, and that the motion of an ion between two collisions is an accelerated one. Thus, the measuring instrument must comprehend a sufficiently large volume, and the measurement must be extended over a sufficiently long period of time. Both volume and time, depend on the gas density. They must be expanded, when measurements in the upper layers of the atmosphere are intended, and the attempt becomes unrealistic if atmospheric pressure becomes smaller than about 1 N/m^2 (or 7×10^{-3} torr).

Second, any measurement of the current provides information on the total current only, and does not distinguish between the "conduction current" mentioned above and other possible types of current, represented by the motion of the same group of ions which represent the conduction current. To evaluate these possibilities, we should discuss the different kinds or shares of current which may exist in the gas or atmosphere under consideration, outside and inside the measuring instrument. Returning to eq. (1), we want to state the introduction of electric forces as the only ones acting from "outside" eq. (3) is a restriction. There may be, in place of them, or in addition to them, other external forces such as gravity forces or the inertial forces of particles which have been accelerated extremely strong at an earlier time and outside of the volume under consideration (penetrating particles). Furthermore, there may be a motion of the binary gas as a whole, depending on the selected coordinate system, and this will be a motion of the particles indicated with the index 1 as well. If these particles (in which we include the penetrating particles also) carry an electric charge all these motions will represent electric currents. If some or all of the mentioned effects (seven in total) are in about the same order of magnitude, and act on the same ion, a complicated pattern of current lines may be the result. Usually, more than one species of ions exist, and the pattern is even more complicated.

Disregarding again grad p and grad T, we may distinguish between the following shares of the electric current:

"Conduction current," represented by eq. (7), applied to all ions existing in the gas mixture

"Convection current" (in the narrower sense of this denomination), represented by the motion of the gas mixture as a whole, including the ions of different kinds

"Gravitational current," included in the third term of eq. (1) if $m_1 \neq m_2$, and applicable to the different kinds of ions

"Penetrating current," if such ions exist

"Diffusion generated electric current," represented by eq. (6).

Sometimes, the last four shares are combined in the denomination "convection current," used in a wider sense and including all motions of ions accelerated by non-electric forces.*

Consequently, to derive mobility from the measured value of the current, we must ascertain, that only the "conduction current" is considered. This may be proven by additional experiments or by theoretical computations if the related parameters are known sufficiently. Fortunately, this task is often an easy one. Convection currents in the narrower sense may be detected easily, if not in magnitude so in direction, and if the conduction current in an instrument can be made to be directed perpendicular to these convection currents, the latter ones are easily cancelled out. Gravitational currents and penetrating currents do occur, but they occur only occasionally, and often are too small to be considered, because either the charges transported are small or because the velocity of this transport is small. In the troposphere, strong gravitational currents are represented by the falling of charged rain drops, etc., while in the mesosphere and stratosphere, penetrating electrons and protons or alpha rays may constitute a current. While charged rain or snow is easily detected, the detection of penetrating charged particles may be difficult, and this possibility should be kept in mind.

Thus, in addition to the conduction current, there remains mostly the "diffusion-generated electric current," which must be considered for all these measurements as a possible and, in principle, always present disturbance.

In a discussion on mobility carried out by applying macroscopic view points, a word must be said on the behavior of this parameter when applied to different ions and in different environments.

---

*The displacement current, although in atmospheric processes often stronger than the other shares, is not discussed here since it does not represent a motion of a charge.

At first, it must be stated, that the mobility of the same kind of ion in the same kind of gas is directly dependent on the inverse value of the density of the gas:*

$$\frac{k_\rho}{k_{\rho_0}} = \frac{\rho_0}{\rho} \tag{15}$$

or

$$\frac{k_p, T}{k_{p_0} T_0} = \frac{p_0}{p} \frac{T}{T_0} \quad . \tag{16}$$

Second, the nature of the atmospheric ions is not well known. It is still a controversial item, whether the atmospheric ions in the troposphere exist of ion clusters or of molecular ions. Also, the chemical nature of these ions is a matter of discussion. Furthermore, it is expected, that the nature of ions changes with height. If there are cluster ions close to ground, more and more non-clustered ions may appear if height increases, and finally even more and more atomar ions will replace the molecular ions. The transition region will be different for chemically different ions.

Since generation of ions, ion equilibrium maintainance, and decay of ions is a never ceasing dynamic process, the time constants for the different processes play the main role here, as has been discussed in section 1. 1, above.

Third, mobility is defined, according to eq. (11), as being independent of the field strength. This condition is mostly fulfilled in the atmosphere. However, under certain circumstances, it may be hurt in an instrument. If the electric field increases, or the pressure decreases, or both, such that

$$\frac{E}{p} > 200 \frac{V/m}{Torr} = 1.5 \frac{Vm}{N} \; ; \tag{17}$$

the definition of eq. (11) is no more applicable. The velocity of the ion does not more increase linearly with the field strength; instead it becomes more close to a relationship such as:

$$v = f(\sqrt{E}) \quad . \tag{18}$$

This fact will be discussed later on (section 1. 7. 3).

Fourth, it may be possible that ions exist which can be destroyed by the application of a small amount of energy. We know from laboratory experiments and theoretical considerations (e. g., E. A. MASON and SCHAMP, 1958; DALGARNO, McDOWELL and WILLIAMS, 1958) that ions with bindings energies as low as

*This simple relationship is often used to "reduce" measured mobility values to the pressure of "ground level", or $10^5 N/m^2$. Such a reduction facilitates the comparison of different kinds of ions, which may exist in different heights, but care must be taken not to confuse the absolute values.

0.014 eV may occur (Cs^+ - He), and we expect to find in the higher atmosphere ions with binding energies in the order of 1 eV. Since any GERDIEN measurement applies stronger fields to the atmosphere than normally existing in undisturbed conditions, the breaking-up of such ions is a possible disturbance* and must be considered. We shall submit a quantitative discussion on this problem for the application in the mesosphere later on (section 1.7.4).

1.2.3 GENERAL MICROSCOPIC DISCUSSION ON MOBILITY

Mobility is sometimes referred to as being a macroscopic expression for the integral--taken over some time and over some space--of a variety of frictional forces which turn the accelerated differential motion of the ion in an unaccelerated integral motion with a definite velocity. This image is a reminder of the motion of a solid particle through a fluid with high viscosity, under the influence of an external force, such as gravity. In fact, as has been shown by ISRAËL (1957, p. 26 and 288) the hydrodynamic law of STOKES, as modified by CUNNINGHAM and MILLIKAN, and valid downwards to particle sizes in the order of the mean distance between the particles:

$$F = \frac{6\pi\eta r_1 v_1}{1 + l/r_1 \left[0.864 + 0.290 \exp\left(-1.25\, r_1/L\right)\right]} \tag{19}$$

smoothly changes over into the formula by LENARD (1913, 1919, 1920) which is supposed to be valid for small particles upwards to the order of the mean free path:

$$F = \frac{\pi \rho (r_1 + r_2)^2 \bar{v}_2 v_1}{Q(m_1, m_2)} \tag{20}$$

where

- F is the force acting on the particles with the index 1
- η is the dynamic viscosity of the gas (atmosphere)
- r_1 and r_2 are the radii of the particles with indices 1 and 2 (ions and gas molecules)
- v_1 is the stationary terminal velocity of the particles with index 1
- l is the mean free path
- ρ is the density of the gas (atmosphere)

* It may be noted here that the usually observed non-fulfillment of Ohm's Law in the measured quantities of the atmospheric electric field, current density, and conductivity may find another explanation (additional to DOLEZALEK, 1960) in the possibility of changing ionic mobility when measuring conductivity.

Q is a factor representing the masses of the particles with the indices 1 and 2 (ions and gas molecules)

$\bar{v}_2$ is the mean velocity of the gas molecules.

If we determine a "mobility" also for the case of the STOKES-CUNNINGHAM-MILLIKAN Law as well as for the LENARD Law, and substitute for F the force acting on an electric charge in an electric field of unity strength, we come to

$$k = \frac{1 + l/r_1 \left[0.864 + 0.29 \exp\left(-1.25\, r_1/l\right)\right]}{6\pi\eta r_1} e_1 \tag{21}$$

and

$$k = \frac{\frac{3}{2\sqrt{m^*}} \frac{1+m^*}{3+m^*} \left[\frac{8(1-m^*)}{\pi(1+m^*)} + \frac{2m^*}{1+m^*}\right] e_1}{\pi \rho (r_1 + r_2)^2 \bar{v}_2} \tag{22}$$

where we have now introduced the explicit value for the Q of eq. (20), with

$$m^* = m_1/(m_1 + m_2) \tag{23}$$

and

m_1 and m_2 being the masses of an ion and of a gas molecule,

e_1 is the electric charge, for "small" or molecular or atomic ions, being 1.6×10^{-19} coulombs.

Since at present we want to discuss the fundamental relations, we may apply (21) for small l/r_1 values, so that

$$k \approx \frac{1}{6\pi\eta r_1} e_1 \tag{24}$$

and, with the usual formula for the dynamic viscosity, written with our symbols:

$$\eta = \frac{1}{3} \frac{m_2 \bar{v}_2}{4\pi\sqrt{2}(r_1 + r_2)^2} \tag{25}$$

(see, for this, e.g., SEARS (1959), eqs. (13-13) with p. 256 last line)

we arrive at the following equation for the "mobility" in STOKES' Law:

$$k \approx \sqrt{8} \frac{r_1}{m_2 \bar{v}_2} e_1 ; \tag{26}$$

where we have taken into account that $r_1 >> r_2$. Introducing:

$$v_2 = \sqrt{\frac{8\,k_B\,T}{\pi\,m_2}}\ , \tag{27}$$

we may also write this as:

$$k \approx \sqrt{\frac{\pi}{k_B\,T\,m_2}}\ r_i\,e_1\ . \tag{28}$$

On the other hand, if we make in LENARD's Law (22) $m_1 >> m_2$ and $r_1 >> r_2$, and apply eq. (27), we have:

$$k \approx \frac{3}{4}\sqrt{\frac{m_2}{8\,\pi\,k_B\,T}}\ \frac{1}{\rho\,r_1^2}\ e_1\ . \tag{29}$$

Not discussing the fact that density ρ is not included in eq. (28), since dynamic viscosity is independent of gas density, and that radii and masses of "ion" and gas molecules have different functional relationships to mobility in eqs. (28) and (29), we see, that in both cases mobility is a function of the electric charge of the ion, the size and/or mass or ion and gas molecules, and the temperature of the gas:

$$k = f(r, m, e, T, \rho)\,; \tag{30}$$

where ρ cancels for very large charged particles (e.g., electrified raindrops).

The problem of giving an analytical expression for eq. (30) is extremely complicated and far from being solved.

The attempts begin with an extended discussion between LENARD (1913, 1919, 1920), who starts from the concept of a solid impact, and LANGEVIN (1902, 1905, and later), who derives one set of his equations from the center-of-force theory, which is expressively doubted by LENARD. In the center-of-force theory, the electric charge of the ion and its mirror charge on the neutral gas molecule are supposed to alter significantly the free path of the ion, and here not only the static fields play a role, but the dipole and quadrupole and higher fields also may be discussed. These discussions considered gas pressures of about 1 atmosphere, and they will be altered if we consider gas densities as they occur in the stratosphere and mesophere. Eq. (22) is the basic LENARD equation.

A basic LANGEVIN equation, which does not yet consider the electric forces, written with our symbols and transferred to MKSA-system, follows:

$$k = 5.5 \times 10^5\ \frac{l}{m_2\,\bar{v}_2\sqrt{m^*}}\ e_1\ . \tag{31}$$

Based on theorectical considerations and laboratory experiments, a series of improvements of this equation has been proposed. By introducing the electrical forces (center-of-force-theory), the mobility becomes independent of the ionic charge, and a function of density, molecular mass of the gas, the dielectric constant and the reduced mass-ratio m^*. For this LANGEVIN-LOEB center-of-force equation, see LOEB (1955). In the same book other derivations are treated, among them that of HASSE and COOK (1931), in which the ionic charge again appears, and the radius of the ion constitutes a factor.

The radius, or more exactly the distance between the centers of ion and molecule at impact, is a complicated parameter, since sphere shapes for the particles involved can not be assumed. In fact, since mobility measurements can be made rather accurately, these equations have been used to determine these center distances.

Another approach can be made by starting from the equation for conductivity as used in ionospheric physics (see, e.g., RAWER (1953)):

$$\Lambda = \frac{n_1 e_1^2}{m_1 \nu} \tag{32}$$

from which, with the usual definition of conductivity:

$$\Lambda = n_i e_1 k \tag{33}$$

we get for the mobility:

$$k = \frac{e_1}{m_i} \frac{1}{\nu} \tag{34}$$

where ν is the collision frequency between ions and gas molecules. Thus, if the collision frequency were known from other measurements, and we can measure n_1 and k, the ionic mass m_1 would be easily derived. Unfortunately, the collision frequency is not independent of the ion mass m_1. For rather coarse considerations, the application of eq. (32) will yield satisfactory results, but for the determination of the ion mass from a mobility spectrum a more accurate solution should be approached.

After the fundamental book of LOEB was published (1955), more investigations on ionic mobilities were done by calculation and in the laboratory. These investigations were often restricted to simple cases, if we compare the situation in the atmosphere. Metallic ions in inert gases, or ions in their atomic parent gas are examples for this type of investigation (see, e.g., DALGARNO, McDOWELL and WILLIAMS, 1958; DALGARNO 1958; E. A. MASON and SCHAMP, 1958). Since the number of possible types of ions is either one or small, and mostly known, and since the neutral gas is not a mixture in most of these investigations, the application of such results to the atmosphere poses some still unsolved problems.

On the other hand, in the region between about 60 and 70 km, there may be a possibility of measuring mobility and ionic mass (without pumping down) at the same time and the same locality. For mobility measurements a great number of collisions within the instrument is required, for mass spectrometry of ions, the number of collisions within the instrument must be very small. In principle, it should be possible to build a rather great mobility instrument and a very small mass spectrometer (using very small distances and high frequencies of the control voltages, such as proposed by EIBER (1965), and to make simultaneous measurements at the same locality. Such a combined measurement would yield borderline values for the upper region, and some extrapolation to mobility values in lower regions certainly is permissible.

In order to give an indication on a mass-mobility relation, we have plotted in figure 2 the dependency of the factor m^* on ionic mass for a neutral gas of 29 amu. These curves hold for all equations, in which mobility is a linear function of the square root of m^*, and in which the parameter does not depend strongly on the kind of ion.

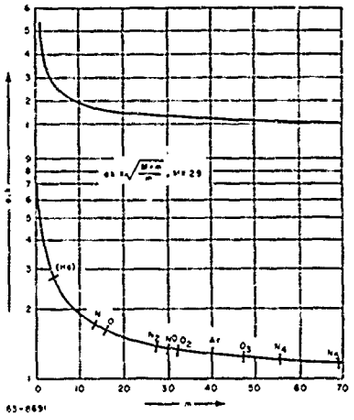

Figure 2 MASS-MOBILITY RELATION ACCORDING TO THE INDICATED FORMULA FOR a_k
(Abscissa: molecular mass in amu; upper curve: same as lower curve, but with linear ordinate.)

1.2.4 CONCLUSION

Knowledge on mobilities of atmospheric ions may be used for a variety of purposes. Electric conductivity is determined in an accurate manner by the numbers of ions in different mobility ranges. A further important application of mobility is the determination of the mean free path, e.g., the LANGEVIN-BRICARD mean free path for ions (BRICARD, 1964). Since the mean free path

plays an essential role in the equations for recombination and attachment coefficients (cf., e.g., SIKSNA, 1964), knowledge on mobility is in many cases still the most desired information.

Under equilibrium conditions, if the combination coefficients are derived in a quiet situation, information on the ionization rate in disturbed situations may be obatined for different heights.

Information on diffusion and diffusion coefficients is another result to be expected from the measurement of the ion spectrum.

Of course, the total ion number densities is an immediate consequence of the ion spectrum. Variations in this number, which occur upon descent through the atmosphere, may indicate changeover points between different kinds or groups of ions. One of such changeover points may concern the variation from molecular to "cluster" ions, and this knowledge may yield a contribution to the study of the ion nature in lower heights.

For given combinations of the involved parameters, the different theories concerning the mobility-mass relation may be compared, and it may be determined to which degree of resolution and accuracy they may yield the same result.

However, if such accuracy is not sufficient in certain cases, and even if it is not known which theory should be applied and how it should be applied, it may still be possible to derive a much more accurate result by a combination of diferent approaches. These would involve the results of laboratory investigations on ionic mobilities in cases of predetermined gases and ions.

Finally, the possibility of carrying out simultaneous measurements of ionic mobility and ionic mass by a common carrier, which seems to be within reach in the next few years for a limited range of altitude, and the further possibility of extrapolating these results downward to a certain extent, and upward for a comparison with other measurements executed in higher ranges, may help considerably to close the gap of knowledge in these mass-mobility relations and to establish a solid basis for statements on the number densities, chemical natures, masses, and mobilities of atmospheric ions.

It may be said, that mobility is the most essential measuring parameter concerning ions in the upper stratosphere and mesophere of the Earth or in similar environments somewhere else.

1.3 MEASUREMENT OF IONIC MOBILITY

1.3.1 THE MEASURING PRINCIPLE OF THE PERPENDICULAR FORCES

If a gas containing ions is drawn through an electrical condenser of capacity C and with a voltage difference U between its plates, a current I which is a measure of the time constant of the gas according to DOLEZALEK (1956) may be measured at either one of the plates:

$$\frac{\lambda}{\epsilon} = \frac{I/U}{C} \tag{35}$$

where

λ is the conductivity of the gas

ϵ is the capacitivity of the gas (permittivity, dielectric constant).

Since I/U is the conductance of the condenser, this equation seems almost to be an identity. In fact, it is the basic equation for the method of the perpendicular forces for the measurement of conductivity and mobility. This method is truly a method to measure the time in which an atmospheric ion travels a certain given and known distance under the influence of an electric field (one force). By the second force, the "wind speed" in the condenser, this time measurement is transferred into measurement of a length.

If the current quoted in eq. (35) is measured at the negative electrode of the condenser, the conductivity λ in the time constant ϵ/λ is the positive polar conductivity, and vice versa, and the total conductivity is the sum of both:

$$\Lambda = \lambda^+ + \lambda^- \; ; \tag{36}$$

and in all cases, only ions with a mobility smaller than a critical value are measured in their full number (a more detailed discussion of this will be given in section 1.3.2., below).

The first quotation of this method is found in RUTHERFORD's paper of 1899. ZELENY and LENARD, both in 1900, and KÄHLER in 1903 applied about the same principle, before GERDIEN turned it (1905) into the most common tool for the measurement of the polar electric conductivities in the atmosphere. Since then, the condenser as used here -- mostly a cylindrical one -- is often referred to as the "GERDIEN-condenser," "GERDIEN-chamber," "GERDIEN-counter," or simply the "GERDIEN."

1.3.2 THE "CRITICAL MOBILITY" OF A GERDIEN CONDENSER*

The "critical mobility" of a GERDIEN condenser is not an atmospheric parameter; it is an instrumental feature of a certain GERDIEN, depending on the type and geometrical configuration of it, and on the applied "driving" voltage and the applied wind speed in the condenser.

To define the "critical mobility," we consider a plate condenser through which air is sucked, and we investigate the motion of the ions under the applied electric field (driving voltage divided by electrode distance) and the velocity of the air.

From figure 3 we derive directly:

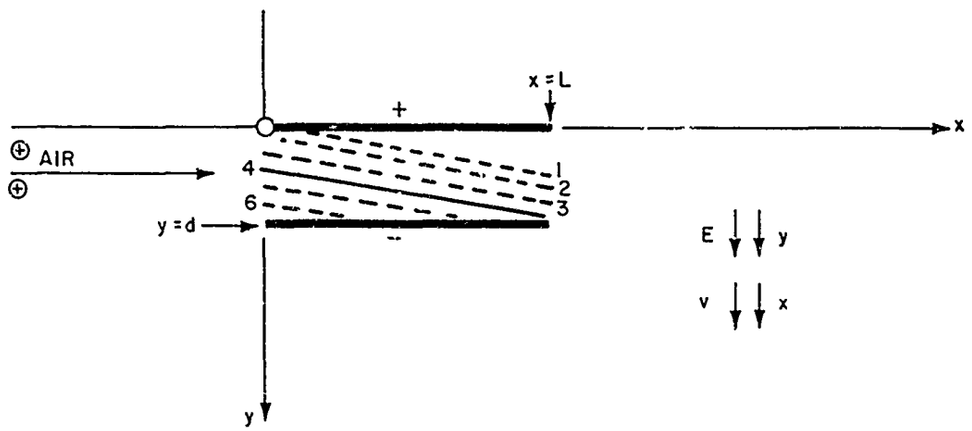

65-12052

Figure 3 DERIVATION OF CRITICAL MOBILITY OF A GERDIEN

movement of ions in horizontal direction:

$$\frac{dx}{dt} = v \tag{37}$$

$$x = vt + x_0; \tag{38}$$

and in vertical direction:

$$\frac{dy}{dt} = kE \tag{39}$$

$$y = kEt + y_0; \tag{40}$$

where E is the electric field, k the mobility, v the velocity of the air, and x_0 and y_0 are integration constants.

The combination of eqs. (38) and (40) gives

* We are following the derivation as it is given by ISRAËL (1957), pp 108 ff.

$$\frac{y - y_0}{x - x_0} = \frac{kE}{v} \quad . \tag{41}$$

This is the equation for the ion paths 1to 6 shown in figure 3. All ions entering the condenser will reach the lower electrode, if

$$\left.\begin{aligned} y &= 0 \quad \text{for} \quad x = 0 \\ y &= d \quad \text{for} \quad x = L \end{aligned}\right\} \tag{42}$$

where d is the distance between the condenser plates, and L the length. With eq. (41), we get the "limiting" or "critical" mobility as follows:

$$k_c = \frac{dv}{EL} \quad ; \tag{43}$$

or, by introducing the capacitance of the condenser C,

$$k_c = \frac{M_0 \epsilon}{CU} \quad ; \tag{44}$$

where $U = Ed$, and M_0 the volume of air which is sucked per second through the condenser.

All ions which have a mobility equal to or greater than k_c, are reaching the lower electrode and thus measured. Ions with a smaller mobility may pass the condenser without being captured, if they enter at a value of y which is small enough. In fact, of ions with a mobility $k < k_c$, just the ratio k/k_c is captured. As can be seen from figure 3, all ions which enter at or below the solid line with the number 4 are captured. They are entering at an y-value $p.d$, where p is a number smaller than unity. Our conditions eq. (42) are now modified to:

$$\left.\begin{aligned} y &= pd \quad \text{for} \quad x = 0 \\ y &= d \quad \text{for} \quad x = L \end{aligned}\right\} \tag{45}$$

and the critical mobility k_c' for the condenser with the distance $d(1-p)$ between the electrodes comes to:

$$k_c' = d(1-p)\frac{v}{EL} \quad . \tag{46}$$

Comparing eqs. (43) and (46), we see that:

$$k_c'/k_c = 1 - p . \tag{47}$$

Since it can easily be shown that the volume of air passing through this smaller condenser, M', is related to the value M according to:

$$M'/M_0 = 1 - p , \tag{48}$$

and since this derivation for k_c' may be repeated for any other of $k < k_c$, our statement is verified that ions with mobility $k < k_c$ are measured with the ratio k/k_c of their number.

1.3.3 APPLICATION OF THE GERDIEN TO THE MEASUREMENT OF THE ION SPECTRUM

The cylindrical condenser as proposed by GERDIEN (1905), i.e., with one "driving" and one "receiving" electrodes (the latter one being the electrode to which the particular species of ions which is to be measured is driven by the applied voltage), and with ions entering across the full opening of the cylinder, can be used for the measurement of the ion spectrum. To show this, we follow the derivation of ISRAËL (1931).

The mobility spectrum is, by definition:

$$\frac{dn}{dk} = f(k) ; \tag{49}$$

where dn is the number of ions/m^3 in the mobility range between k and $k + dk$; k is the mobility, and $f(k)$ is a function of the mobility.

If ions of different mobilities are intercepted at the "receiving electrode" of the aspiration condenser, the current represented by these ions, is generally given by

$$I = M_0 e \frac{1}{k_c} \int_0^{k_c} k f(k)\, dk + M_0 e \int_{k_c}^{\infty} f(k)\, dk ; \tag{50}$$

where M_0 is the amount of air passing through the aspiration condenser (m^3/sec); e is the charge per ion (1.6×10^{-19} Cb); and k_c is the "critical mobility" of the condenser (see section 1.3.2).

If mobility is entered in (m/sec) / (V/m), the current in eq. (50) becomes in A. If we want to derive the mobility spectrum from the GERDIEN-characteristic, i.e., from the current versus voltage curve of the GERDIEN condenser, we are looking for a relation between f(k) and the parameters "current" I and "voltage" U of the GERDIEN condenser. In eq. (50) we have a relation between I and k_c. Another relation, that between k_c and U, may be derived as follows.
The critical mobility is a constant of the measuring apparatus, the GERDIEN condenser. It is defined as (see eq. (44)

$$k_c = \frac{M_0 \epsilon}{CU} \; ; \tag{51}$$

where C is the effective capacity of the condenser (i.e., the capacity without consideration of the capacity of the connected wiring, supports, etc.), and ϵ is the capacitivity of the air (8.86×10^{-12} F/m). By differentiation we get:

$$\frac{dk_c}{dU} = - \frac{C}{\epsilon M_0} k_c^2 \; . \tag{52}$$

Combining eq. (50) after differentiation, and eq. (52) we get

$$\frac{dI}{dU} = \frac{dI}{dk_c} \frac{dk_c}{dU} = \frac{Ce}{\epsilon} \int_0^{k_c} k f(k)\, dk \; ; \tag{53}$$

for the second differentiation, we apply

$$\frac{d^2I}{dU^2} = \frac{d}{dk_c} \left(\frac{dI}{dU} \right) \frac{dk_c}{dU} \tag{54}$$

and get:

$$\frac{d^2I}{dU^2} = - \frac{e \epsilon M_0^2}{CU^3} f(k_c) \; . \tag{55}*$$

* This derivation was first demonstrated by H. BENNDORF. For the differentiations the rule of LEIBNIZ has been applied, namely, for the differentiation of eq. (50) in the form:

$$\frac{\partial}{\partial y} \int_{x=0}^{y} F(x,y)\, dx = \int_{x=0}^{y} \frac{\partial F(x,y)}{\partial y} + F(y,y);$$

and for the differentiation of eq. (53), with eq. (54), in the following form:

$$\frac{\partial}{\partial y} \int_{x=0}^{y} F(x)\, dx = F(y) \; .$$

We may replace here k_c by k, if we are doing the measurement in such a way that the particular k under consideration is always just the k_c and this is done by proper adaptation of U. Thus, we arrive at:

$$f(k) = \frac{dn}{dk} = - \frac{C U^3}{e\epsilon M_0^2} \frac{d^2 I}{dU^2} ; \qquad (56)$$

or, specified for a cylinderical condenser:

$$\frac{dn}{dk} = \frac{2L U^3}{\pi e v^2 (R^2 - r^2)^2 \ln R/r} \frac{d^2 I}{dU^2} \qquad (57)$$

with L as the length, and R and r as the radii of the outer and the inner electrodes, respectively, and ln being the logarithm to the basis 2.71828...
It is shown by eqs. (56) and (57), that the ion spectrum can by measured by the GERDIEN condenser, if the applied driving voltage U is varied ("swept") while the current from the receiving electrode is measured, so that the secon derivative may be calculated of taken from the I over U curve.

1.3.4. GENERAL OPERATING CONDITIONS OF THE GERDIEN CONDENSER

A certain number of conditions must be fulfilled if the measurements made by a GERDIEN condenser are to give correct values.

The life time of the ions to be measured must be so long, that the ion number density does not change due to combination or attachment to other particles while the ions are traveling inside the GERDIEN condenser. The number of ions, as compared with the number of neutral gas molecules, and the average distances between the ions must be neglected as compared with the electric field applied to the chamber. There must be no space charges of a magnitude so as to compete with the applied field.

The number density of ions inside the chamber must be the same as it is outside the chamber. That means that no ions which approach the chamber in a cylindrical volume of air of the diameter of the orifice of the chamber are intercepted at the entrance or moved to a location outside the chamber; in other words, the so-called "edge-effect" must be avoided. The edge effect usually is created by electric stray fields at the front end of the condenser, generated by the applied driving voltage or by potential differences between the instrument and its environment. This effect has been studied a great deal since 1905.

The density of the air inside the chamber must be the same as outside of it.

That means, that the chamber must not provide a remarkable air flow resistance, and there must be no deviation in the direction of the relative air flow in front of the chamber.

The air flow in the chamber must be a laminar one, i.e., it must not be turbulent. Also this effect has been studied by a number of authors.

Since edge effectand turbulence disturbances, in the general meaning, do not play a role in the case of the particular "modified GERDIEN chamber" to be particularly discussed in this report, we refer to the literature as quoted in the textbooks on atmospheric electricity, and do not discuss these effects here.

The possibility of disturbances given by any motion of ions due to other forces than electrical and convection with the air motion in the chamber is already indicated in eq. (1) (section 1.2.1); in particular, diffusion is to be mentioned here. Also this is discussed extensively in the literature, and we shall consider this influence later on.

At the same place (i.e., in chapter 1.7), some more limitations and disturbances, which occur with measurements of ion number densities, conductivities and mobilities in the upper stratosphere and in the mesosphere, will be investigated.

Almost none of the conditions quoted here can be fulfilled with a perfect accuracy. Thus, the influences of the different deviations must be weighted to determine the accuracy of a measurement.

1.3.5 VARIATIONS IN THE DC-OPERATED GERDIEN CHAMBER

In section 1.3.3, we have shown that the ion spectrum may be derived from a "usual" GERDIEN chamber, if the driving voltage U is varied ("swept") and the measured current is differentiated twice to this voltage. "Usual" means that the cylindrical condenser has only the two electrodes, and both are not subdivided, and that ions are taken in through the full opening of the cylinder.

Since a double differentiation generally reduces the accuracy obtainable with a measurement, means of developing instruments, which would do with only one or even without any differentiation have been investigated.

A classification of these varied GERDIEN chambers has been proposed by TAMMET (1960). He calls the "usual" GERDIEN chamber an "integrated chamber". Next he quotes two different kinds of "differential chambers of the first order". In both cases, the mobility spectrum is derived by sweeping the driving voltage and differentiating the measured current but once. Finally, there is the "differential GERDIEN chamber of the second order", with which the measured current gives the mobility spectrum directly. In figure 4, the principle of these four varieties is shown in the example of the plate condenser.

(1) INTEGRAL GERDIEN CHAMBER:

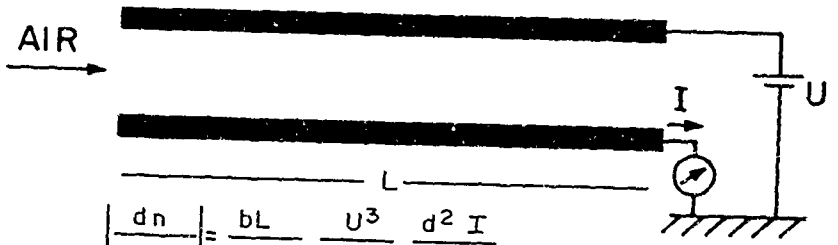

$$\left|\frac{dn}{dk}\right| = \frac{bL}{d}\,\frac{U^3}{eM_0^2}\,\frac{d^2I}{dU^2}$$

(2) DIFFERENTIAL GERDIEN CHAMBERS, IST ORDER

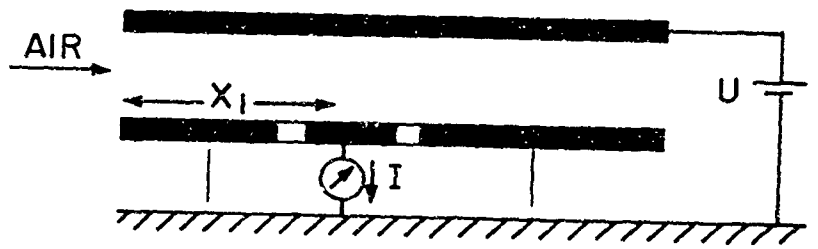

(a) $$\left|\frac{dn}{dk}\right| = \frac{X_1 b}{d}\,\frac{U^2}{eM_0^2}\,\frac{dI}{dU}$$

(3) DIFFERENTIAL GERDIEN CHAMBER, 2ND ORDER

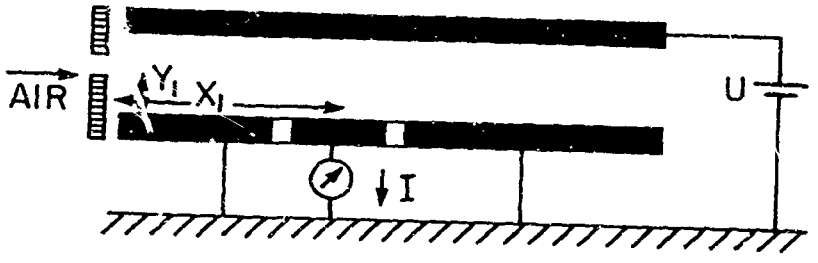

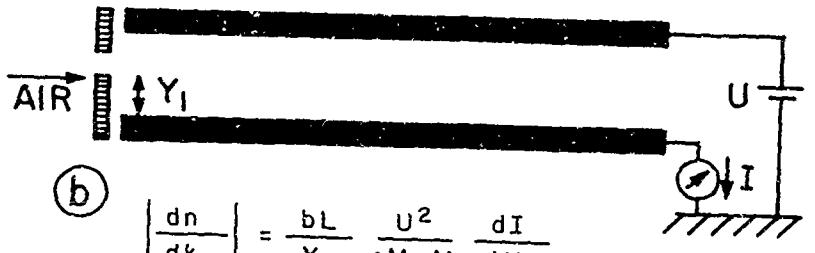

(b) $$\left|\frac{dn}{dk}\right| = \frac{bL}{Y_1}\,\frac{U^2}{eM_0 M_G}\,\frac{dI}{dU}$$

$$\left|\frac{dn}{dk}\right| = \frac{X_1 b}{Y_1}\,\frac{U}{eM_0 M_G}\,I$$

65-903

Figure 4 SCHEMATIC SURVEY ON DC-OPERATED GERDIEN CONDENSERS (PLATE CONDENSERS)

(The formulas give the analytical expressions for the mobility spectrum dn/dk, i.e., the number density of ions n per mobility range dk; b is the width of the condenser, M_0 is the amount of air passing per second through the whole cross section of the condenser, M_G is the amount of air passing through the ion gate (ion intake) only; and e is the electric elementary charge.)

The same principles of variation apply to cylindrical (and other) condensers: while the integrated chamber allows the ions to enter through the full crosss section, and has them intercepted all at the same "receiving electrode," and while the differential chamber of the second order lets the ions pass only through a narrow slit and makes the interception at a subdivided receiving electrode, the two kinds of differential chambers of the first order apply either one of these two additional features.

The analytical expression for the mobility spectrum for the integrated chamber has been derived above, in section 1. 3. 3. Specified for the plate condenser, it is entered in figure 4.

To derive the mobility spectrum formula for the dc-operated differential chamber of the second order, we start from figure 5, for both the plate and the cylindrical condenser form.

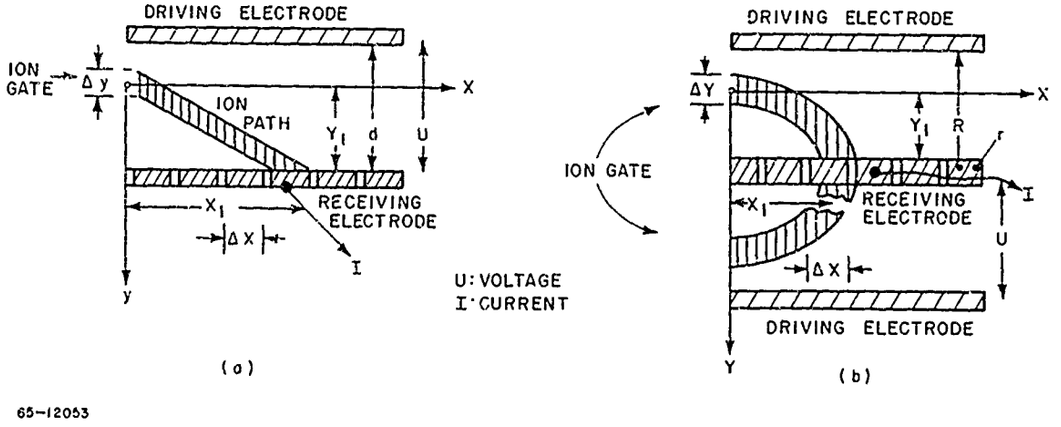

Figure 5 SCHEMATIC FIGURE FOR THE DERIVATION OF THE FORMULA FOR THE MOBILITY SPECTRUM FOR THE DIFFERENTIAL GERDIEN CHAMBER OF THE SECOND ORDER
(a - plate condenser, b cylindrical condenser.)

Since, in a differential ion counter of the second order, ions are entering only at a predetermined slit, the calculation of the mobility spectrum is rather simple. The current I is given by the number density of ions times their electric charge times the product ($\Delta y\, b\, v$) which is the numbers of unit volumes entering per time unit through the slit Δy is the width of the slit or intake opening, b is the width of the condenser, and v is the air velocity):

$$I = n_e \, \Delta y \, b \, v; \tag{60}$$

or, written for n

$$n = \frac{1}{e \, \Delta y \, b \, v} \, I. \tag{61}$$

Because of the obvious relation:

$$\frac{dx \,/\, dt}{dy \,/\, dt} = \frac{x}{y} = \frac{x_1}{y_1} = \frac{v}{k \, E} = \frac{v \, d}{k \, U} \tag{62}$$

eq. (61) can be written as follows:

$$n = \frac{y_1}{e \, \Delta y \, b \, k \, E \, x_1} \, I; \tag{63}$$

and then be differentiated to get the mobility spectrum:

$$\frac{dn}{dk} = \frac{x_0}{y_0} \quad \frac{U}{v^2 \, d \, b \, e \, \Delta y} \tag{64}$$

(not noting the sign)
which is, with

$$v \, b \, d = M_0 \tag{65}$$

and

$$v \, b \, \Delta y = M_G \tag{66}$$

the equation for the mobility spectrum as entered in figure 4:

$$\frac{dn}{dk} = \frac{x_1 \, b}{y_1} \quad \frac{U}{e \, M_0 \, M_G} \, I. \tag{67}$$

By the application of any one of the many possibilities for substitution given with eq. (62), a number of modified expressions for eq. (67) may be derived, and this may be helpful for an interpretation of this mobility spectrum formula. Considering:

$$M_G = v \, \Delta y \quad 2\pi(y_1 + r) \tag{68}$$

(compare figure 5) and replacing eq. (61) by

$$n = \frac{1}{ve\ \Delta y\ 2\pi (y_1 + r)}\ I \tag{69}$$

and eq. (62) by

$$\frac{y_1^2}{x_1} = \frac{1}{v}\ \frac{2Uk}{\ln R/r}\ , \tag{70}$$

we derive, in a similar way, the formula for the cylindrical condenser:

$$\left|\frac{dn}{dk}\right| = \frac{x_1/y_1 \qquad U}{\pi\ e\ v^2\ \Delta y\ y_1 (y_1 + r)\ \ln R/r}\ I\ ; \tag{71}$$

which has been written here in a form comparable to eq. (57), and which may be modified in various forms by substitutions such as given in eq. (70).

In figure 4, the corresponding formulas for the differential GERDIEN of the first order are quoted, namely, for type a (i. e., full intake, subdivided receiving electrode):

$$\frac{dn}{dk} = \frac{x_1\ b}{d}\ \frac{U^2}{e\ M_0^2}\ \frac{dI}{dU} \tag{72}$$

and for type b (i. e., subdivided intake, full receiving electrode:

$$\frac{dn}{dk} = \frac{bL}{y_1}\ \frac{U^2}{e\ M_0\ M_G}\ \frac{dI}{dU} \tag{73}$$

The detailed derivation of these equations is not given here.

Historically, the differential ion chamber of the first order has already been applied by BLACKWOOD in 1920, and the differential chamber of the second order was used by ERIKSON in 1921 (ERIKSON 1921, 1922, 1924, 1929 MAHONEY 1929, and Seville CHAPMAN 1937).

Recent reports on the measurement of ion spectra have been published by MISAKI especially for large ions close to ground (1950, 1961, 1964); TSVANG (1956); E. WHIPPLE (1960); and, for ions in the troposphere, by HOPPEL (1963) and HOPPEL and KRAAKEVIK (1964). Disturbances occurring in GERDIEN chambers have been discussed recently (after many others since 1905) by KOMAROV (1960 a and b) and TAMMET (1962). The paper by TAMMET (1960) in which the chambers are classified, has already been mentioned.

Surveys on methods to measure ionic spectra are given by LOEB (1949, 1955) and by KNOLL, EICHMEIER, and SCHÖN (1964, pp. 198-205).

1.3.6 RESOLUTION OF THE DC-OPERATED GERDIEN CHAMBERS

An important problem is given by the fact that the resolution of all types of GERDIEN chambers decreases with increasing mobility. By differentiation of eq. (62), we get

$$\left|\frac{dx}{dk}\right| = \frac{1}{k^2}\,\frac{v\,y_1\,d}{U} \tag{74}$$

for the resolution. The driving voltage U cannot be decreased beyond a level which is given by the unavoidable noise. This noise is due mostly to the VOLTA effect. Since the condenser has to be exposed to the free atmosphere, pollutions of the surfaces of the electrodes and other differences between the electrodes can hardly be avoided, and the VOLTA effect plays a role (compare ISRAËL and DOLEZALEK, 1957). The smallest applicable voltage will be between 1 and 5 V, and it is advisable to stay well over that.

The wind velocity v should not be increased beyond the speed of sound, because otherwise the shock wave may bring disturbances. The geometrical dimensions in radial direction y_1 and d have certain limits, too. Finally, the length Δx must be kept great enough to allow for the disturbances due to diffusion.

Obviously, this is the difficulty which explains why no direct measurements of conductivity, let alone mobility, have been presented for altitudes higher than about 30 km. If we want to extend the measurements into higher ranges, either v or U, or both parameters in eq. (74) should be replaced by another one. In other words, a new measuring principle must be found.

1.4 THE MODIFIED GERDIEN CHAMBER

1.4.1 THE MEASURING PRINCIPLE

It has been said above (section 1.3.1), that the measuring method of the perpendicular forces is essentially a measurement of the time in which an ion travels over a given distance. Since, for great mobilities, the resolutions become too small to allow a successful measurement with instruments of practical size and applicable voltages and air speeds, it seems reasonable to try to enlarge that "given distance" without changing the diameter of the chamber. In order to verify this, one or more of the parameters in eq. (74) must be replaced by another one.

There are a number of possibilities for this approach. One of them is the replacement of U by a parameter U/ω where ω is the circular frequency of an ac voltage - in other words, to replace the dc driving voltage discussed so far in this report by an ac driving voltage. It will turn out that by introducing the ac voltage, the wind velocity does not influencing the resolution anymore, see below.

Here a word should be said with respect to our application of the denomination ac. In the past, GERDIEN chambers have been proposed which operate with an ac voltage, but in these cases, the frequency was so small that for the movement of a particular ion on a dc field was effective. If one of the GERDIEN chambers quoted in section 1.3.5 should be used for ions of both signs, and with a sweeping driving voltage, the solution of the application of a low frequency ac is a natural one. However, in all these cases, the length of the ion motion is not essentially changed, and the equations of section 1.3.5 and 1.3.6 basically apply.
If we want to increase the length of the ion paths within the condenser by the application of an ac driving voltage, the applied frequency must be so great that the ions follow a sinusoidal path. This principle was proposed by DOLEZALEK in 1962 and discussed by DOLEZALEK (1963) and by DOLEZALEK and OSTER (1963, 1964, 1965).

Figure 6 shows the principle and figure 7 demonstrates the difference in resolution for dc and ac chambers. The lower part of figure 6 shows the influence of a superimposed dc voltage of a magnitude comparable to the amplitude of the ac driving voltage, and it indicates how this influence can be minimized. As can be seen, the ions are forced to follow a sinusoidal pattern inside the chamber, the amplitude of which is constantly increasing while the ions travel downstream. The increase in the amplitude of the driving voltage along the chamber's axis is done by a rather fine subdivision of the driving electrode, and by a network of relatively small resistances every partial driving electrode is supplied

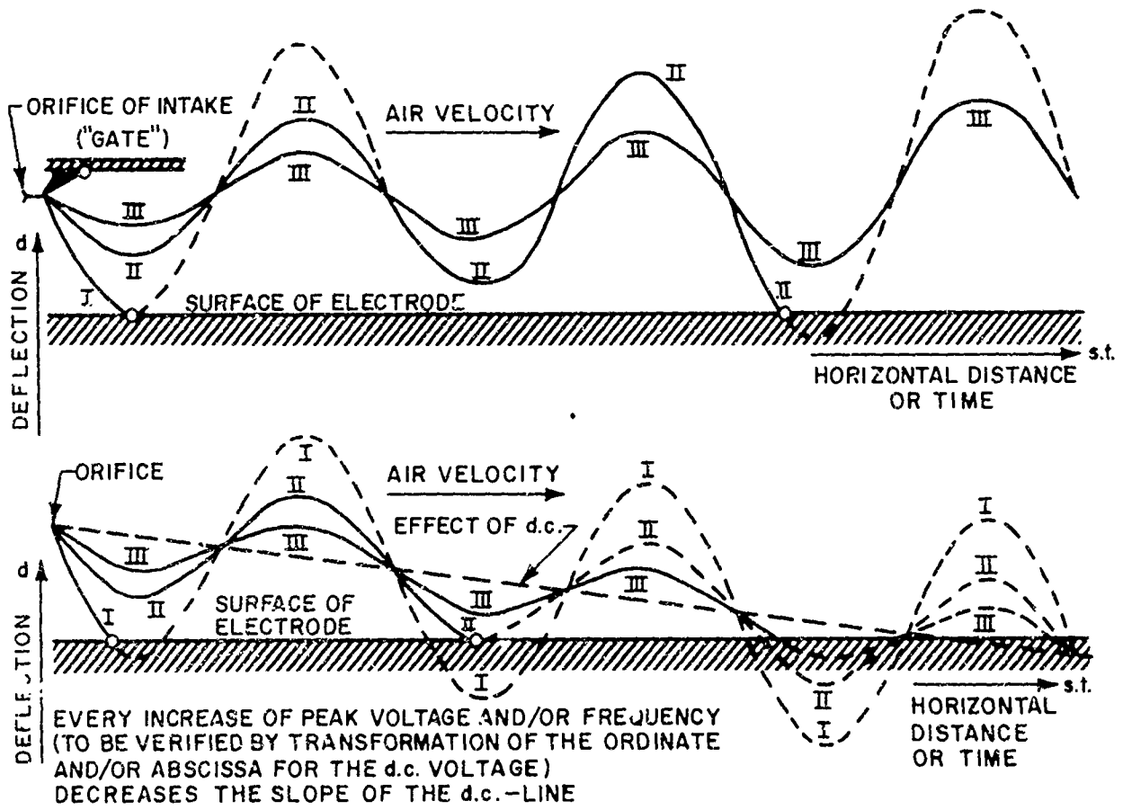

Figure 6 ION MOVEMENT IN A PLATE CONDENSER WITH AN AC VOLTAGE INCREASING FROM LEFT TO RIGHT, AIR FLOW FROM LEFT TO RIGHT

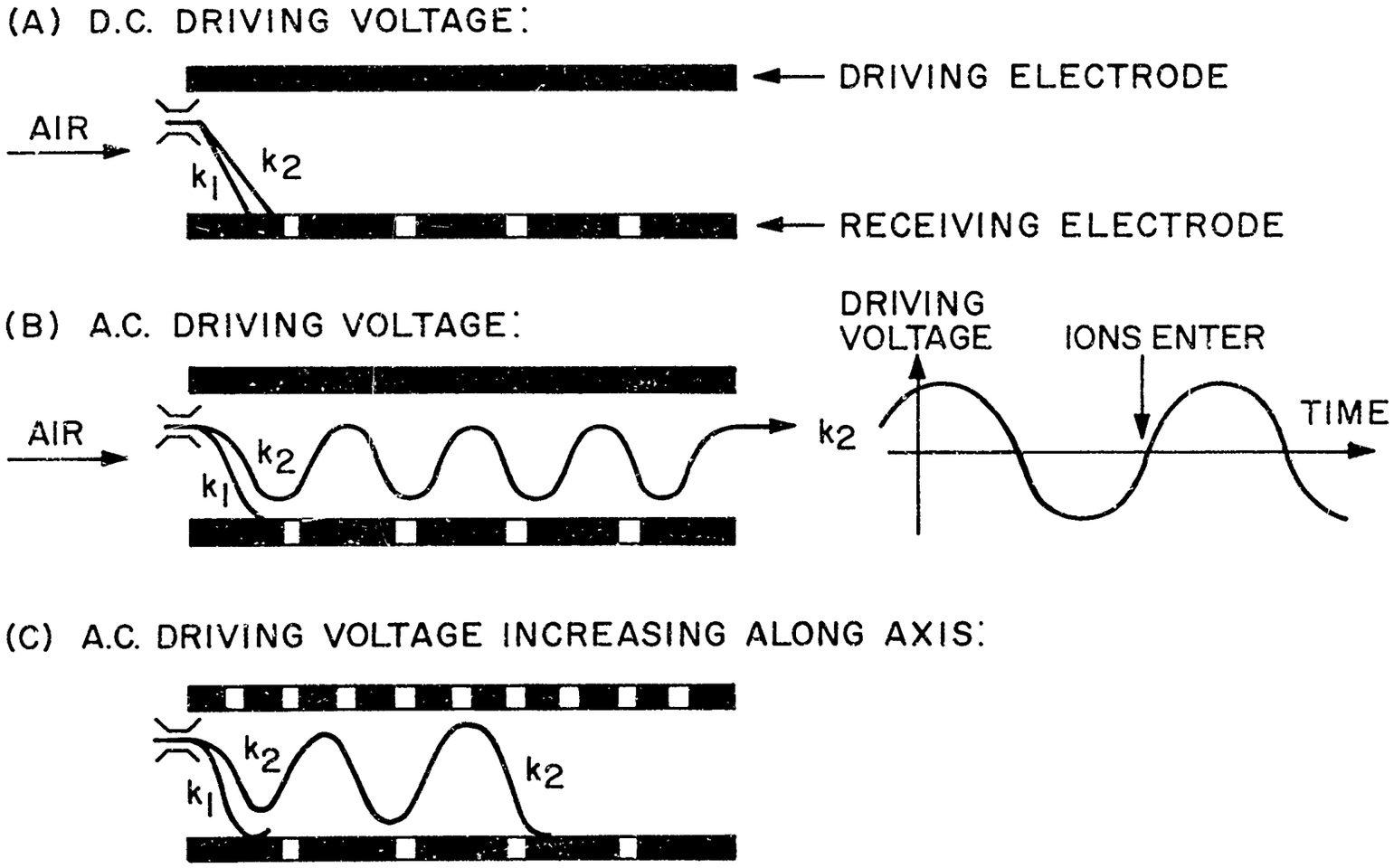

Figure 7 ION PATHS IN DIFFERENTIAL GERDIEN CHAMBERS OF THE SECOND ORDER
(Two ions with mobilities k_1 and k_2 enter from the ion gate into the chamber at the same time.)

with a slightly greater ac amplitude than its upstream neighbor. This increase must be done by small resistors to avoid phase delays, and it must be done smoothly to avoid any phase shifts for the ions traveling downstream.

The actual ion paths for a given cylindrical condenser have been calculated:

$$\rho = \sqrt{\frac{2kU}{\omega \ln R/r}\sin(\omega t + \phi) + C_1} \quad .$$

Here, ρ is the radial location of the ion at the time t, Φ is the phase of the sinusoidal driving voltage, and C1 is an integration constant. The significance of the other letters used is as before (see figures 4 and 5); however, U is now "amplitude" of the driving voltage, i. e., the zero-peak potential difference and ω is the circular frequency of it.

Figure 8 shows an example for these ion paths, demonstrated for ions of one mobility only, but entering at different times with respect to the zero point of the driving voltage. It can be seen from this figure that, for example, an ion entering at t = 5/8 T would not reach a receiving electrode placed at r = 1.5 cm during the first sine wave it follows in the chamber, but because of the increasing U, it may intercept during one of the following waves. However, only ions with a smaller mobility are supposed to intercept more downstream. For this reason, only ions which arrive at t = 0 will be allowed to enter. This poses a new technical problem for the realization of the method.

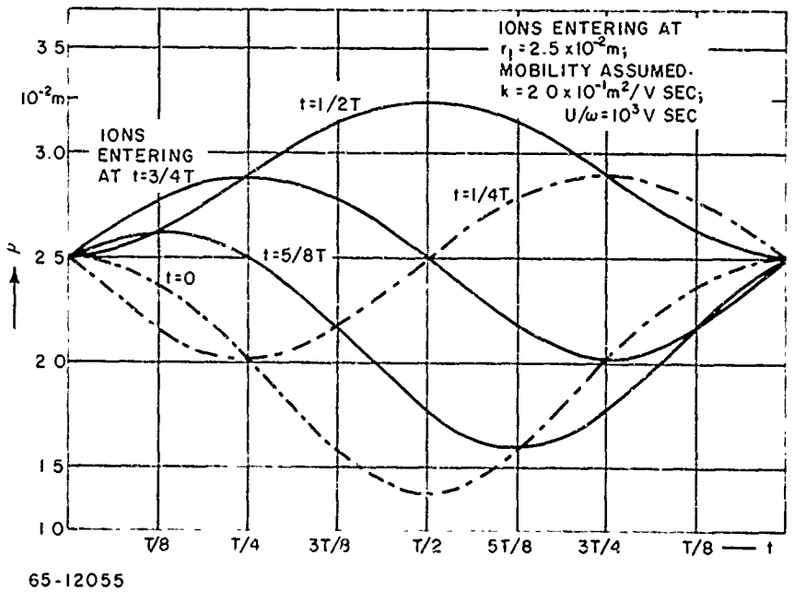

Figure 8 ION PATHS IN A CYLINDRICAL CONDENSER WITH AN A.C. DRIVING VOLTAGE. IONS OF ONE MOBILITY ONLY. IONS ENTERING AT THE SAME ORIFICE (ION GATE) AT DIFFERENT MOMENTS, NAMELY AT 0T, 1 4T, 1 2T, 5 8T, 3 4T. T: DURATION OF ONE PERIOD OF THE SINE WAVE.

By positioning a "collecting electrode " - in the case of figure 8 - at about 2.6 cm and with a length reaching downstream to about T/8, all ions with a phase other than zero would be caught there. This solution of the problem is applicable in the case of known wind speed, since the abscissa in figure 8 is time and the length of the collecting electrode must be chosen according to velocity. The collecting electrode must not be longer than corresponding to T/8 because of the increase of driving voltage along the axis.

Another method of solving this problem is given by the possibility of making the ion orifice to an ion gate, which is closed all the time with the exception of a short duration at t = O in figure 8. This can be achieved by a particular generator triggered by the driving voltage. Figure 9 shows its principle. At the upstream end of the modified GERDIEN chamber, there are three sets of rings, the purpose of which will be discussed in the next figure. The ion gate is located between rings 13 and 14. Between these rings, a dc voltage which is great enough to capture all ions of the expected mobility range is maintained. Only during the time τ this dc voltage is removed and ions will pass. Since the rings 03, 04, 14, 23, and 24 are always on the same potential, ions will not meet an electric field while passing between 03 and 04 and while passing between 23 and 24. (All actual rings and their numbers in this example refer to the laboratory model of the 'modified GERDIEN chamber', the so-called "Model A," which will be described in Part 2 of this report).

The purpose of the rings 11 to 18, as indicated in the upper left part of figure 9, is to allow the air to pass between them, but to remove all ions out of it. To do this, dc voltages are maintained between all these rings. This same set of rings is to be seen in figure 10 as well; in the same figure we also see the two other sets of rings, parts of which are already shown in the upper left part of figure 9. The purpose of these two sets of rings is explained below.

The first set of rings, numbers 00 to 07, are to cancel the so-called edge effect. Because of the strong dc voltages to be maintained between the pairs of rings of the set 10 to 17, stray fields would occur going across the inlet to the pair 13-14. The effect of these stray fields would be to reject, more or less, ions of one sign, and to promote ions of the other. Since this would falsify the number densities, the rings 00 to 07 had to be added. They are all on the same potential as ring 14. Thus, during the time τ (figure 9) when there is no potential difference between 13 and 14, ions entering between 03 and 04 will feel no electric field while passing. The same had to be done at the downstream side of rings 10 to 17. However, this side faces the interior of the chamber and there is a field. For this reason, the rings of the set 20 to 27 are all carried on different potentials. Each ring gets the potential which a point with the same radius as the ring would have in an infinitely long cylindrical condenser. This is done with one exception: rings 23 and 24 both have the same potential, namely, that of the point with the radius $(r_{23} + r_{24})/2$ in an infinity long cylinder. The consequence of this is that an ion entering between 03 and 04 will "see" no elec-

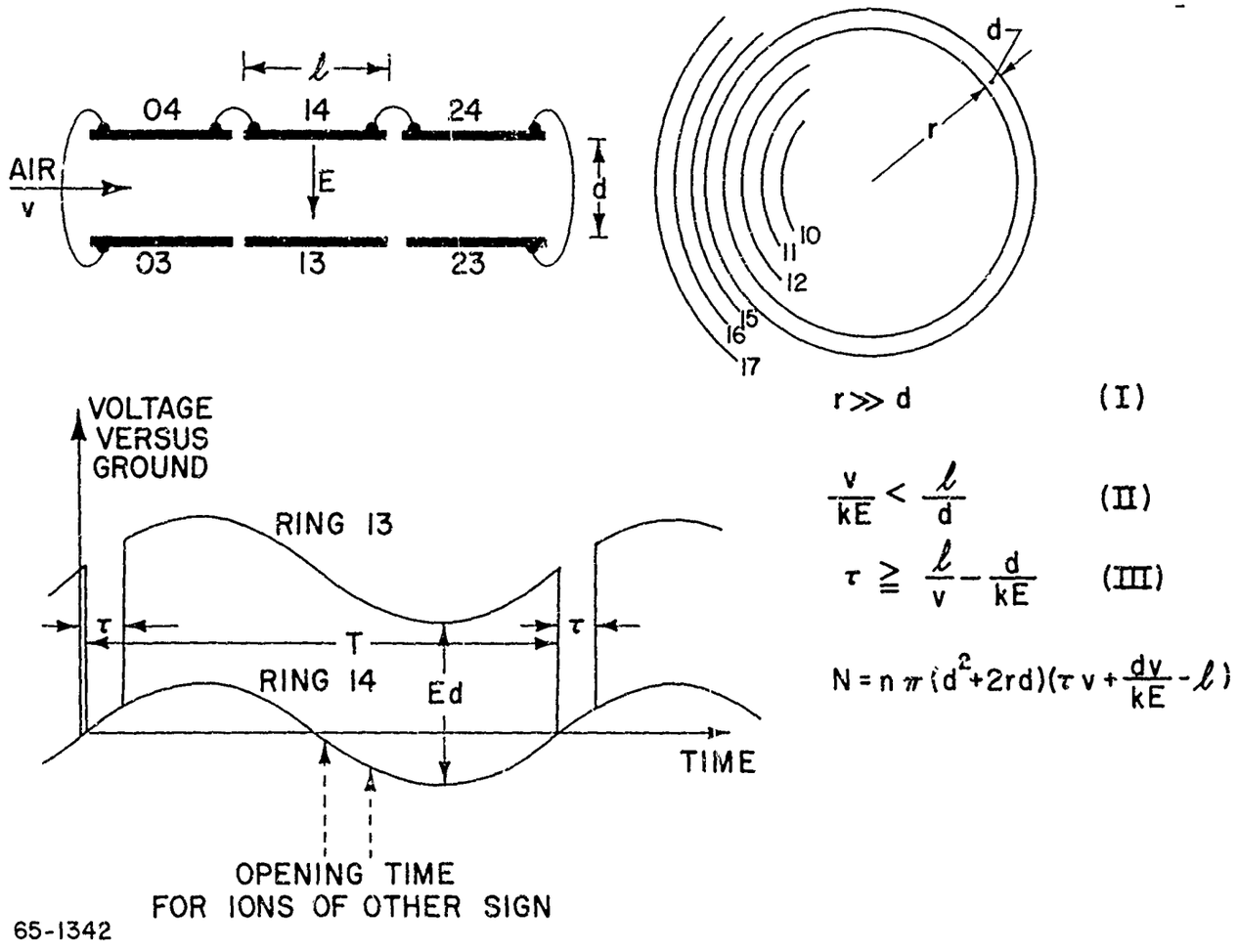

$$r \gg d \qquad \text{(I)}$$

$$\frac{v}{kE} < \frac{\ell}{d} \qquad \text{(II)}$$

$$\tau \geq \frac{\ell}{v} - \frac{d}{kE} \qquad \text{(III)}$$

$$N = n\pi(d^2 + 2rd)\left(\tau v + \frac{dv}{kE} - \ell\right)$$

Figure 9 OPERATION OF ION GATE DEMONSTRATED WITH THE LABORATORY MODEL OF MODIFIED GERDIEN CHAMBER ("MODEL A")

Upper left: three pairs of the sets of rings at the upstream end of modified GERDIEN chamber with the ring numbers as indicated in figure 10.

Upper right: Schematic view of the rings as seen when looking parallel to the axis of the chamber.

Lower left: Variation of voltage versus ground at rings 13 and 14 with time; T is the period of the driving voltage.

Lower right: The three conditions for the operation of the ion gate: (I) is the condition for applying formulas of the plate condenser; (II) is the condition for capturing all ions of mobility k during the closing time of the gate; and (III) is the condition for the passage of ions of mobility k during the opening time of the gate. N is the total number of ions of mobility k which will pass during one gate opening τ, when the ion number density prior to entering the gate is n.

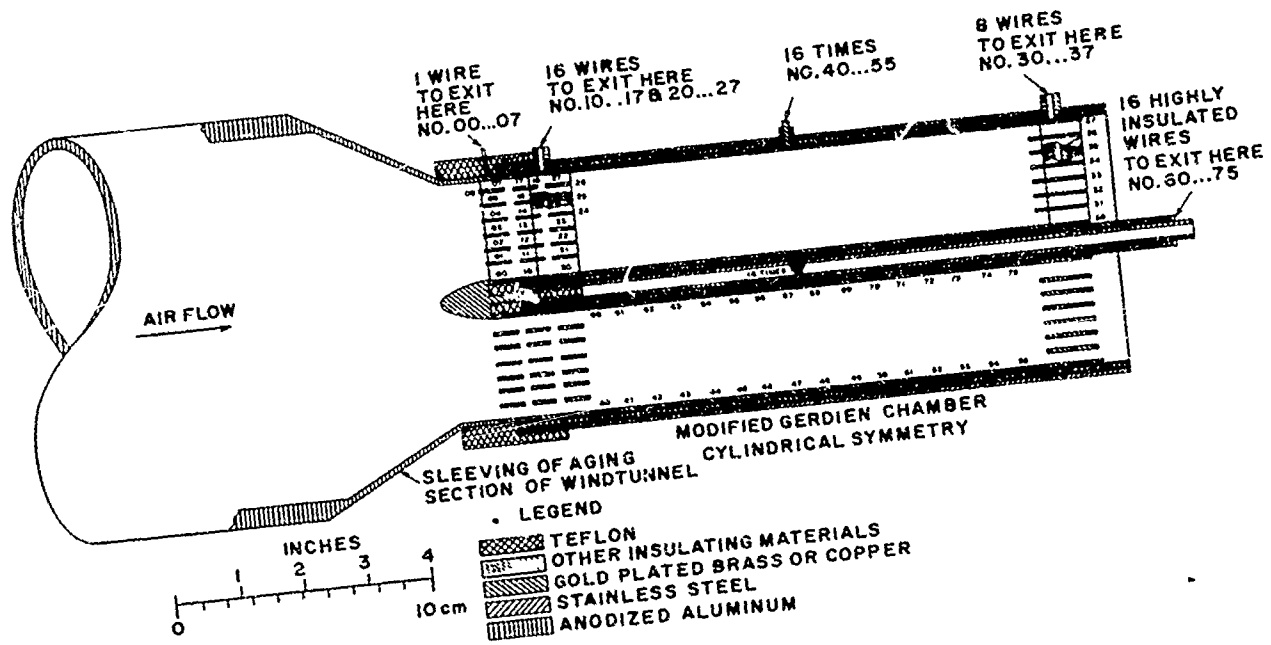

ELECTRODES AND RINGS (ALL GOLD PLATED):

FIRST SET OF RINGS, NO. 00...07 : EQUALIZING RINGS, EXTERNAL (EDGE EFFECT CANCELLATION)
SECOND SET OF RINGS, NO. 10...17 : ION FENCE WITH ION GATE
THIRD SET OF RINGS, NO. 20...27 : EQUALIZING RINGS, INTERNAL, UPSTREAM (FIELD EQUALIZING)
FOURTH SET OF RINGS, NO. 30...37 : EQUALIZING RINGS, INTERNAL, DOWNSTREAM (FIELD EQUALIZING)
OUTER ELECTRODES, NO. 40...55 , USED AS RECEIVING ELECTRODES
INNER ELECTRODES, NO. 60...75 , USED AS DRIVING ELECTRODES

EXAMPLE FOR ELECTRIC CONNECTIONS: IF THE ION GATE IS BETWEEN 13 AND 14, THE FOLLOWING RINGS WILL BE DIRECTLY CONNECTED TO EACH OTHER: 23-24-14-00-01-02-03-04-05-06-07-11-16 AND TO THE SLEEVING OF THE AGING SECTION OF WIND TUNNEL. ALSO 10-12-15-17 WILL BE INTERCONNECTED. THE FENCE VOLTAGE IS BETWEEN 10 AND 11. THE GATE VOLTAGE IS BETWEEN 13 AND 14.

THE RINGS ARE MOUNTED ON THREE TEAR SHAPED LEGS. ALL RINGS CAN BE TAKEN OUT AND REPLACED BY A SET OF THREE LEGS WITHOUT INTERMEDIATE RINGS (FULLY OPEN INTAKE AND OUTLET).

64-11372

Figure 10 CROSS SECTION OF MODIFIED GERDIEN CHAMBER--MODEL A (Laboratory model).

tric field prior to entering the chamber proper, and this is what must be requested. To avoid any fields outside the chamber for the laboratory experiments done in the wind tunnel, the wind tunnel is lined by an electrically insulated sleeve, and this is carried along at the same potential as the rings 00 to 07 have. The beginning of this sleeve is shown at the left hand end of figure 10.

The rings 20 to 27, furthermore, serve to equalize the electric field in the neighboring part of the chamber, which otherwise would show the well known effect at the end of a cylindrical condenser. For the same reason, another set of rings, 30 to 37, is located at the downstream end of the chamber (figure 10).

The potentials of all these rings are functions of the driving voltage. This is to be seen from the fact that the "undisturbed potentials" at the locations of rings 20 to 27 (and 30 to 37) are determined by the potential of the adjacent driving electrode (which is No. 60 and No. 75 in the case of figure 10, where the inner electrodes represent the driving electrodes, and the outer ones are used as receiving electrodes). Since this potential is a sinusoidal one, all other potentials are as well, and the additional dc voltages as applied to rings 11 to 17 are "riding" on this sinusoidal wave.

The selection of the outer electrodes as receiving electrodes was determined by the necessity to keep the input capacity of the electrometers connected to them as small as possible.

In the following sections, some more theoretical aspects of this chamber will be discussed. In Part 2 of this report, the actual design of this model will be described and the laboratory experiments and their results will be reported.

For the actual measurements in the free atmosphere, the modified GERDIEN chamber will descend from peak latitude, while a parachute or decelerating body will keep the falling speed below the velocity of sound.

1.4.2 THE MOBILITY SPECTRUM OF THE MODIFIED GERDIEN CHAMBER

The chamber, as shown in figure 10, is designed as a differential GERDIEN chamber of the second order. However, if all driving electrodes are connected to each other, and if all receiving electrodes are also connected to each other, it may be applied as a differential chamber of the first order (type b) as well.

The analytic expressions for the mobility spectra are not derived here. They are for the first order mode:

$$\frac{dn}{dk} = \frac{T/\tau}{y_1 d} \quad \frac{\left(2\frac{U}{\omega}\right)^2}{e M_G} \quad \frac{dI}{d(U/\omega)} \tag{76}$$

and for the second order mode:

$$\frac{dn}{dk} = \frac{T/t}{y_1 d} \quad \frac{2U/\omega}{e M_G} \quad I \; ; \tag{77}$$

in both cases for plate condensers. The same letters as before are used. Both modes are demonstrated in figure 11.

Again, it can be seen, that for the first order mode the first derivative must be used, while the spectrum is directly given in the second order mode. The current measured for the same ion number density per mobility range is the greater the more ions are sucked into the chamber per second (M_G), but the parameter M_o (the total amount of air passing through the chamber) is no more contained in these equations, as it was in the dc case (eqs. (67) and (73)). That means that the air flow velocity in the chamber does not influence the resolution anymore. This also becomes evident from figure 7(C): the location for the interception of ions of a certain mobility is determined by the voltage which is sufficient to move the ion within one period of the sine wave towards the receiving electrode.

The resolution of the measurement can be made very good with the first-order mode, but the accuracy is much smaller than with the second-order application. The resolution with the second-order mode depends on the number of receiving electrodes, and on the overall range of mobility to be comprehended in one measurement, since this in turn determines the dU/dx, or the increase of driving voltage along the axis of the chamber.

The fact that the mobility spectrum does not depend on M_o is advantageous for measurements in higher altitudes. For several reasons, it is difficult to measure wind speed in an atmosphere of low density. Any errors made in such a measurement influence the mobility spectrum only linearly, and not in its square, as in the case with the dc-operated chamber.

Resolution and accuracy of the measurement depend on many factors. The more essential ones will be discussed in the following sections, and a particular discussion of the limitations will be presented in one of the following chapters.

1.4.3 MEASURING ION NUMBERS BY MEASURING CURRENT

In the original conductivity apparatus (RUTHERFORD, 1899; GERDIEN, 1905; and others) the "receiving electrode" was fully insulated. Either the "charging" or the "discharging" methods have been applied. In the first case, the receiving electrode had no charge at the beginning, and the rate of charging was determined by measuring electrometrically the potential difference between this electrode and ground. After a while, the electrode was artificially discharged and the process began again. Correspondingly, with the discharging method, the receiving electrode was charged at the beginning of a measuring cycle and

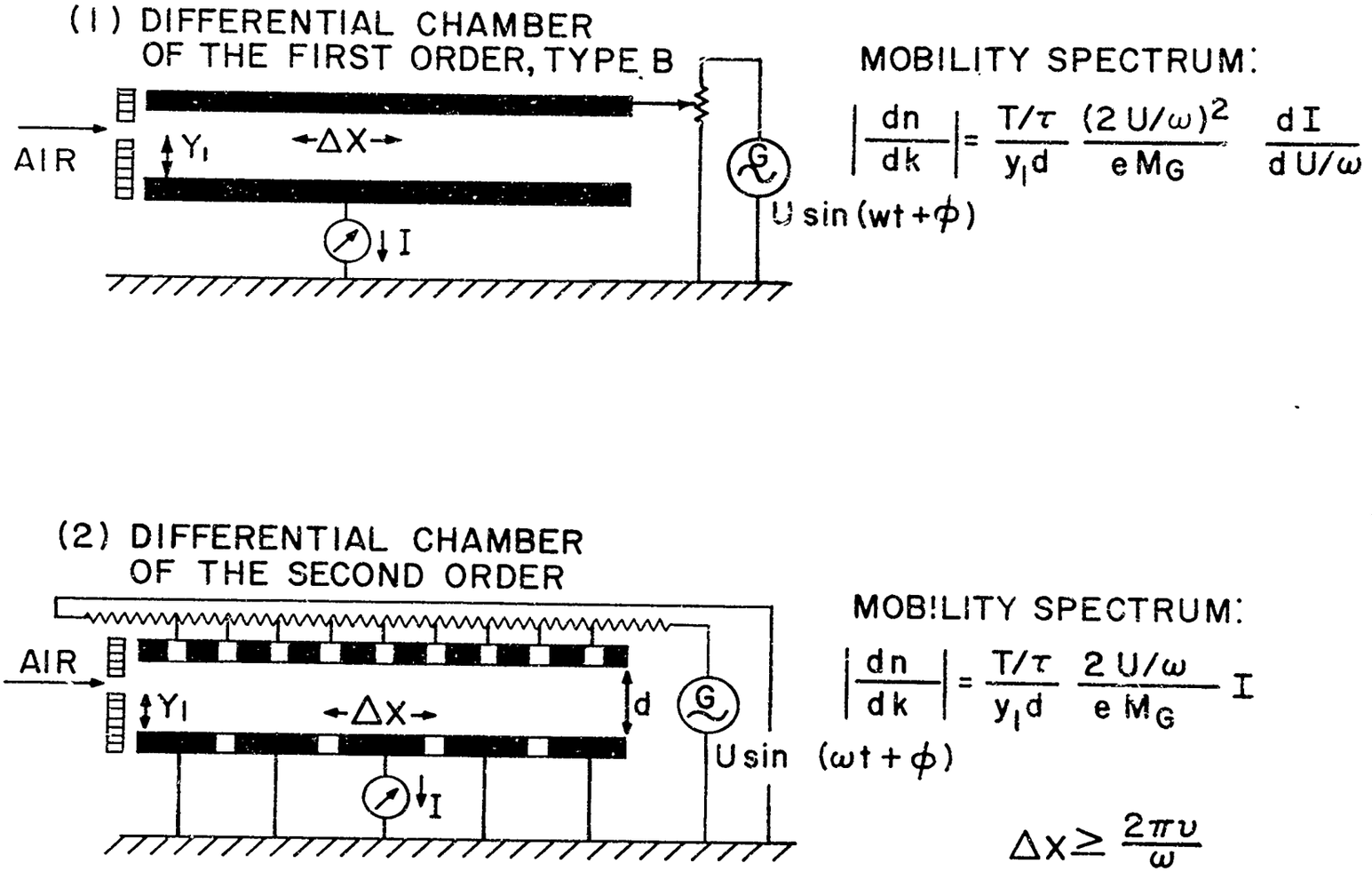

Figure 11 SCHEMATIC SURVEY ON AC-OPERATED GERDIEN CONDENSERS WITH THE ANALYTICAL EXPRESSIONS FOR THE MOBILITY SPECTRUM
(Symbols as explained in figure 4. τ is the ratio of period of driving voltage over opening time of ion gate (see figure 9); ω is the circular frequency of driving voltage, U_k is the mean effective amplitude at the point of measurement, and v is the velocity of the air flow in the chamber. Equations apply to plate condenser.)

then discharged by the arriving ions of the opposite sign. In these two cases (which are discussed extensively in the literature) the capture of the ion determined the signal which was read in the electrometer. Later on, the application of the GERDIEN method was frequently changed by the introduction of the so-called current method. Here, the receiving electrode is connected to ground by a high-ohmic resistor. The current through this resistor is measured, and it is supposed that this current represents the number of impacting ions times their charges. Some discussion on this principle and on the problem of whether or not this supposition is correct has been conducted in recent years. For the integral GERDIEN chamber this supposition will hold; deviations will be small and hardly noticeable.

With the modified GERDIEN chamber, the situation is different. During a discussion at a meeting in 1963 (DOLEZALEK, 1963), it was stated that transients caused at a receiving electrode by ions which pass by, but do not hit it, do not disturb the measurement if only the actual charges of impacting ions are measured by applying an integration over a sufficient time. A more accurate expression was derived later on by KADANOFF (1964), who calculated the current caused by the moving ion on the basis tha cylindrical symmetry can be supposed.

The charges induced on the inner and outer electrodes of a cylindrical condenser by an electric charge moving between them are (not regarding edge effects)

$$Q'_{inn} = - Q \frac{\ln (R/\rho)}{\ln (R/r)} \tag{78}$$

$$Q'_{out} = - Q \frac{\ln (\rho/r)}{\ln (R/r)} \quad ; \tag{79}$$

where Q is the moving charge, Q' is the induced charge, R and r are the radii of the outer and inner electrodes, respectively, and ρ is the radius of the location of Q at a given time. The current I flowing from the outer and inner electrode, respectively, can be calculated by differentiation over time (t) as follows:

$$I_{out} = \frac{d Q'_{out}}{dt} = \frac{Q}{\ln (R/r)} \frac{1}{\rho} \frac{d\rho}{dt} \tag{80}$$

$$I_{inn} = \frac{d Q'_{inn}}{dt} = - \frac{Q}{\ln (R/r)} \frac{1}{\rho} \frac{d\rho}{dt} \quad . \tag{81}$$

With these formulas, and supposing certain mobilities and values for the entrance point of the ions into the chamber (location of ion gate) as well as radii of the electrodes, the location of the ion in the assumed chamber, the velocity of this ion in the chamber, and the current induced in the high-ohmic resistor between the outer electrode and ground have been calculated. They are entered

the velocity of the air flow in the chamber. Equations apply to plate condenser.)

in figures 12, 13, and 14. When interpreting these figures, we must keep in mind, that the driving voltage has a sinusoidal shape. This determines the form of these curves. A qualitative interpretation of the figures and the equations leads to the following result.

A current is caused by an incoming ion as soon, as the respective receiving electrode "sees" that ion. For the first one of the receiving electrodes, this occurs when the ion enters through the rings 23 and 24 into the chamber. If this ion is not to hit the receiving electrode, the current caused by it flows in one direction as long as the ion approaches the receiving electrode, and in the opposite direction when the ion moves away from it. It ceases to flow, when the electrode cannot "see" the ion anymore whether it be that the ion is intercepted at another receiving electrode, or that it moved too far downstream the chamber. In both cases the time integral of the current extended over the full period is zero. However, if the ion hits that particular receiving electrode, the measurement is done at this very moment, the time integral is not zero, but has the magnitude of the charge of that ion. In figures 12, 13, and 14, the parameters have been chosen in such a way that the ion almost hits the receiving electrode. It can be seen, that these three curves would be very nearly the same if the ion would hit. That means that during the passing of an ion, an electrometer with a very short time constant attached to this electrode would not be able to distinguish between ions which would hit and others which would not. In other words we again approach the charge measurement method as used with GERDIEN chambers in early days - and it can be the "charging" of the "discharging" mode. This depends on the immediate history of the receiving electrode under consideration.

If one would allow ions of both signs to be measured (i. e., open the ion gate twice per period of driving voltage), one would operate essentially with a discharging mode. This would require a rather precise setting of the integrating time for each individual measurement. On the other hand, of one opens the gate only once per period (compare figure 9), only ions of one sign enter and the charging mode applies. In this case, the individual measurement can be extended over several or even many periods of the driving voltage, and it becomes independent of the wind velocity in the chamber. This is preferable. The discharging of the receiving electrode may then be done by grounding it, or by switching the ion gate to let the ions pass with the other sign. Again, the grounding would be preferable, since then one always operates with the charging mode.

In conclusion, the time constant of the electrometer attached to the receiving electrode must be great enough to obtain an integral over a time which is longer than the time in which an ion travels from the exit of the ion gate to the receiving electrode under consideration. The electrometer time constant must be shorter than the period of time between the switching over from one sign to the other. If these conditions are fulfilled, the electrometer should show how the capacity of the receiving electrode versus ground is charged up by the intercepted ions. Because of the high ohmic resistance across this capacity, this

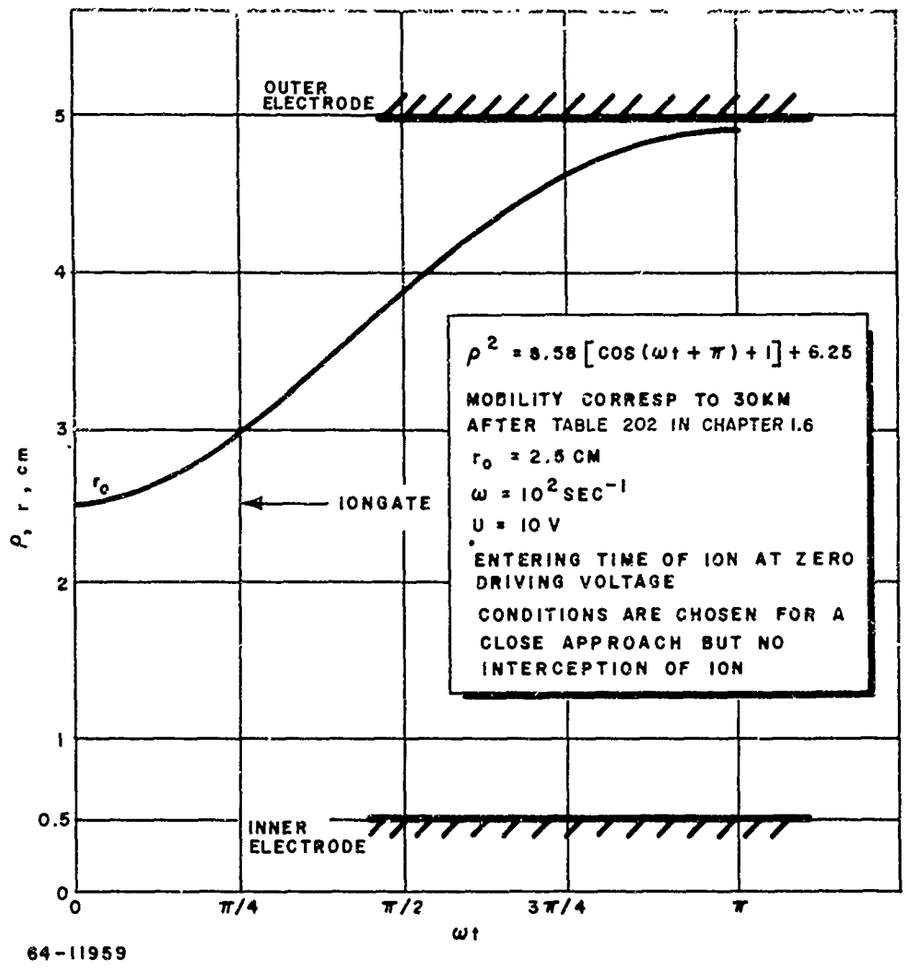

Figure 12 LOCATION OF MOVING ION IN MODIFIED GERDIEN CHAMBER
(Outer electrode is receiving electrode.)

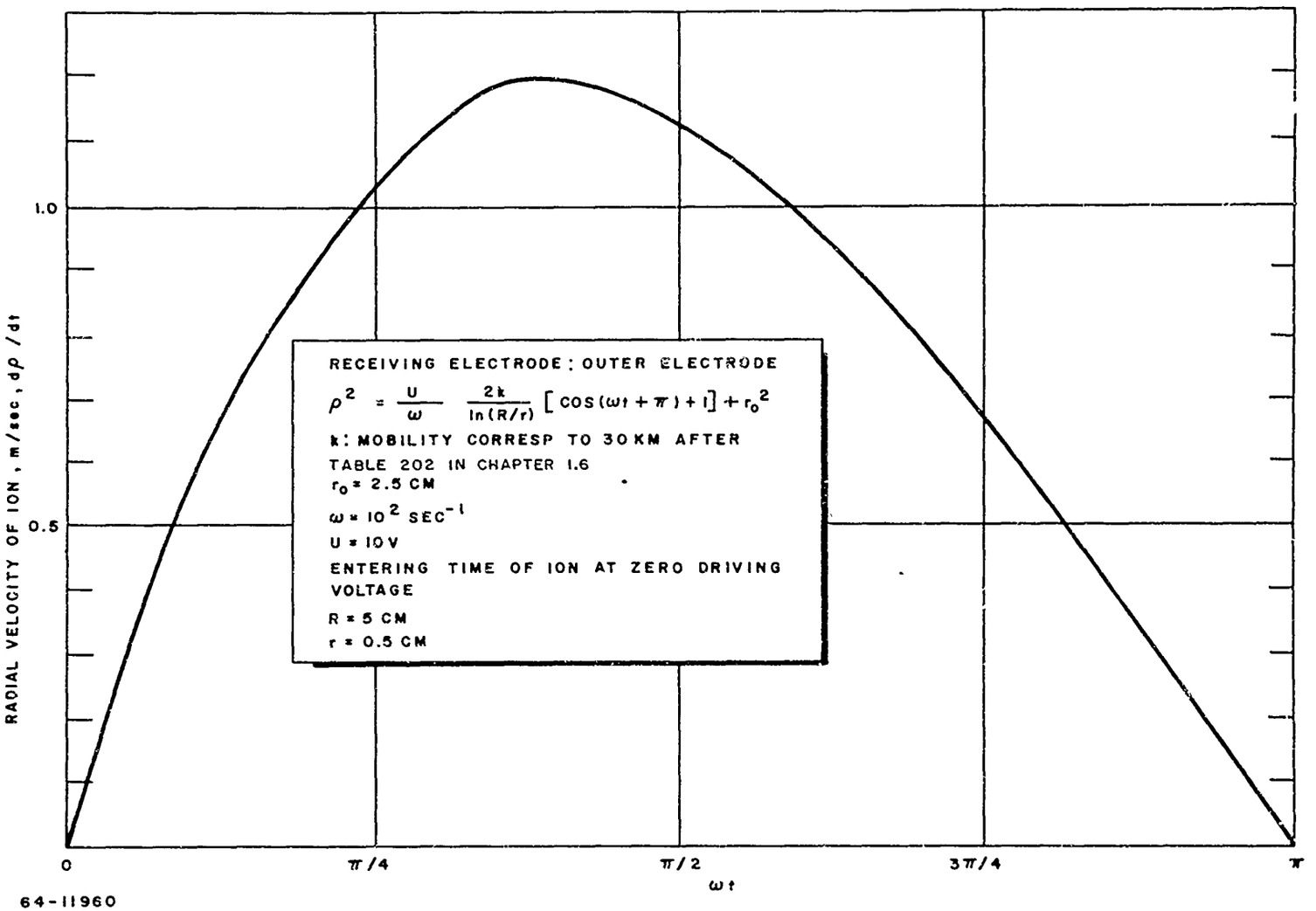

Figure 13 VELOCITY OF ION IN MODIFIED GERDIEN CHAMBER

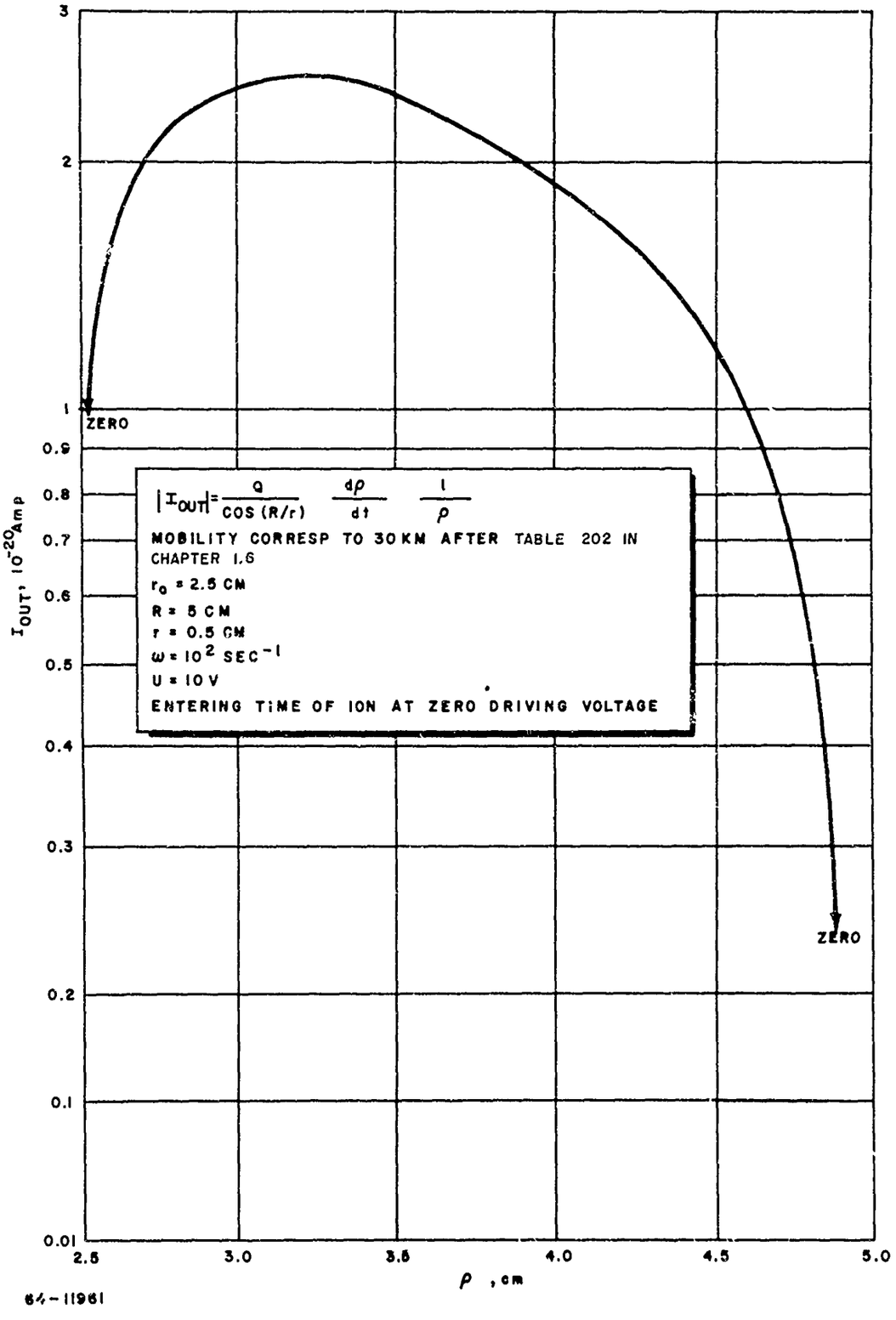

Figure 14 CURRENT IN RESISTOR BETWEEN ONE RECEIVING ELECTRODE AND GROUND AS INDUCED BY A MOVING ION

charging-up process occurs according to an exponential function which, at a closer sight, dissolves into a number of stepwise increases and decreases, each pair of which has the duration of one period of the driving voltage. If the high ohmic resistor is too small, however, there may be no increase at all. If one should be chosen too high, one would risk getting an unkown leak resistance between electrode and ground.

1.4.4 DETERMINATION OF DRIVING VOLTAGE PARAMETERS

The discussion of the preceding section encompasses essentially the general theory for the ion motion in the chamber. The formula for the location of an ion which entered the chamber through the ion gate located at the radius $(r + y_1)$ is:

$$\rho^2 = \frac{U}{\omega} \frac{2k}{\ln (R/r)} [\cos (\omega t + \pi + \phi) + \cos \phi] + (r + y_1)^2 \; ; \tag{82}$$

and, for an ion entering when the driving voltage passes the value zero (i.e., $\phi = 0$)

$$\rho^2 = \frac{U}{\omega} \frac{2k}{\ln (R/r)} [\cos (\omega t + \pi) + 1] + (r + y_1)^2 \; . \tag{83}$$

If ρ is replaced by either R or r, the equations provide the U/ω values for a tangential impace on either the outer or inner electrode, respectively.

It is obvious from figure 8 (in section 1.4.1) that tangential impact is the desirable method for measuring the ion spectrum. This fact is confirmed by the quantitative discussion of the preceding section.

However, it has been shown by DOLEZALEK and OSTER (1964) that even with ions impinging at a greater angle, information on the ion spectrum may be derived. This fact may add valuable information in cases with a swept or stepped driving voltage.

For the case of tangential impact, U/ω values are shown in figure 15, covering the mobility range which corresponds to altitudes between about 30 and 80 km. The four curves shown are valid for (a) ions entering at zero driving voltage exactly ($\phi = 0$) and in the middle between rings 23 and 24 of the laboratory model of modified GERDIEN chamber (model A), and for (b) ions entering at $\phi = \pm 10$ degrees, again in the middle between the rings, and, finally, (c) and (d) for ions entering at $\phi = 0$ but very close to rings 23 and 24, respectively. After the selection of the adequate U/ω values, the individual parameters U and ω must be chosen.

The amplitude of the driving voltage, U (peak to zero) must be greater than disturbing dc voltages which may occur in the chamber (compare figure 6, lower part), but its size is limited also by the necessity of avoiding some pos-

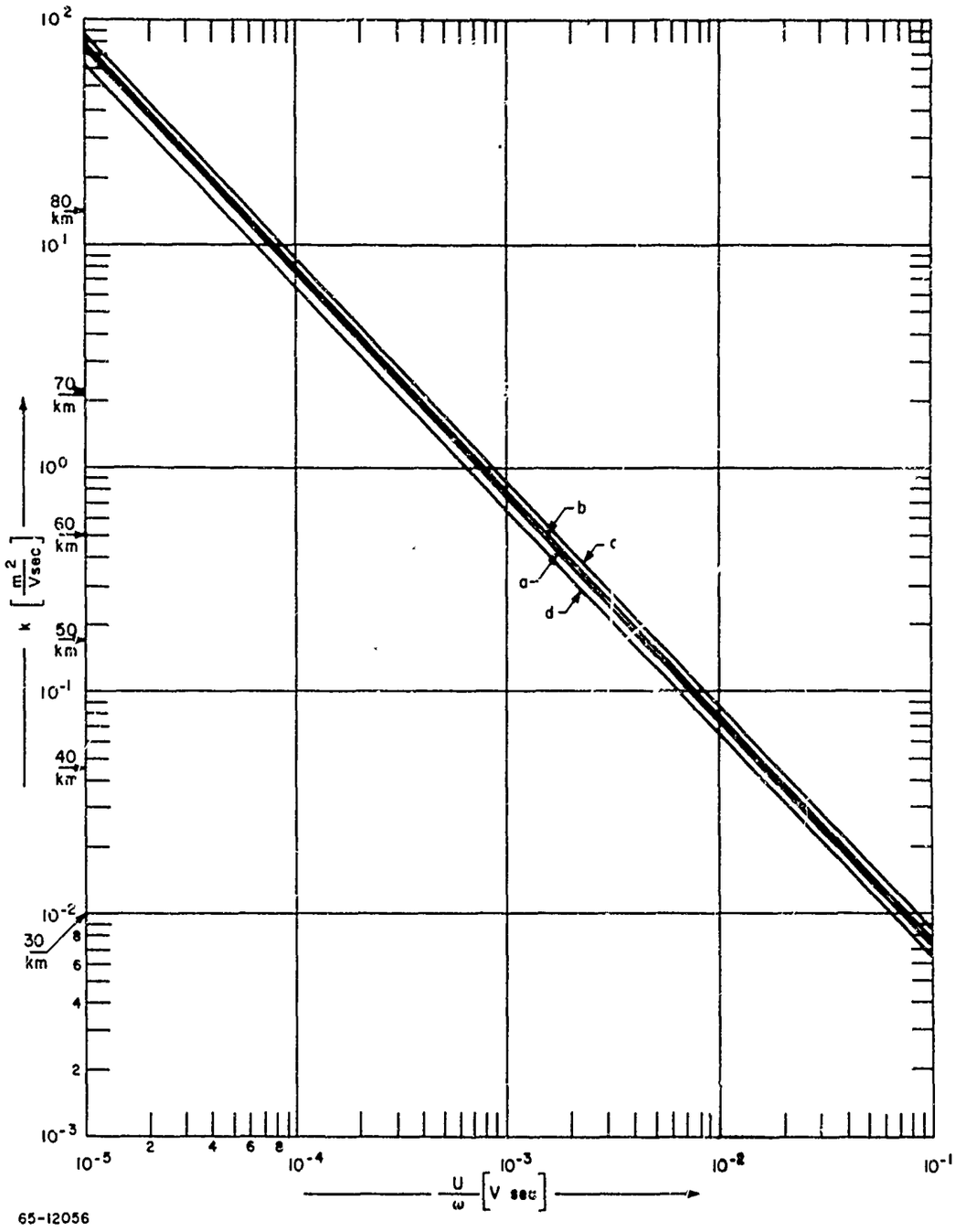

Figure 15 DRIVING VOLTAGE PARAMETERS U/ω FOR TANGENTIAL IMPACT OF IONS (Model A of modified GERDIEN chamber: (a) ions entering in the middle between rings 23 and 24 and at zero driving voltage (i.e., $\phi = 0$). (b) ions entering in the middle between rings 23 and 24, at a phase of 10 degrees prior or after zero driving voltage; (c) ions entering very close to ring 23 at zero driving voltage; and (d) ions entering very close to ring 24 at zero driving voltage.

sible disturbances to be discussed in chapter 1.7. Furthermore, U must be small enough to avoid ionization by collision in the chamber to avoid corona discharges between the rings 20 to 27, and between them and the adjacent rings of the set 10 to 17. On the other hand, the greater U, the smaller the disturbing influence of diffusion.

The frequency of the driving voltage, $\omega = 2\pi\nu$ is determined by several factors as well. Since we want tangential impact at the receiving electrode, the distance between the impact point of the first electrode and rings 23/24 in the axial direction should be:

$$\Delta x = Tv = \frac{v}{\nu} = \frac{2\pi v}{\omega} \quad . \tag{84}$$

Thus, for a given wind speed in the chamber v and given geometrical dimensions of the chamber, a minimum ω is determined. The same consideration applies for the distances between the first and subsequent receiving electrodes, or simply for the electrode length. This is plotted in figure 16 for two different wind speeds. On the other hand, the frequency of the driving voltage must be kept in a range in which it is possible to construct a properly working ion gate impulse generator (compare figure 9 and section 1.4.7 below); it should be kept small enough to allow a sufficient cancellation of the main displacement current (see section 1.4.5 below). Furthermore, the frequency of driving voltage determines the opening period of the ion gate (to a certain extent), and since the barring voltage in the gate must stay well below the onset of corona discharge, there is a dependence between frequency and length of gate rings (rings 13 and 14 in model A).

1.4.5 ION CURRENT AND DISPLACEMENT CURRENT

If the number density of ions of one mobility range is n_k, and if all these ions have but one elementary charge, the electric current as carried by these ions to the receiving electrode is given by:

$$i_k = M_G n_k e = v \Delta y \, 2\pi (y_1 + r) n_k e \quad . \tag{85}$$

As pointed out in the preceding section, the cancellation of the displacement current induced in the receiving electrode by "passing-by" ions requires the summing up of the current measurement for a time at least as long as that required for one ion to pass downstream the length of one receiving electrode. In this period of time, $\Delta x/v$, the charge accumulated on an insulated receiving electrode of length Δx will be:

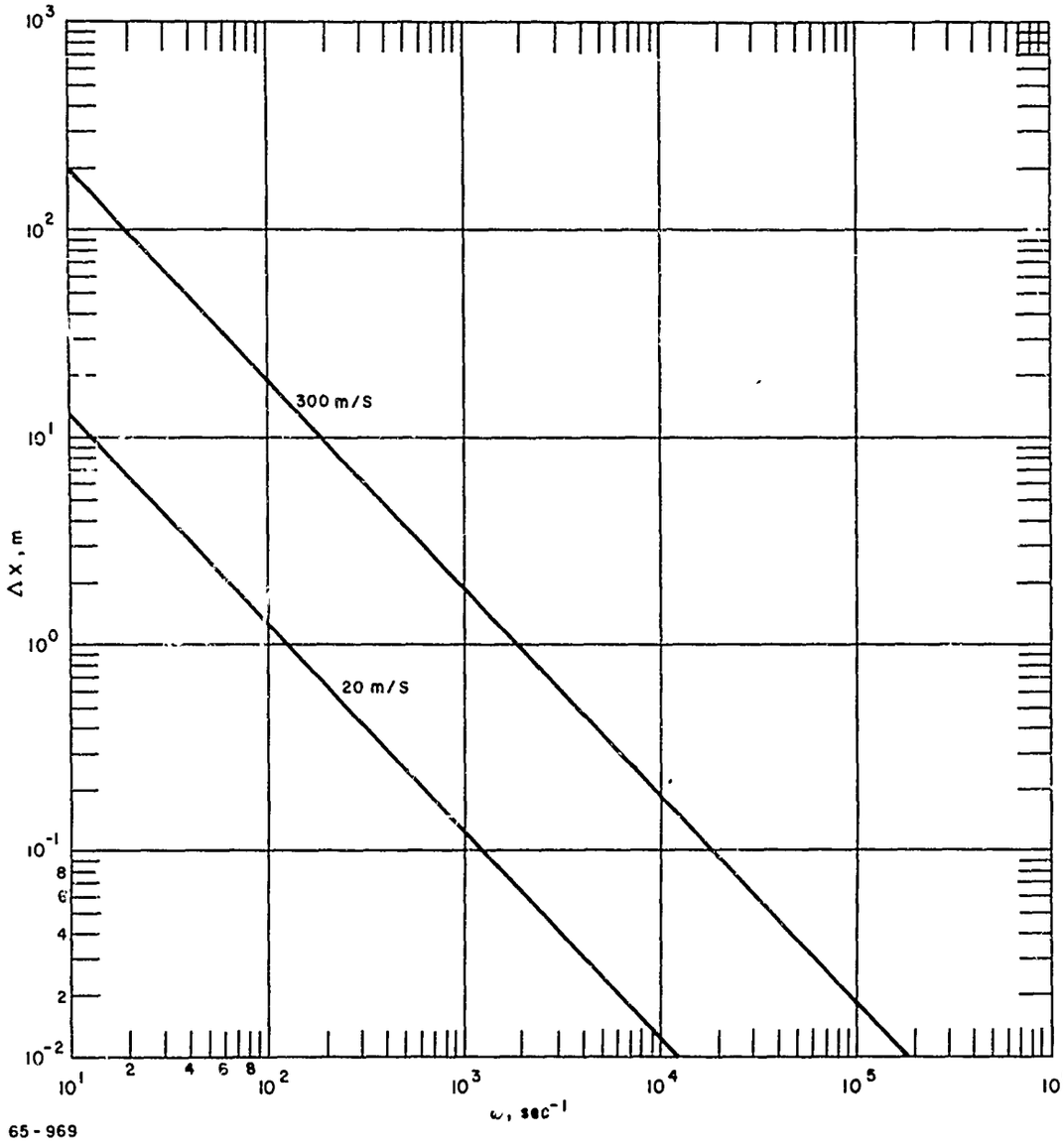

CIRCULAR FREQUENCY OF DRIVING VOLTAGE FOR A GIVEN LENGTH OF RECEIVING ELECTRODE ACCORDING TO $\omega = \frac{2\pi v}{\Delta X}$

Figure 16 RELATION BETWEEN FREQUENCY OF DRIVING VOLTAGE AND LENGTH OF RECEIVING ELECTRODES

$$Q_2 = \Delta x \; \Delta y \; 2\pi \; (y_1 + r) \; n_k \; e \quad . \tag{86}$$

If the current is collected over one period of the driving voltage, one samples all ions entered in the time r. This quantity may be derived from figure 9 and amounts to:

$$Q_3 = n_k \; e \; \pi \; [\Delta y^2 + 2\Delta y \; (r + y_1)] \quad \left[rv + \frac{v \, \Delta y}{k \, E_G} - l \right] \tag{87}$$

where the letters d and r of figure 9 have been replaced by the symbols Δy and $(r + y_1)$. Here, E_G is the voltage applied to the ion gate for closing it, and l is the length of the ion gate (ring 14 or 13).

If the receiving electrode under consideration has, versus ground, a capacity of C_k and if the leak resistance is sufficiently great so that the product of C_k with it is much greater than the duration of one period of the driving voltage, this capacity will get a voltage of:

$$U_3 = \frac{n_k \; e \; \pi}{C_k} \quad [\Delta y^2 + 2\Delta y \, (r + y_1)] \quad \left[rv + \frac{v \, \Delta y}{k \, E_G} - l \right] \tag{88}$$

from the ions of one mobility range entering during one period of driving voltage.

In addition to the displacement current induced by "passing-by" ions, we also have the displacement current induced directly by the driving voltage. Since the driving electrodes are supplied by an ac voltage, we will get another ac voltage with a 90 degree phase shift on the receiving electrodes as well, even if there were no ions in the chamber at all. If we were to measure the current per receiving electrode exactly for one period or for a full number of periods, this "main displacement current" would just cancel. However, there are two reasons why we should not count on this automatic cancellation: at first, it would be very difficult to arrange the measurement to a full number of periods exactly, and since this main displacement current will be much greater than the current provided by the ions, any small error in the timing would cause great disturbance. Second, the main displacement is assumed to be so great that it would quickly saturate any sensitive electrometric amplifier. It is known that the desaturation of these amplifiers occurs with an extremely long time constant. Thus, the amplifiers would just jump from positive to negative saturation and vice versa, and no measurement would be possible.

For these reasons, a more detailed discussion on the main displacement current is necessary.

To obtain some numerical values, we take the more disadvantageous case, -- that the admittance between receiving electrode and ground:

$$Y_k = \sqrt{\frac{1}{R_k^2} + \omega^2 C_k^2} \tag{89}$$

is, due to a relatively high frequency, determined by the capacitance. For $\nu = 100$ Hz (i.e., $\omega = 628$ sec^{-1}), this is the case, if the numerical value of R_k in Ohm is more than $1.6 \times 10^{-2} / C_k$, where C_k is measured in Farads; e.g., if the capacity is 10 pF, the resistance must be greater than 1.6 Gigaohm to have a contribution of less than 1 per cent to the admittance. For $\nu = 1$ kHz, the resistance must only be greater than 160 megohms. In this case, the displacement current may be calculated by the series connection of C_k and C_D, where C_D is the effective capacity between one receiving electrode and the driving electrodes:

$$I_D = U \frac{C_k C_D}{C_k + C_D} \omega \; ; \tag{90}$$

this is the amplitude (peak to zero) of the main displacement current.

For example, if the modified GERDIEN chamber is moving through the atmosphere at, say, an approximate altitude of 50 km with half the velocity of sound, and the number density of all ions is 5×10^9 m^{-3}, and we want to measure in a mobility range where 5×10^8 m^{-3} ions exist, we derive, from eq. (85), an ion current to the adequate receiving electrode of about (using the dimensions of figure 10):

1.13×10^{-11} A.

On the other hand, with $\omega = 6.28 \times 10^3$ sec^{-1} and U =40V (using the U/ω value from figure 15), and with $C_k = 50$ pF and $C_D = 15$ pF, we get for the peak value of the main displacement current to the same receiving electrode:

2.88×10^{-6} A.

The intended accumumulation of charge would reduce the difference, and if one measurement is made by integrating over a great number of periods, the signal can be increased by several orders of 10, while the noise due to displacement current never will become greater than the charge accumulation during one half period.

However, for a safe measurement, the displacement current must be eliminated. Figure 17 shows a workable principle. It requires a duplication of the driving voltage amplitude. The critical point of the arrangement of figure 17 is the potentiometer P_D, which must allow a very sensitive regulation. In fact this potentiometer was made up by an arrangement of eleven sensitive single potentiometers. This done, the displacement current could be cancelled with a remaining part of slightly less than 10^{-12}A. An even better cancellation would probably be possible by a better shielding and a more sophisticated application of the condenser of about 8 pF. The whole arrangement of figure 17 must be carefully kept free of phase shifts.

1.4.6 THE AMPLIFICATION OF THE SIGNAL

According to eq. (85) the current to be measured, will be smaller than 10^{-11}A, and it should be tried to amplify a current of about 5×10^{-13} A in order to provide ample flexibility. This current will be ac and it would be desirable, if a frequency of several kHz still could be handled. A discussion of the problems involved has been presented by DOLEZALEK and OSTER (1964) and will not be repeated here.

A promising beginning to solving this problem is given by the so-called" admittance neutralizer" (VOLKERS, 1963/4). Here, an input stage with a relatively great impedance (better than 10^8 Ω) is provided. In addition, artificial "negative capacitances" and "negative conductances" are fed into the input, with the goal of raising the input resistance to infinity and to lower the input capacitance to zero. In principle, this goal could be reached, and we succeeded in measuring alternating currents of about 3×10^{-12} A at 2 kHz. It turned out, however, that a further decrease was impossible because of the existing noise and it was already then difficult to get the proper settings of the regulation potentiometers. It seems promising, to increase the "natural" input impedance to about 10^{14} by applying a good electrometer tube or a modern field effect transistor in the input stage of the admittance neutralizer. In addition, a filter for frequencies greater than about 10 kHz may decrease much of the thermal noise. It has not as yet been possible to test this possibility by an experiment.

Another possibility is given by the combination of an electrometric input stage and an operational amplifier. A practical arrangement, following a proposal of SAPPUPO (1964) is shown in a later chapter of this report. Here, the critical point is the proper balancing of the zero signal put into one of the two inputs of the operational amplifier by an artificial voltage put into the second one. Experimentally, we had good results down to current of 10^{-13} A and even less, with frequencies up to several hundred Hertz. This arrangement could be made more sophisticated by applying the bridge electrometer of DOLEZALEK (1956, 1961) and feeding the outputs of the two members of the bridge into two operational amplifiers, which then could be combined by a third one. The main advantage of the bridge principle is the provision for the cancellation of disturbing elements; in the case of the modified GERDIEN chamber, it could be for a cancellation of the main displacement current.

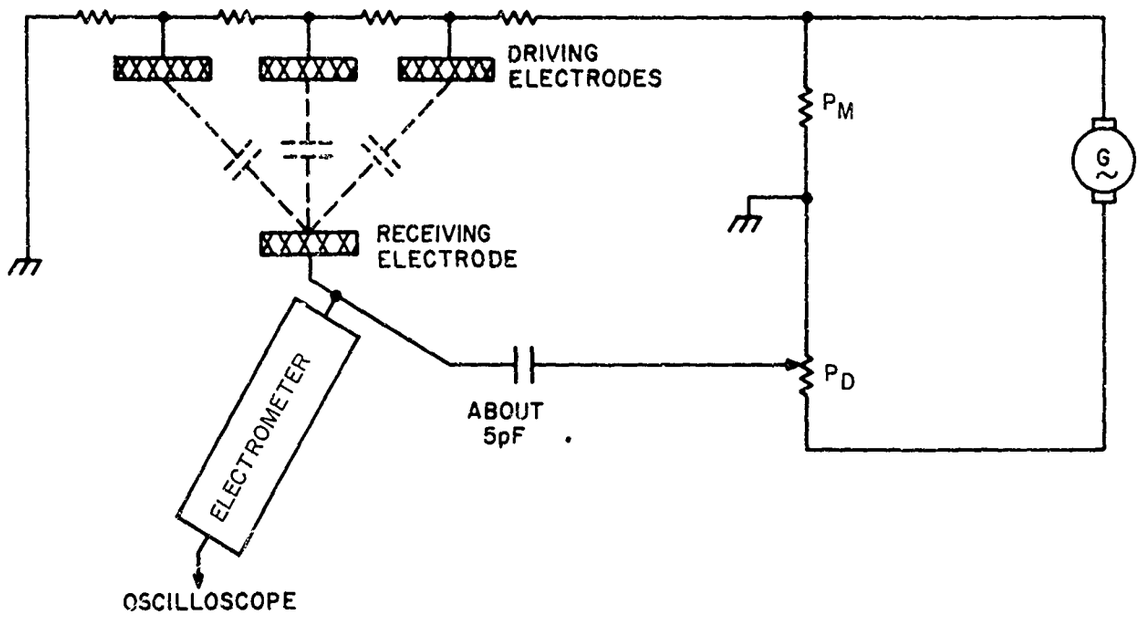

Figure 17 PRINCIPLE FOR THE CANCELLATION OF THE MAIN DISPLACEMENT CURRENT IN THE MODIFIED GERDIEN CHAMBER

1.4.7 ION FENCE AND ION GATE

As discussed in section 1.4.1, air is flowing through the full cross section of the modified GERDIEN chamber, but ions are entering only through a circular slit. From the rest of the air, the ions are removed by the application of strong dc fields.

We call this the ion filter or the ion fence, and in Model A (Laboratory Model) it was made up by rings 10 to 13 and 14 to 17 (figures 9 and 10). The field to be applied must be stronger than:

$$E > \frac{vd}{kl} \tag{91}$$

where v is the wind velocity through these rings, d is the distance between two adjacent rings, k is the smallest expected mobility, and l is the axial length of the rings. The relation between $U_G = Ed$ and length l is plotted in figure 18. Here, the mobility values are converted into altitude values according to table 202 in section 1.6.4, and velocity values have been taken from PEDERSEN (1964). It should be mentioned, however, that the d-values applied in figure 18, being 1 cm, may well be lessened for the measurement.

On the other hand, the applied voltage must be so small that no corona discharge occurs. Because of the considerable length of the cathode fall under low pressures, the PASCHEN curve will have a minimum at rather high voltages (in the order of a few hundred Volt). This has been proven experimentally in a bell jar (see figure 43).

In Model A, the "ion gate" is situated between rings 13 and 14. Again, the barring voltage during the time in which the gate has to be closed, must suffice eq. (91), while the shortest possible opening period is given by:

$$\tau \geq \frac{l}{v} - \frac{\Delta y}{kE} \ . \tag{92}$$

The number of ions entering into the chamber during this time has already been given by eq. (88) in section 1.4.5. All of these equations--(88), (91), and (92)--are easily derived from figure 9. The letter d of figure 9 and eq. (91) is replaced by Δy in eq. (92), since Δy was used by us for the denomination of the slit-width of the ion orifice.

The practical verification of a generator to supply the pulses for ion gate (triggered by the driving voltage), riding on that portion of driving voltage which is adequate to rings 23 and 24, poses many difficulties. In fact, this generator and the amplification of the signal have made necessary many experiments and required much effort.

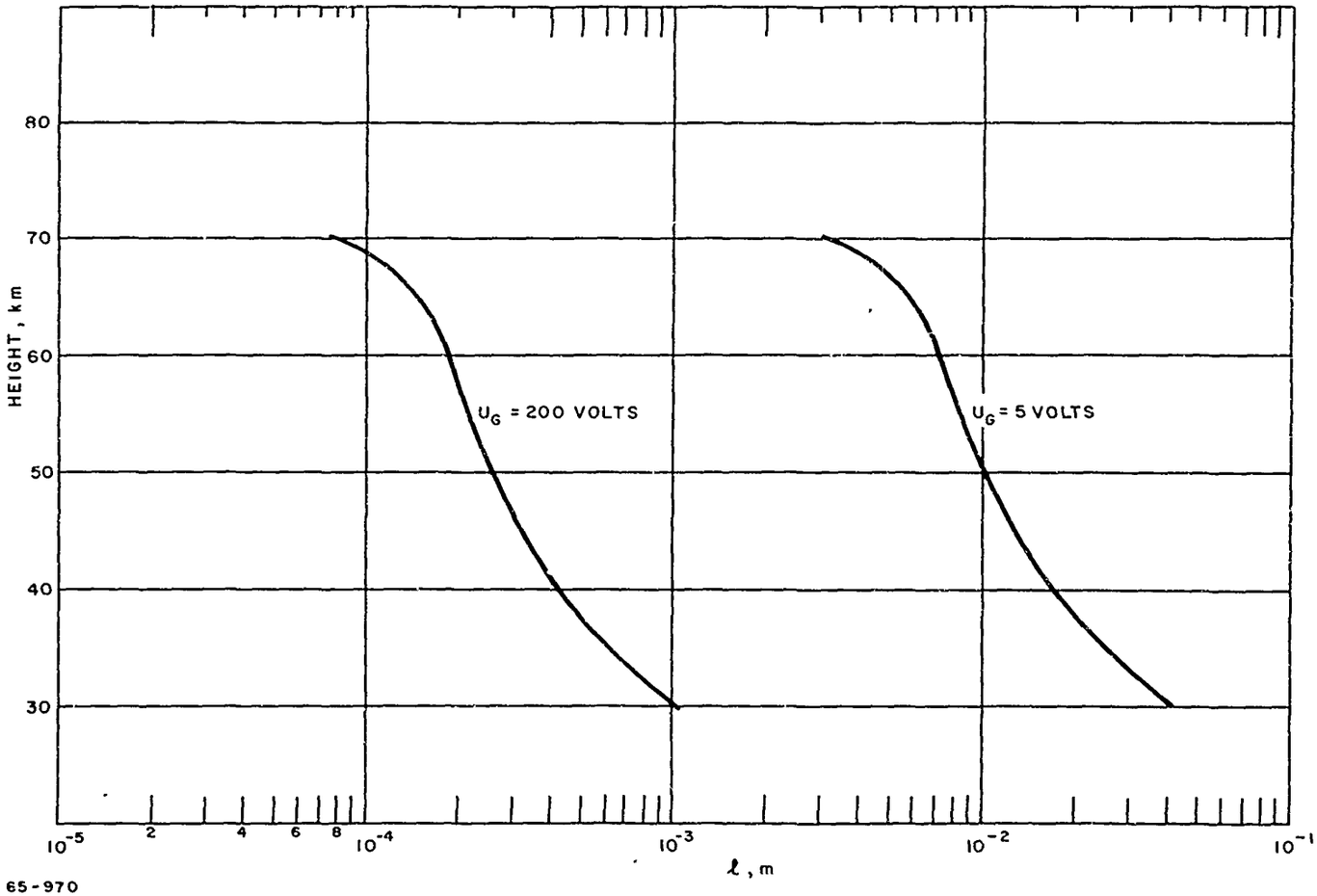

Figure 18 MINIMUM LENGTH OF ION GATE TO SECURE CLOSING EFFECT FOR TWO VALUES OF BARRING VOLTAGE U_G
(Width of ion gate d = 1 cm; mobility values transferred to altitude values according to table 2u2 (section 1.6.4) using the experimental values for falling velocities from PEDERSEN (1964.)

1.4.8 THE LENGTH OF THE RECEIVING ELECTRODES

In the preceding section eq. (92) also determines practically the length Δx of the receiving electrodes. This can be seen from the following consideration:

The opening period for the ion gate r, should only be a small portion of the period T of the driving voltage. Otherwise, the resolution of the measurement would go down and the ion number densities in the lower mobility ranges would be falsified (see section 1.4.1). To keep r small enough, the wind velocity v must be great enough.

On the other hand, we want the ions to be moved by a full period while passing one receiving electrode,

$$\Delta x \geq \frac{2\pi v}{\omega} \tag{93}$$

(compare figure 16 and eq. (84)). If we assume a value T/r of 10, the combination of eqs. (92) and (93) gives approximately:

$$\Delta x \geq \frac{2\pi v}{\omega} \geq 10\, l \tag{94}$$

here the second member on the right hand side of eq. (92) has been neglected.

Eq. (94) is essential for the determination of the overall length of the modified GERDIEN chamber. Lastly, the limits are set by the smallest practical length of ion gate l and the greatest allowable barring field in the gate (see eq. (91)).

1.5 AIR FLOW IN THE GERDIEN CHAMBER

Two characteristics of the air flow inside the GERDIEN chamber may influence the measurement of mobility and conductivity: turbulence and rounded wind profiles. For turbulence, refer to section 1.3.4. The fact, that the air inside the GERDIEN chamber will not have the same velocity at all places in the cross section will be discussed in this chapter.

In a GERDIEN chamber operated by a dc driving voltage, the accurate knowledge of the wind velocities for all radii which are crossed by the moving ion is essential. In the "modified GERDIEN chamber," operated by ac driving voltage, it is sufficient, if a consideration of wind speeds leads to the conclusion, that they do not interfere with the measurement. This is the case if the ion during its vertical motion is not carried past the adequate receiving electrode by too great a wind velocity for some portion of its path.

M. BERNSTEIN (1965) has conducted theoretical investigations on the wind velocity profile for the modified GERDIEN chamber, Model B1. This model will be used, at first, for some dc measurements. It is described in Part 3 of this report. The following presentation reflects the result of BERNSTEIN's investigations.

Neglecting the influence of the "spider legs" (i.e., the four legs at the upstream end of chamber, supporting the sets of rings), the velocity distribution is given by the equation

$$v(r) = \bar{v}\,[B - k(r)^2 + \phi \log r] \tag{95}$$

where the significance of the letters is different from that given in the list of symbols:

$v(r)$ is the limiting flow velocity in the region from r to $r + dr$;*

r is the distance from the axis of the chamber;

$\bar{v}$ is the mean flow velocity in the region;

$$B = 2\,\frac{a^2 \ln a - (a^2 - 1) \ln a\, R_1}{(a^2 + 1) \ln a - (a^2 + 1)}$$

$$k = 2\,\frac{\frac{\ln a}{}}{R_1^2\,(a^2 + 1)\,\ln a - (a^2 + 1}$$

$$\delta = 2\,\frac{a^2 - 1}{(a^2 + 1)\,\ln a - (a^2 + 1)}$$

* "Limiting" flow velocity refers to the "final" velocity distribution which is asymptotically approached when $x \gg d$ (refer to eq. (96)).

$\alpha = R_2/R_1$, the ratio of the outer to the inner radius of a "region," and a "region" is a cylindrical layer within the cylindrical condenser, determined, in a particular case, by two adjacent coaxial rings at the upstream end of the chamber.

Aerodynamic assumptions behind this expression, eq. (95), are that the flow is steady, viscous, and incompressible, and that the entering wind is at a uniform velocity throughout a region.

Comparing the flow in the "regions" as defined above with the simpler case of flow between parallel planes (making the approximation that the flow in the individual regions of the GERDIEN chamber may be considered as a flow between parallel planes ($R_2 - R_1 \ll R_1$)), limiting velocities are shown in figure 19 for seven different regions, defined in caption to figure 19.

From figure 19 it is seen that the flow in the parallel plane case is a good approximation of the flow in the coaxial-cylinder-enclosed regions of the chamber, using the limiting velocity distribution as a criterion. Thus, an analysis of the flow in the parallel-plane case will yield useful information.

To determine the shape of the flow velocity distribution in the parallel-plane case, a parameter ϕ is introduced by

$$\phi = \frac{4 x \nu}{d^2 \bar{v}} \tag{96}$$

where

x is the distance parallel to the velocity vectors, counted from the upstream end of the chamber

ν is the kinematic viscosity of the air,

d is the separation between the parallel planes.

In figure 20 velocity distributions corresponding to several selected values of ϕ are given. For $\phi \geq 0.16$, the flow profile becomes indistinguishable from the limiting velocity distribution.

For region 6, however, information on ϕ is not sufficient to determine the actual velocity distribution; four other factors must also be considered. They are:

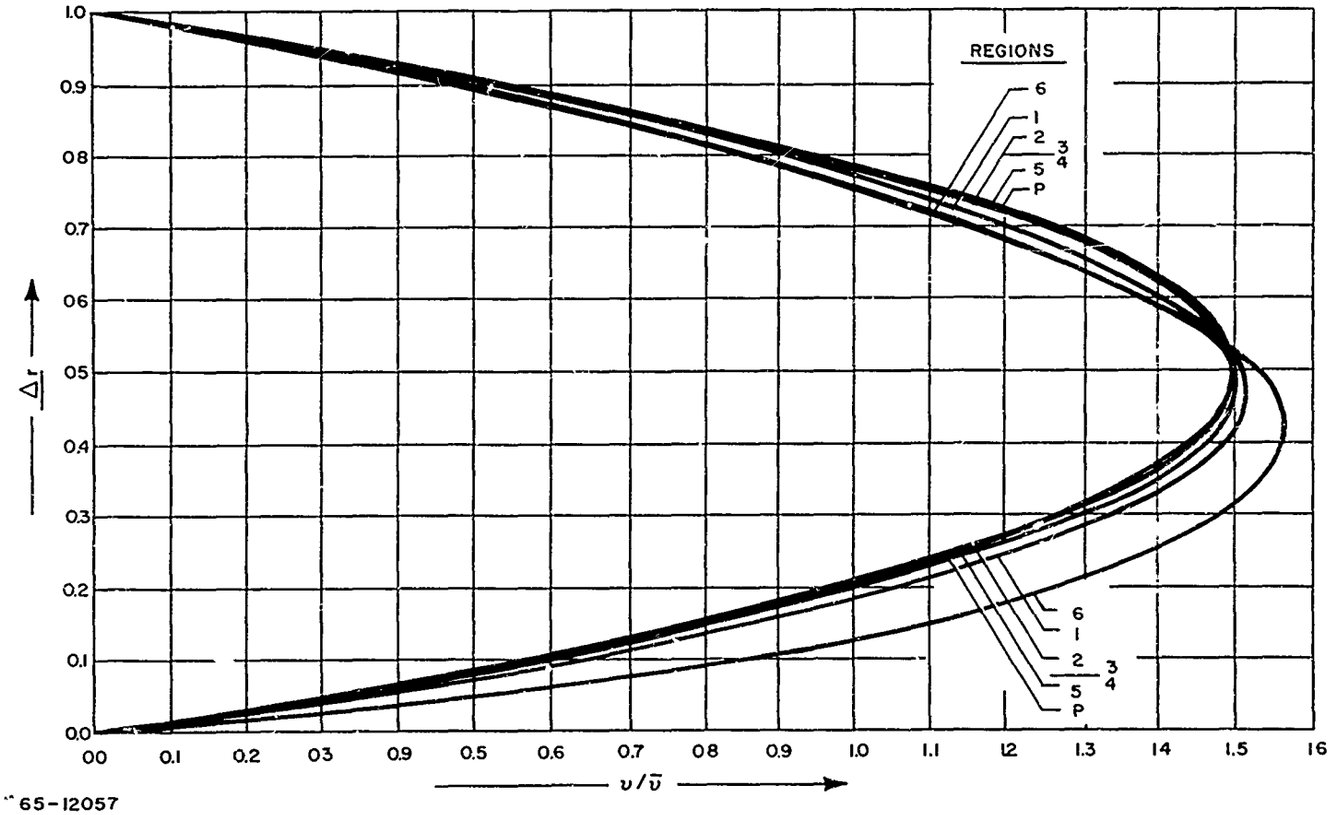

Figure 19 THE RATIO $v/\bar{v}$ FOR THE SIX "REGIONS" OF THE MODEL B1 MODIFIED GERDIEN CHAMBER, AND FOR A PLATE CONDENSER
(See text for definition of regions)

DEFINITION OF REGIONS

Curve No...	graphs the limiting velocity of region	..which is defined by the rings numbered
1	1	01, 11, 21 and 02, 12, 22
2	2	02, 12, 22 and 03, 13, 23
3	3	03, 13, 23 and 04, 14, 24
4	4	04, 14, 24 and 05, 15, 25
5	5	05, 15, 25 and 06, 16, 26
6	6	01, 11, 21 and 06, 16, 26
P	between parallel planes.	

r is the normalized radial separation between the region's boundaries;

$$\frac{r - R_1}{R_2 - R_1} = \Delta r$$

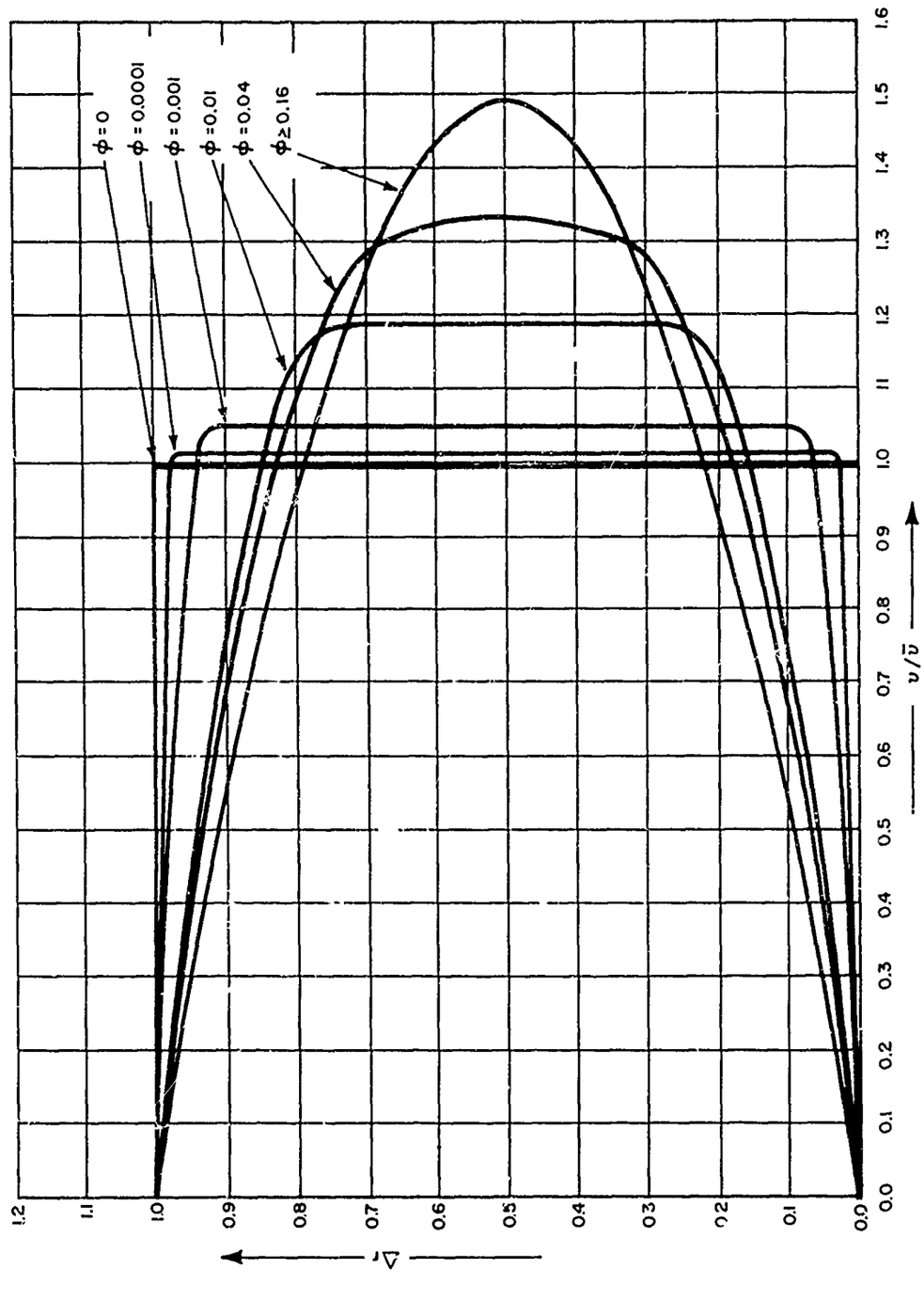

Figure 20 THE RATIO $v/\bar{v}$ FOR DIFFERENT PARAMETERS Φ

(1) that there is actually a difference between the flow velocity distribution in region 6 and the studied parallel-plane case flow velocity distribution; (2) that the velocity profile is decidedly non-uniform at the entrance of region 6; (3) that there are turbulent values from the rings and their supports ("spider legs"); and (4) that the flow may not be laminar in region 6. For a quantitative evaluation of these four factors, knowledge of the actual mean wind velocity $\bar{v}$ in the chamber is necessary. This wind velocity may be found upon considering the requirement that laminar flow must be maintained in region 2 (ion gate) for obvious reasons, together with the desire to increase the mean wind velocity as much as possible. As it is well known, undamped turbulence does not occur, if the REYNOLD'S number

$$Re = \frac{\bar{v}\, d}{\nu} < 1400 \tag{97}$$

For region 2, we may derive, by using $v_2 = 1400 \frac{\nu}{d}$ (98)

and $\bar{v}_2 = v_\infty (A_\infty / A_{ent}) = 1.41\ v_\infty$ (99)

where v_∞ is the falling velocity of the chamber

A_∞ is the area of entering flow far ahead of chamber

A_{ent} is the available area inside the chamber

that the maximum allowable falling velocity is

$$(v_\infty)_{max} = 1.00 \times 10^5 \times \nu\ . \tag{100}$$

Kinematic viscosity is given for the altitude h in km by

$$\nu = 10^{(0.0694\, h - 5.17)}\ m^2/sec\ . \tag{101}$$

Thus we arrive at a value of

$$v_\infty = 10^{(0.0336\, h + 0.211)}\ m/sec\ * \tag{102}$$

From this value for v_∞ the parameter $\bar{v}$ and the parameter ϕ can be calculated, for each region, and for any altitude between 10 and 40 km. This has been done, and the result is communicated in the following table:

* It should be remembered, however, that laminar flow may still exist, if Re > 1400. This should be tested experimentally in the wind tunnel. For our theoretical consideration, we stay at values of Re < 1400.

PARAMETER FOR REGIONS 1 TO 5 IN DIFFERENT HEIGHTS

(Calculated for the downstream end of each region between adjacent rings (exit from rings into chamber proper))

h in km	Parameter ϕ for Region No.					Values to be multiplied with
	1	2	3	4	5	
10	4.7	6.0	6.3	6.0	3.8	$\times 10^{-2}$
15	6.1	8.6	9.0	8.6	3.4	$\times 10^{-2}$
20	9.9	13.0	13.0	13.0	7.9	$\times 10^{-2}$
25	1.5	1.6	1.6	1.6	1.2	$\times 10^{-1}$
30	1.6	1.6	1.6	1.6	1.2	$\times 10^{-1}$
35	1.6	1.6	1.6	1.6	1.2	$\times 10^{-1}$
40	1.6	1.6	1.6	1.6	1.2	$\times 10^{-1}$

At the exits from the rings into the chamber proper, the velocity distributions in region 1 to 5 begin to influence the ion trajectories in region 6. Figure 21 is a plot of the parameter ϕ for different altitudes; here x is the distance measured from the end of regions 1 to 5 or the beginning of region 6.

From the knowledge of parameter ϕ, velocity distributions in regions 1 to 5 can be derived, and a first approximation to the velocity distribution in region 6 can be found, applying the information from figures 19 and 20. The average velocity in region 6 is given by

$$\bar{v}_{(6)} = 1.15\ v_{\infty} \quad .$$

For a better approximation to the velocity distribution in region 6, the other three factors, as listed above, may be studied. It can be shown that the non-uniformity of the entrance profile at the upstream end of region 6 is absorbed in about 0.1 meter, and that the difference between flow velocity inside the wake and outside of it is not more than 0.5 m/sec. Furthermore it can be shown, by application of the REYNOLD'S number criterion, that a fully developed turbulence in region 6 cannot occur if $h > 26$ km . Since no perturbation mechanism seems to be present in region 6, it is entirely possible that the flow will never become a fully turbulent flow. However, even if it does, velocity distributions could be calculated.

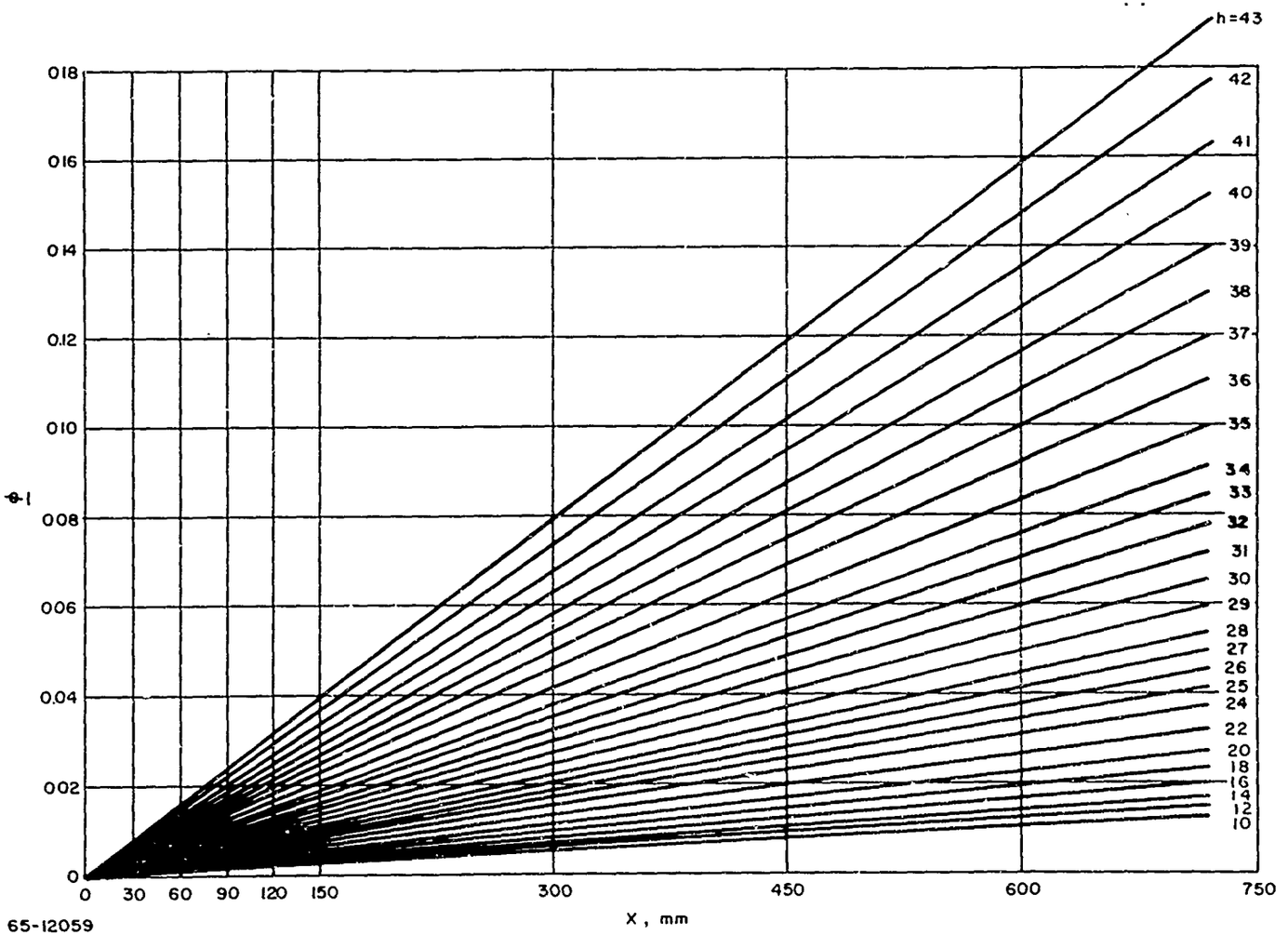

Figure 21 PARAMETER Φ AS A FUNCTION OF LENGTH x FOR ALTITUDES FROM 10 TO 43 km

For the genuine modified GERDIEN chamber with ac operation, this discussion on the air flow inside the chamber for a given falling speed is sufficient. However, if the chamber will be used in a dc operation, a more detailed discussion for region 6 may be required. This discussion can at best be conducted, if the motion of the ions under the influence of the electric field is considered. This would then be a special case for the dc operation, and will not be reported here.

1.6 EXPECTED ENVIRONMENTAL CONDITIONS FOR ION MEASUREMENTS IN THE TERRESTRIAL STRATOSPHERE AND MESOSPHERE

1.6.1 INTRODUCTION

It has often been said, that the range between 30 and 80 km is the least known one in the terrestrial atmosphere. Nevertheless, for the design of any instrument which is to make measurements in this range, some theoretical or observed values must be assumed. To create a basis for out discussion, we have compiled such values from other publications. Since this was done a few years ago, some more reliable or accurate values have been published. In this respect, we refer, above all, to the paper of COLE and PIERCE (1965). While the more accurate values are presently being used for the improvement of our design and will be used later on, the earlier tables still are valuable for any first approximation. For this reason, they are printed unchanged in the following sections 1.6.3 and 1.6.4.

1.6.2 REMARK ON THE MEAN FREE PATH

Table 104 in section 1.6.3 communicates two sets of values for the mean free path of neutral particles. For some of our later discussions, approximate data on the actual free paths--in particular, data on the occurrences of free paths longer than the mean one--is important. Therefore, in figures 22 and 23, the percentage of free paths longer than the mean ones are presented, calculated by use of MAXWELL's velocity distribution function, for the two sets of values in table 104.

Of course, the free path for ions is different from the path for neutral particles. For a recent discussion refer to SIKSNA 1964.

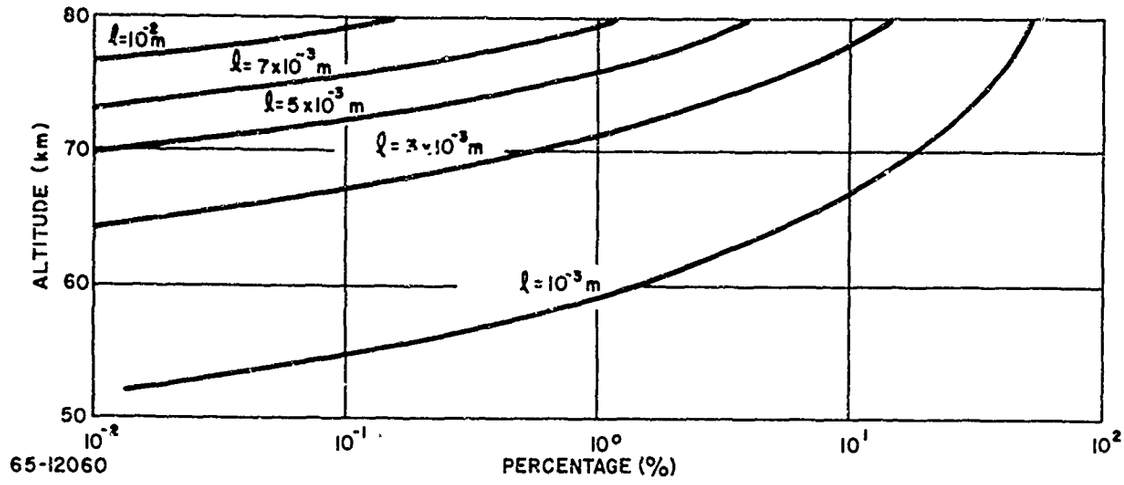

Figure 22 PERCENTAGE OF NEUTRAL PARTICLES IN THE ATMOSPHERE, WHOSE FREE PATH IS LONGER THAN l

(The results are obtained by using the mean free path values from the first column of table 104.)

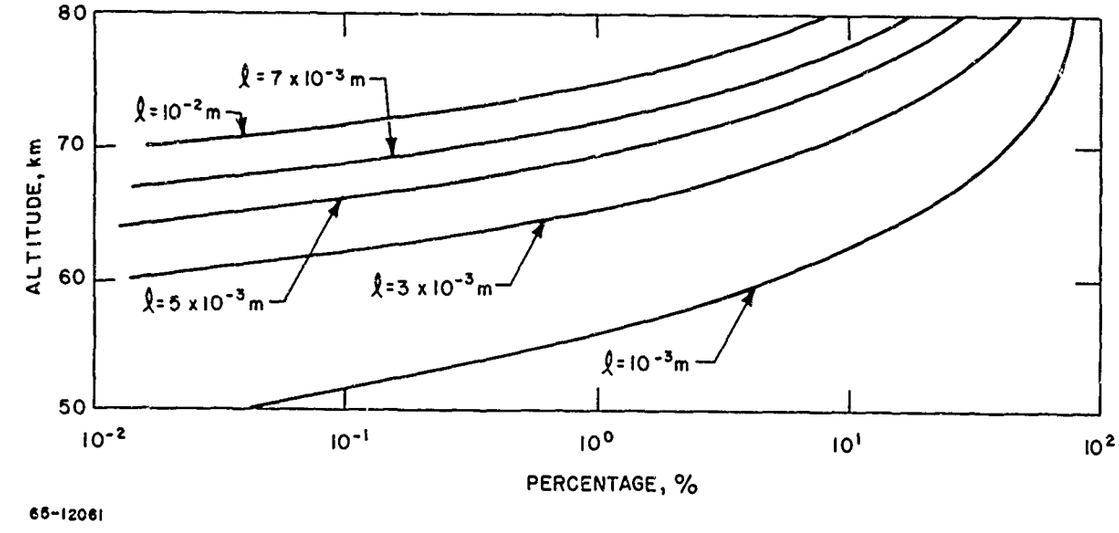

Figure 23 PERCENTAGE OF NEUTRAL PARTICLES IN THE ATMOSPHERE, WHOSE FREE PATH IS LONGER THAN l

(The results are obtained by using the mean free path values from the second column of table 104.)

101 TEMPERATURE

h [km]	T [°K]	T/To [-]	To/T [-]	$(To/T)^{2.35}$ [-]
0	288	1	1	1
10	223	0.775	1.29	1.819
20	217	0.755	1.325	1.937
30	231	0.803	1.246	1.683
40	261	0.906	1.103	1.259
50	283	0.984	1.018	1.044
60	245	0.850	1.175	1.461
70	173	0.602	1.669	3.314
80	168	0.584	1.712	3.538

The T-values are taken from:
F.S. JOHNSON, Satellite Environment Handbook
Stanford University Press
Stanford, California, 1961
Page 20

102 AIR DENSITY

h [km]	ρ [kg/m³]	ρ_o/ρ [-]	$(\rho_o/\rho)^3$ [-]	ρ/ρ_o [-]
0	1.22x10⁰	1	1	1
10	4.1 x10⁻¹	2.98x10⁰	2.05x10¹	3.35x10⁻¹
20	8.9 x10⁻²	1.37x10¹	2.57x10³	7.30x10⁻²
30	1.17x10⁻²	1.04x10²	1.14x10⁶	9.60x10⁻³
40	4.0 x10⁻³	3.05x10²	2.85x10⁷	3.78x10⁻³
50	1.08x10⁻³	1.13x10³	1.46x10⁹	8.85x10⁻⁴
60	3.7 x10⁻⁴	3.29x10³	3.56x10¹⁰	3.11x10⁻⁴
70	9.4 x10⁻⁵	1.30x10⁴	2.70x10¹²	7.70x10⁻⁵
80	1.38x10⁻⁵	8.97x10⁴	7.70x10¹⁴	1.12x10⁻⁵

The ρ-values are take from:
F.S. JOHNSON, Satellite Environment Handbook
Stanford University Press
Stanford, California, 1961
Page 20

103 ATMOSPHERIC PRESSURE

h [km]	P [kg m^{-1} sec^{-2}]	P [mb]	Po/P [-]	P/Po [-]	$(P/Po)^{0.3}$ [-]
0	1.01×10^{5}	1.01×10^{3}	1	1	1
10	2.65×10^{4}	2.65×10^{2}	3.82×10^{0}	2.68×10^{-1}	6.736×10^{-1}
20	5.5×10^{3}	5.5×10^{1}	1.836×10^{1}	5.45×10^{-2}	4.177×10^{-1}
30	1.19×10^{3}	1.19×10^{1}	8.47×10^{1}	1.18×10^{-2}	2.640×10^{-1}
40	3.0×10^{2}	3.0×10^{0}	3.36×10^{2}	2.975×10^{-3}	1.747×10^{-1}
50	9.0×10^{1}	9.0×10^{-1}	1.12×10^{3}	8.94×10^{-4}	1.217×10^{-1}
60	2.55×10^{1}	2.55×10^{-1}	3.956×10^{3}	2.53×10^{-4}	8.325×10^{-2}
70	4.7×10^{0}	4.7×10^{-2}	2.243×10^{4}	4.45×10^{-5}	4.982×10^{-2}
80	6.6×10^{-1}	6.6×10^{-3}	1.528×10^{5}	6.55×10^{-6}	2.785×10^{-2}

kg m^{-1} sec^{-2} = N m^{-1}

The P-values are taken from:
F.S. JOHNSON, Satellite Environment Handbook
Stanford University Press
Stanford, California, 1961
Page 20

104 MEAN FREE PATH OF NEUTRAL PARTICLES

h [km]	λ [m] WARFIELD	λ [m] PENNDORF
0	--	--
10	--	--
20	1.02×10^{-6}	1.3×10^{-6}
30	4.8×10^{-6}	6.4×10^{-6}
40	2.5×10^{-5}	3.9×10^{-5}
50	9.1×10^{-5}	1.3×10^{-6}
60	2.4×10^{-4}	3.5×10^{-4}
70	5.6×10^{-4}	1.2×10^{-3}
80	1.6×10^{-3}	4.3×10^{-3}

The λ-values are taken from:

C. N. WARFIELD, NACA Techn. Note 1200 (1947)
R. PENNDORF, Meteor. Zs. 58 (1941) 103

105 PARTICLE VELOCITY

h [km]	v [m/sec]
0	--
10	4.38×10^2
20	4.32×10^2
30	4.33×10^2
40	4.76×10^2
50	5.27×10^2
60	4.94×10^2
70	4.58×10^2
80	4.18×10^2

The v -values are taken from:

. PEHLDORF, Meteor. Z. 58, (1941, 103

106 NUMBERS OF PARTICLES

h [km]	[m^{-3}]
0	2.5×10^{25}
10	8.6×10^{24}
20	1.85×10^{24}
30	3.7×10^{23}
40	8.3×10^{22}
50	2.3×10^{22}
60	7.53×10^{21}
70	1.9×10^{21}
80	2.0×10^{20}

The N-values are taken from:
F.S. JOHNSON, Satellite Environment Handbook
Stanford University Press
Stanford, California, 1961
Page 20

107 C O L L I S I O N S P E R V O L U M E - U N I T

$\left[\frac{h}{km}\right]$	$\left[m^{-3}\ \nu\ sec^{-1}\right]$
0	--
10	5.6×10^{33}
20	3.0×10^{32}
30	1.2×10^{31}
40	3.7×10^{29}
50	3.7×10^{28}
60	5.0×10^{27}
70	4.6×10^{26}
80	2.8×10^{25}

The ν-values are taken from:

R. PENNDORF, Meteor. Zs. 58 (1941) 103

108 C O L L I S I O N S P E R P A R T I C L E

$\left[\frac{h}{km}\right]$	$\left[sec^{-1}\right]$
0	--
10	7.6×10^{8}
20	1.7×10^{8}
30	3.2×10^{7}
40	6.0×10^{6}
50	2.0×10^{6}
60	7.4×10^{5}
70	2.2×10^{5}
80	4.8×10^{4}

The ν'-values are calculated after

$$\nu' = \frac{\nu}{N}$$

using the figures of tables 106 and 107.

109 KINEMATIC VISCOSITY

h [km]	η [m^2/sec]
0	--
10	--
20	--
30	7.5×10^{-2}
40	4.8×10^{-1}
50	2.2×10^{0}
60	5.6×10^{0}
70	1.1×10^{1}
80	2.8×10^{1}

The η-values are taken from:

C.N. WARFIELD, NACA Techn. Note 1200 (1947)

110 TEMPERATURE 'GRADIENT'

h [km]	dT/dh [$^{o}K/m$]
0	--
10	-0.8×10^{-2}
20	$+0.4 \times 10^{-2}$
30	$+1.9 \times 10^{-2}$
40	$+3.0 \times 10^{-2}$
50	$\pm 0 \times 10^{-2}$
60	-6.0×10^{-2}
70	-1.1×10^{-2}
80	-0.6×10^{-2}

Extreme values:

55	$+3.2 \times 10^{-2}$
65	-8.1×10^{-2}

The dT/dh-values are graphically destined using the T-values of table 101

111 UPPER AIR WINDS
EAST-WEST COMPONENTS

h [km]	v_w [m/sec] East		West	
0	--	--	--	--
10	--	--	--	--
20	10(1);	8(2)	--	--
30	18(1);	9(2)	--	--
40	32(1);	7(2)	--	--
50	42(1);	--	--	9(2)
60	48(1);	--	--	16(2)
70	45(1);	6(2)	--	--
80	120(3);		80(3)	

Remarks: (1) average values for June, July, August
(2) average values for September
(3) extreme single values

The v_w-values are taken from:
AUFM KAMPE, SMITH, and BROWN; Journ. Geophys, Res., 67 (1962) 4243.

112 UPPER AIR WINDS
NORTH-SOUTH COMPONENTS

h [km]	v_w [m/sec] North	South
0		
10		
20	3 (1)	--
30	1.5(1)	--
40	1 (1)	--
50	5 (1)	--
60	5 (1)	--
70	up to 20(2)	25(3)
80	25 (3)	65(3)

Remarks: (1) average velocities for June, July, August, September
(2) the same, however, large distribution
(3) individual maximal values

The v_w-values are taken from:
AUFM KAMPE, SMITH, and BROWN; Journ. Geophys. Res., 67 (1962) 4243.

113 RELATIVE TEMPERATURE AND RELATIVE PRESSURE

h [km]	$\frac{P_o}{P} \times \frac{T}{T_o}$ [-]	$(\frac{P_o}{P})(\frac{T_o}{T})^{2.35}$ [-]	$(\frac{P_o}{P})^{0.3}(\frac{T_o}{T})^{2.35}$ [-]
0	1	1	1
10	2.96×10^{0}	4.875×10^{-1}	1.225
20	1.38×10^{1}	1.056×10^{-1}	8.091×10^{-1}
30	6.80×10^{1}	1.986×10^{-2}	4.443×10^{-1}
40	3.05×10^{2}	3.752×10^{-3}	2.199×10^{-1}
50	1.10×10^{3}	9.333×10^{-4}	1.270×10^{-1}
60	3.36×10^{3}	3.696×10^{-4}	1.216×10^{-1}
70	1.35×10^{4}	1.475×10^{-4}	1.651×10^{-1}
80	8.9×10^{4}	2.317×10^{-5}	9.853×10^{-2}

These values are calculated from the values of tables 101 and 103

201 IONIZATION RATE

h [km]	q [m^{-3} sec^{-1}]
0	--
10	4.36×10^{7}
20	1.87×10^{7}
30	2.63×10^{6}
40	4.40×10^{5}
50	1.17×10^{5}
60	3.67×10^{4}
70	9.12×10^{3}
80	1.38×10^{3}

q = number of ion pairs generated per cubic meter and second by cosmic radiation

The q-values are calculated after

$$q = q_o \frac{p\,T_o}{p_o T}$$

using the $\frac{p\,T_o}{p_o T}$ -values of table 113. The q_o-values are taken from GANGNES, JENKINS, and VAN ALLEN (Phys. Rev. 75, 1949, 57-69), using the number of 5.6 ions/cm^3 per count/sec, as proposed by BOURDEAU, WHIPPLE, and CLARK (Journ. Geoph. Res. 64, 1959, 1363-1370)

202 MOBILITY OF IONS

h [km]	k [$m^2/(V \cdot sec)$]
0	1.5×10^{-4}
10	4.44×10^{-4}
20	2.07×10^{-3}
30	1.02×10^{-2}
40	4.58×10^{-2}
50	1.65×10^{-1}
60	5.04×10^{-1}
70	2.025×10^{0}
80	1.335×10^{1}

The k-values are calculated after

$$k = k_o \frac{p_o T}{p\,T_o}$$

using the $\frac{p_o T}{p T_o}$ values of table 113 and starting with $k_o = 1.5 \times 10^{-4}$ $m^2/(V \cdot sec)$.

203 NUMBERS OF IONS

h [km]	$[n\ m^{-3}]$ $\alpha = \alpha_0 (p/p_0)$	$\alpha = \alpha_0 (p/p_0)^{0.3}$
0	--	--
10	7.50×10^9	4.71×10^9
20	3.33×10^9	3.81×10^9
30	9.10×10^9	1.92×10^9
40	8.57×10^9	1.12×10^9
50	8.86×10^9	7.60×10^8
60	7.97×10^9	4.34×10^8
70	6.22×10^9	1.86×10^8
80	1.93×10^9	9.35×10^7

The n-values are calculated after

$$n = \sqrt{q/\alpha}$$

using the q-values of table 201 and the two sets of α-values of table 205.

204 DISTANCES BETWEEN IONS

h [km]	$[d_i\ m]$ $\alpha = \alpha_0 (p/p_0)$	$\alpha = \alpha_0 (p/p_0)^{0.3}$
0	--	--
10	4.05×10^{-4}	4.74×10^{-4}
20	5.32×10^{-4}	5.08×10^{-4}
30	3.80×10^{-4}	6.37×10^{-4}
40	3.91×10^{-4}	7.63×10^{-4}
50	3.83×10^{-4}	8.70×10^{-4}
60	3.98×10^{-4}	1.05×10^{-3}
70	4.31×10^{-4}	1.29×10^{-3}
80	2.96×10^{-4}	1.75×10^{-3}

The d_i-values are calculated after

$$d_i = \frac{1}{\sqrt[3]{2n}}$$

using the two sets of n-values of table 203. d_i, accordingly, is the average distance between ions without considering the signs of the ions.

205 RECOMBINATION COEFFICIENTS BETWEEN IONS

h [km]	$\alpha = \alpha_0 (p/p_0)$	$\alpha = \alpha_0 (p/p_0)^{0.3}$
	α [m^3/sec]	
0	1.60×10^{-12}	1.60×10^{-12}
10	7.80×10^{-13}	1.96×10^{-12}
20	1.69×10^{-13}	1.29×10^{-12}
30	3.18×10^{-14}	7.11×10^{-13}
40	6.00×10^{-15}	3.52×10^{-13}
50	1.49×10^{-15}	2.03×10^{-13}
60	5.91×10^{-16}	1.95×10^{-13}
70	2.36×10^{-16}	2.64×10^{-13}
80	3.71×10^{-17}	1.58×10^{-13}

The α-values are calculated after

$$\alpha = \alpha_0 (p/p_0)^x (T_0/T)^{2.35}$$

with x = 1 and x = 0.3, according to the discussion by H. Israël, Atmosphärische Elektrizitat, I, p. 133/134, based on experimental values of "Explorer II". The p/p_0 and T_0/T values are taken from table 113. α_0 is supposed to be 1.6×10^{-12} m^3 sec^{-1}.

206 FIELD STRENGTH

h [km]	E [V/m]
0	--
10	2.83×10^{0}
20	1.36×10^{0}
30	1.01×10^{-1}
40	2.38×10^{-2}
50	6.43×10^{-3}
60	2.34×10^{-3}
70	7.45×10^{-4}
80	3.53×10^{-5}

REMARK: These E-values seem to be about one order of magnitude smaller than most measured values at altitudes of 10 and 20km. If we take column A of table 207 the coincidence is better. The E-values are calculated after Olm's Law

$$E = i/\Lambda$$

using $i = 3 \times 10^{-12}$ A m^{-2} and the Λ-values of column "F" of table 207.

h [km]	Column A	B	C	D	E	F
	Λ [cm^{-1} m^{-1}]					
0	--	--	--	--	--	--
10	2.4×10^{-13}	--	--	--	1.2×10^{-12}	1.0×10^{-12}
20	1.5×10^{-12}	--	3.5×10^{-12}	3.0×10^{-11}	8.9×10^{-12}	2.21×10^{-12}
30	6.8×10^{-12}	--	8.0×10^{-12}	5.0×10^{-10}	3.8×10^{-11}	2.97×10^{-11}
40	--	6.1×10^{-11}	2.5×10^{-11}	5.0×10^{-9}	1.7×10^{-10}	1.26×10^{-10}
50	--	2.0×10^{-10}	3.5×10^{-11}	4.5×10^{-8}	6.4×10^{-10}	4.07×10^{-10}
60	--	6.0×10^{-10}	6.0×10^{-11}	2.5×10^{-7}	1.0×10^{-9}	1.28×10^{-9}
70	--	2.5×10^{-9}	1.0×10^{-10}	1.3×10^{-6}	3.3×10^{-9}	4.03×10^{-9}
80	--	1.0×10^{-8}	2.0×10^{-10}	9.8×10^{-6}	2.0×10^{-8}	8.5×10^{-8}

Remark: The values of the columns A,B,C,D,E are not based on the values of the tables 101, 103, 201, 202, and 205; however, the values of column F are.

The Λ-values are taken from:

Column A: CORONITI et al., 1954, AFCRC-TR-54-206
" B: BOURDEAU, WHIPPLE, AND CLARK 1959
" C:
" D: } ISRAËL and KASEMIR, 1949 { without electrons, $(\phi/p)^{0.3}$ = const.; with electrons, (ϕ/p) = const.
" E: } { without electrons, (ϕ/p) = const.
" F: calculated after $\Lambda = 2$ ekn, using the k-values of table 202 and the n-values of table 203, colum. $\phi = \phi(p/p_o)$; and $e = 1.6\times10^{-19}$ A sec.

h [km]	D [m^2/sec]
0	--
10	8.54×10^{-6}
20	3.87×10^{-5}
30	2.03×10^{-4}
40	1.03×10^{-3}
50	4.03×10^{-3}
60	1.06×10^{-2}
70	1.83×10^{-2}
80	1.93×10^{-1}

The D-values are calculated after

$$D = \frac{k\,kT}{e}$$

where $k = 1.38\times10^{-23}$ W·sec·degr^{-1} is the BOLTZMANN-constant, and $e = 1.6\times10^{-19}$ A·sec the elementary charge. The values of k (mobility) and T (temperature) are taken from tables 202 and 101, respectively.

209

ION FLUX DUE TO DIFFUSION

h [km]	$\lvert\vec{Z}\rvert$ [$m^{-2}\,sec^{-1}$] d = 1cm	d = 1mm
0	- +	--
10	0.4×10^{6}	0.4×10^{7}
20	1.27×10^{7}	1.27×10^{8}
30	1.85×10^{8}	1.85×10^{9}
40	8.85×10^{8}	8.85×10^{9}
50	3.57×10^{9}	3.57×10^{10}
60	8.45×10^{9}	8.45×10^{10}
70	1.14×10^{10}	1.14×10^{11}
80	3.72×10^{10}	3.72×10^{11}

The $\lvert\vec{Z}\rvert$-values are calculated after

$$\vec{Z} = -D \cdot \operatorname{grad} n, \text{ and,}$$

by making some simplifications:

$$\lvert\vec{Z}\rvert = D \cdot \frac{\Delta n}{d} = D \cdot \frac{n}{d}.$$

Thus, it is assumed, that the concentration of particles at one end of d is n, and at the other end is and stays zero. The n- and D-values are taken from tables 203 and 208, respectively.

210

RELATIVE ION FLUX DUE TO DIFFUSION

h [km]	$\lvert\vec{Z}\rvert/n$ [m/sec] d = 1cm	d = 1mm
0	--	--
10	8.54×10^{-4}	8.54×10^{-3}
20	3.87×10^{-3}	3.87×10^{-2}
30	2.03×10^{-2}	2.03×10^{-1}
40	1.03×10^{-1}	1.03×10^{0}
50	4.03×10^{-1}	4.03×10^{0}
60	1.06×10^{0}	1.06×10^{1}
70	1.83×10^{0}	1.83×10^{1}
80	1.93×10^{1}	1.93×10^{2}

The $\lvert\vec{Z}\rvert/n$-values give a measure which portion of ions disappear under the pre-assumption of table 209. It is

$$\lvert\vec{Z}\rvert/n = D/d;$$

the D-values are taken from table 208.

21. CRITICAL FIELD PRESSURE

h [km]	E/p [(V/cm)/(mm Hg)]	E/p [(V/cm mb)]
0	--	--
10	1.42	1.07×10^{-2}
20	3.40	2.48×10^{-2}
30	1.20	8.42×10^{-3}
40	1.08	7.94×10^{-3}
50	0.99	7.14×10^{-3}
60	1.30	9.20×10^{-3}
70	2.26	1.59×10^{-2}
80	0.77	5.35×10^{-3}

Remarks: It is not astonishing that the E/p - values are almost constant. Introducing the original values, from which E was calculated, we obtain:

$$E = \frac{1}{2e\varepsilon_0}\ \sqrt{\frac{\beta\alpha_0}{q_0}}\ \frac{q_0^{1.68}}{p_0}\ \frac{p}{T^{1.68}}$$

in which only q_0, T and p vary with altitude. The variation of q_0 and T remains in the same order of magnitude; consequently, the variation of p, being extended over six orders of magnitude, is the essential factor. Thus, E/p varies only relatively little.

The values for E and p were taken from tables 206 and 103, respectively.

Exceptionally, other dimensions are used for the first column, enabling an easier comparison with the textbooks on gaseous electronics.

22. ARTIFICIAL IONIZATION

A 20 mc-alpha source will yield:

h [km]	q' [$m^{-3} sec^{-1}$]	n' [m^{-3}]	n'' [m^{-3}]
0	--	--	--
10	2.20×10^{15}	7.30×10^{12}	5.4×10^{12}
20	2.39×10^{11}	1.94×10^{12}	1.48×10^{12}
30	5.31×10^{8}	1.08×10^{11}	2.80×10^{11}
40	2.12×10^{7}	6.67×10^{10}	5.99×10^{10}
50	4.14×10^{5}	1.70×10^{10}	1.07×10^{10}
60	1.70×10^{4}	6.48×10^{9}	5.35×10^{9}
70	2.75×10^{2}	1.96×10^{9}	1.08×10^{9}
80	8.41×10^{-1}	2.83×10^{8}	1.50×10^{8}

The n'- and n''-values are calculated after $n' = \sqrt{q'/\beta'}$ and $n'' = q'/\beta'$. Here, $\beta' = \beta_0 (p/p_0)$, in other words, for the case of pressure simulation and no temperature simulation. $\beta = \beta_0 (p/p_0)(T_0/T)^{2.35}$, i.e. for pressure and temperature simulation, is taken from table 20), the p/p_0-values from table 103. $\beta_0 = 1.0\times10^{-12}\ m^3\ sec^{-1}$.

The q'-values are calculated after $q' = q_0' (\varrho/\varrho_0)^3$, where $(\varrho_0/\varrho)^3$ is taken from table 102. q_0' is the number of ion pairs per cubic metre, created by a 20 mc Ionotron-Foil (20 mg Ra). The foil emits 7.5×10^5 α-rays per second which make 10^7 ion pairs in a sphere of $1.05\times10^{-4}\ m^3$. This give $q_0' = 0.05\times10^{14}$ ion pairs per cubic meter.

Here, it is assumed, that the space under consideration is evenly filled with the ionization caused by the α-rays. Of course, the application of the formula $n = \sqrt{q/\beta}$ to this problem is only a very rough approximation. This formula is derived for a volume with equilibrium of ionization and recombination. The air under consideration here is, however, only for a short time exposed to α-radiation.

213 RELATIVE ARTIFICIAL IONIZATION

as provided by a 20 μc - Alpha Source.

h [km]	q/q' [-]	n/n' [-]	n/n'' [-]
0	--	--	--
10	1.91×10^{-6}	1.02×10^{-3}	1.38×10^{-3}
20	7.95×10^{-5}	2.03×10^{-3}	2.82×10^{-3}
30	4.95×10^{-3}	5.41×10^{-2}	3.25×10^{-2}
40	2.08×10^{-2}	1.28×10^{-1}	1.44×10^{-1}
50	2.84×10^{-1}	5.21×10^{-1}	5.31×10^{-1}
60	2.16×10^{0}	1.23×10^{0}	1.49×10^{0}
70	3.31×10^{1}	3.27×10^{0}	5.75×10^{0}
80	1.64×10^{4}	6.82×10^{1}	1.29×10^{2}

The q- and n-values are taken from tables 201 and 203 (first column), respectively. The q'-, n'-, and n''-values are taken from table 212.

214 RELATIVE ION DENSITY

h [km]	n / N [-]
0	--
10	8.7×10^{-16}
20	1.8×10^{-15}
30	2.5×10^{-14}
40	1.0×10^{-13}
50	3.8×10^{-13}
60	1.1×10^{-12}
70	3.2×10^{-12}
80	6.8×10^{-12}

The values for n and N are taken from tables 203 and 105. The values for n are from the first column of table 203. With the second column of 203, the n/N values are up to about one order of magnitude smaller.

1.7 LIMITATIONS FOR THE MEASUREMENT OF IONIC MOBILITY IN THE UPPER ATMOSPHERE

1.7.1 INTRODUCTION

When discussing the characteristics of atmospheric ions and the definition of ionic mobility in the earlier chapters, we have also laid the foundation for a discussion of some of the facts which determine the limits of the applicability of these definitions. When ascending in the atmosphere, the free paths of the atmospheric constituents increase, the number of collisions between the particles decreases, and parameters which involve a great number of collisions become more and more inapplicable.

This gradual changeover is of great theoretical and practical interest. The focal point is given by the problem of ontology--"how far up" we still can use the denomination mobility. At an altitude of about 80 km, the mean free paths become so long, that it becomes unfeasible to construct instruments which could measure mobility. Thus, we cannot measure it any more; but for a larger scale treatment of atmospheric processes; the parameter mobility may still be applicable. Still higher up, this possibility also ceases. In this transition region, the application of denomination, such as mobility and conductivity, must be done with caution, and it is an open question as to how far out this may still be tolerated.

The different aspects of mobility and the different problems of measuring it get into these difficulties at different heights. For this reason, we have to discuss these changeovers if we want to establish safe limits for the application of our measuring method. On the other hand, some of the difficulties of the measurement of ionic mobilities and conductivities existing in the lower atmosphere (see section 1.3.4) become less difficult in the upper atmosphere. This is so, for example, for the problem of laminary and turbulent flow inside a GERDIEN chamber. In a more rarefied atmosphere, the REYNOLD's numbers are such that laminary flow is always ascertained. Other difficulties change their nature, such as the problems provided by the diffusion.

1.7.2 DIFFUSION

In the modified GERDIEN chamber, diffusion effects provide disturbances at two locations: in the "ion gate" and in the chamber itself. In the ion gate, no electric field exists while the ions pass through. There will be a loss of ions to the rather closely situated walls. Inside the chamber, diffusion effects will tend to broaden the ion path and thus create a loss in resolution, and some ion loss to the electrodes where the ion path approaches them closely.

Three different types of diffusion have to be considered:

1. Gas kinetic diffusion, governed by the "diffusion coefficient, D, and the gradient of ion density, grad n

2. "Electric diffusion" caused by the mirror-charge effect attracting ions to walls and electrodes

3. "Eddy diffusion" due to turbulent flow of the air containing ions by which a much greater number of ions is put into locations, where great density gradients cause them to follow diffusion.

The diffusion coefficient is related to the mobility of the ions according to EINSTEIN's law, which we write in the form

$$D = k \frac{k_B T}{e} \tag{103}$$

where

D = diffusion coefficient of FICK's Law in $m^2\ sec^{-1}$

k = ion mobility in $m^2\ V^{-1}\ sec^{-1}$

k = BOLTZMANN constant, 1.4×10^{-23} Wsec degree^{-1}

T = temperature in degrees KELVIN

e = elementary charge, 1.6×10^{-19} Coulomb.

Values for D, calculated according to eq. (103), are listed in table 208 in section 1.6.4.

In the same section, in tables 209 and.210, some other parameters are derived from D, namely, flux numbers and relative flux numbers. These relative flux numbers give the ratio of ions removed due to diffusion out of an ion stream under certain ion number density gradients. In fact, table 210 gives a removal velocity, and this velocity can be compared with the wind velocity in the modified GERDIEN chamber for a first approximation to the measuring errors caused by diffusion. This statement is based on the fact that the walls represent absolute ion sinks, all ions touching the wall are lost, they deposit their electric charge and turn to neutral molecules. In fact, it is not even necessary for them to touch the wall, since mirror-charge become very great when the ions approach closely; they are practically lost as soon as they achieve a certain approach. While, in principle, this method for an estimation of ion losses due to diffusion (to walls as well as the broadening of an ion trail in an otherwise neutral gaseous environment) is certainly a correct* one, it is difficult to apply it

* Within the vaguely defined limits of FICK's diffusion laws.

for a more accurate consideration, since the definition of ion density gradients becomes difficult.

Before dealing with another approach, we want to use the numbers of table 210 of section 1.6.4., and other similarly derived numbers for a first approximation.

We see from table 210 that in an altitude of 80 km the ion removal velocity for ions in the first millimeter is about half the speed of sound. However, at the other end of the table, the removal speeds are in the order of very little fractions of 1 m/sec, and thus negligible. Disturbances, according to this consideration, may be expected in altitudes greater than 60 to 70 km, and it is here where loss factors should be determined experimentally.

For another approximation, based on the same concept, we use the values of table 204 (section 1.6.4.), dealing with average distances between ions. From them, we determine the thickness of the "first layer" of ions to $\frac{1}{2}\sqrt{3}$ of this distance. Thus, we obtain ion density gradients for this first layer in the order of 10^{11} to 10^{14} m^{-4}. The great discrepancy stems from the fact that the average distance is calculated according to two different assumptions, both hypothetical ones, as explained in section 1.6.4. The relative ion flux, calculated for the first layer, then comes to values between 600 and 2000 m/sec for the height of 80 km. That means that here the first layer disappears completely (for a wind velocity of 300 m/sec, we get a traveling distance paralled to the wall of only 0.3 m). For the "second layer," the situation is somewhat different. Since these ions are not directly confronted with an absolute ion sink, the ion density gradient is smaller.

A more sophisticated approach may be taken by starting from equations quoted by L. B. LOEB (1955, p. 199). Here a parcel of gas is considered, which contains a great number of "particles" (molecules), which move at random due to their temperature. The density of the considered type of particles in the parcel is N_o; outside of it this density is zero at the time $t = 0$.

The parameter

$$N_x = \frac{N_o}{\sqrt{4\pi D t}} \exp\left(-\frac{x^2}{4Dt}\right) dx \qquad (104)$$

indicates the number of particles of the considered type, which have, after a time t has passed, displacement components along the x-axis in the magnitude between x and $x + dx$. The square root of the average squared displacement along the x-axis derived from eq. (103) is:

$$\sqrt{\bar{x}^2} = \sqrt{2Dt} \qquad (105)$$

and the average displacement is

$$\bar{x} = \sqrt{4Dt/\pi} \quad . \tag{106}$$

By using the diffusion coefficients from table 208 of section 1.6.4, we calculate for the different heights the average displacement per second (see the following table):

AVERAGE DISPLACEMENT OF IONS PER SECOND
DUE TO GAS KINETIC DIFFUSION

Height [km]	$\sqrt{\bar{x}^2}$ [m]		$\bar{x}$ [m]	
10	4.13×10^{-3}	$\sqrt{t}$	3.30×10^{-3}	$\sqrt{t}$
30	2.02×10^{-2}	$\sqrt{t}$	1.60×10^{-2}	$\sqrt{t}$
50	8.95×10^{-2}	$\sqrt{t}$	7.15×10^{-2}	$\sqrt{t}$
80	6.70×10^{-1}	$\sqrt{t}$	4.96×10^{-1}	$\sqrt{t}$

With a wind velocity equal to that of sound, ions travel downstream with an average velocity of, for example, 300 m/sec. That means that they pass the zone of rings at the upstream end of the modified GERDIEN chamber, being about 3 cm long, in 10^{-4} sec, and $\sqrt{10^{-4}} = 10^{-2}$. With the same velocity, which would apply to the uppermost ranges of falling height, the ions would traverse the whole modified GERDIEN chamber of about 1 m in 1/300 second, the square root of which is 5.8×10^{-2} $\sec^{-1/2}$. The values of the table for the range of 80 km must be multiplied by these square roots of time in order to determine the effect of diffusion on (a) ion losses in the ring zone, and (b) ion path broadening inside the chamber.

For an application of the GERDIEN chamber in lower heights, at 10 km, the rings must be longer, for example, 12 cm, and the wind velocity may be as small as 5 m/sec.

This leads to square root of time values of 4.9×10^{-2} $\sec^{1/2}$ for the ring zone, and 4.45×10^{-1} for the chamber proper. Thus we get the actual average displacement as indicated in the following table:

EXTREME CASES OF AVERAGE DISPLACEMENT

	$\bar{x}$ for ring zone [m]	$\bar{x}$ for chamber proper [m]
at 10 km	1.6×10^{-4}	1.47×10^{-3}
at 80 km	4.96×10^{-3}	2.28×10^{-2}

The true displacement occurs due to a MAXWELLIAN curve. From the last table we see, that gas kinetic diffusion creates a small concern for the height of 10 km, but must be taken into account at 80 km. In fact, it prevents another limitation for the application of the modified GERDIEN chamber in altitudes approaching 80 km; if the distance between the rings is 10 mm, and the displacement according to the table is in the average about 5 mm, only half of the ions will pass, roughly speaking, and the resolution of mobilities at the lower end of the range will become rather poor at that extreme height.

In conclusion, all our different approaches lead to the fact, that for 80-km diffusion disturbances are severe, and that post-calibration must investigate the influence of diffusion at altitudes of 70 and 60 km or less.

The "electric diffusion" caused by the mirror-charge effect leads to the following facts. If we again take a distance between ion and wall in the order of 1mm, the electric field generated by the mirror-charge effect, is in the order of mV/m. With the mobility values for altitudes between ground and 80 km, the resulting ion velocity towards the wall is in the order of a few mm per second at 80 km, and of less than a thousandth of that at 10 km. Thus, the effect of the electric diffusion can be neglected; in lower altitudes it does not play a role at all, and at the maximum altitude, where it may begin to be noticeable, its effect is much smaller than the effect of gas-kinetic diffusion.

The most severe influence is that of eddy diffusion. Eddy diffusion occurs as soon as the flow of the air, containing ions, is turbulent. For the lower atmosphere, GUNN (1964) has discussed this effect.

Losses of about 39 percent of the small ions occurred when the CARNEGIE expedition used a special type of GERDIEN chamber. In this chamber, eddy diffusion was produced at the upstream end, because coaxial rings, 40 cm long, and about 2 cm spaced were inserted here. GUNN does not discuss to what extent this changed the mobility spectrum of the incoming ions. While in gas kinetic diffusion the loss is a function of mobility, the losses in eddy diffusion presumably depend on mobility to a much less degree. However, this degree is not known and cannot be determined theoretically. For this reason, it is planned to avoid turbulence during the measurements with the modified GERDIEN chamber.

The probable diffusion losses will be determined after each flight. Since these investigations belong to the velocity-density dependent complex, they will be included in the post-calibration periods.

1.7.3 FIELD-STRENGTH DEPENDENT MOBILITY UNDER LOW PRESSURE

If the ions can gain much energy between collisions, i.e., when moving in a gas of low density under the influence of a great electric field, their velocity is no more a linear function of the field strength

$$v_i \sim E \quad ; \tag{107}$$

and it finally becomes dependent on the square root of the field

$$v_i \sim E^{1/2} \; . \tag{108}$$

Eq. (107) applies when the kinetic energy acquired by the ions from the electric field is small in comparison to their thermal energy:

$$l e \, E \ll k_B \, T \tag{109}$$

where

l = mean free path

E = electric field strength

k_B = BOLTZMANN constant

T = temperature in degrees KELVIN

e = electric charge of the ion.

Energy transfer between neutral particles (molecules) and ions is small when the respective masses are quite different. If this is the case, the ions may store energy through many collisions:

$$\left(\frac{m_2}{m_1} + \frac{m_1}{m_2} \right) e \, E \, l \ll k_B \, T \tag{110}$$

where m_2 and m_1 are the masses of neutral molecules and ions, respectively. This may be expressed also as follows, substituting the mean free path by the collision cross section:

$$\left(\frac{m_2}{m_1} + \frac{m_1}{m_2} \right) e \, E \ll p \sigma \tag{111}$$

where

p = pressure

σ = collision cross section.

For $m_1 \approx m_2$ and introducing the magnitudes for the other parameters, we get

$$\frac{E}{p} \ll 200 \ \frac{V/m}{torr} \ . \tag{112}$$

The limit determined in eq. (112) is never surpassed in the free atmosphere, since the atmospheric electric field strength is small where the pressure is low. However, in the GERDIEN chamber, stronger fields have to be applied. Since it is a cylindrical condenser, the limiting field with decreasing pressure will at first be reached close to the inner (driving) electrode. Even then, the influence on the measurement would be small, for three reasons: (1) the transition between the regions of field-independent and field-dependent mobilities is a smooth one; (2) the surpassing of the critical E/p value is smooth as well, and (3) ions move mostly close to the outer electrode where the transition occurs at last. However, part of the ion path at altitudes higher than 60 to 70 km will certainly be affected. Thus, the evaluation of measurements requires a consideration of this effect.

Based on the studies of G. H. WANNIER and L. B. LOEB, the following formula, which describes the movement of ions in the cylindrical condenser, has been derived:

$$\rho = \left[\left(\frac{3}{\omega \sqrt{2}} \quad \frac{(m_2 + m_1)^{1/4} \ m_1^{1/4}}{m_2^{1/2}} \right) \left(\frac{eU}{m_1 \ n_2 \ \sigma \ \ln (R/r)} \right)^{1/2} \right.$$
$$\left. \left(E \left(\frac{\pi}{4} ; \ \phi \right) \ - \frac{1}{2} \ F \left(\frac{\pi}{4} ; \ \phi \right) \right) \ + C_1 \right]^{2/3} \tag{113}$$

where

ϕ = arc cos $\sqrt{\cos 2 \omega t}$

ρ = distance from the center of the modified Gerdien chamber

m_2 = molecular mass

m_1 = ionic mass

e = ionic charge

U = voltage applied between the two electrodes of the modified Gerdien chamber

n_2 = number density of the molecules

σ = collision cross-section of ions and molecules

R = radius of outer electrode of the Gerdien chamber

r = radius of inner electrode of the Gerdien chamber

E = elliptical integral of second order

F = elliptical integral of first order

C_1 = integration constant

This formula becomes more and more inaccurate above a certain frequency limit--in the Earth's atmosphere about 1 MHz at 30 km and 10 kHz at 80 km.

1.7.4 CHANGES OF THE NATURE OF IONS BY DRIVING VOLTAGE

The possibility that ions exist which can be destroyed by the application of a very small energy has been indicated in section 1.2.2. If ions could really exist with binding energies as low as 0.014 eV, we certainly could destroy them in the GERDIEN chamber. Thus, if we do not find mobilities which may be attributed to such ions, the existence of these ions is not yet refuted experimentally. However, the probability is small.

The existence of O_2 ions, on the other hand, is very probable. Their electron affinity is 0.9 ± 0.1 eV (NAWROCKI and PAPA, 1961), i.e., it is smaller than that of all other probable constituents.

Here, the problem exists, whether the electric field in the GERDIEN chamber could destroy the ions and thus change the mobility values prior to the measurement itself. In order to do this, the electric field must become so great that it conveys more energy to the ions than they have due to their own thermal motion (see section 1.7.3.). Thus, there is a common lower limit for the "WANNIER effect" and the possible ion destruction.

For a closer estimate, we consider the occurrence of long free paths as plotted in figures 22 and 23 of section 1.6.2. Supposing a maximum field strength inside the GERDIEN chamber of 110 V/m exists for measurements in 70 or 80 km, and of 7.6 kV/m in 30 km, we can easily calculate that:

at 80 km. about 10 percent

at 70 km about 10^{-2} percent

at 30 km less than 10^{-4} percent

of the ions may acquire energies of 0.8 eV or more.

1.7.5. SHIELDING BY A SPACE CHARGE LAYER

From the domain of electrochemistry, the concept of shielding off any electric field by a layer of space charges of opposite sign in front of any electrode has been introduced into the domain of atmospheric physics. The general applicability of this concept is still vague. However, the so-called DEBYE-length (or DEBYE shielding-distance):

$$L_D = \left(\frac{k_B \, T_\epsilon}{n_e \, e^2} \right)^{1/2} \tag{114}$$

--with n_e = electron number density--is often quoted. We have to show, that the possibility of a shielding effect of this kind does not disturb our measurements.

It is intended to keep the field outside the Modified GERDIEN chamber free of any disturbing electric fields which may be generated from the instrument. The first set of rings (Nos. 00 to 07 in Model A) is constructed for this purpose. That means that there is no field which could build up a shielding space charge layer by the electrode effect.

Inside the GERDIEN chamber, the electron density is practically zero, since all electrons which are not removed by diffusion between the rings will immediately be destroyed by the electric field in the chamber. A shielding effect of the ions caused by the electrode effect, however, certainly does not occur over so short a distance as given in the chamber.

1.7.6 ACQUISITION OF AN OWN CHARGE BY THE INSTRUEMENT

Basically there are two possibilities that the whole modified GERDIEN chamber, including everything which is electrically connected to it, may adopt an electric charge. This is a well known event at higher altitudes. If this were so in our case, the intake of ions would be a selective one, depending on the sign and even on mobility of the aeroions. It can be shown, however, that the probability of such a charge-up process is very small.

An external charge-up would occur if more ions of one sign would impact on the outside of the instrument. This already is unlikely to have a great effect, since

it is intended to move the instrument at a much slower rate than the thermal velocities of both ions and electrons. And even if this occurs, the instrument, together with the carrier, is so much greater than the mean free path that the concept of conductivity applies to its full extent. This has the consequence that the rather great surface of the instrument will be discharged very quickly, once it has obtained a potential difference with respect to the environmental atmosphere.

An internal charge-up would occur, if inside the chamber not all ions are intercepted. That means, if ions of predominantly one sign would exit at the chamber's rear end with the airstream, a certain charge-up may occur. Again, conductivity is so great that the potential will very quickly be equalized. If so wanted, the aft rings of the chamber (30 to 37 in Model A) may be subdivided into two sets. Then, there are several easy possibilities to establish a workable ion fence or filter, and no ions would exit any more.

1.7.7 DISTURBANCES BY COSMIC PARTICLES

There is basically a possibility that the internal space of the modified GERDIEN chamber will show an additional ionization due to cosmic rays. The walls of the chamber are thick and partially built by heavy materials, and cosmic rays penetrating them may give rise to secondary effects which, in turn, would ionize many neutral particles in the chamber.

For a first approximation, we compare our instrument with ionization chambers used for the measurement of cosmic rays in the upper atmosphere. These ionization chambers must be constructed in such a way as to avoid the indicated disturbances. The ionization chamber described by NEHER (1953) and used by him still in 1963 (NEHER & ANDERSON, 1964) was essentially a sphere of 25 cm diameter, made of steel, with a thickness of 500/μm. This gives a mass thickness of 3.9 kg/m^2. The chamber has been used to altitudes of about 30 km, and an air mass of 100 kg/m^2 was still overhead of it.

In the modified GERDIEN chamber, Model B1, the receiving electrodes are made of steel with a thickness of 250 μm. However, there are aluminum beams to support the structure against the expected great accelerations, and in the most unfavorable case, a ray may penetrate 25 mm of Al before entering the chamber, which corresponds to a mass of 67.5 kg/m^2. If secondary particles will have but small angles with respect to the primary ray, only a small fraction of the chamber's volume would be affected. To obtain still another number, one may divide the chamber's whole mass, 9.1 kg, by its surface, 5.6×10^{-2} m^2, and arrive at 1.63 kg/m^2, which is less than the 3.9 kg/m^2 of NEHER's ionization chamber.

It is difficult to draw a conclusion from these numbers. In addition, it must be remembered that the 100 kg/m^2 of air above NEHER's chamber are practically not existing, if the modified GERDIEN chamber is to measure at a 70-km alti-

tude. Thus, the total material mass would be slightly smaller or much smaller in the case of the GERDIEN than in the case of NEHER's ionization chamber.

1.7.8 OTHER LIMITATIONS AND DISTURBANCES

Limitations of a more technological nature are given by the fact, that a velocity below that of sound could hardly be maintained in altitudes much higher than 80 km. Also, the rather high frequency of the driving voltage which then would be necessary would pose problems with respect to the generation of the ion gate pulses and the amplification. The driving voltage cannot be lowered under a limit given by VOLTA potential differences, which cannot be avoided.

The low temperature of the atmosphere around the instrument, which comes up from lower layers, may cause difficulties for the required high insulation. Ice deposits on the insulating surfaces, however, may be precluded by heating up the atmosphere at the surface of the insulators to about 10°C above the temperature of the atmosphere.

The most obvious limitation of the application of the instrument is, of course, given by the fact that the requirement of many collisions between the ion and neutral particles cannot be satisfied more where the mean free path comes into the order of magnitude of the instrument dimensions. This has been treated at different locations in the preceding chapters.

1.7.9 CONCLUSION

A general upper limit for the application of the method of the modified GERDIEN chamber--and that means for the possibility of measuring the mobility spectrum in general--cannot be given. Partially, the values of involved parameters are not yet known, and information is to be expected from our intended measurements. Partially, the upper limit depends on time variable atmospheric features, and no general number can be quoted. And, in part, the limit depends on the actual measurement itself inasmuch as a certain combination of wind velocity in the chamber and density of the atmosphere and total ion number density determines whether a measurement still can be evaluated. This combination will not be known prior to the measurement.

To give a rough estimate, we may say that no reason can be seen why measurements up to about 60 km should not give reliable results. However, the accuracy at 60 km may already be slightly smaller than at 55, 50, 40, or 30 km. Furthermore, there is hope, that reliable information may be obtained up to 70 or 75 km, while values from a height of 80 km probably cannot be evaluated further to obtain a mobility spectrum. However, some information still may be derived from these measurements at the peak.

PART 2

LABORATORY EXPERIMENTS

2.1 LOW PRESSURE WIND TUNNEL

2.1.1 INTRODUCTION

The wind tunnel to be described in the following pages has been constructed for the simulation of the atmosphere between ground and about 80 km, as seen from a body moving with velocities between zero and about the speed of sound. These limits have been chosen for the following reasons.

For many in situ measurements in the free atmosphere it is desirable to avoid the shock wave which is generated by a body moving with a speed greater than that of sound (Mach 1). Such shock waves may alter the atmospheric parameters to be measured - at higher speeds, even create additional ionization - or disturb the measurement otherwise. A measuring platform moving through the atmosphere with subsonic speeds may be provided by the application of modern forms of parachutes for atmospheric heights below about 80 km. Since the mean free path at that height comes in the order of the geometric dimensions of many practicable instruments, and since it is there where the atmospheric conditions undergo a typical change (the mesopause), the height range between ground and about 80 km may be considered a more or less uniform environment for the development of in situ instrumentation. The possibility of providing subsonic falling speeds and the critical length of the mean free path occurs in the atmospheres of other planets at other altitudes, but again they constitute the upper limit of environmental conditions favorable for the application of many instruments. An additional requirement for the wind tunnel was given by the fact that the simulation of the environment had to be maintained for times comparable to measuring times in the free atmosphere, which often will count by thousands of seconds or more.

The actual wind tunnel in its present configuration allows for the fulfillment of these requirements in a continuous operation which may last for hours: wind speeds between zero and more than 350 m/sec for any desired pressure between about 10 and 10^{-2} torr, and to a certain extent for higher pressures as well. It is, in addition, possible to exceed these velocities and to lessen the pressure to a certain degree. For a short-time-measurement the wind speed can be increased considerably: the tank of about 300 m^3 content pumped down to about 10^{-3} torr then serves as a surge action vacuum of strong capacity.

Provisions are made to simulate the ion content of the atmosphere as well, and temperature simulation may be added if so desired.

The test section of the wind tunnel consists of a pipe with a variable diameter. For our experiments the diameter of the pipe varies between 10 and 20 cm. However, this diameter as well as a number of other features can easily be changed if the system is to be adapted to particular experiments. The construction of this wind tunnel has been made necessary for the development and calibration of the modified

GERDIEN chamber, intended to measure in altitudes between 30 and 80 km, because we have been unable to find another facility which would have met the quoted requirements.

It is not surprising that no other facility of this kind exists. There are three main difficulties to overcome: (1) mechanical pumps have but a small effectiveness below a pressure of about 1 torr and diffusion pumps cannot be used for pressures higher than a few tenths of a torr. Thus, rather great mechanical pumps in connection with a great tank are the only means of providing sufficient wind speed in the whole range of pressure; (2) the maintainance of small wind velocities, i. e., of a small constant and unidirectional air flow, requires a high degree of tightness of the whole system, higher than is usually required for this pressure range. This is made difficult by the necessity of providing many ports and feedtroughs, and to combine the tunnel of a rather great number of different sections. This problem could be solved. The remaining leak rate corresponds to a wind velocity of about 10 cm/sec, which is much below the limit of all measuring instruments; and (3) it is difficult to measure small wind velocities under the required low pressures.

The wind tunnel is briefly described below, the principle of its operations is indicated, the attached instrumentation for the determination of pressure and wind speed is discussed, and information on actual performance is given.

2. 1. 2 DESCRIPTION OF THE SYSTEM

Figure [24] shows an overall drawing of the wind tunnel and Figure [25] is a general sketch of the overall wind tunnel. The wind tunnel (figure [26]) is attached directly to a big tank (figure [27]) whereas the pump system (figure [28]) is connected at the opposite end of this tank. Figure 29 shows a cross section of the wind tunnel. Pressurized air or gas is inserted in the wind tunnel through valves. The inside of the wind tunnel is nickel-plated so that during the operation of the wind tunnel no dust can be created by the joining air stream. The jet of air is smoothed out by the baffling in the first section before entering the test section. The aging section can be used for a temperature control of the air. Presently it is used for the generation of ions. The test section as used in figure 29 is 60 cm long and has a diameter of 20 cm. It is accessible through a rectangular port. The smoothing section and the baffling section (II) prevent the air from being disturbed in the test section when valves (C) are opened.

By changing the openings of valves A and valves C and by using different valves B in the bleeding section , the whole pressure-velocity range can be obtained. Three sets of pumps are used (figures 24, 25, and 28). The first set of pumps consists of three 11 kw pumps in parallel, the second of the three 8 kw pumps in parallel. For the third stage, two 37 kw pumps are used. The air removal of the pumps amounts to about $15 m^3/sec$ at 10^{-1} torr. A short pipe with a 60-cm diameter connects the pipes to the tank.

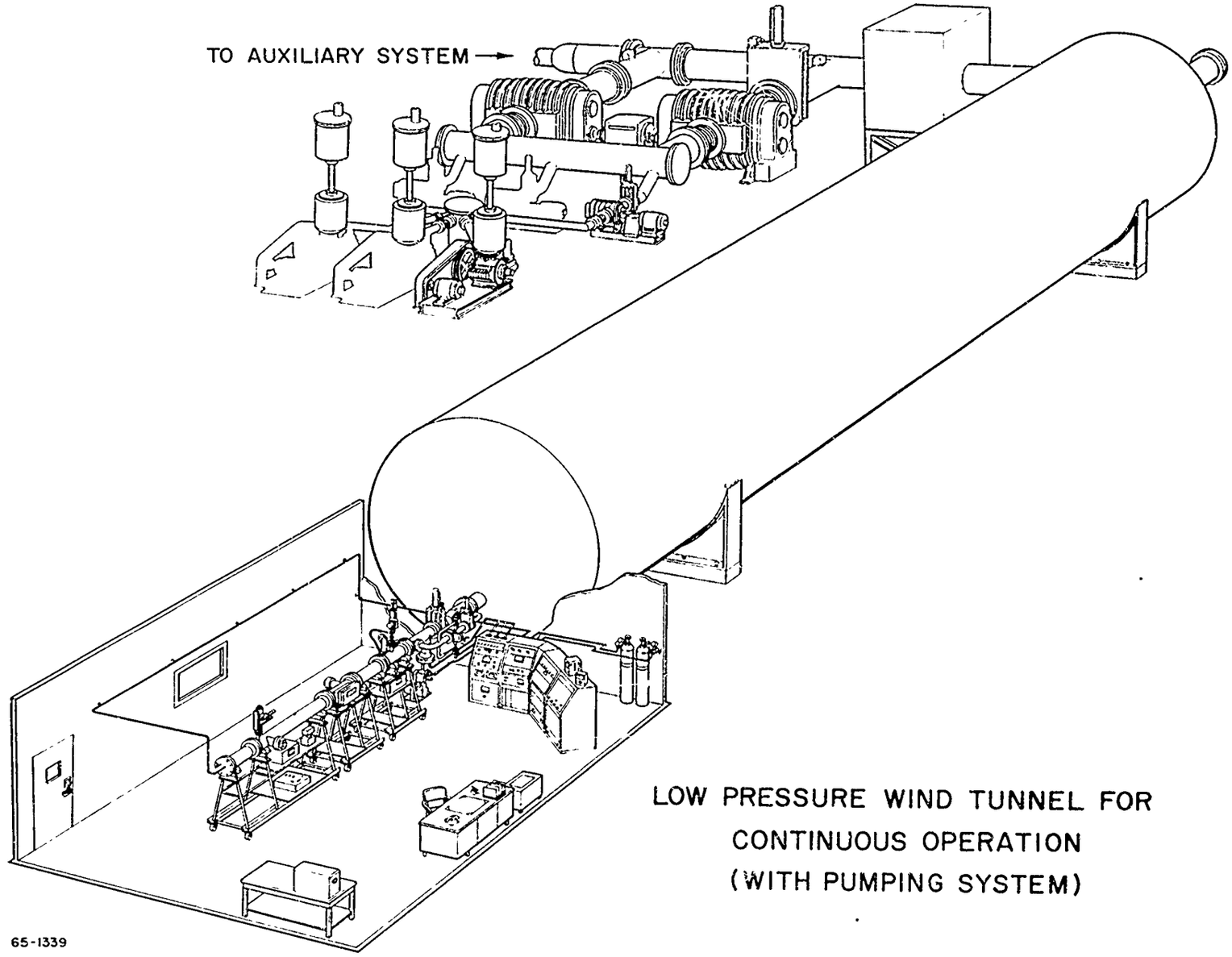

Figure 24 LOW-PRESSURE WIND TUNNEL FOR CONTINUOUS OPERATION
(WITH PUMPING SYSTEM)

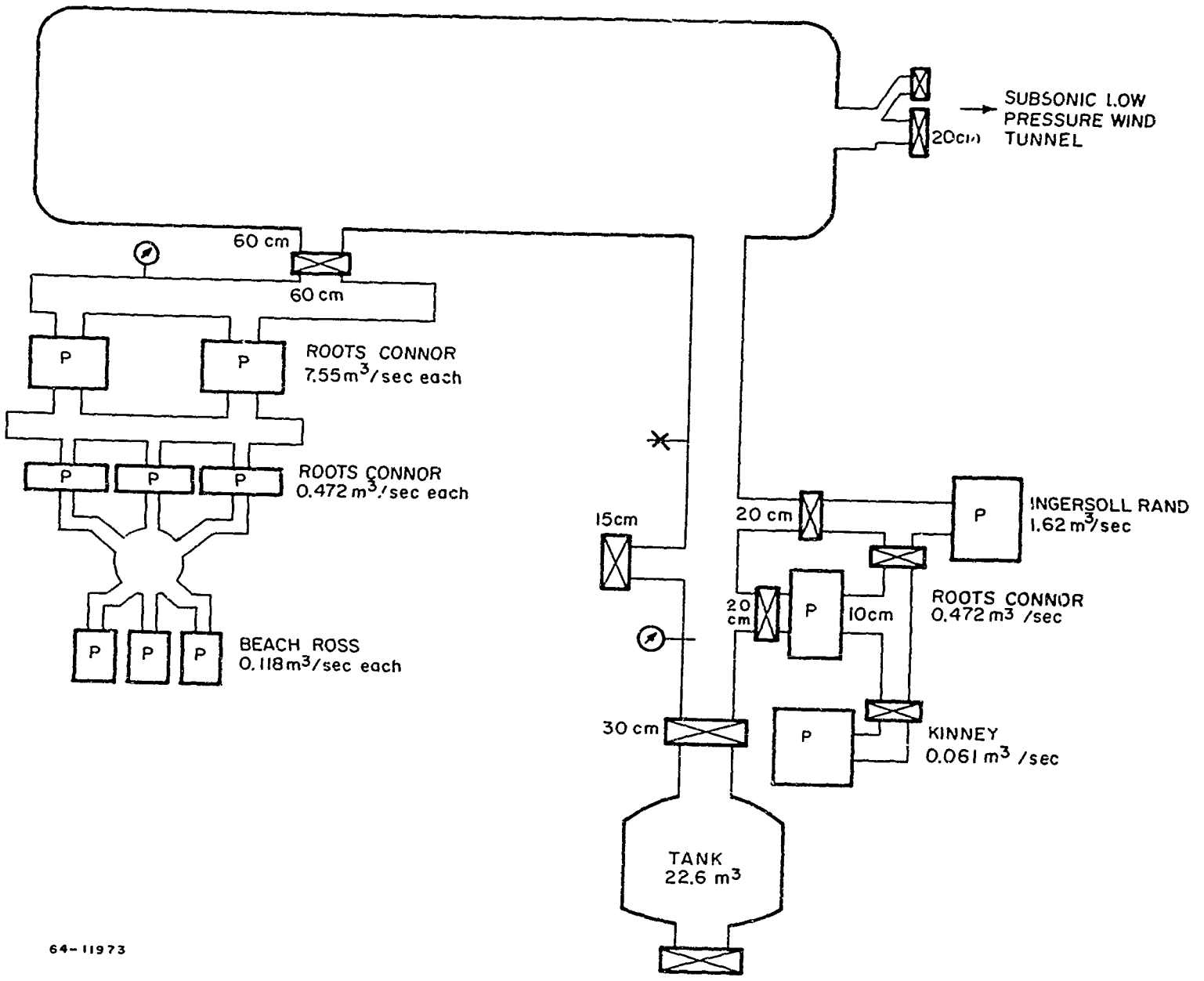

Figure 25 OVERALL SYSTEM OF THE SUBSONIC LOW-PRESSURE WIND TUNNEL

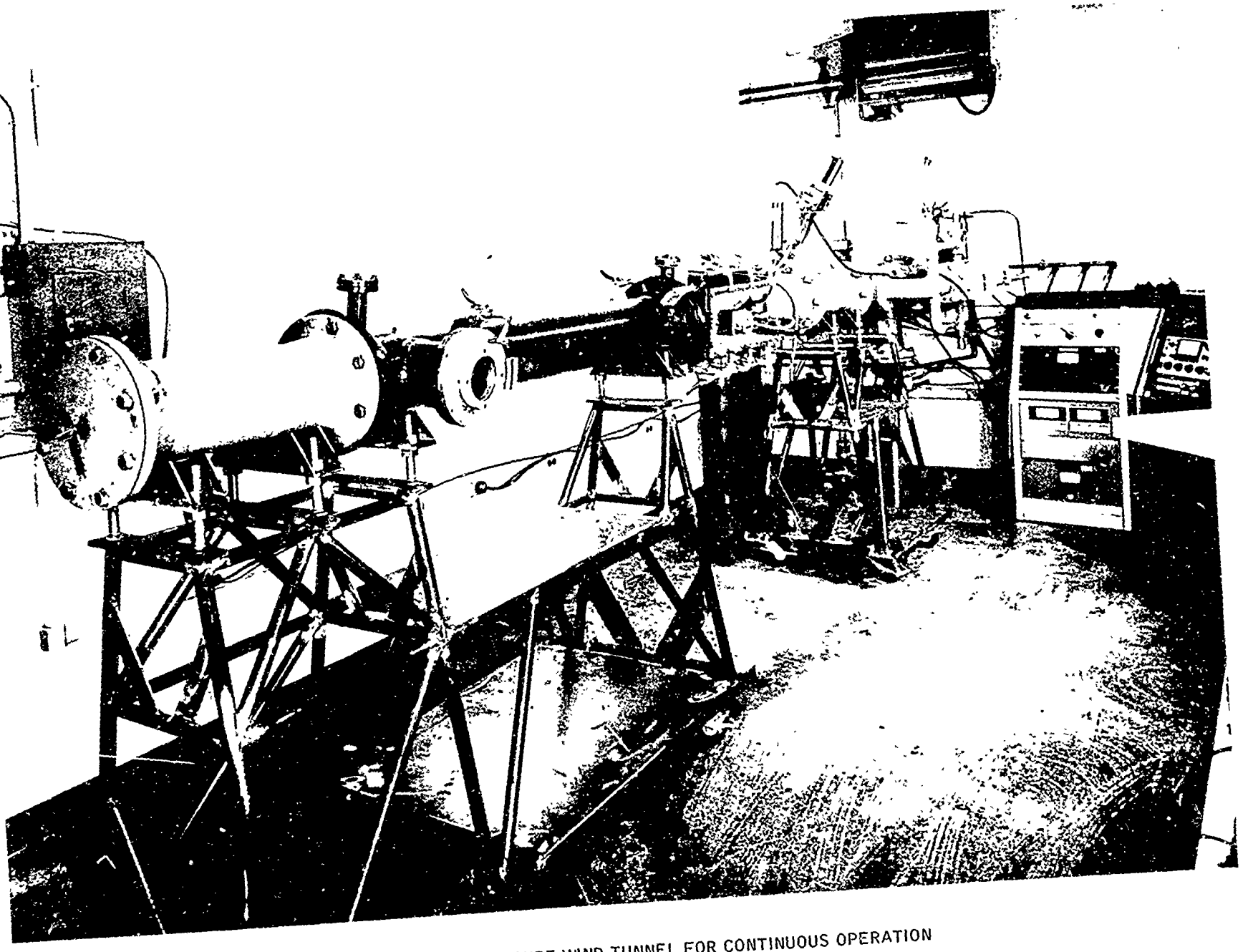

Figure 26 LOW-PRESSURE WIND TUNNEL FOR CONTINUOUS OPERATION
(Tunnel Proper in the Wind Tunnel House)
P12363A

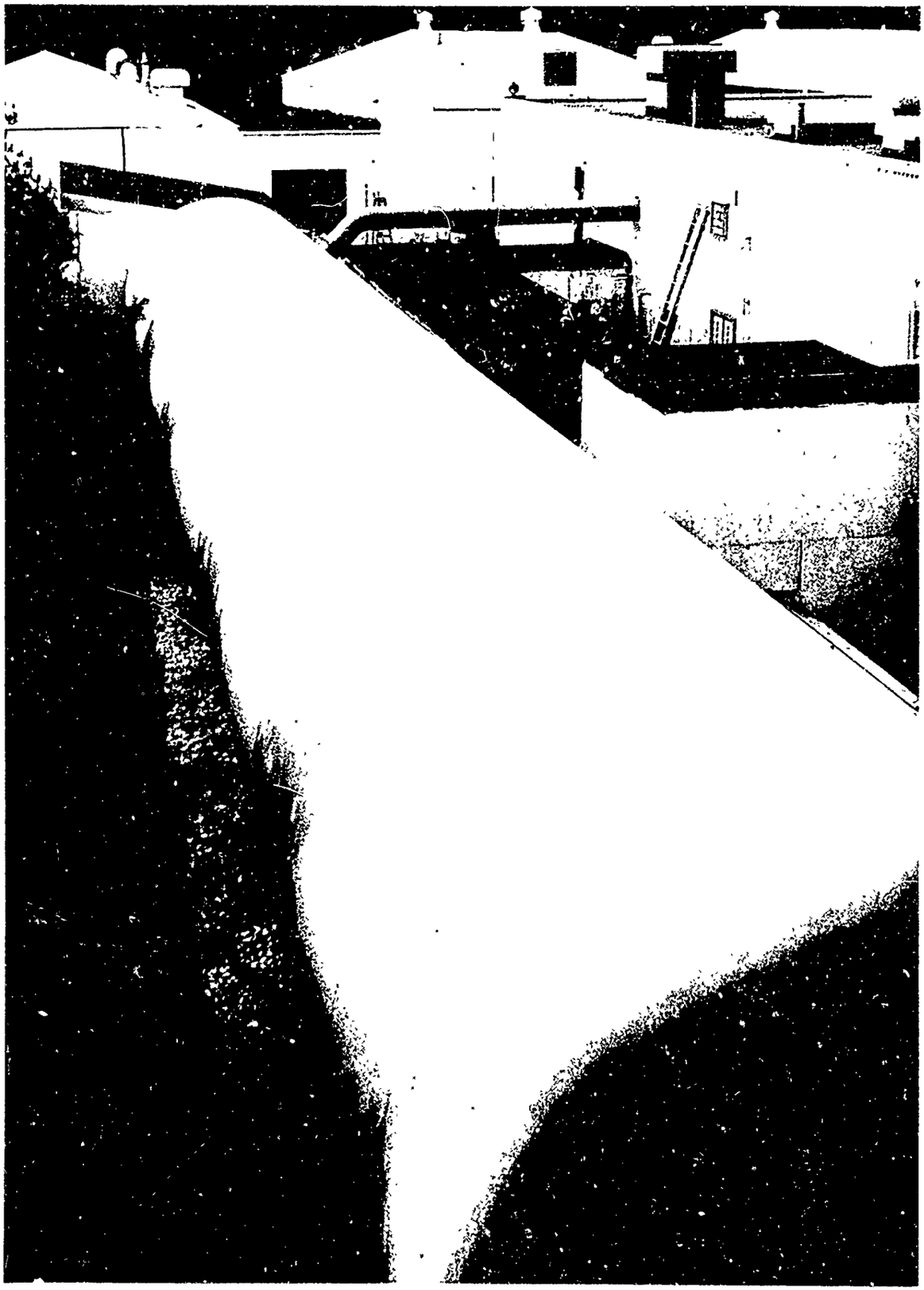

Figure 27 THE TANK, AT THE FAR END IS THE WIND TUNN.. HOUSE
P12294A

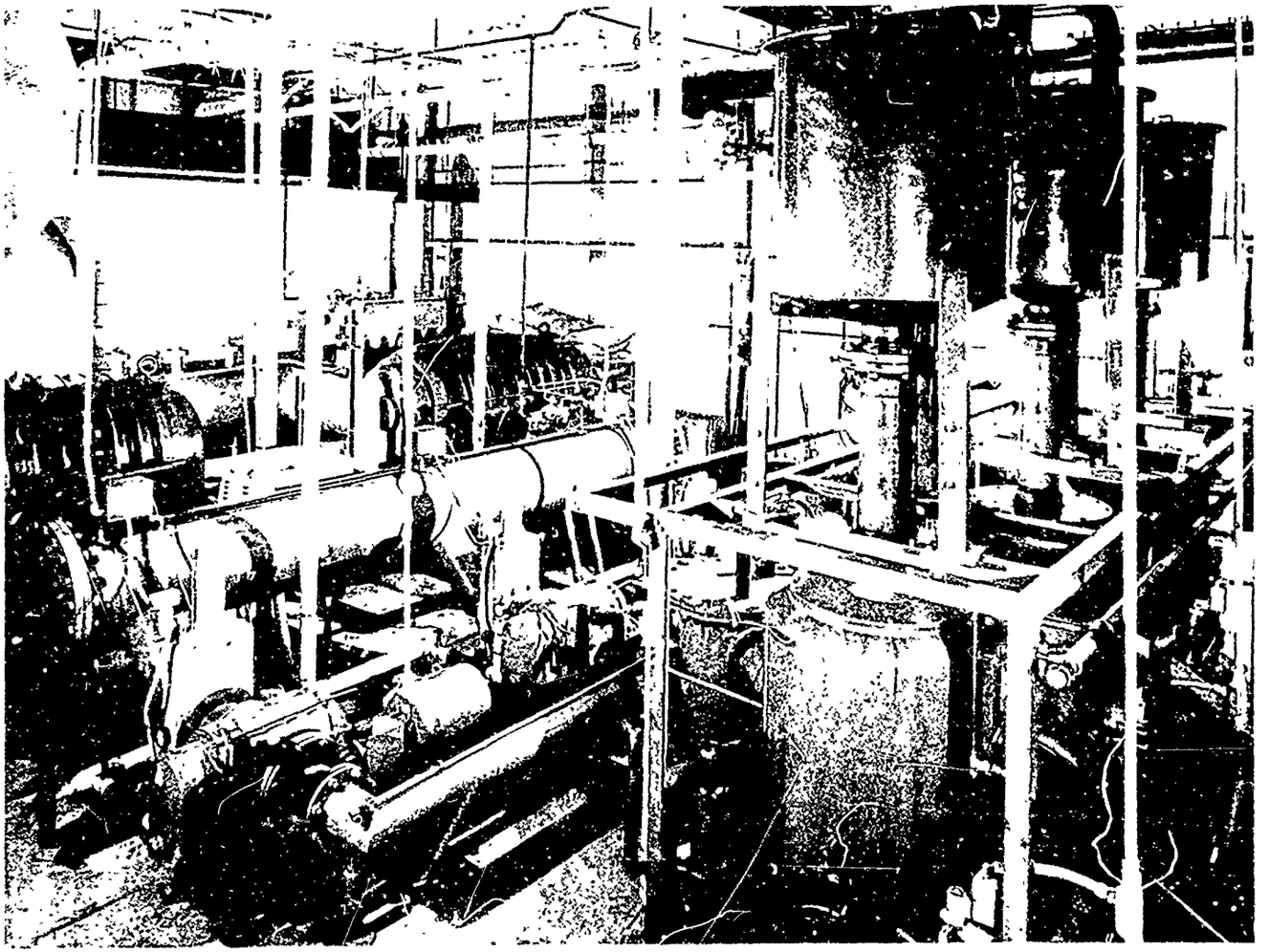

Figure 28 MAIN PUMPING SYSTEM SERVING THE LOW-PRESSURE WIND TUNNEL
(Right, the three pumps of the first stage; center, two of the three (smaller) pumps of the second stage; left, one and a half of the two (great) pumps of the third (low-pressure) stage; connection to the tank (outside building, at far left.)
P11991A

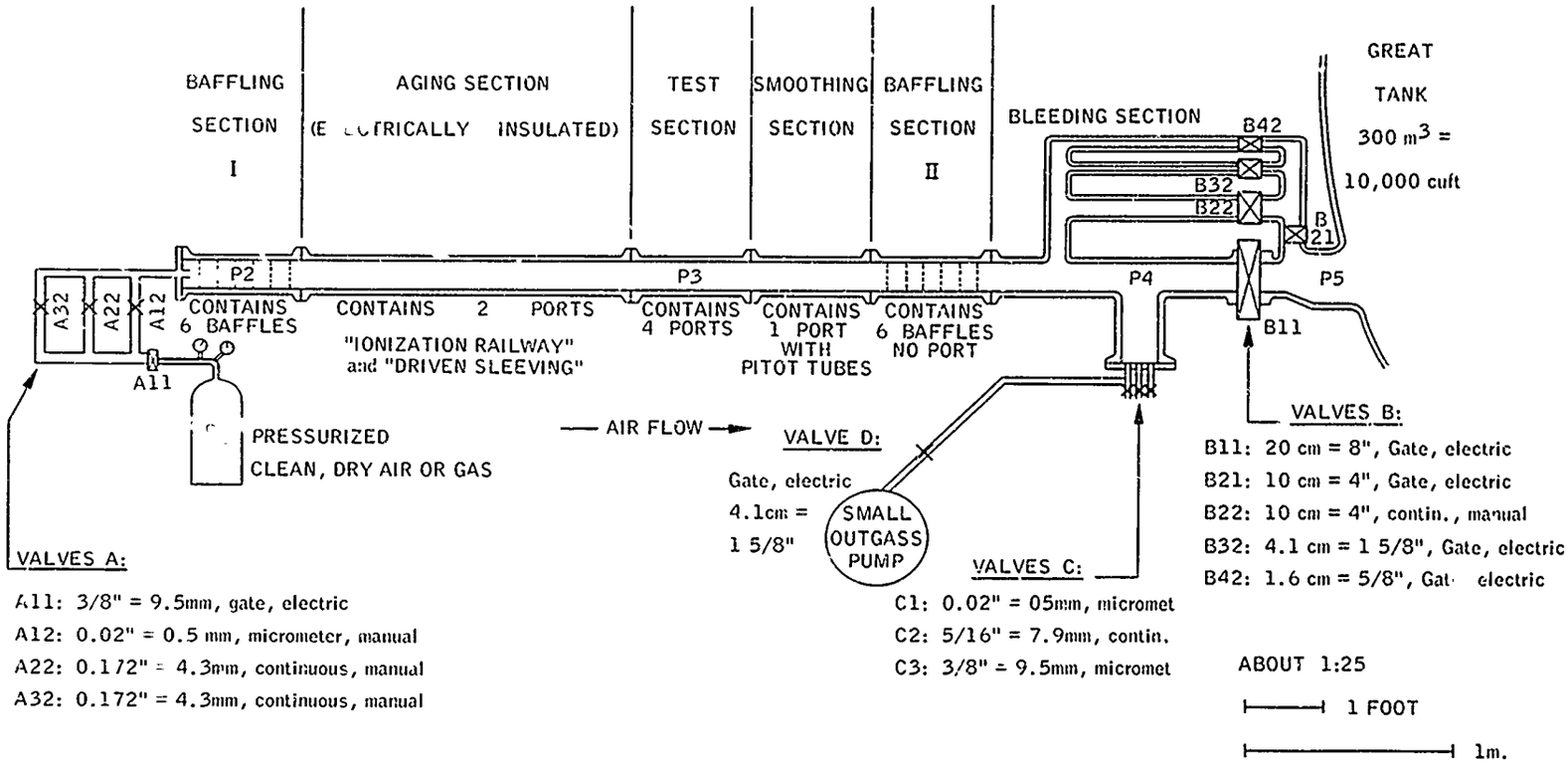

64-11968

Figure 29 CROSS SECTION THROUGH LOW-PRESSURE WIND TUNNEL FOR CONTINUOUS OPERATION SHOWING SECTIONS AND VALVES

The tank to which the pumps are connected has a volume of 283 m^3. One purpose of this big tank is to smooth out all pulsations of the pump system. In fact, a steady air stream is obtained. The pumps are operative to below 10^{-2} torr. Against a blank flange, they will pump the big tank down to about 10^{-3} torr.

A smaller pump system may be used in addition (figure 25). Here, the air removal amounts to about 1.5 m^3/sec only, and the lowest obtainable pressure is about 6×10^{-2} torr.

2.1.3 OPERATION OF THE SYSTEM

In a fully developed flow in a pipe, either laminar or turbulent, the velocity of a gas is given by a function ϕ of the following form (ROHSENOW and CHOI, 1961):

$$v = \phi (p_1, p_2, \rho, R, \nu, e); \tag{115}$$

where

- v =velocity of the gas inside the tube
- p_1 =pressure at the front end of the pipe
- p_2 =pressure at the rear end of the pipe
- R =resistance of the pipe
- ρ =density of the gas
- ν =kinematic viscosity of the gas
- e =internal energy of the gas per unit mass.

Assuming laminary flow in the pipe, the velocity distribution in a cross section is given by

$$v(y) = \frac{p_1 - p_2}{4 \nu \rho l} (y_r^2 - y^2); \tag{116}$$

where y =distance from the axis of the pipe
y_r =the radius of the pipe

The density of the gas (air) in the pipe in the middle between the two ends is as follows:

$$\rho_m = \frac{\frac{p_1 - p_2}{2}}{k_B T} m \tag{117}$$

where m =the mass of a gas molecule
k_B =the BOLTZMANN constant, 1.38×10^{-23} Ws/degree
T =the temperature of the gas.

By eqs. 116, and 117, it is shown that with independent control of the pressures p1 and p2 , i.e., the pressures at both ends of the pipe, gas density and gas velocity in the pipe can both be controlled independently within certain limits.

This is the basic idea for the operation of the wind tunnel: by maintaining a certain pressure in a vessel at the upstream end of the tunnel (i. e., baffling section), and maintaining another pressure at the downstream end (bleeding section), the desired values for density and wind velocity can be set. There are five practical means of obtaining this result: (1) the pressure in the gas container (P_1 in figure 29); (2) the set of valves A; (3) the set of valves B; (4) the set of valves C; and (5) the gas removal speed of the pumps. Because of technological reasons, the gas removal speed of the pumps cannot be controlled at will, but the remaining four regulation possibilities are sufficient.

In fact, the stability of the system is such, that a point in the density-velocity diagram, set on Friday afternoon, is again obtained when the system is put to operation on Monday morning.

To obtain the gas resistance between the pumps and the wind tunnel proper, the pressure has been measured at two points of the system with the following result:

pressure at connection tank - wind tunnel	6	4	3.5	11	15	19	millitorr
pressure at pump	4.2	3.8	3.4	6.6	10	15	millitorr
quotient of both	1.4	1.08	1.02	1.67	1.5	1.26	

That means that the flow resistance between the wind tunnel and the pumps is small.

During the experiments, the gas pressure is monitored continuously at different points of the wind tunnel, as indicated in figure 8.

2.1.4 DETERMINATION OF PRESSURE AND VELOCITY

For the determination of the wind velocity in the tunnel, Pitot tubes are used. Depending on the range, Pitot tubes for subsonic flow with a very short time constant, or Pitot tubes for supersonic speeds with a somewhat larger time constant (shown in figure 30) are applied. In the smoothing section, a Pitot tube for static pressure is fixed, and a Pitot tube for the total pressure can be moved by a motor across a diameter of the tunnel. Another set of Pitot tubes has been applied inside the test section itself during some of our experiments. The pressure differences between the two tubes of each set of Pitot tubes is measured by a "Baratron" differential pressure gauge type 77, equipped with several heads of different sensitivity. The smallest pressure difference to be read is about 3×10^{-5} torr. Its operation principle is a variable condenser (capacitive sensor) in a bridge circuit and in a heated atmosphere; phase sensitive ac voltage and polarized dc voltage are provided for recording and controlling.

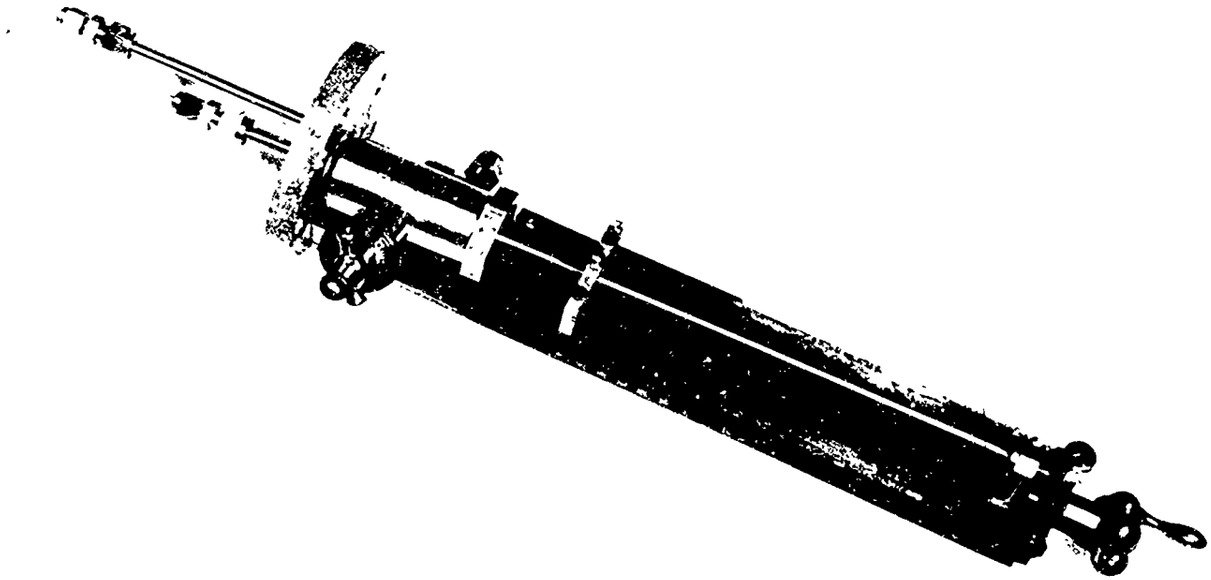

Figure 30 SET OF PITOT TUBES FOR OPERATION IN SUBSONIC AND SUPERSONIC WIND SPEEDS

(Impact probe, left, measuring total pressure, is movable through "feed-through" in a vacuum-tight operation.)

P12147B

The static pressure is measured simultaneously at six different locations along the wind tunnel (figure 31) mostly by thermocouple gauges. For a more accurate determination of static pressure, an Alphatron absolute pressure gauge, model 530, is attached to the smoothing section. It allows the measurement of pressures from 760 to less than 10^{-4} torr with an accuracy of ± 5 per cent of full scale in the 0...1 millitorr range and with linear response. A STOKES' gauge is attach d to the smoothing section as well. Figure 32 shows the instrument panel with the pressure gauges, valves A and C, and part of the electronic instrumentation for a particular experiment. The measuring head of the Alphatron and one measuring head of the Baratron are visible in figure 26, sitting on the smoothing section of the tunnel.

2.1.5 MEASUREMENT OF STATIC PRESSURE

For the measurement of static pressure (and wind speed) in the axis of the tunnel, a cone of internal diameter of 5mm was fixed close to the axis in the smoothing section and, in some of the experiments, in the test section as well. This relatively large diameter was chosen for measurements in the subsonic range on the basis of experiments to obtain a short response time. The central positioning of the cone helped to avoid errors due to radial changes of static pressure in the range of about 10^{-2} torr or below.

The exact correction value for the applied cone are not known. However, from measurements with similar cones (TALBOT, 1954), it was derived that the remaining error at about 10^{-2} torr would not exceed 15 per cent (TALBOT, 1954; ENKENHUS, 1957). Including the possible error of the Baratron instrument, the total error for 10^{-2} torr and about Mach 1 comes to 20 per cent.

It decreases rapidly with increasing pressure; e.g., for Mach 1 and 10^{-1} torr it is already below 5 per cent.

2.1.6 MEASUREMENT OF IMPACT PRESSURE

As mentioned above, the open-end impact probes can be moved by motors in radial direction across the tunnel. The diameter of the orifice is about 5 mm. The external diameter of the probe, being about 7 mm, was taken as a characteristic length for the determination of the Reynolds number. With Reynolds numbers greater than 100, the continuum flow theory can be applied, and errors introduced by slip flow or molecular flow can be neglected (ENKENHUS, 1957). Smaller Reynolds numbers occur at lower pressures. At about 2×10^{-1} torr (Reynolds number 50), the total error due to outgassing* and viscosity is estimated to be 10 per cent for a wind speed of Mach 1. At still smaller pressures, the error increases rapidly and amounts to about 40 per cent at 5×10^{-2} torr and Mach 1 (Reynolds number 10). Corrections with respect to viscosity have not been applied because available correction factors differ very much and do not seem to be reliable enough for our particular task.

*Outgassing from the material in the pressure gauge can last for many hours. Under rather low pressures, either it must be awaited that long, or the error must be estimated and accounted for.

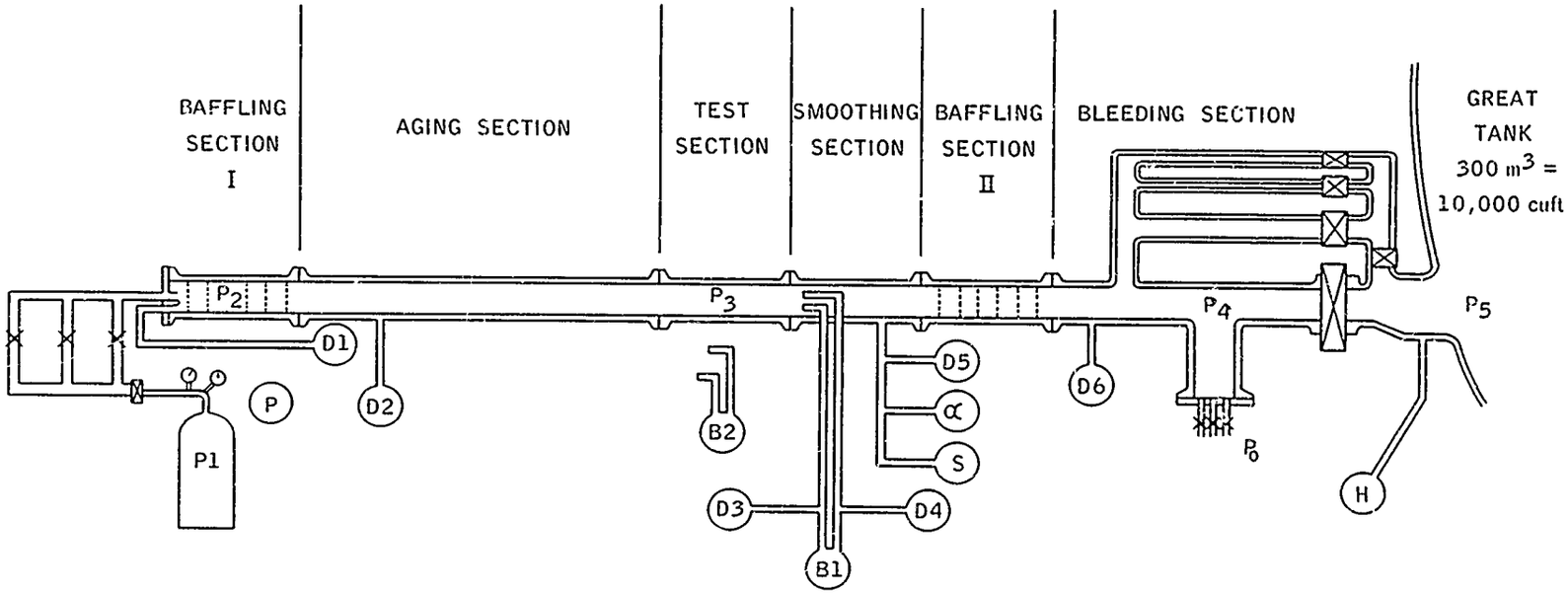

Pressure Gauges:
- α : Alphatron-Gauge, 760 mm to 0.02 μm Hg
- B : Baratron Differential Pressure Gauges, 3 heads, down to 0.01 μm Hg
- D : Dresser Gauges, six channels, 1mm to 1 μm Hg
- H : Hastings Gauge, with recorder
- P : manometers, up to about 5000 mm Hg
- S : STOKES-Gauge
- in reserve: five channels Hastings Gauges 1 mm to 1 μm Hg
  additional Alphatrons

64-11969

Figure 31 MEASUREMENT OF PRESSURES AT LOW-PRESSURE WIND TUNNEL

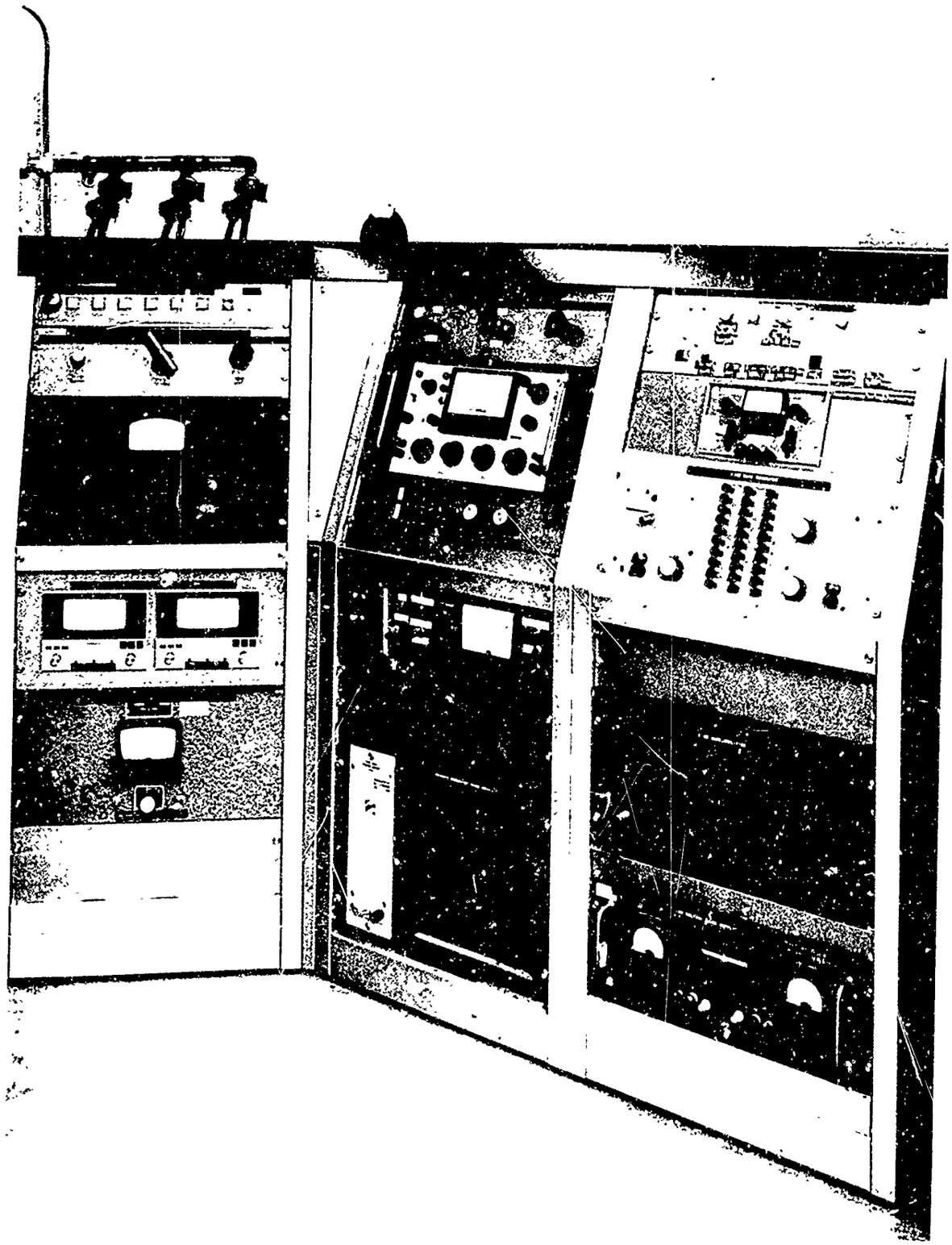

Figure 32 PARTIAL VIEW OF INSTRUMENT RACK FOR LOW-PRESSURE WIND TUNNEL
P12769A

2.1.7 DETERMINATION OF FLOW VELOCITY (Wind Speed)

Two different equations for the determination of the flow velocity may be quoted, and in both cases the velocity is given by Mach numbers and not in a temperature-independent scale. For subsonic flow ($M \leq 1$), we have

$$\frac{p_t}{p_s} = \left(1 + \frac{\gamma - 1}{2} M^2\right)^{\frac{\gamma}{\gamma - 1}} ; \qquad (118)$$

and for supersonic flow ($M \geq 1$) the RAYLEIGH formula may be applied:

$$\frac{p_t}{p_s} = \left(\frac{\gamma + 1}{2} M^2\right)^{\frac{\gamma}{\gamma - 1}} \left(\frac{2\gamma}{\gamma + 1} M^2 - \frac{\gamma - 1}{\gamma + 1}\right)^{-\frac{1}{\gamma - 1}} \qquad (119)$$

In both formulas are

p_t = the total or impact pressure
p_s = the static pressure
M = the Mach number or ratio v/c with c = speed of sound
γ = the ratio of specific heating: c_p/c_v
(for air at 20°C, $\gamma \approx 1.4$).

These formulas are valid under certain assumptions, and their reliability decreases when the pressure gets low. A study of these assumptions and of the inaccuracy under the low-pressure conditions has been made, and it was decided, that for the purpose of our measurements, eqs. (118) and (119) may be applied. The resulting error for the determination of the wind speed comes, for wind speeds of Mach 1, to about 10 per cent for altitudes of about 60km, and to about 20 per cent for 70 km, increasing rapidly if altitudes of more than 70 km are to be simulated. Since these accuracies have been sufficient for our purposes, no attempt was made to improve the measurement by the application different types of probes and the execution of a series of particular experiments.

2.1.8 SIMULATION OF OTHER PARAMETERS THAN DENSITY AND WIND SPEED

For the simulation of the ionic state of the free atmosphere, there are provided two possibilities to create ions. To simulate the conditions up to heights of about 40 km, polonium-foils are inserted in the aging section of the wind tunnel. Depending on the desired ion density, more or less radioactive material is used. This ion source can be moved by a motor along the axis of the aging section. This possibility allows the provision of older or younger ions to the test section; furthermore

it yields a rather sensitive regulation of the ion number density since recombination and diffusion losses depend on the traveling time.

To get a sufficient ion density for higher altitudes, a box containing (at present) 400 millicurie polonium is used. This box is connected by a thin tube and a valve with a pressurized air bottle. During the operation of the wind tunnel, the air streaming through this box is highly ionized, since the air pressure is then about atmospheric. The ionized air is released through a nozzle of 4-mm diameter into the wind tunnel proper. In this nozzle, the pressure reduces to the operating pressure maintained in the tunnel. Many ions are lost in the nozzle due to diffusion, but it is still possible to obtain a number density in the test section, which corresponds to a height of 70 km. By changing the pressure in the box and the diameter of the nozzle, a still greater ion density could be obtained.

The wind tunnel described here is not a recirculating system. That means that fresh gas supply is possible throughout the operation. Thus, every gas or gas mixture which can be provided from pressurized bottles and which does not disturb or endanger the functions of the wind tunnel and the pumps can be used. However, it must be remembered that even the purest gases purchased from industry or stored in bottles will be contaminated by aerosol particles. This fact may considerably disturb the simulation of the conditions in the free atmosphere. To avoid this disadvantage, "absolute filters" can be inserted. These filter out aerosol particles of the 0.5 μm size to better than 99.97 per cent, and particles of greater or smaller size to 100 per cent, practically.

If the ionization box, as described in the preceding section, is applied, it may be fed directly with a gas other than that used in the wind tunnel. In this way, it is possible, to a certain extent, to have ions of one chemical nature in a neutral gas of another one.

No provisions have been made, so far, to control the temperature or to simulate in the wind tunnel the radiative environment given in the free atmosphere. Simulation of temperature is possible to a certain extent, and facilities for radiation simulation may be installed within certain limits.

2.1.9 EXPERIMENTALLY OBTAINED VELOCITY PROFILES AND MAXIMUM VELOCITIES

All results which are given in the following are values which have been obtained during continuous operation within the test section, which during these experiments had a diameter of 10 cm.

In figure 33, as an example, a few wind profiles are given which have been obtained at different pressures. Figure 34 shows in which pressure-velocity range the wind tunnel can be operated in our present setup. Each point in this figure gives the value of the maximum velocity of one wind profile inside the test section and the

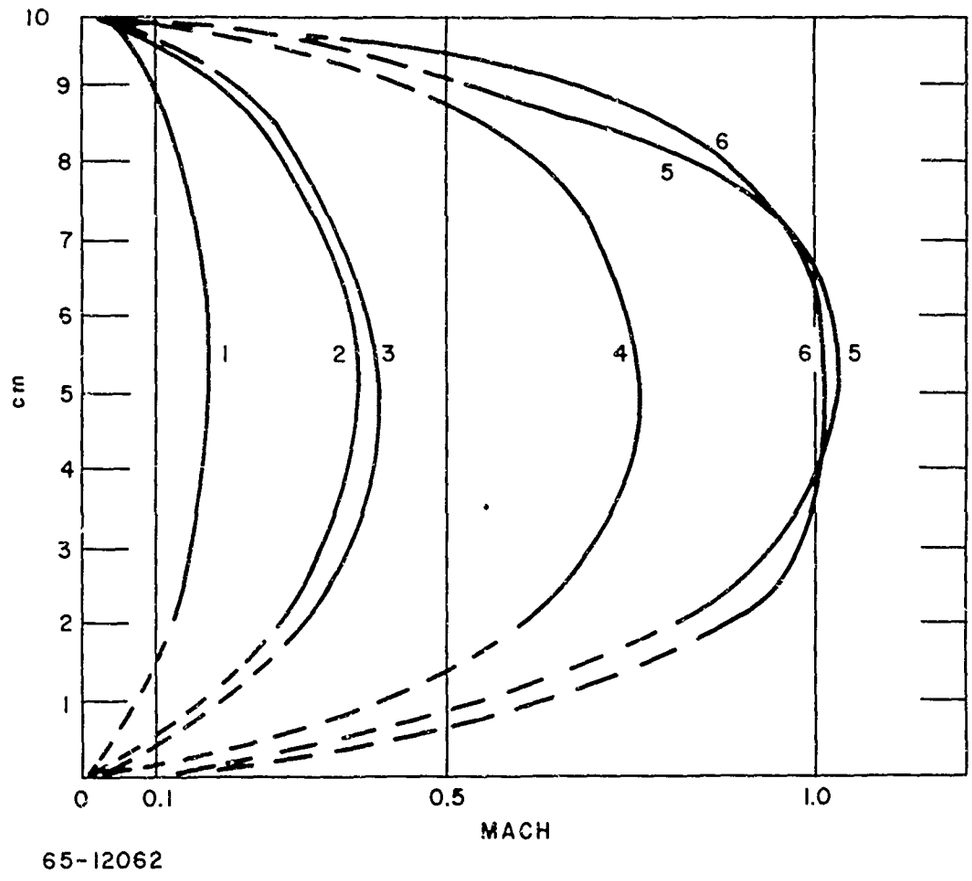

Figure 33 EXAMPLES FOR VELOCITY DISTRIBUTIONS IN PRESENT SET-UP OF TEST SECTION

(Each curve is obtained by 8 to 15 measurements and calculations.)

(1) static pressure 0.24 Torr, valves B21, B22, and C partially open

(2) static pressure 0.068 Torr, valves B21 and B22 partially open

(3) static pressure 0.35 Torr, valves B11 and C partially open

(4) static pressure 0.034 Torr, maximum obtainable speed

(5) static pressure 0.16 Torr, maximum obtainable speed

(6) static pressure 0.28 Torr, maximum obtainable speed

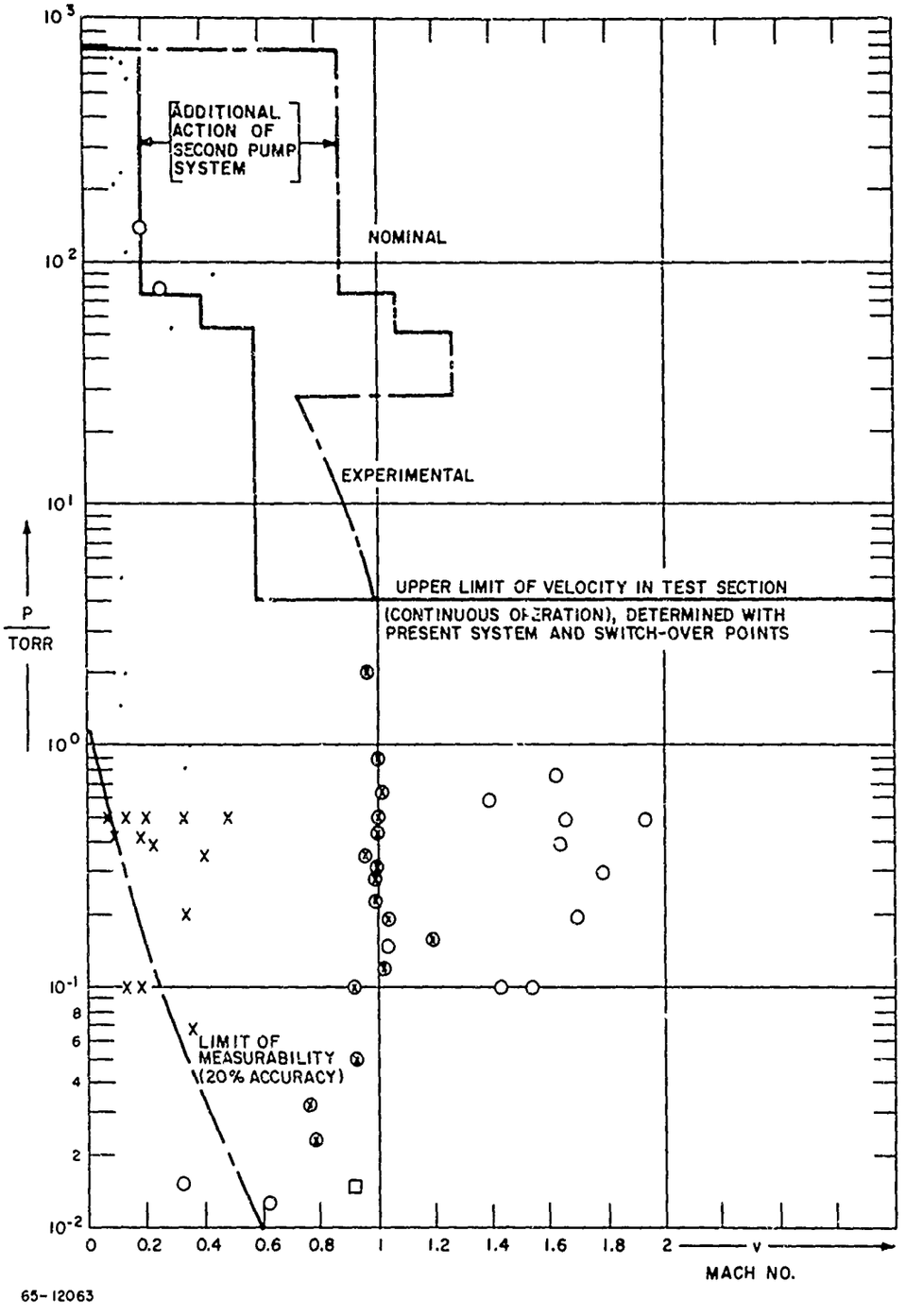

Figure 34 PV-DIAGRAM OF LOW PRESSURE WIND TUNNEL FOR CONTINUOUS OPERATION

(Points: Experimental values obtained under different experimental conditions)

corresponding static pressure. It can be seen that pressure and velocity can be regulated independently from each other. For example, at a static pressure of 500 millitorr (corresponding to a height of 55 km), a number of different wind speeds between 2 and 0.1 Mach have been simulated. Even much slower wind speeds as those given in this figure can be obtained at this static pressure. However, the accuracy of the velocity measurement becomes more and more inaccurate the lower the velocity of the streaming air.

The maximum wind speed which can be obtained with a given test section can be determined from the pumping speed of the pumps. The lines in figure 34 give the theoretical obtainable values. As can be seen only at pressures above 10 torr (corresponding to a height of about 30 km), the obtainable velocity is less than 0.3 Mach. Higher velocities in this pressure range can be obtained by operating an additional pump system (see figure 26).

As can be seen from these figures, in the present set-up of the tunnel and with the indicated test section, velocities up to about Mach 1 can be obtained for a continous operation in all pressure ranges. In the range between 10^{-2} and 10 torr, about Mach 2 can be reached.

Exact measurements of the higher velocities obtainable in a surge operation have not as yet been made.

2.2 MODIFIED GERDIEN CHAMBER, MODEL A, LABORATORY MODEL

2.2.1 INTRODUCTION

It has not been possible to find a method for measuring the wind speed in the GERDIEN chamber without introducing probes into it. The production of visible smoke balls traveling in the air stream ceased to be feasible for pressures below 0.4 torr. The introduction of probes into the chamber proper whould have disturbed the electric field in it and thus prohibited the intended measurements. For this reason, it was necessary to construct a "dummy model" with exactly the same dimensions but without the electrical parts. Aerodynamic probes (Pitot tubes) have been inserted in the dummy model. While a velocity profile was obtained in the dummy model, a second velocity profile was measured some 50 cm downstream of it. Then the dummy model was replaced by the chamber proper, and the wind velocity at the second, downstream location, was set as before. It was then assumed that the velocity profile in the chamber was the same as in the privious dummy model.

2.2.2 MODEL A

The dimensions of the laboratory model (Model A) have been chosen on the basis of earlier instruments. The receiving as well as the driving electrode have each been divided into 16 highly insulated and gold-plated parts. Thus it is possible to exchange their functions.

A cross section, which is nearly accurate with respect to sizes, has been shown in figure 10 (section 1.4.1). The first set of rings, 00 to 07, was added after the initial experiments, because it turned out that the edge effect across the ion gate (rings 13-14), created by the potential differences between 12 and 14 as well as between 15 and 13, increased the number of entering ions of one polarity and decreased that of the other polarity. This was immediately avoided, after the additional rings had been mounted, together with a "sleeving" of the aging section of the wind tunnel in which the ions were generated. Thus, the ions did not "see" any electric field prior to entering the free volume in the chamber proper.

In figure 10 (section 14.1.), data on the material used to construct the chamber are given as well.

Figure 35 shows the assembled chamber*. To reduce capacity, the outer electrodes have been used as receiving electrodes; they could be connected to the feedthroughs of the wind tunnel with the shortest length. Figure 36 shows the chamber mounted to the cover plate of the test section of the wind tunnel, and

*The individual parts of Model A, prior to assembly, have been shown in figures 2a, 2b, and 2c of Quarterly Progress Report No. 1 (1963) of the same contract.

Figure 35 MODIFIED GERDIEN CHAMBER, MODEL A, ASSEMBLED
(The 16 connections to the outer electrodes are seen on top. Seventeen wires are connected to the three sets of front rings and come out above. The 8 connections to the aft rings are seen coming out behind the 16 outlets. The 16 wires, Teflon insulated, connecting the inner electrodes, exit in the rear.)
P9619D

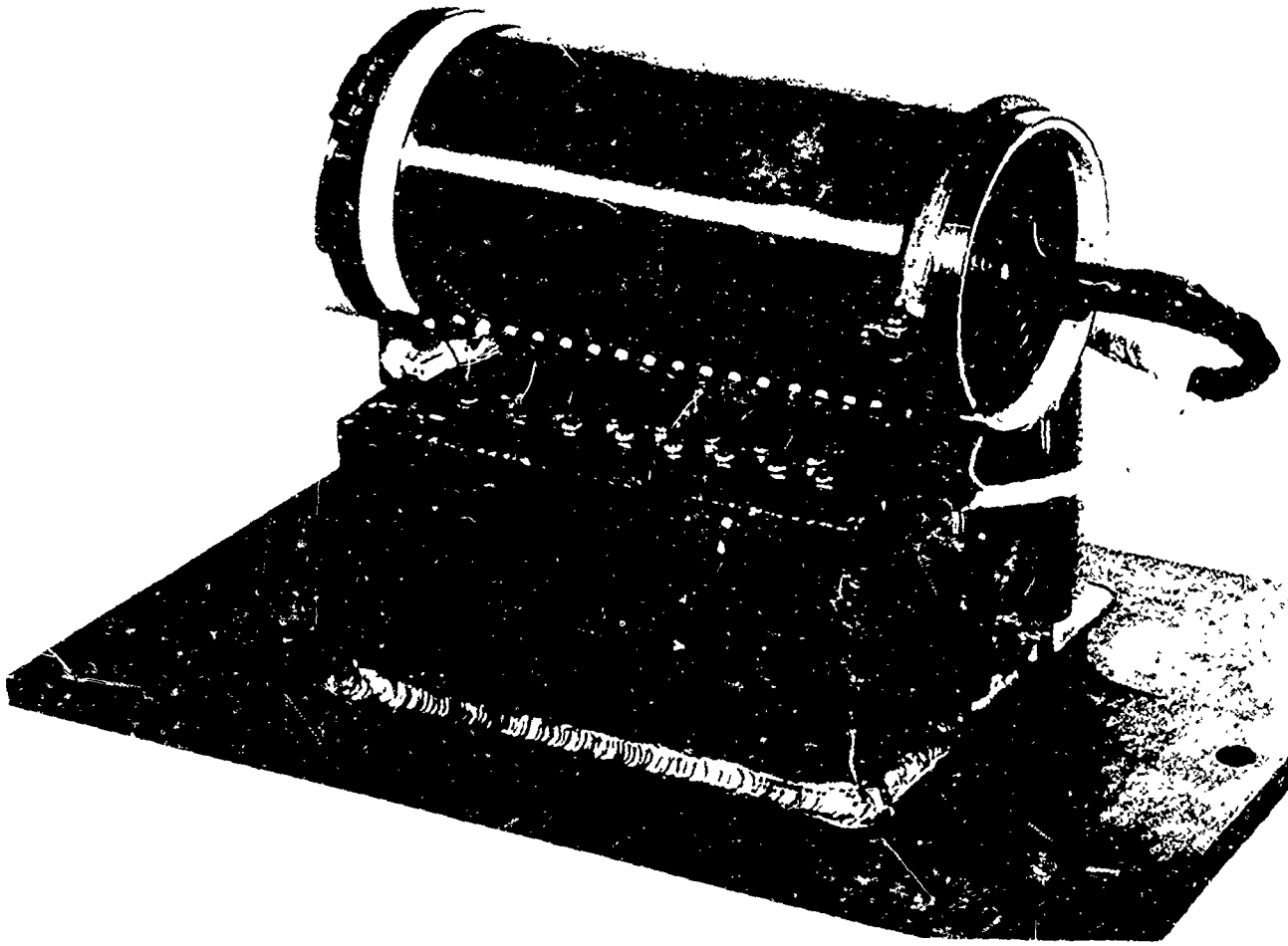

Figure 36 MODEL A OF MODIFIED GERDIEN CHAMBER MOUNTED TO THE COVER PLATE OF THE WIND TUNNEL. HIGHLY INSULATED VACUUM TIGHT FEED-THROUGHS CONNECT THE SIXTEEN OUTER ELECTRODES OF THE CHAMBER TO THE ELECTROMETERS OUTSIDE OF THE WIND TUNNEL

in figure 37 one sees, above, the extremely highly insulated feed-throughs for the receiving electrode and the box for inserting the electrometers, and, below, the inputs to the driving electrodes and the rings and to the shields of some critical connections.

Figure 38 shows the dummy model mounted on its cover plate for the wind tunnel, with one set of Pitot tubes inserted. Another set of Pitot tubes has been shown in figure 30 (section 2.1.4).

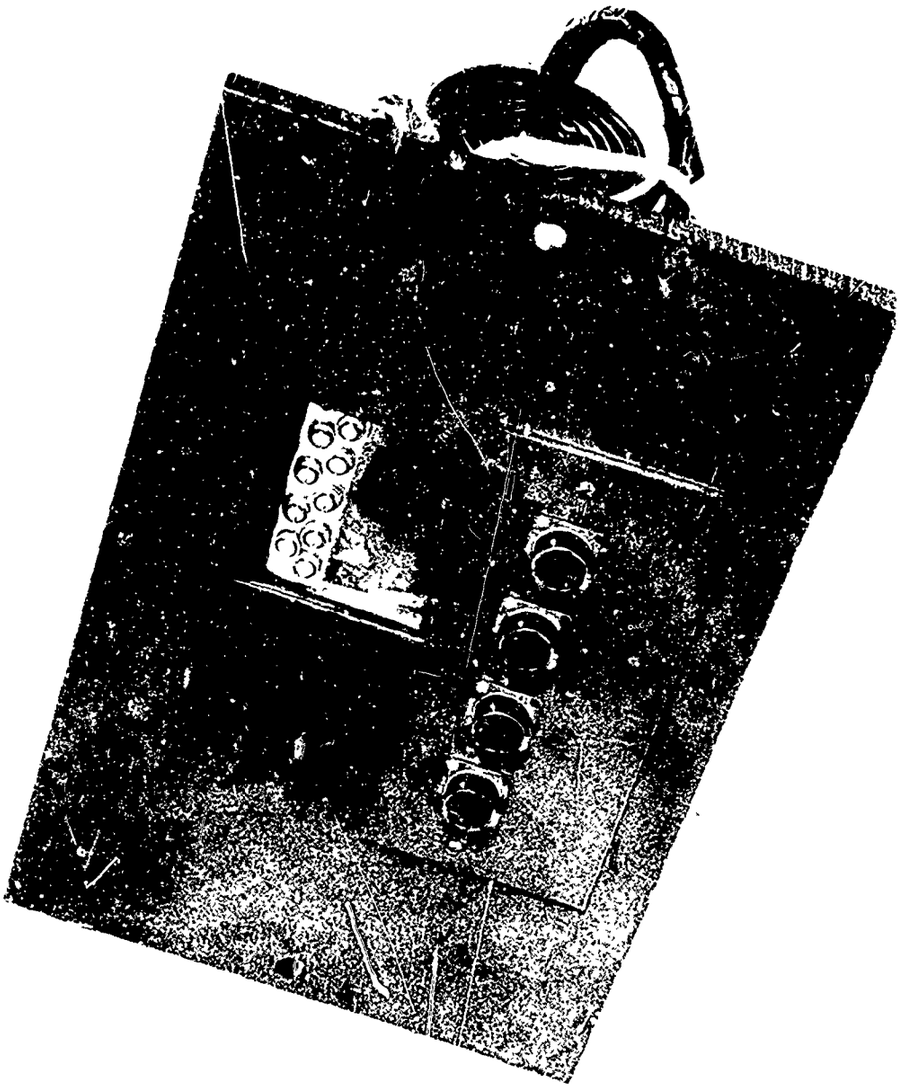

Figure 37 COVER PLATE OF TEST SECTION OF WIND TUNNEL WITH THE MODEL A OF THE MODIFIED GERDIEN CHAMBER MOUNTED BEHIND IT
(above: Box for insertion of electrometers, below: 5 x 19 connections to electrodes and rings and shields of chamber below.)
P12363C

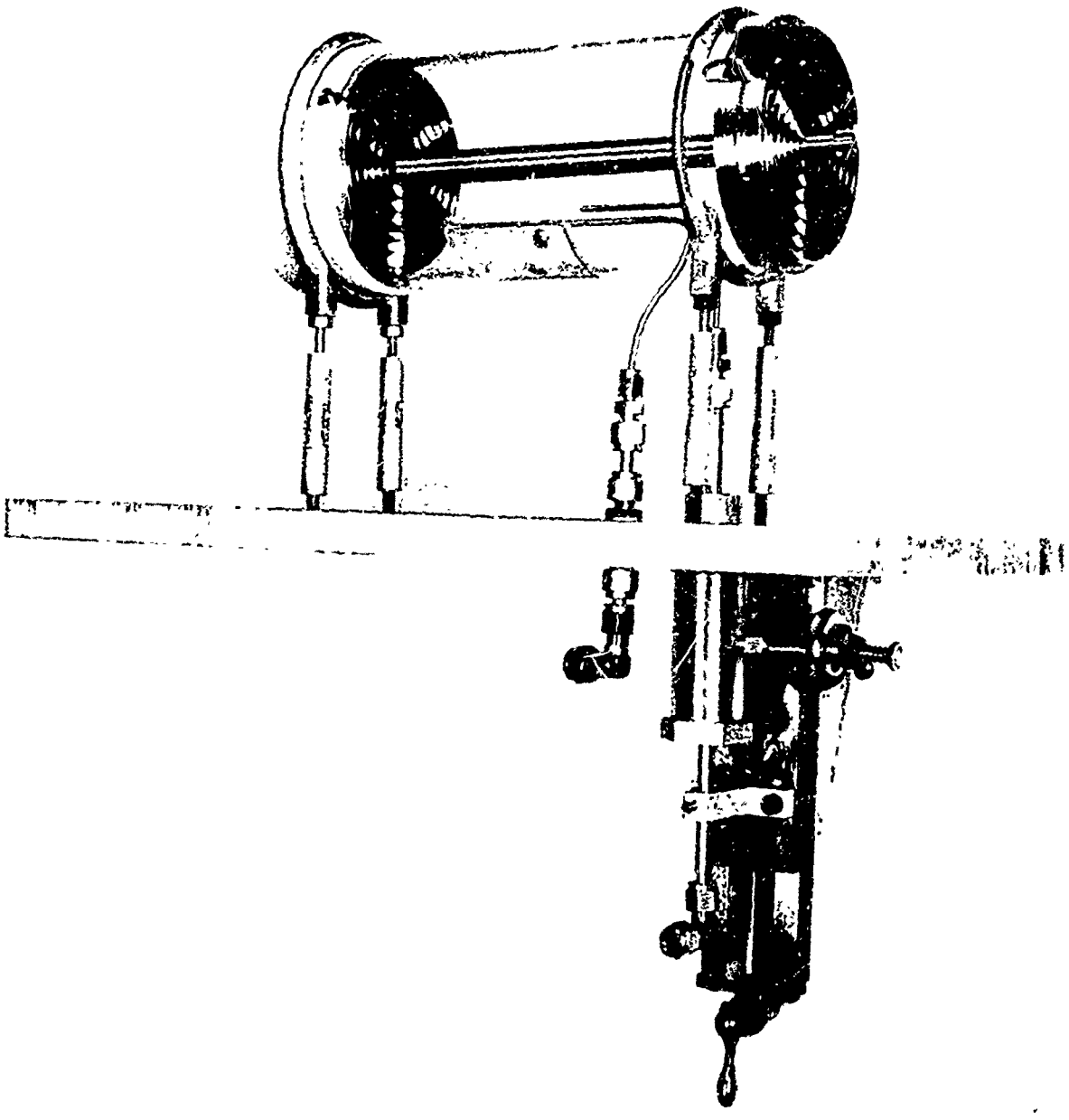

Figure 38 DUMMY MODEL OF MODEL A MODIFIED GERDIEN CHAMBER MOUNTED ON A COVER PLATE FOR TEST SECTION OF WIND TUNNEL
(Two Pitot tubes are inserted, one of which can be moved radially from outside.)

P12147A

2.3 SUPPLY AND AMPLIFICATION

2.3.1 PROVISION OF SUPPLY VOLTAGES

The modified GERDIEN chamber, Model A, has 16 receiving electrodes (which may be used in any combination, down to just 1) plus 48 other electrodes (including rings) to which a maximum of 29 different potentials plus the "ground" potential must be provided. Except for the ground potential, all these potentials are functions of time. Of these potentials, 27 are sine wave potentials oscillating versus ground as their zero line, one is a sine wave plus a superimposed constant potential, and another one is a sine wave plus superimposed constant potential plus superimposed square wave pulses, triggered by the sine wave. In addition, a sine wave with a 180-degree phase shift must be provided for the cancellation of the main displacement current (see section 1.4.5 and figure 17).

The capacitive load for the supply units is considerable, since the generator for the ion gate pulses, including its power supplies, and the "sleeving" of the aging section of the wind tunnel must follow the sine wave variations without delay. For this reason, a specific powerful supply for ring 24 was provided.

For the experiments in the laboratory, it was desirable to be able to vary the supply to every electrode, if possible, independent of the potential applied to other electrodes. Also, independent measurements with voltmeters and oscilloscopes of each of these potentials was desired. The final schematic of the overall supply system is given in figure 39, which, if taken together with figure 10, hardly needs explanation. Figure 39 also contains the schematic for serving the electric valves of the wind tunnel (see section 2.1.2 and figure 29). Figure 40 shows the special rack for the generation of the supply voltages. The related power supplies, however, have been mounted on the racks shown in figure 32 (section 2.1.4.) and located in some distance to avoid electromagnetic disturbances from them. A careful grounding system, using own grounders free of any noise in a loop connection, and grounding leads poor in capacitance and inductance as well as resistance, is essential.

2.3.2 AMPLIFICATION OF THE SIGNAL FROM THE RECEIVING ELECTRODES

The experiments conducted to find the best method for the amplification of the signal coming from the receiving electrodes, and thus for the measurement of numbers of electric charges, are not reported here. In part, they have been described by DOLEZALEK and OSTER (1964).

For the measurement of dc voltages or currents the following methods have been applied:

The LINDEMANN-Electrometer by Spindler & Hoyer

SUPPLY CIRCUIT FOR MODIFIED GERDIEN CHAMBER
FEBRUARY 1965

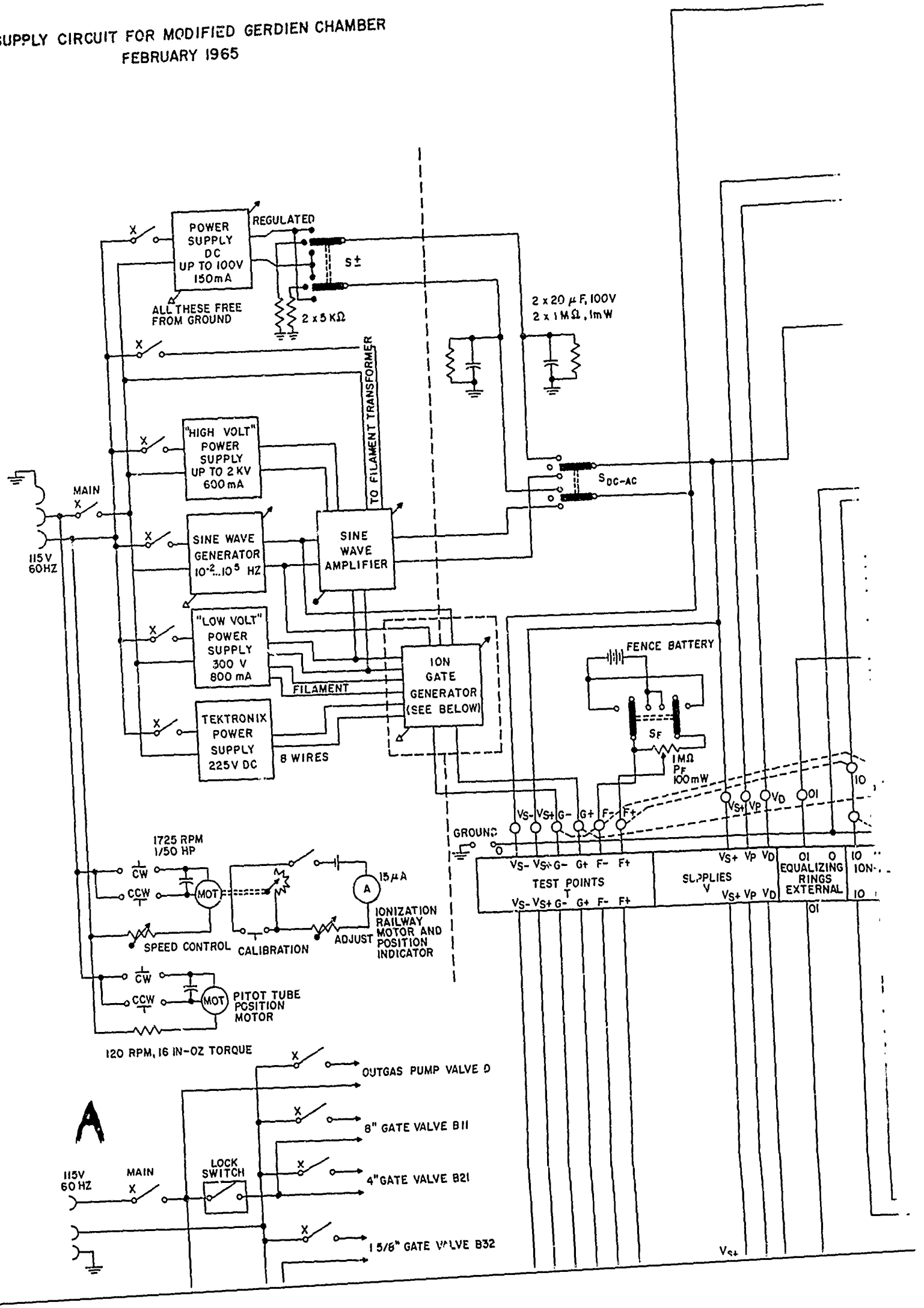

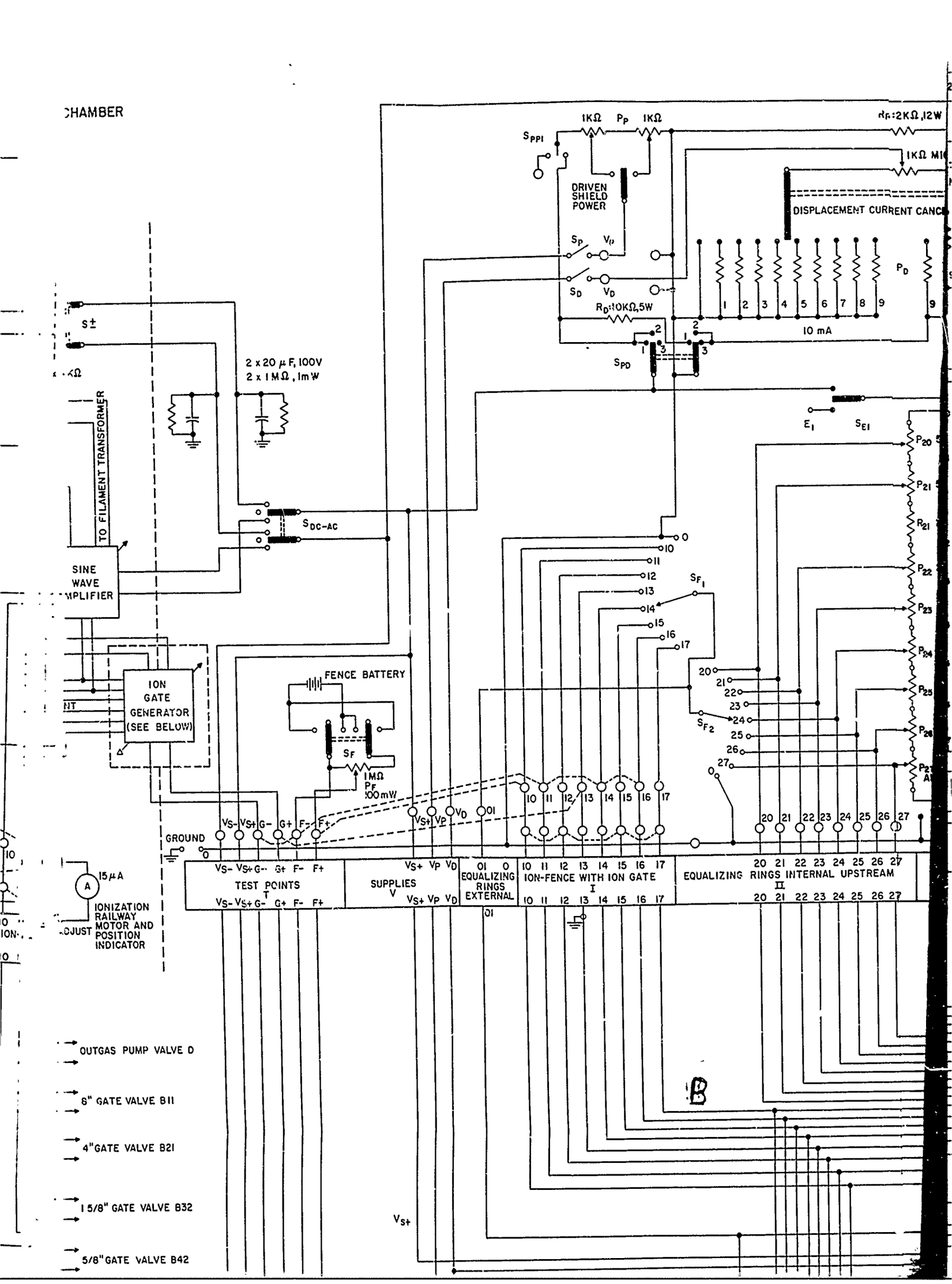
CHAMBER
1KΩ P_P 1KΩ
S_PPI
DRIVEN SHIELD POWER
DISPLACEMENT CURRENT CANCE
S_P V_P
S_D V_D
R_D:10KΩ,5W
P_D
10 mA
S_PD
S±
2 x 20 μF, 100V
2 x 1 MΩ, 1mW
TO FILAMENT TRANSFORMER
S_DC-AC
SINE WAVE AMPLIFIER
ION GATE GENERATOR (SEE BELOW)
FENCE BATTERY
S_F
1MΩ
P_F
E_1
S_E1
S_F1
S_F2
P_20
P_21
R_21
P_22
P_23
P_24
P_25
P_26
GROUND
Vs- Vs+ G- G+ F- F+
Vs+ Vp VD
01
10 11 12 13 14 15 16 17
20 21 22 23 24 25 26 27
TEST POINTS T
SUPPLIES V
EQUALIZING RINGS EXTERNAL
ION-FENCE WITH ION GATE I
EQUALIZING RINGS INTERNAL UPSTREAM II
15 μA
IONIZATION RAILWAY MOTOR AND POSITION INDICATOR
OUTGAS PUMP VALVE D
6" GATE VALVE B11
4" GATE VALVE B21
1 5/8" GATE VALVE B32
5/8" GATE VALVE B42
B

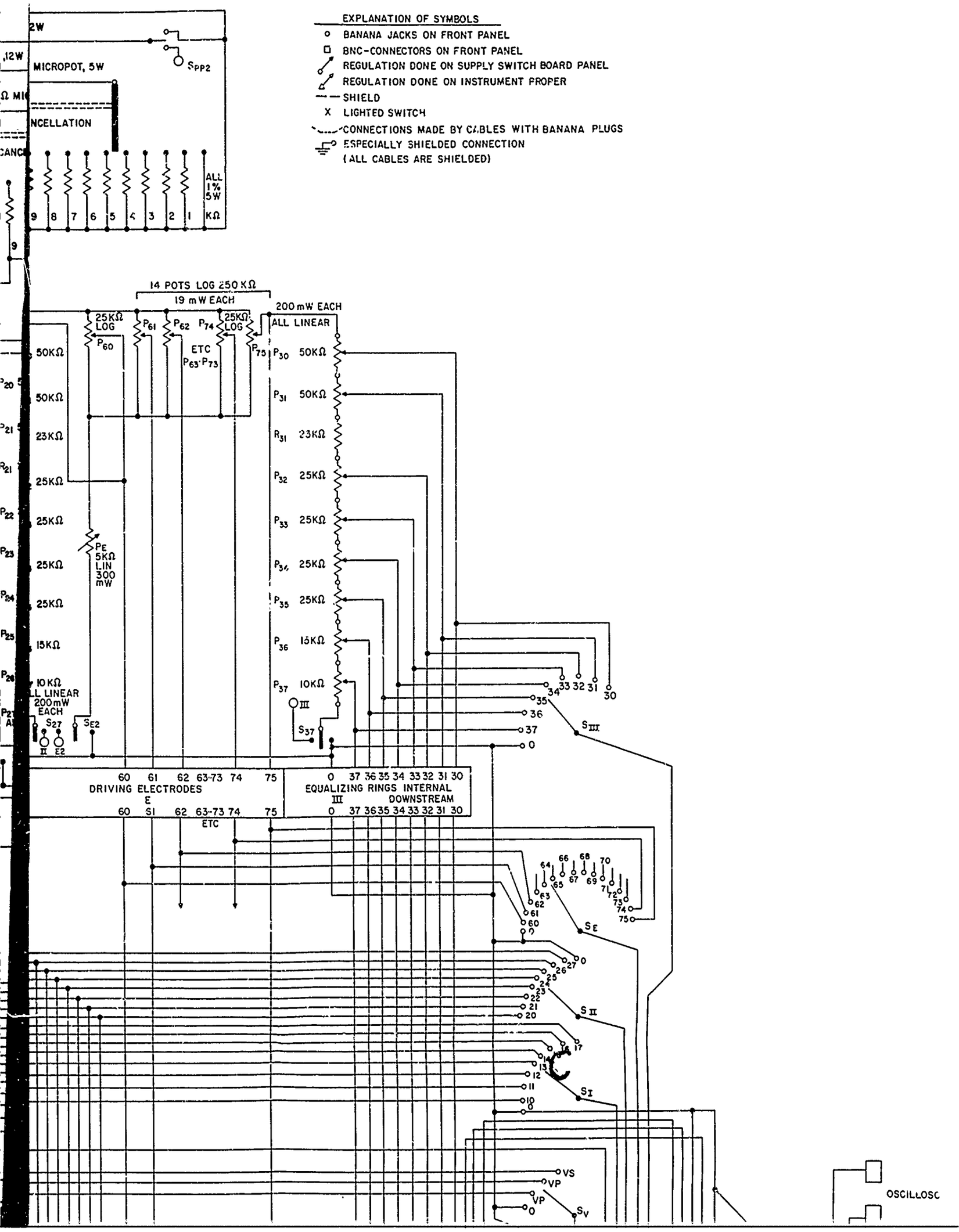
EXPLANATION OF SYMBOLS
BANANA JACKS ON FRONT PANEL
BNC-CONNECTORS ON FRONT PANEL
REGULATION DONE ON SUPPLY SWITCH BOARD PANEL
REGULATION DONE ON INSTRUMENT PROPER
SHIELD
LIGHTED SWITCH
CONNECTIONS MADE BY CABLES WITH BANANA PLUGS
ESPECIALLY SHIELDED CONNECTION
(ALL CABLES ARE SHIELDED)
MICROPOT, 5W
ALL 1% 5W
9 8 7 6 5 4 3 2 1 KΩ
14 POTS LOG 250 KΩ
19 mW EACH
200 mW EACH
ALL LINEAR
25KΩ LOG
ETC
50KΩ
23KΩ
25KΩ
15KΩ
10KΩ
5KΩ LIN 300 mW
DRIVING ELECTRODES
EQUALIZING RINGS INTERNAL
DOWNSTREAM
ETC
OSCILLOSC

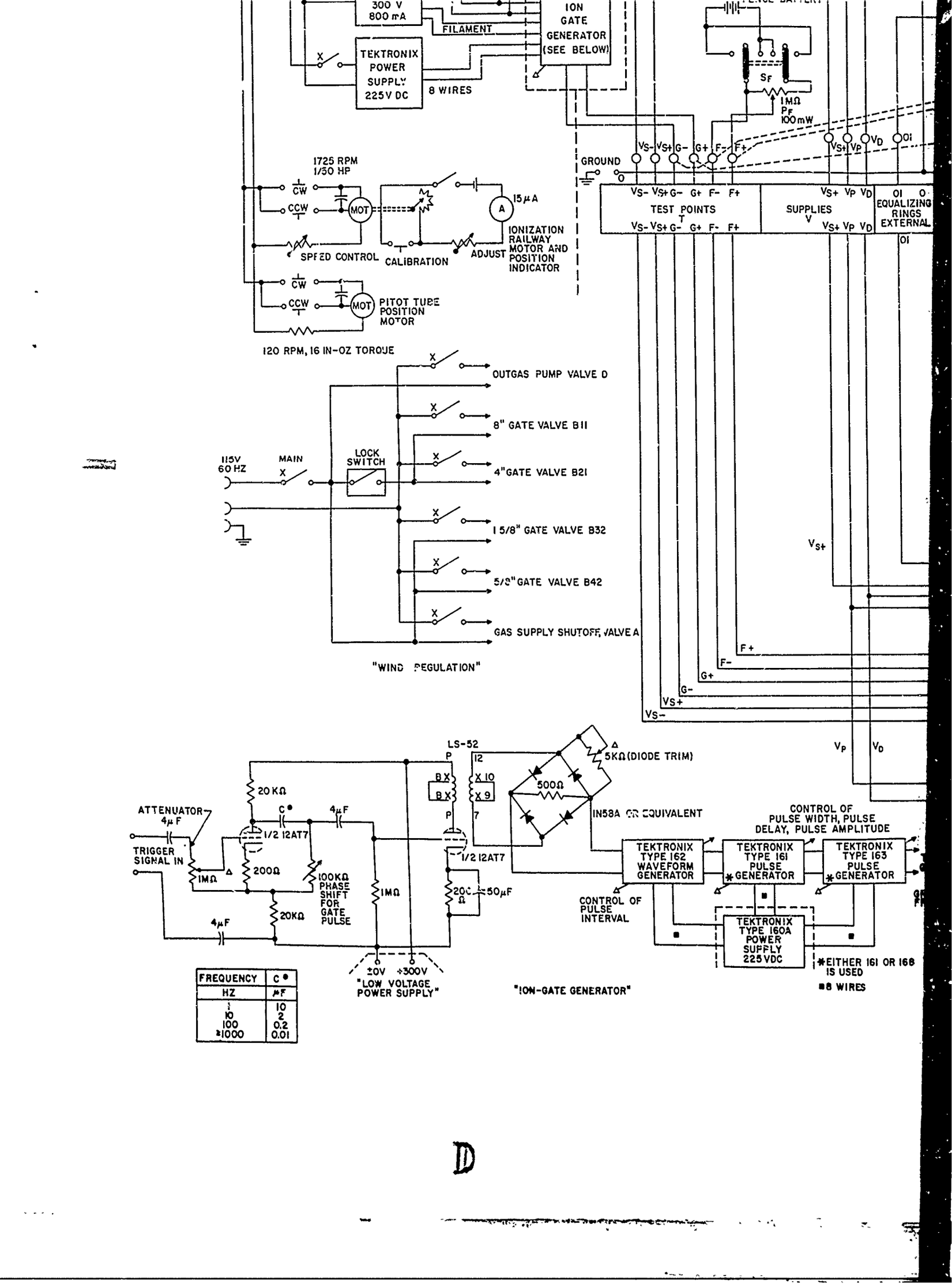

FREQUENCY	C ●
HZ	μF
1	10
10	2
100	0.2
≥1000	0.01

D

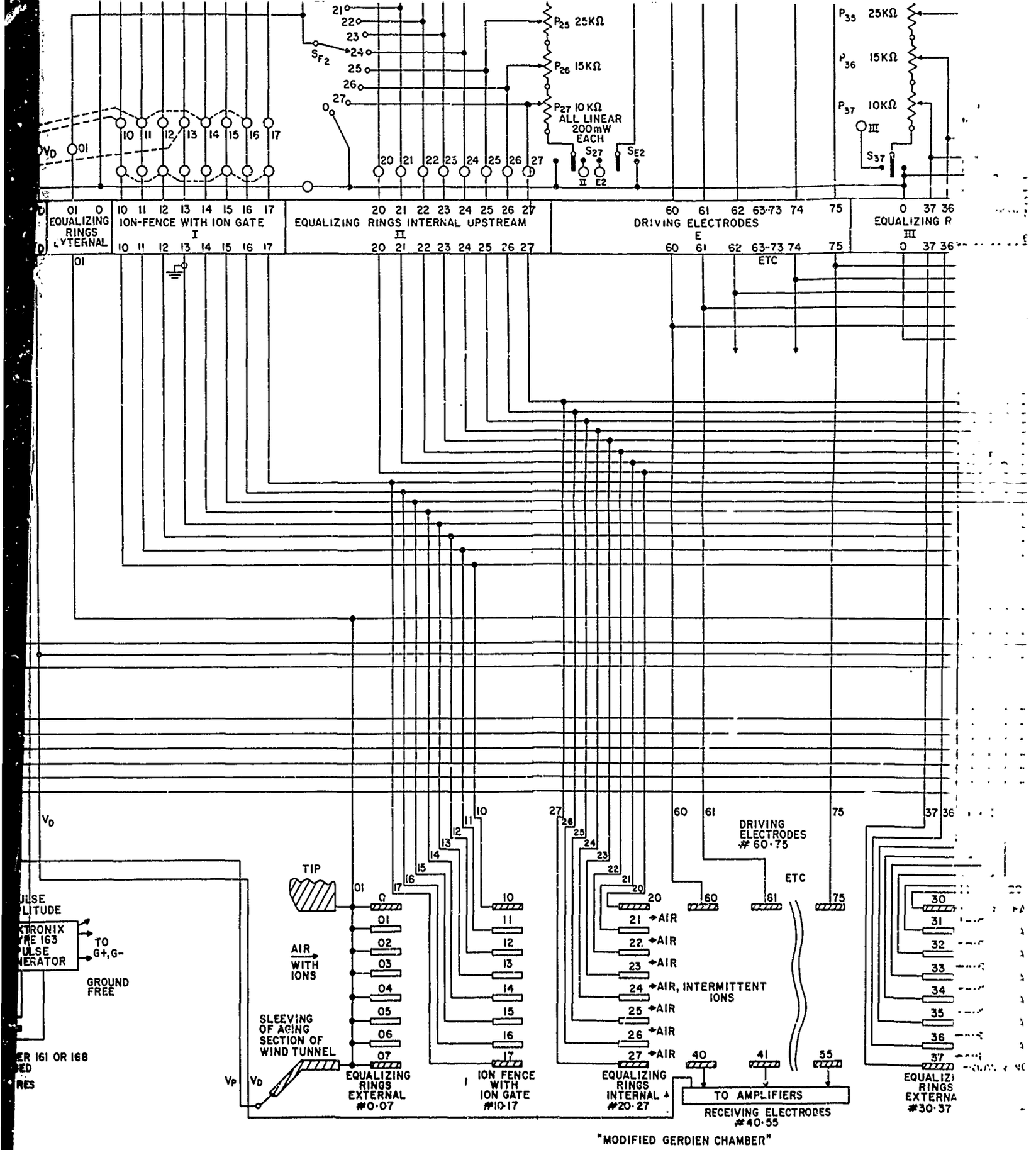

Figure 39 TOTAL SUPPLY SYSTEM FOR MODEL A OF THE MODIFIED GERDIEN CHAMBER

E

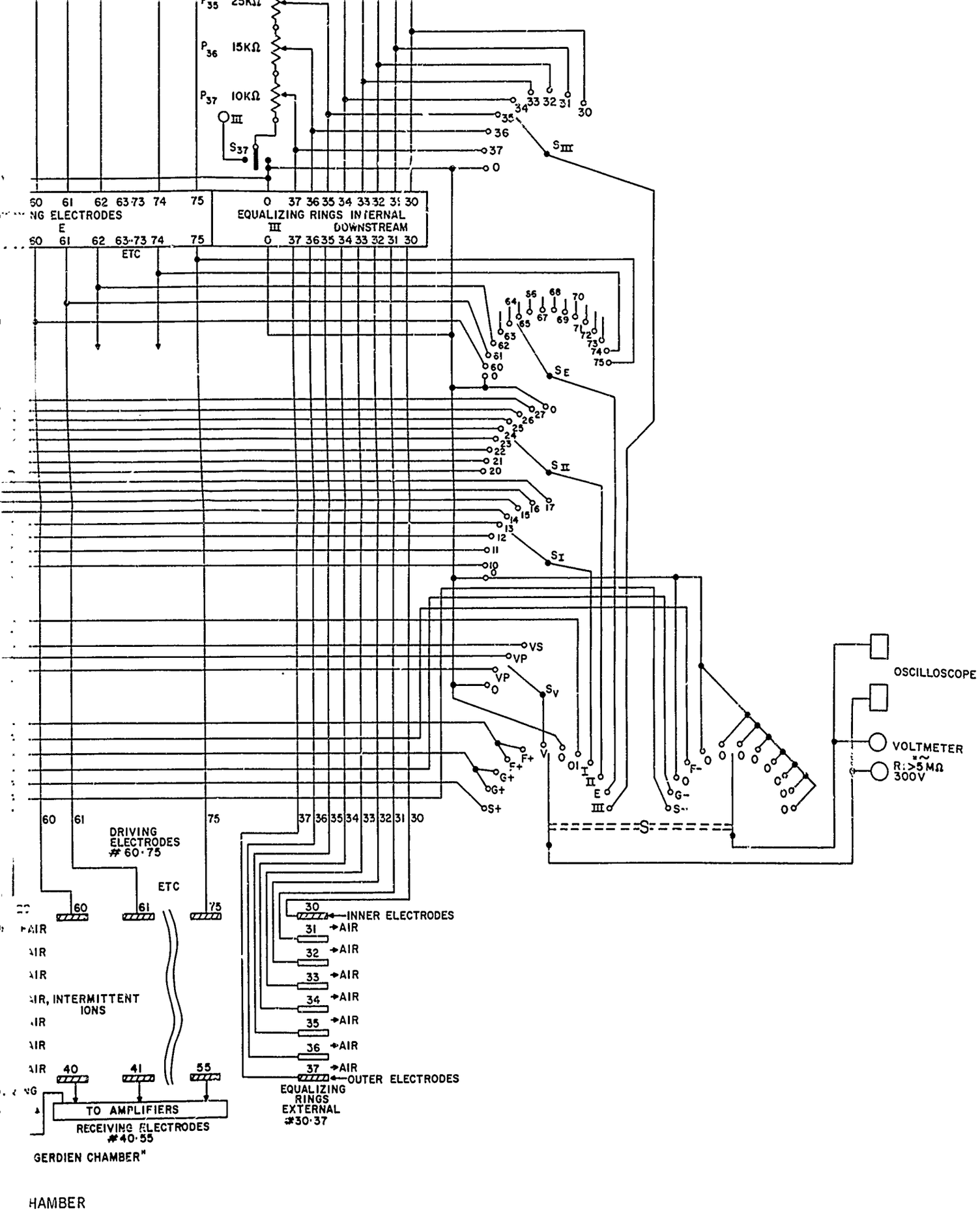
P35 25KΩ
P36 15KΩ
P37 10KΩ
III
S37
33 32 31 30
34
35
36
37
0
SIII
60 61 62 63-73 74 75
NG ELECTRODES
E
60 61 62 63-73 74 75
ETC
0 37 36 35 34 33 32 31 30
EQUALIZING RINGS INTERNAL
III
DOWNSTREAM
64 66 68 70
65 67 69 71
63 72
62 73
61 74
60 75
0
SE
0
27
26
25
24
23
22
21
20
SII
17
16
15
14
13
12
11
10
0
SI
VS
VP
VP
0
SV
F+
G+
V
0
01
I
II
E
III
F-
G-
S-
S+
S
OSCILLOSCOPE
VOLTMETER
R i>5MΩ
300V
60 61
DRIVING
ELECTRODES
#60-75
75
37 36 35 34 33 32 31 30
ETC
60
61
75
30
INNER ELECTRODES
31
32
33
34
35
36
37
OUTER ELECTRODES
AIR
AIR
AIR
AIR, INTERMITTENT
IONS
AIR
AIR
AIR
AIR
40
41
55
EQUALIZING
RINGS
EXTERNAL
#30-37
TO AMPLIFIERS
RECEIVING ELECTRODES
#40-55
GERDIEN CHAMBER"
HAMBER

F

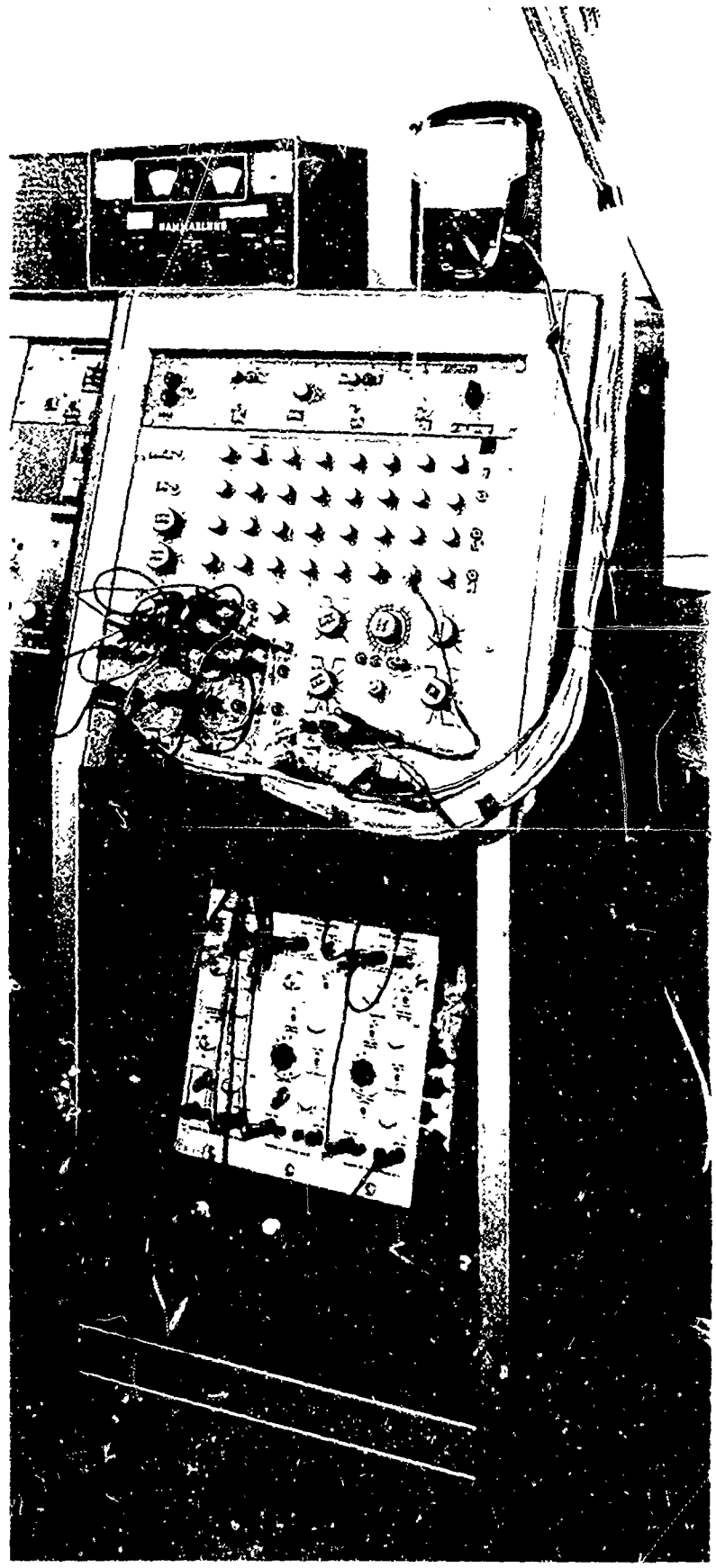

Figure 40 RACK FOR THE PROVISION OF SUPPLY VOLTAGES TO THE RINGS AND ELECTRODES FOR THE MODEL A MODIFIED GERDIEN CHAMBER
(The lower part, recessed for shielding purposes, is the pulse generator for the ion gate.)

P12769B

The Electrostatic Voltmeter by Trüb, Täuber & Co.

The Cary 31 Vibrating Reed Electrometer by Applied Physics Co.

A Valve Electrometer of the straight-forward bridge circuit type (after DOLEZALEK 1956, 1961).

For the ac measurements, the following methods were used:

The Bridge-Electrometer, after DOLEZALEK, with a sensitive double beam oscilloscope.

The Admittance Neutralizer by Micronia Corp. with oscilloscope

A combination of electrometer input stage, operational amplifier by Philbrick Co., and a 10^{12} Ohm feedback, following the schematic by SAPUPPO (1964).

The schematic of the DOLELALEK bridge electrometer has been shown by DOLEZALEK and OSTER (1964). There also the basic schematic of the SAPUPPO electrometer is presented. The actual schematic applied in our measurements is given in section 3.2.3. (figure 55, sheet 2) below, while calibration results are presented in figures 41, a and b. The results represented in figure 41b have later on been improved toward better sensitivity.

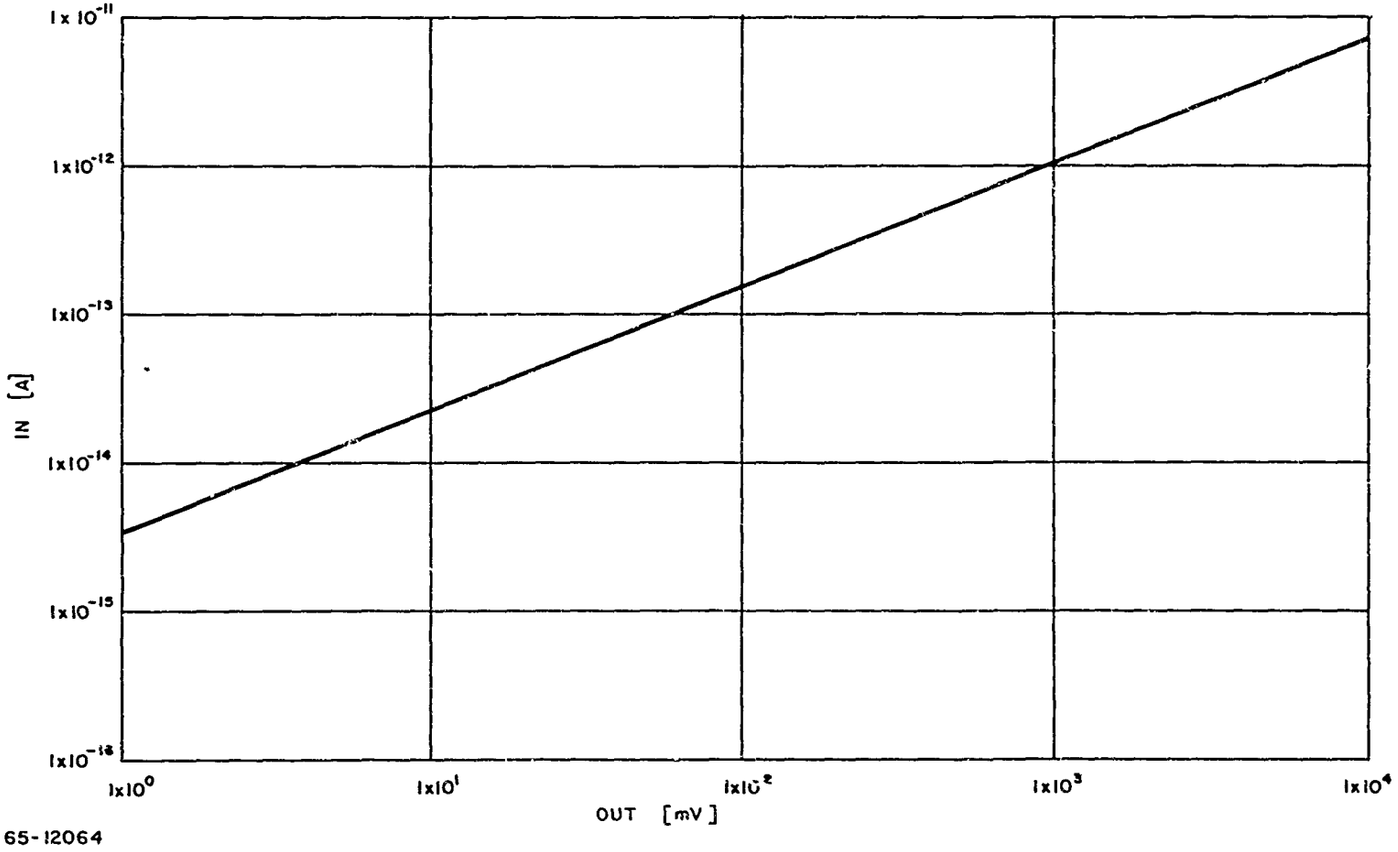

Figure 41a CALIBRATION CURVE OF THE ELECTROMETER AFTER SAPPUPO (1964), WITH A FEEDBACK RESISTOR OF 10^{12} OHM, AND AN IMPUT SERIES RESISTOR OF 10^{10} OHM - DC OPERATION

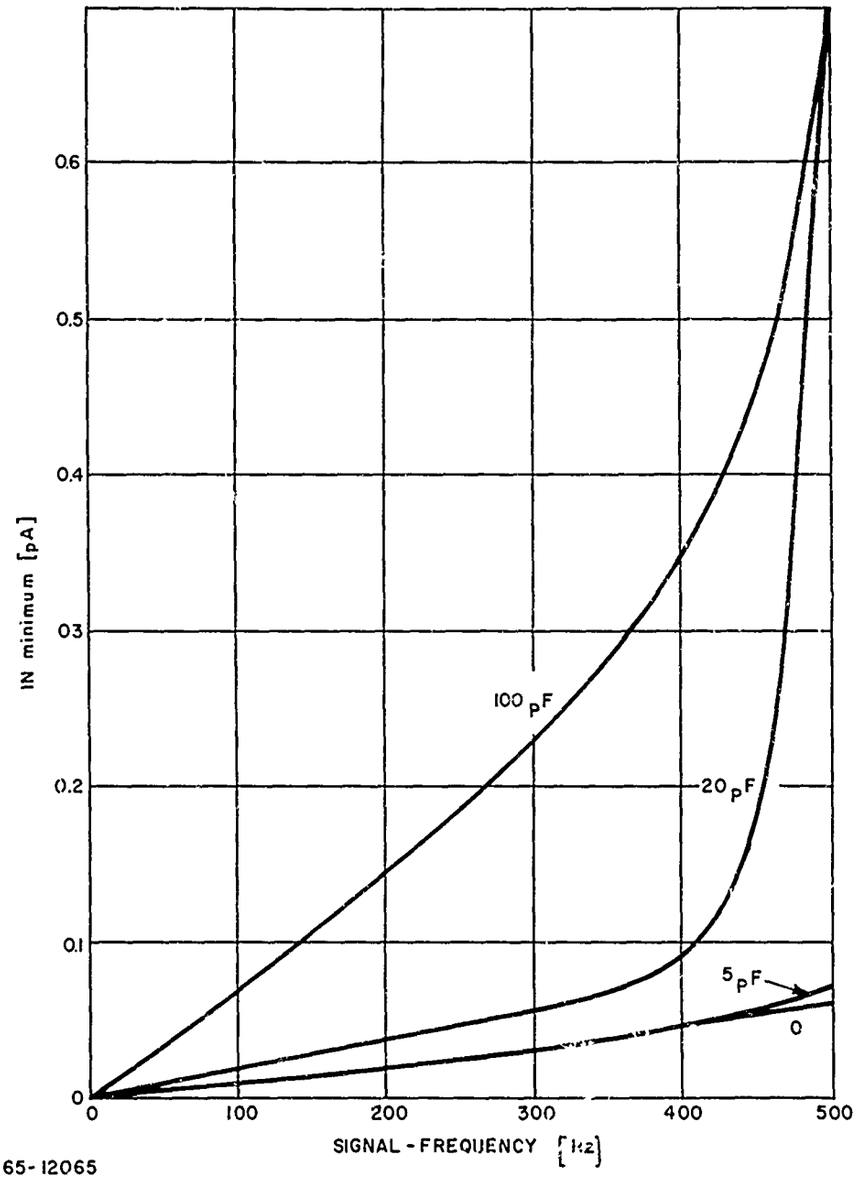

Figure 41b MINIMUM INPUT a.c. CURRENT, WHICH STILL GIVES A READABLE OUTPUT OF 70 mV FROM THE ELECTROMETER, AFTER SAPPUPO, WITH $\Delta\ 10^{12}$ OHM FEEDBACK RESISTOR

The curves present the minimum measurable current as a function of frequency and of input capacitance between zero (i.e., only the natural capacitance of the input) and 100 x 10^{-12} Farad (i.e., in addition to the natural input capacitance).

2.4 LABORATORY EXPERIMENTS

2.4.1 INTRODUCTION

In this chapter, laboratory experiments which have been conducted to determine the characteristic features of the modified GERDIEN chamber and to measure mobility spectrum of ions generated artificially in air (from pressurized bottles) are reported . A report on experiments for the design and improvement of the wind tunnel and the facilities to measure pressure and air velocity in it, as well as on other supplementory experiments, such as generation of the supply voltages and pulse voltages, cancellation of displacement current, elimination of noise, and amplification of the signal is not given here. These experiments have been reported in the monthly and quarterly reports prepared for this contract.

2.4.2 INITIAL EXPERIMENTS

After an extended measuring period used to determine all insulation resistances and all capacitances between the rings and electrodes in the modified GERDIEN chamber, at first, the so-called "GERDIEN characteristic" was measured. That is the current output of the chamber as a function of the applied driving voltage, measured in constant wind speed and with a constant ion supply. This was done under atmospheric pressure, in a FARADAY cage, with dc, and for four combinations of receiving electrodes. Here, the inner electrodes have been used as receiving electrodes. Figure 42 shows the result. For these experiments, the edge effect at the intake of the chamber was not cancelled (rings 00 to 07 had not yet been applied, and no sleeving was provided for the ion generation); for this reason, the right hand parts of the characteristics show the typical decrease of output with increasing driving voltage and thus increasing edge effect.

Next, an experiment was conducted to determine the maximum voltage applicable to the ion fence (or ion filter, rings 10 to 17) without causing corona discharge. The result, presented in figure 43, corresponds to the well-known PASCHEN curve, and may be explained by the fact, that the length of the cathode fall increases with decreasing gas density, and that a self-sustained gas discharge cannot occur without the provision of this length. In the experiments, the onset of corona discharge was determined by measuring electrometrically the current between the two involved rings.

Then, preliminary ion spectra have been measured in the low-pressure wind tunnel, under relatively high pressure and applying a dc driving voltage to all driving electrodes, which were interconnected. Here, the outer electrodes have been used as driving electrode. The result is shown in figure 44. Air pressure in the wind tunnel was about 2 torr, corresponding to 40 km.

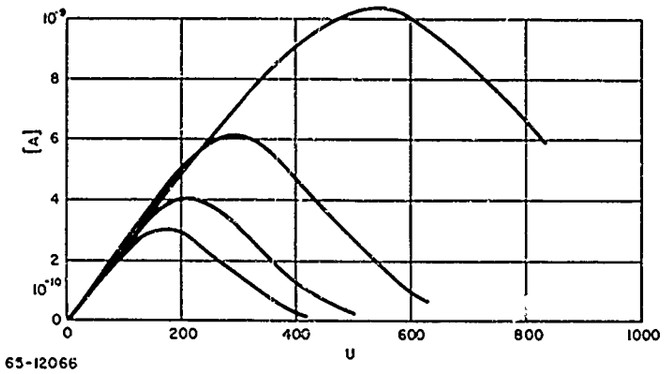

Figure 42 DC GERDIEN CHARACTERISTICS
(Atmospheric pressure, artificial ionization of laboratory air. Receiving electrode of modified GERDIEN chamber divided into four parts of equal length; abscissa: driving voltage; ordinate: current from Receiving Electrode. The maxima of current are shifted to smaller driving voltages with increasing distance of receiving electrode from front-(upstream) end of chamber.)

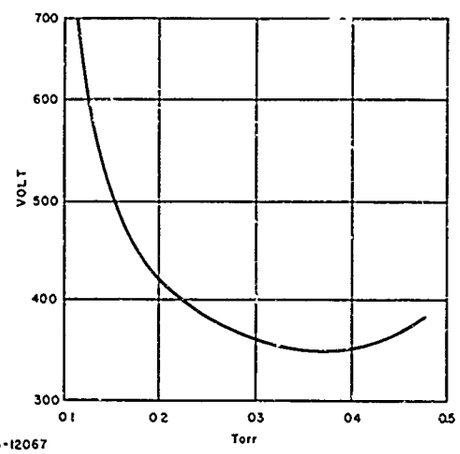

Figure 43 ONE EXAMPLE FOR THE ONSET OF CORONA DISCHARGE BETWEEN TWO ADJACENT COAXIAL RINGS AT THE INTAKE OF THE MODIFIED GERDIEN CHAMBER

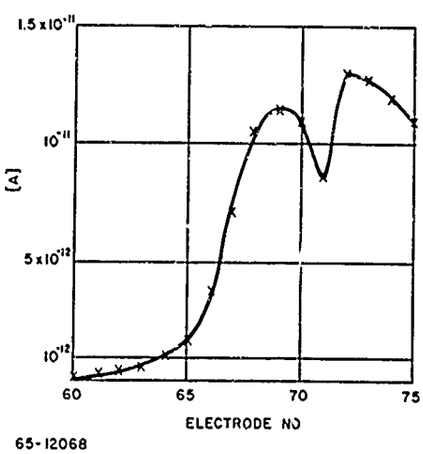

Figure 44 RELATIVE ION SPECTRUM OBTAINED WITH DIFFERENTIAL ION COUNTER OF THE SECOND ORDER AND DC DRIVING VOLTAGE

The driving voltage, equal for all driving electrodes, was +10 V. The ion fence was closed. The ion gate was kept open all the time; it was located between the fourth and fifth of the coaxial rings, counted from the inner electrode, including the ring which is flush with it. The wind velocity was very high, about the speed of sound. Because of the edge effect, the numbers at the ordinate of figure 44 should be taken only as relative ones.

The abscissa shows the receiving electrodes which have been measured one by one--a total of 16 electrodes. The first electrode counted from the upstream (front-) end has number 60, the last one at the rear end of the chamber has number 75. Thus, with increasing numbers of electrodes, the mobility of intercepted ion decreases. It is obvious that ions with a still smaller mobility existed as well but have not been measured, since the driving voltage was not high enough for this wind speed. An increase of driving voltage was not attempted, since this would automatically increase the edge effect.

Experiments with ac driving voltages, applied in a great variety, have been conducted as well in the preparatory stage, and some of them have been used to derive information on the ion spectrum (see DOLEZALEK and OSTER, 1964). On this basis, the conditions for the actual laboratory measurements have been determined.

2.4.3 PROCEDURE FOR LABORATORY MEASUREMENTS IN THE WIND TUNNEL

By describing this procedure, the significance of the many different parameters discussed in this and in our earlier reports will become clearer.

At first an altitude to be simulated is selected, and the appropriate air pressure is derived from a table or curve. Then, a reasonable wind velocity is chosen, based on parachute flights with instruments made by previous workers and recalling that it is possible to reduce the wind velocity inside the chamber, but hard to increase it if the fall velocity must be kept below the speed of sound.

For the selected altitude, a range of expected ion mobilities is estimated, extending between k_1 and k_2. From these values, the U/ω values are determined. For the case of a plate condenser with distance y_1 between the plates, and distance y_1 between the ion gate and receiving electrode, the equation $2 U_k/\omega = dk/y_1$ is easily derived, where U_k is the driving voltage measured from zero to peak. For the present model of modified GERDIEN chamber, the U/ω value can be taken directly from figure 15 in section 1.4.4. Thus, two U/ω values are determined, corresponding to maximum and a minimum expected mobility (k_1 and k_2).

The driving voltage frequency will be the same for all electrodes, while the amplitude U will increase along the axis of the chamber. For the determination of the frequency, we use the equation $\omega > 2\pi v/\Delta x$, where v is the wind speed, and

Δx the length of one partial receiving electrode. This equation is obvious from the fact that at least one full cycle of driving voltage should occur while an ion is passing in front of one partial receiving electrode. Only then are we sure that it will reach this electrode, and the ion with the next smaller mobility will reach the next electrode. Thus, we get a minimum frequency, and now with our two U/ω values, two minimum voltages for the first and the last driving electrodes. In fact, we shall apply this higher voltage to the driving electrode which is next to last, and apply a much higher voltage to the very last electrode order in to ensure that all ions are intercepted. Then the intermediate voltages are selected to follow either an arithmetical or geometrical series or some other sequence.

The next steps aim at the determination of opening time τ of the ion gate. Unfortunately we are not completely free to select this time, if the effective length of the ion gate l and the length of the partial receiving electrodes Δx are of the same order. To understand this, see equation $\omega > 2\pi v/\Delta x$ and equation III from figure 9 in which we set $q = \tau/T$, and take the case that the second right-hand side member is small (E sufficiently large):

$$\omega < \frac{2\pi v q}{l}$$

By inserting our minimum frequency ω, derived from wind speed and length of receiving electrodes, into equation III we determine l, the fraction of opening time of ion gate to the full cycle of driving electrode, and can set our ion gate pulse generator accordingly (consider, however, the significance of length as discussed above).

We are now ready to perform the measurement. At first we determine whether sufficient ions are created by using the modified GERDIEN chamber as an ion counter with a large dc driving voltage, then we determine the actual length of ion gate as indicated above, and apply the calculated driving voltages and frequencies, and measure the current coming from each of the receiving electrodes.

2.4.4 DISCUSSION OF A RESULT FROM THE LABORATORY MEASUREMENTS

As discussed in section 1.4.2., the modified GERDIEN chamber can be operated in two ac modes: as a differential chamber of the first order, or as a differential chamber of the second order. The result of an experiment, made under otherwise equal conditions with these two modes, is shwon in figures 45 and 46.

For the measurement according to the differential chamber on the first order, all receiving electrodes have been connected as well as all driving electrodes. The driving voltage was swept, while the U/ω value was kept constant, and the current from the receiving electrode was measured. The results have been plotted, and the mobility spectrum has been derived by graphical differentiation. Unless the curve is a polygonic trace, it may be difficult to decide how many tangents can be put to it and where to place them. The more tangents one may reasonably apply, the better becomes the resolution but the accuracy suffers. In particular, it may be difficult to determine whether any smooth transition between straighter parts of the curve presents the existence of ions of intermediate

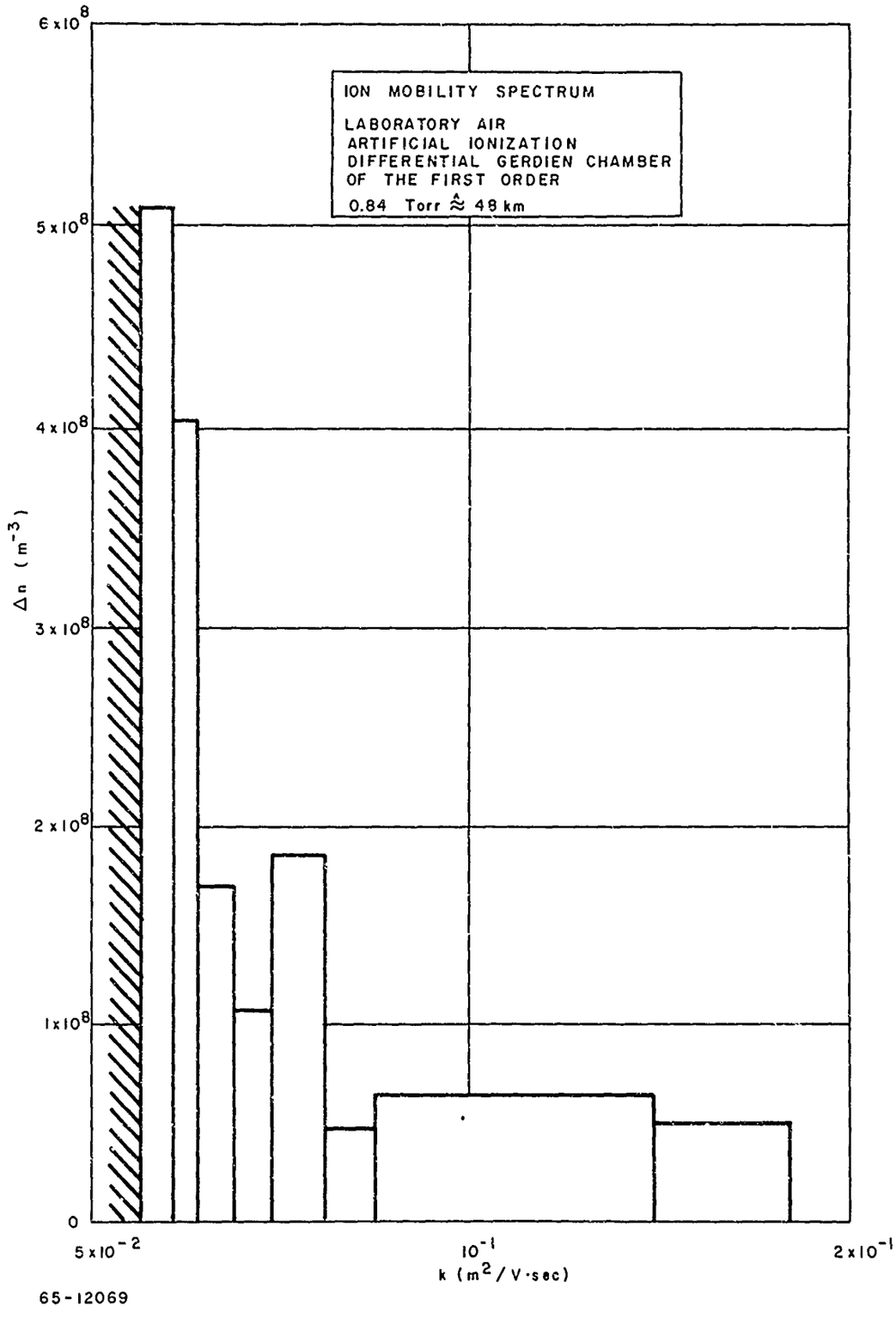

Figure 45 ION MOBILITY SPECTRUM IN THE LABORATORY
(Differential chamber of the first order; Pressure: 0.84 Torr)

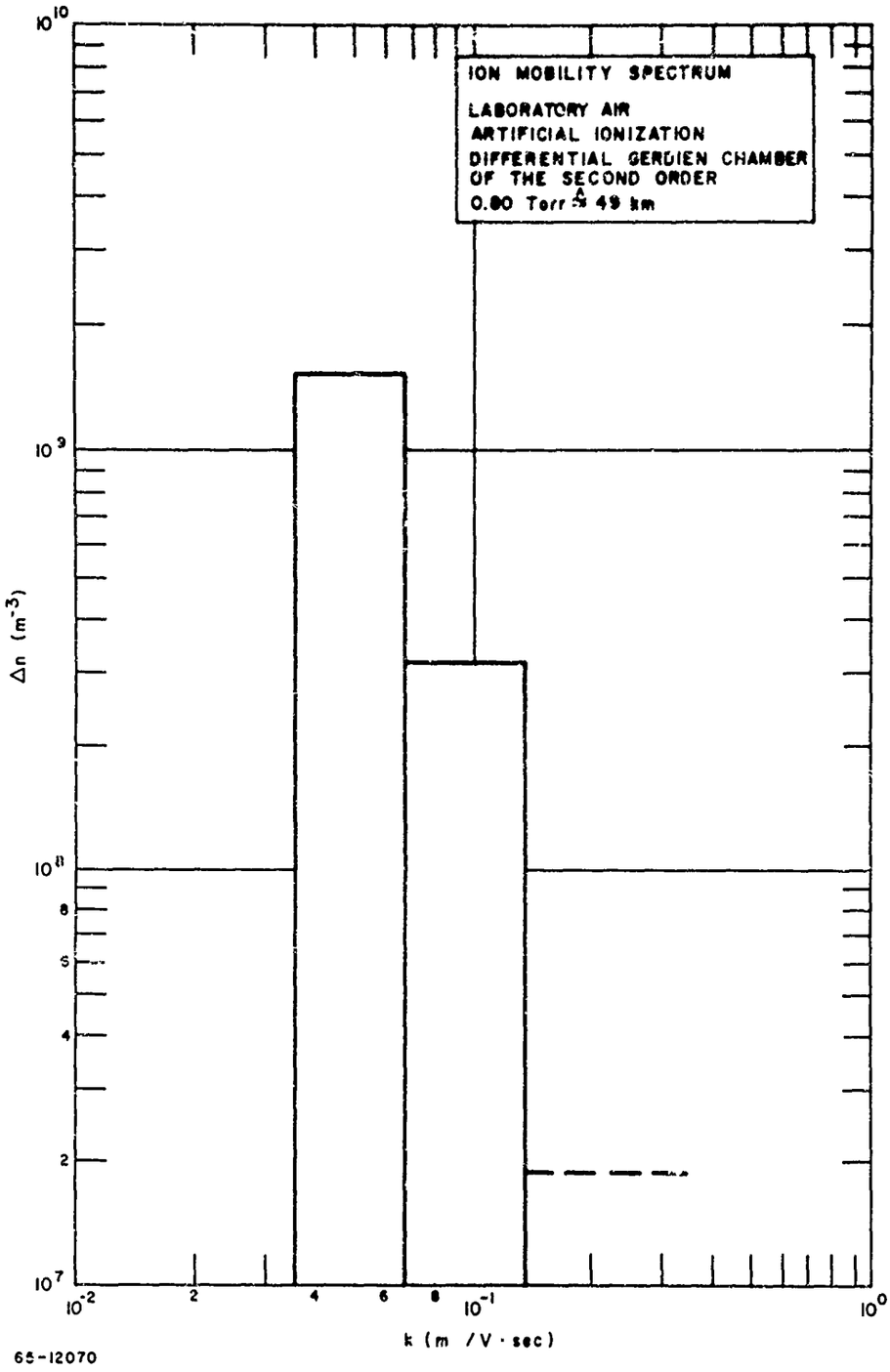

Figure 46 MOBILITY SPECTRUM (Differential chamber of the second order; pressure = 0.8 Torr.)

mobility or is just the result of the interception of ions straying because of diffusion. We decided to divide the curve into eight different slopes. The result is shown in figure 45.

For the measurement with the differential chamber of the second order, a smooth increase of driving voltage was applied by bringing different voltages in small steps to each of the 16 driving electrodes. The receiving electrodes have been divided into only three portions--5, 5, and 6 individual electrodes. Thus, the resolution is not better than given by this number of three, and it cannot be said where the upper limit of mobility was situated. On the other side, the accuracy is much better. The reliability of the measurement could be demonstrated by applying, e.g., the driving voltage responsible for one receiving electrode to the next one: no more ions were then intercepted there.

The number of ions per mobility range, of course, is determined to the degree of artificial ionization maintained in the wind tunnel during the experiments. Thus, the height of the columns in figures 45 and 46 does not give an information on natural conditions. However, if the two figures are compared to each other, it comes out that for the same mobility range the same number of ions was measured with the two methods, thus again confirming the reliability of the measurement.

If we compare the measured mobilities with the values expected for the height of about 50 km in the free atmosphere (see figure 47, which is plotted from table 202 in section 1.6.4, and table 103 in section 1.6.3.), we find that the coincidence is good. No attempt, however, was made to determine the chemical nature of the ions measured. The pollution of the wind tunnel seemed to be too great to allow a reliable determination, since no special precaution was taken to secure a completely dust-free air for these experiments.

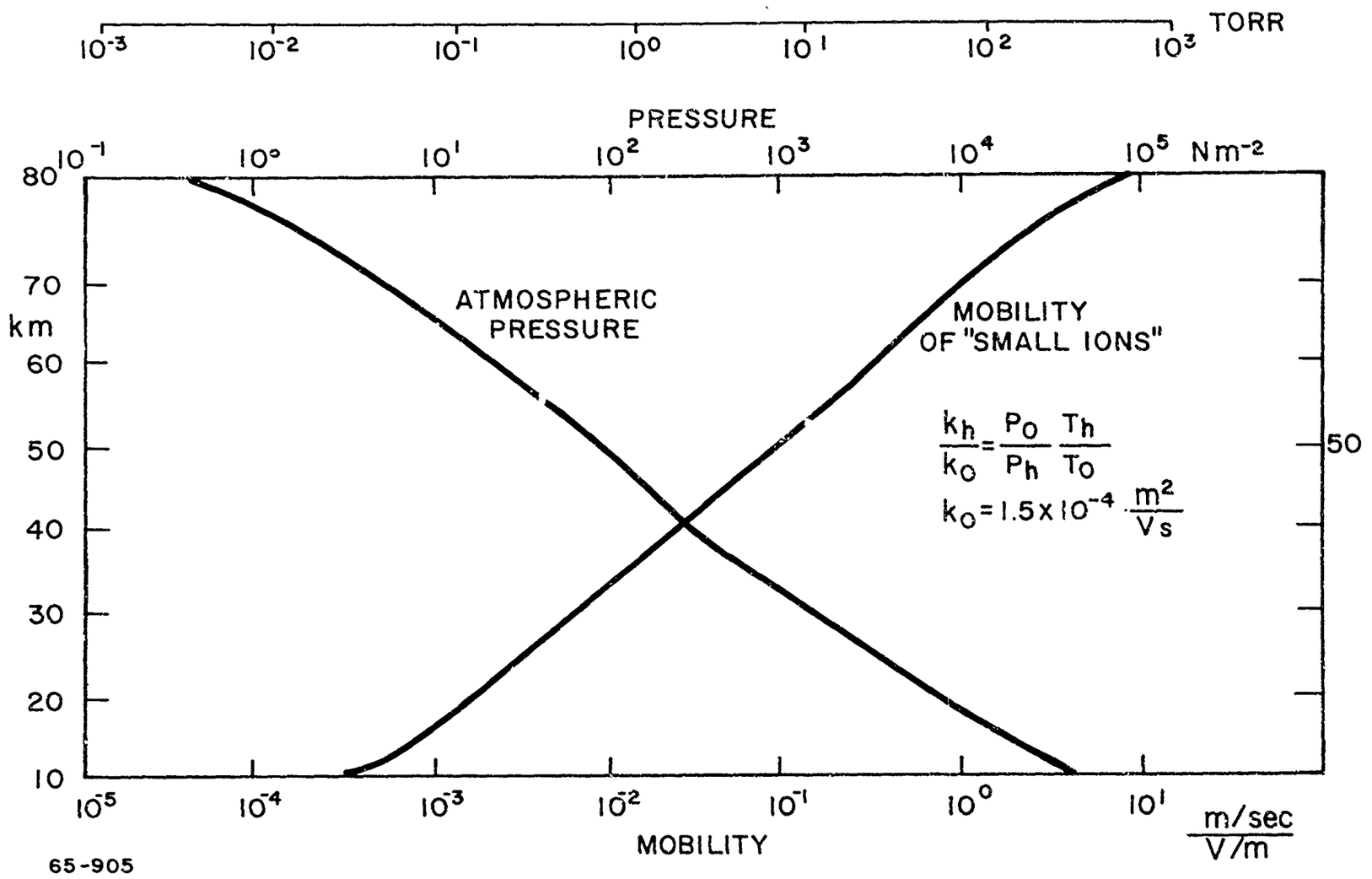

Figure 47 ESTIMATED MOBILITY VALUES FOR DIFFERENT HEIGHTS

PART 3

DESIGN OF ION-SPECTROMETER

3.1 DETERMINATION OF DIMENSIONS FOR MODEL B1

3.1.1 INTRODUCTION

Based on the theoretical considerations reported in Part 1 of this report, and on the laboratory experiments described in Part 2, the modified GERDIEN chamber or ion spectrometer for the measurements in the free atmosphere has been designed. While the actual measurements in the mesophere and upper stratosphere will be conducted by the instrument, falling down under a parachute from a height of about 80 km (to which it must be carried by a rocket), it is intended to execute at first a series of measurements in lower heights. It is supposed that the instrument will be carried to about 30 km by a balloon and then make the measurements while falling down under a parachute. Recovery is intended. Measurements in the lower stratosphere will be made by applying a dc driving voltage and using the instrument as a differential chamber of the second order.

With these intentions, it was decided to build the instrument proper (i.e., the receiving and driving electrodes, the aft rings, and the hull) to be suitable for the ac measurements at greater heights, but to attach the front rings which are suitable for dc measurements at lower heights. These rings can be replaced by the shorter rings for ac measurements, if the instrument is recovered in a good state after the dc measurements. The supply unit was constructed for the dc measurements, while the amplifiers will be the same ones for both series.

The general decision of the size of the chamber was derived from the considerations communicated in section 1.4.8 of this report. There it has been stated that the length of the individual receiving electrode must be greater than the length of the rings constituing the ion gate. Since we did not want to reduce the length of the ion gate very much, we had to make the receiving electrodes much longer than in Model A. This has the consequence that the overall length of the chamber also increased considerably; it is now about 90 cm.

The principal technological difficulty was given by the fact that the instrument should withstand accelerations of 300 g, which may occur in the process of ejecting the instrument with the parachute from the rocket. Another difficulty for measurements in the free atmosphere is given by the necessity of avoiding losses of insulation caused by the possible condensation of water vapor on the insulating surfaces, and of maintaining a constant temperature in the enviroment of the high-ohm resistors in the amplifiers which have a great temperature coefficient. To overcome these difficulties, a heating is provided: (a) for the maintenance of a temperature at the insulation surfaces slightly higher than that of the enviroment by covering the whole chamber with "heating blankets" (bifilar wiring to avoid magnetic fields), and (b) in the preamplifiers by a heater and a thermostat and a temperature probe. In addition, ample temperature insulation has been applied.

3.1.2 DETERMINATION OF DESIGN PARAMETERS

The inner electrode will serve as the driving electrode. It is divided into 45 individual rings, numbered 201 to 245, and insulated from each other. All rings are connected to wires, which are led out through the boring in the inner electrode and which lead to two connectors mounted on the outside of the chamber (but under the outer layer of thermal insulation). By plugging other connectors into them, which contain resistors, any distribution of driving voltages to the 45 individual electrodes can be supplied (see figure 55, sheet 6). For the dc experiment, all individual driving electrodes are interconnected.

The outer electrodes will be used as receiving electrodes. There are fifteen of them, but for the dc experiments they will be connected in groups, resulting in a number of only six actual electrodes. These receiving electrodes are mounted on very small teflon insulating stripes, so that most of the dielectricum between them and the outer hull is air. This was done to reduce the capacitance. To avoid conduction through the air between them and the outer hull, the backside of the receiving electrodes is covered with a thin layer of highly insulating material. The receiving electrodes are made of stainless steel. The preamplifiers will be mounted directly over the heating blankets which serve as the hull around the receiving electrodes. These heating blankets are covered with a highly conductive layer for electrostatic shielding.

Since, for a dc operation, no ion gate pulsation is needed, a number of adjacent rings of the three different sets at the upstream end can be electrically connected. In this case, they have been made simply of one piece. The rings of the ion fence or ion filter, numbered 11 to 16, are much longer than in Model A to avoid the otherwise necessary great fence voltages for the measurements in the lower stratosphere, which could give rise to corona discharges (see sections 1.4.7 and 2.4.2). The first set of rings, serving to reduce the edge effect, is numbered 01 to 06, while the third set at the upstream end and the set at the downstream end are numbered 21 to 26 and 31 to 36, respectively (see figure 53), all numbers counting from inward out.

3.1.3 DETERMINATION OF ELECTRICAL PARAMETERS

To derive the electrical parameters for Model B1, we started from figure 48, which presents the results of calculations, made on the basis of the geometrical dimensions of the chamber as well as on some assumptions on the air velocity inside the chamber. These calculations concerned the location of the receiving electrodes for different driving dc voltages, under the assumption of certain mobilities being theoretically representative for the different heights between 40 and 10 km. Since these mobilities have been theoretically extrapolated from measured values at much lower altitudes, they are rather unexact. For this reason, curves have been added, which correspond to mobilities being by factors of 3 either greater or smaller than the assumed values.

To arrive at the results of figure 48, at first certain calculations had to be made with respect to the air velocity inside the chamber. Based on the actual dimensions, and on a number of "pessimistic" presumptions, REYNOLDS' numbers have been calculated, and from these the maximum velocities may be determined by experiments in the wind tunnel. Table 1 gives these values.

TABLE 1

MAXIMUM AIR VELOCITIES IN A MODIFIED GERDIEN CHAMBER FOR LAMINARY FLOW
(Pessimistic Values for the Later Theoretical considerations)

Height (km)	Maximum Velocity Inside Chamber (m/s)
10	5.15
20	11.08
30	24.65
40	52.07

For the derivation of these numbers, a flat wind profile inside the chamber was assumed. A correction must be made after the flight, when the actual average velocities for any given pressure are known and the actual wind profile can be better estimated.

The curves of figure 48 suggest a subdivision of the 15 receiving electrodes of the chamber to the six planned electrometer amplifiers, according a geometrical series. It was decided to connect the amplifiers as shown in table 2.

TABLE 2

CONNECTION OF ELECTROMETER AMPLIFIERS TO RECEIVING ELECTRODES

Amplifier No.	Is Connected to Receiving Electrode No.
A1	101
A2	102
A3	103, 104
A4	105, 106, 107
A5	108, 109, 110, 111
A6	112, 113, 114, 115

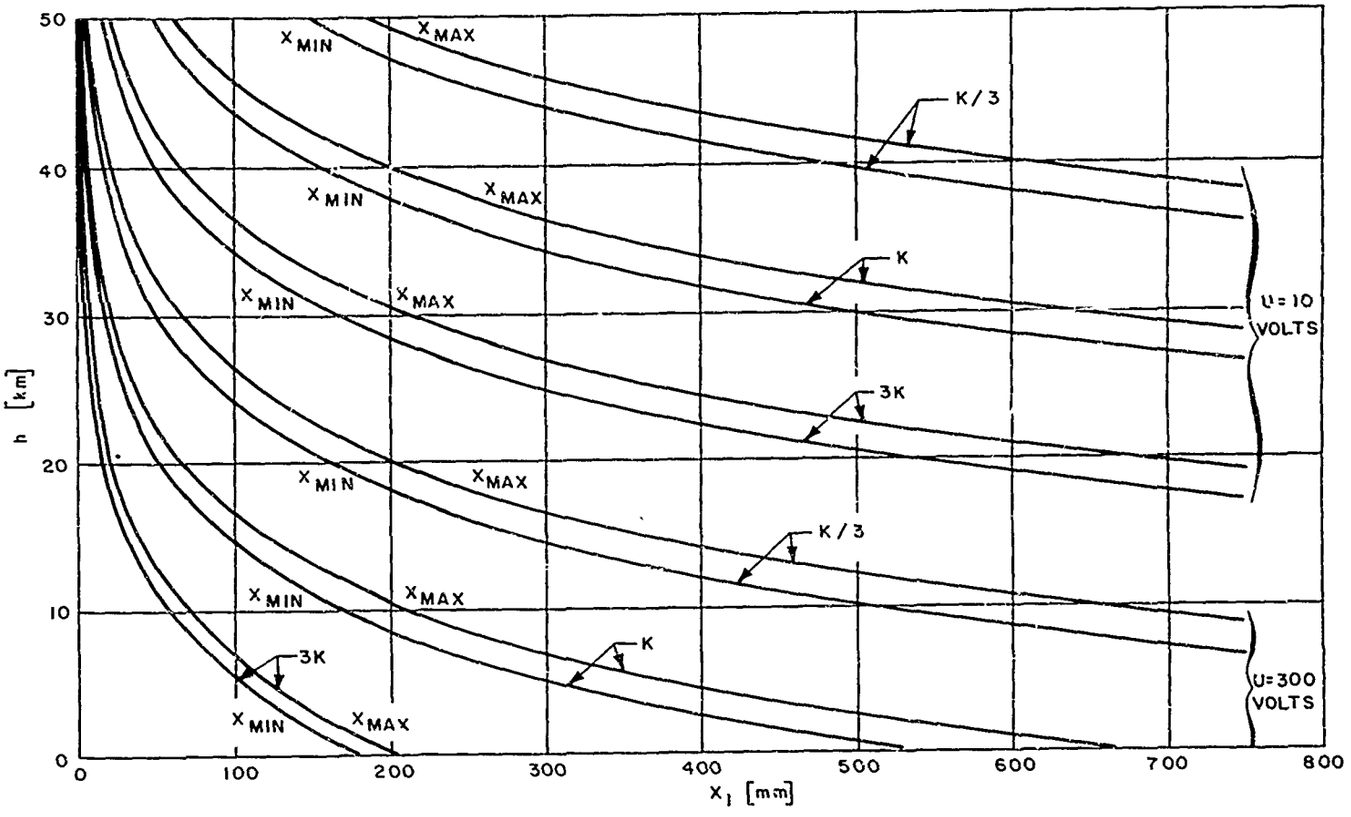

Figure 48 DETERMINATION OF LOCATION OF RECEIVING ELECTRODES

(For the mobilities, about expected for the altitudes indicated at the ordinate (according to table 202, section 1.6.4) and for the values of one-third and of three times K, the location of the receiving electrodes are shown for two different driving voltages. Minimum and maximum values are related to the finite width Δy of the ion gate -- calculated for dc operation in Model B1 and for supposed wind speeds).

It had been decided at an earlier time that the driving voltages for the dc experiment with the GERDIEN chamber would be stepped through the whole intended range over the whole altitude range of the flight. According to the curves of figure 48, 10 V would be a good value for the driving voltage in an altitude of 40 km, and 300 V would be good for 10 km. It was decided, however, to extend the range of driving voltages from 5 to 300 V, because this has the effect of increasing the dynamic range for the measurement of current coming from the receiving electrodes, at the lower end, by a factor of 2. Under these circumstances, and a subdivision of driving voltages according to a geometrical series, the values of table 3 have been chosen.

TABLE 3

DRIVING VOLTAGES FOR MODIFIED GERDIEN CHAMBER
(d. c. Experiment 5, 10, 25, 60, 140, 300 V)

Every voltage is applied simultaneously to all driving electrodes, Nos. 201 to 245, which are all interconnected for this particular experiment.

The next decision had to be made with respect to the "programming," the sequence and duration of switching processes. Two requirements had to be considered. At first, the commutator of the telemetry channel allows one measurement per channel each 0.2 second. Secondly, if one full cycle is accomplished in the time of 1 minute, we shall obtain one full cycle of measurements for the following falling distances:

TABLE 4

ROUGH VALUES FOR MEASURING CYCLES OF D.C. EXPERIMENT
(Starting from an Assumed Height of 40 Km)

40 ... 37 km
37 ... 35 km
35 ... 33 km
33 ... 31.5 km
31.5 ... 30.0 km
30.0 . 28.5 km
28.5 ... 27.0 km

about all 600 to 1200 m from 27 to 20 km
about all 30 to 600 m from 20 km down to 10 km altitude.

These numbers are very rough, because they do not take into account the difference between air speed in the chamber and falling speed of the instrument with respect to a ground fixed frame. However, a number of approximately 80 to 150 full cycles could be measured during the falling from 40 to 10 km. Thus, a duration of a full cycle of 1 minute is certainly not too long.

Each cycle consists of six measured curves. This may be explained in the following way. Before a particular driving voltage is applied, all receiving electrodes are shortly grounded. After they are disconnected from ground and the driving voltage is applied, ions will begin to sediment on the receiving electrodes and will raise their potential in the form of a curve of the type $y = 1 - \exp(-x)$. Since for each cycle six different driving electrodes are applied, this will happen six times for each cycle, i. e., for every curve there is a time of roughly 10 seconds. In this period, "10"/0.2 $\approx$ 45 single points of these curves will be measured. Unless a curve has reached its maximum value in a period less than 0.4 second, the curve itself can be determined from these points. This remains true, even if the time to reach maximum is considerably greater than 9 or 10 seconds. Thus, the maximum value may be determined by calculation even in these cases, though it is preferred to directly measure the height of the curve. There is a great chance that during each cycle there will be at least one case in which this is possible for each of the six amplifiers. This is a consequence of the stepping of driving voltages according to table 3.

It is furthermore planned that each amplifier be checked on time during each cycle, and that the zero point be tested six times during each cycle. This "checking" of the amplifier is not a full calibration, because we did not want to include the high-ohmic resistance in this control process so as not to endanger the good insulation. Also, a correct calibration of an electrometer takes a considerable amount of time. Always, when the driving voltage is changed, the amplifiers are grounded. Thus, a saturation of the amplifiers due to displacement current is avoided.

For the first flight, only ions of one sign will be measured. The instrument is built in such a way, however, that by desoldering one wire it will be able to measure alternatively ions of both signs, Then, one cycle would measure positive ions, the next negative ions, etc. It should be noted that the values of table 4 are derived from maximum falling speeds. If measurements of less distant regions are desired, and if the falling speed of the instrument can be reduced by a greater parachute, the spacing could be made much closer.

Finally, it had to be determined how sensitive the electrometer-amplifiers had to be made. The general rule applied here was that for the first flight it should be preferred to risk saturation and the risk of missing measurements due to insufficient sensitivity should be reduced.

The calculation has been made for ion number densities of 10^9 and 10^{10} m^{-3}, since the expected values should be in between these limits. Considering the

actual area of the ion gate, the numbers of incoming ions has been calculated. From these, and by considering figure 3, the following limitations for the current measurements have been derived (table 5).

TABLE 5

LIMITS OF CURRENT MEASUREMENT BY THE ELECTROMETER AMPLIFIERS
(Assuming a Mobility Range of 10)

Height (km)	Currents per Amplifier for the Driving Voltages of:		
	300 Volt	10 Volt	5 Volt
10	average per amplifier: 0.1 ... 1 pA	less than 0.1 pA	less than 0.1 pA
40	amplifier A1 gets 5 ... 50pA; A2 ... A6: nothing	average per amplifier: 0.8 ... 8 pA	amplifiers A1 ... A3: nothing; amplifiers A4 ... A6 in the average 0.8 ... 8 pA

The dynamic range of the electrometer-amplifier can be made rather great, since the amplifier is able to measure less than 1 fA. However, the dynamic range of the telemetry system is limited to about 25. Remembering our general decision, rather being too sensitive than too insensitive, we propose a dynamic range of the electrometer amplifiers as follows:

TABLE 6

DYNAMIC RANGE OF ELECTROMETER AMPLIFIERS

0.1 ... 25 pA.

With this range, we should measure at least something for all cases of table 5, and in the cases where the expected current is greater than 25pA, we should be able to extrapolate the measured curve in order to derive the value of equilibrium between charging of the receiving electrode by sedimented ions and discharging it by amplifier input resistance. We should remember, however, that, due to the stepping of driving voltages, every point of the mobility spectrum is measured

or approximated several times. All these values will be checked as soon as the calculation is made for the bent wind velocity distribution curves. However, we do not expect essential variations.

It was decided to monitor the driving voltages all the time. Since the dynamic range of driving voltages is greater than the dynamic range of the transmitter, two transmitter channels have to be used, which previously were called Alpha and Beta here. Table 7 shows the applied voltages.

TABLE 7

MONITORING OF DRIVING VOLTAGES

Output from Switches 81 to 86 (Volt)	Transmitting Channel Alpha Gets	Transmitting Channel Beta Gets
300	2.5 V	2.5 V (zener)
140	1.16 V	2.5 V (zener)
60	500 mV	2.5 V (zener)
25	(208 mV)	2.5 V
10	(83 mV)	1.0 V
5	(42 mV)	500 mV

3.2 CONSTRUCTION AND INTEGRATION OF CHAMBER

3.2.1 OVERALL DESIGN

Mechanically, the whole instrument will consist of four parts. When falling down, the foremost part is the chamber proper. It consists of the inner and outer electrodes, the insulators for the outer electrodes, the heating blankets as a huli around the outer electrodes with some distance in between, the preamplifier directly attached to pins reaching from the outer electrodes through the blankets without touching them, the connector plugs for the subdivision of driving voltages and the connectors for the supply to the rings, the front and aft sets of rings, the thermal insulation layers, the thin outer hull, and an intake ring in the form of half a doughnut.

This chamber is made of a frame consisting of four beams in axial direction and bracers forming a periphery. The four beams are extended backwards (upwards when falling) to allow the uninhibited exit of the air streaming through the chamber, and ending at a conical cover for the other parts.

Behind (above when falling) this cone there is at first a setup of three "decks." Two of them carry the second-stage amplifiers, while the third one is carrying the supply units and the programmer. After these three decks there come the compartments for the 28-V battery (batteries) and for the transmitter. At last comes the parachute. The parachute, the transmitter, and the batteries will be supplied by the contracting agency and are not described here. The batteries deliver 28 Vdc, unregulated.

3.2.2 THE CHAMBER PROPER AND THE "DECKS"

Figures 49, 50, 51, and 52 show the chamber proper. Figure 49 shows the chamber without the preamplifiers and the thermal insulation; one looks at the frame and at the heating blankets between the parts of the frame. In figure 50, the thermal insulation has been added partially, while figure 51 shows the fully assembled instrument with the outer hull. In figure 52, the same is shown as seen from the front end. The ruler is scaled in inches.

Figure 53 gives an overall sketch of the instrument, partially cut to show internal parts.* Photographs of the internal parts have been submitted with Monthly Report No. 16 of this contract.

In figure 54, the assembled decks can be seen. The lowest deck and the middle deck carry the six second-stage amplifiers, essentially consisting of operational amplifiers (type Philbrick PP 65a, solid state). The uppermost deck caries the cylindrical programmer, and below it at the left hand side, the four converters

*A complete set of detail drawings in scale 1:1 has been made, but is not included in this report.

for the supply of regulated voltages, and at the right hand side the box for the polarity inverter.

The programmer was developed and constructed by the Geophysics Section of Avco RAD. Two arms which carry small magnets, driven by an electric motor by the way of a great set, rotate in a completely sealed cylindrical box. The magnetic fields penetrate the hull of this cylinder and may so activate magnetic reed switches, which are mounted on the outer side of the cylinder, inserted in rings of plexiglass (covered by the black tape). These reed switches operate in a sealed-in atmosphere themselves. Thus, motor, rotating arms, and switching action are independent of the outer atmosphere and its pressure.

The polarity inverters consist essentially of a relay, triggered by the programmer once with every revolution. The time for one revolution of the programmer is set to approximately 1 minute.

3.2.3 THE ELECTRICAL SCHEMATIC

Figure 55, consisting of eight sheets, presents the whole electrical schematic of the system, with the exception of the transmitter.

Sheet 1 shows the general connections between the electrodes and rings and preamplifiers mounted on the chamber proper on one side, and the second-stage amplifiers as well as the supply units, programmer, and connections to the transmitter on the other side.

The other sheets give the details of individual parts, including a survey on the electric program. They are understandable without further explanation.

The preamplifiers are small units of about 6x4x2 cm in a curved shielding box, mounted on a printed circuit board. Including the small heater, the thermostat, and the heat probe, they are potted with a heat-conducting material, but the input connections, which have to maintain an extremely high insulation, are not included in the potting. The second-stage amplifiers are mounted, three by three, on printed boards as well. The voltage inverters are industry items. Photographs of the printed boards as well as of the details of the programmer have been submitted with Monthly Report No. 16. Vacuum tightness is obtained with O-rings.

Part of the electrical connections are fully shielded electrically. This has been made possible by the application of special connectors which allow the insertion of unshielded pins as well as shielded ones. Sheet 1 of figure 55 indicates the shielded connections as well as the placing of connectors.

The requirement for power for the heating blankets is considerable. However, it has been calculated that the applied 28-V batteries will be sufficient. If necessary, the supply for the heating blankets can be made independent of the supply for the other parts.

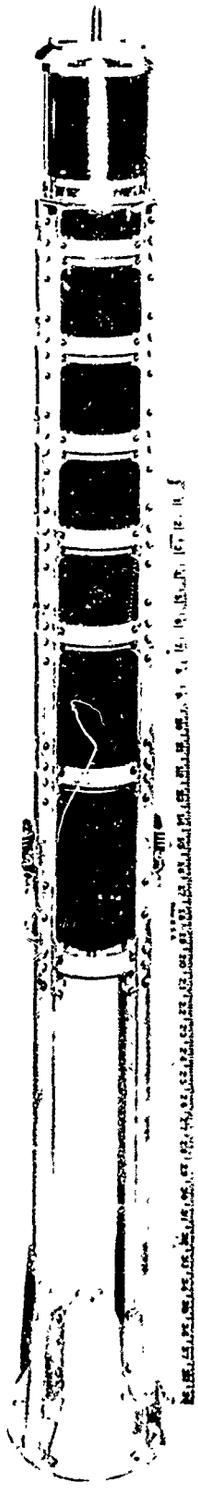

Figure 49 THE MODIFIED GERDIEN CHAMBER, MODEL B1, WITHOUT PREAMPLIFIERS AND THERMAL INSULATION
P13471A

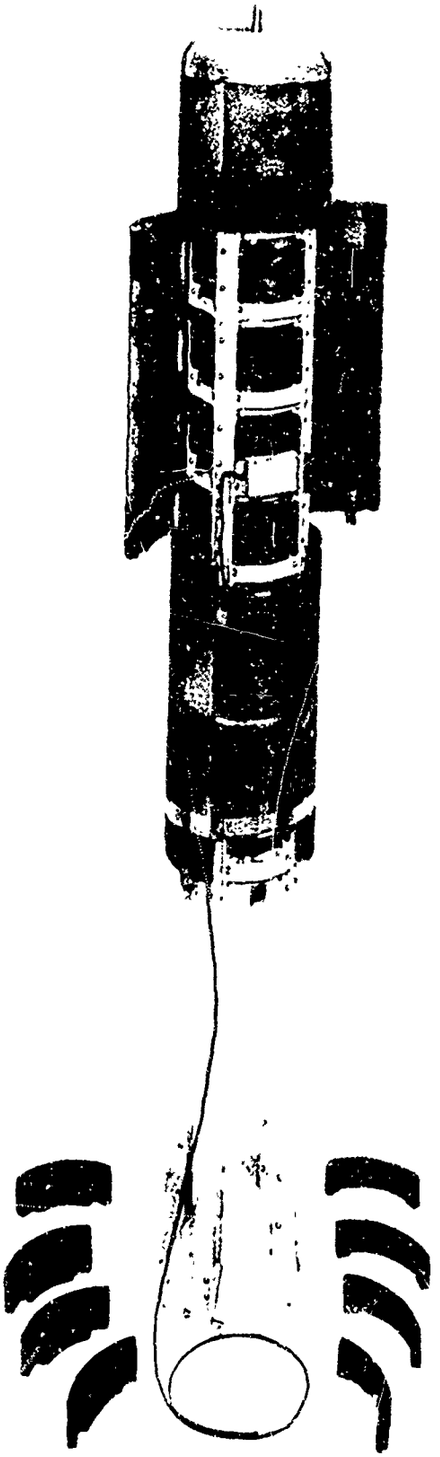

Figure 50 THE MODIFIED GERDIEN CHAMBER, MODEL B1, WITH ONE PREAMPLIFIER AND PART OF THE THERMAL INSULATION
P13471B

Figure 51 MODIFIED GERDIEN CHAMBER, MODEL B1, FULLY COVERED
P13471C

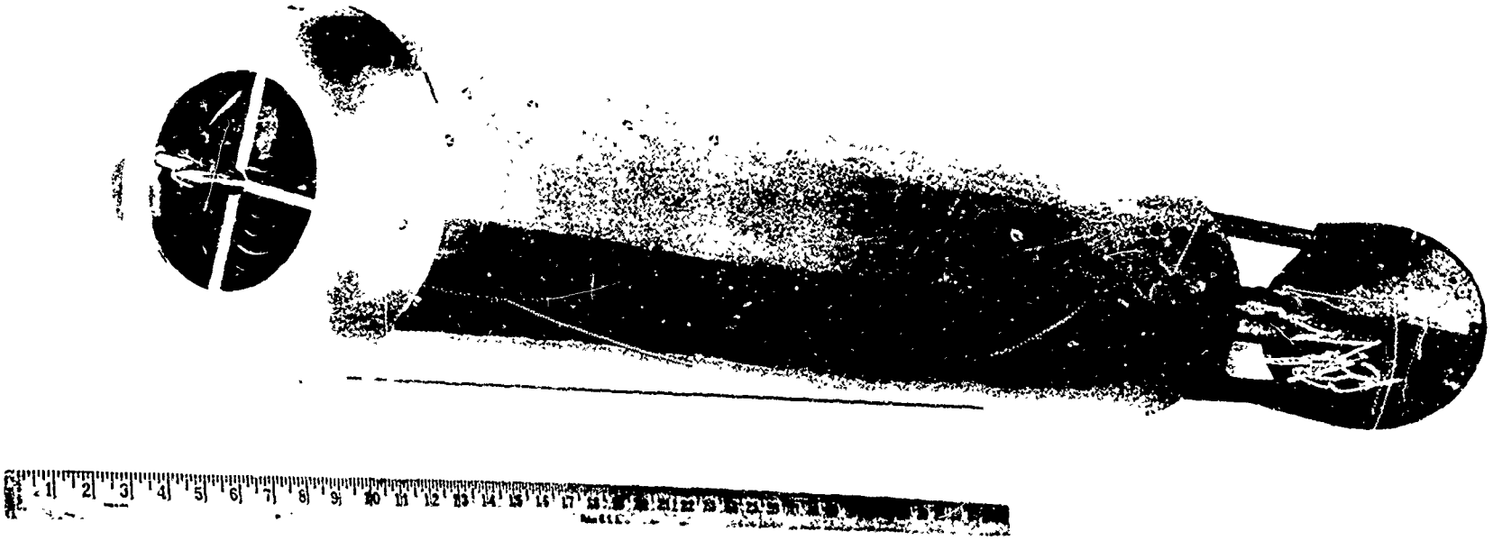

Figure 52 MODIFIED GERDIEN CHAMBER, MODEL B1, ASSEMBLED
P13471D

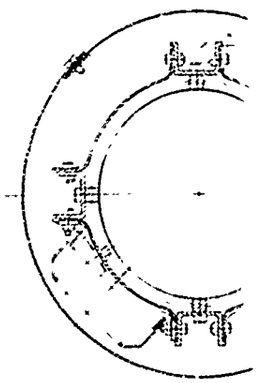

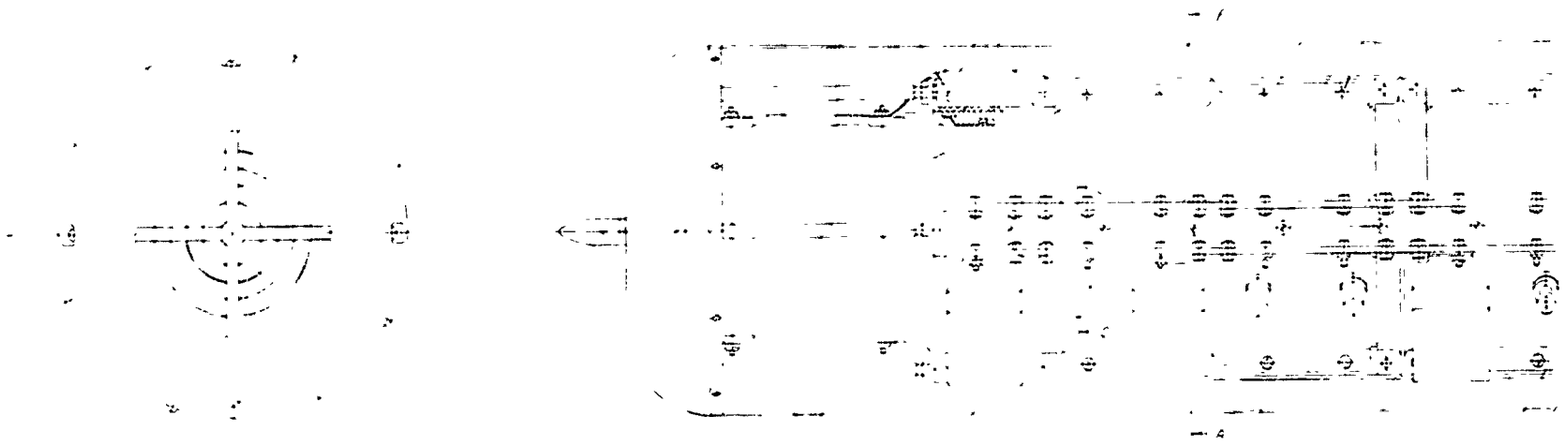

Figure 53 DETAIL

A

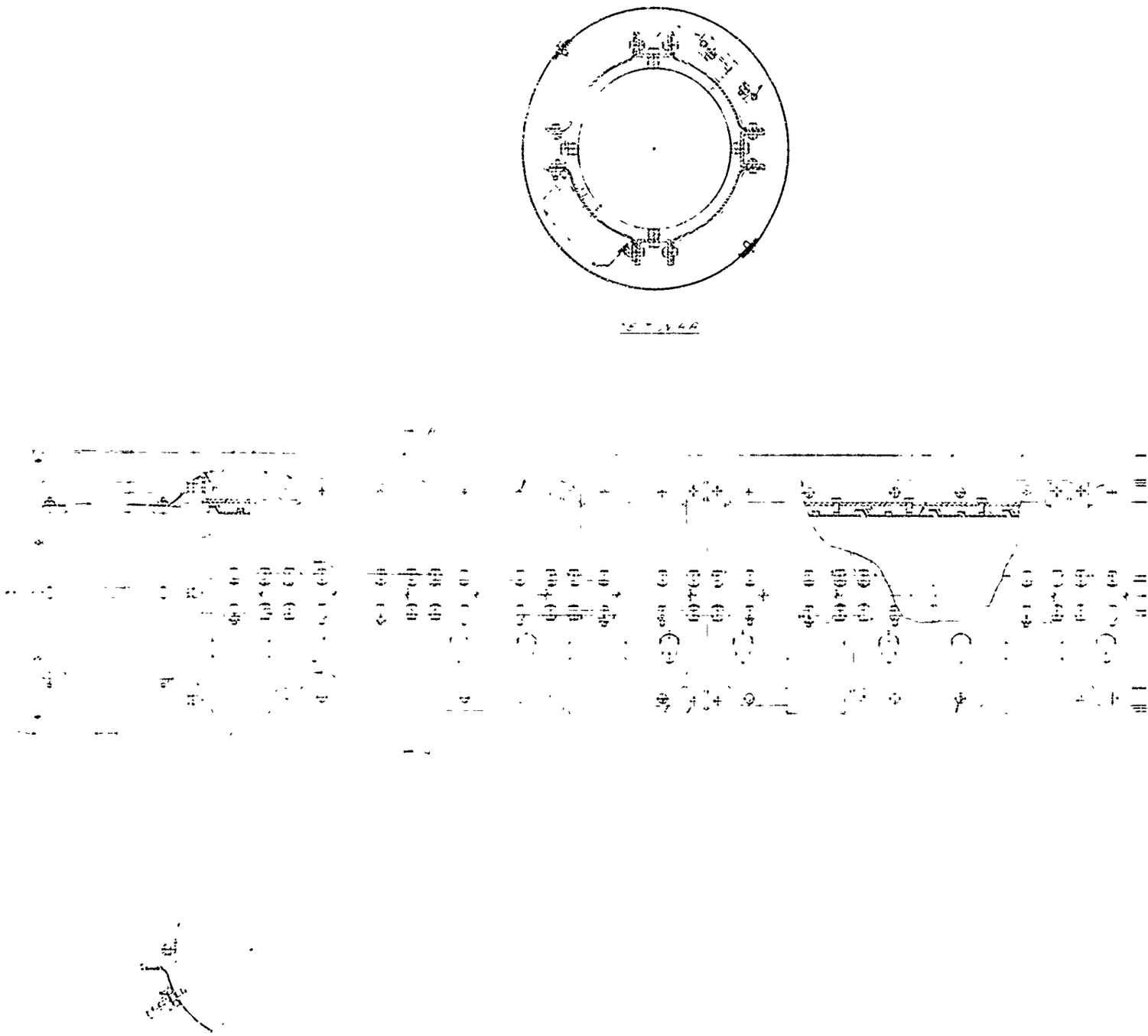

Figure 53 DETAILS OF MODIFIED GERDIEN CHAMBER, MODEL B1

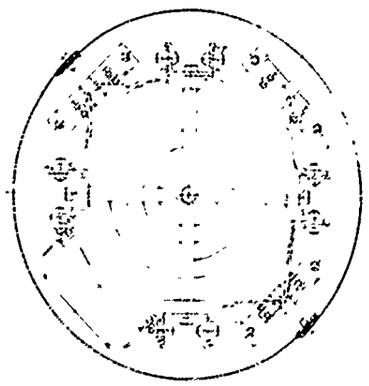

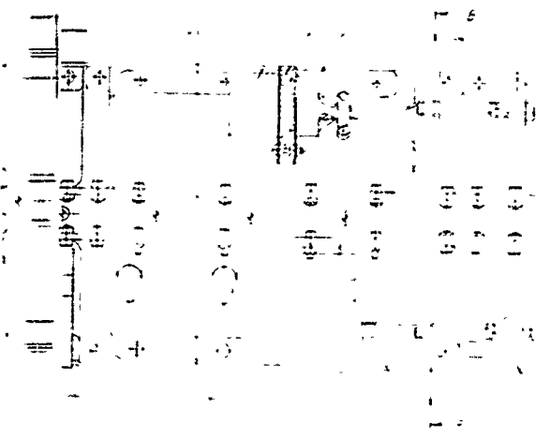

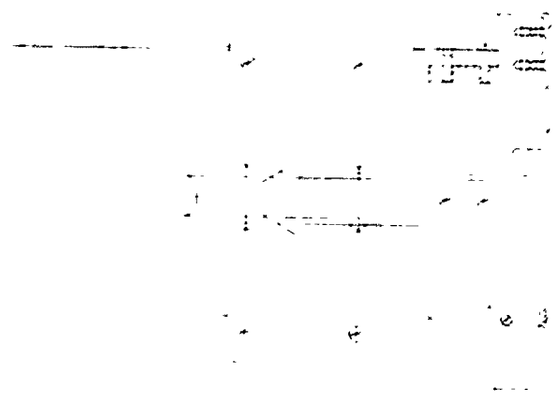

C

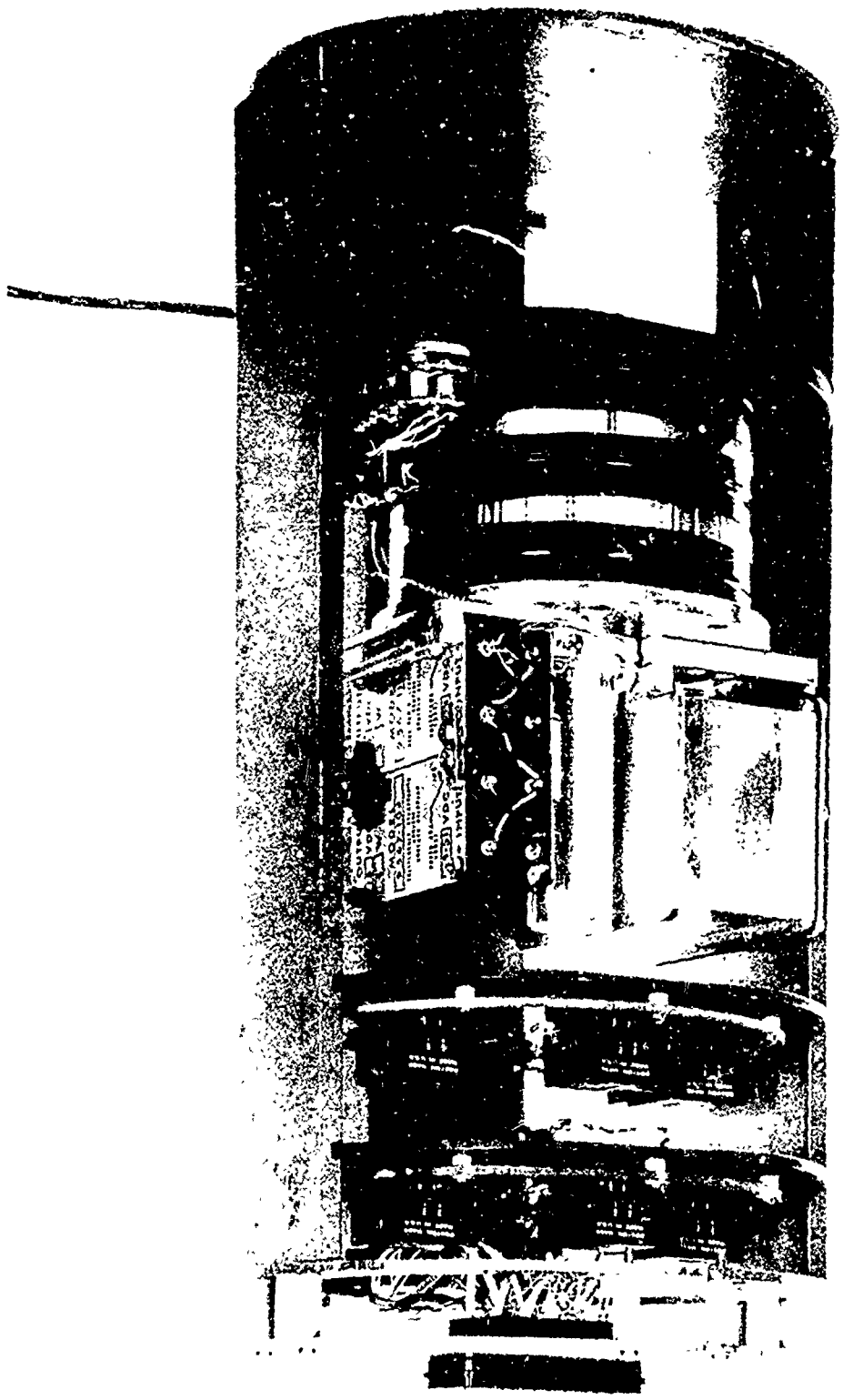

Figure 54 SECOND-STAGE AMPLIFIERS, SUPPLY UNITS, AND PROGRAMMER OF MODIFIED GERDIEN CHAMBER, MODEL B1
P13595C

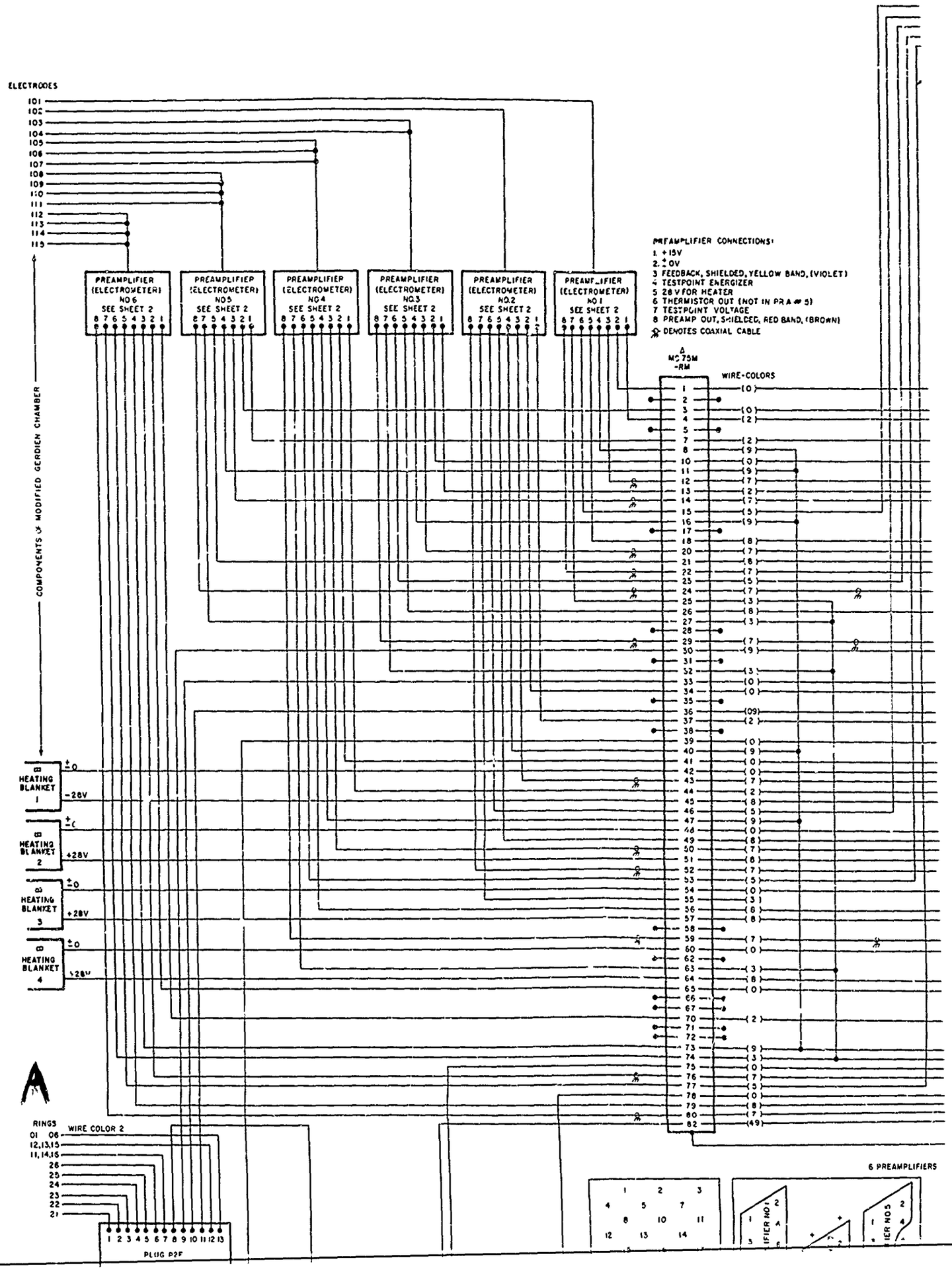
ELECTRODES
101
102
103
104
105
106
107
108
109
110
111
112
113
114
115
COMPONENTS OF MODIFIED GERDIEN CHAMBER
PREAMPLIFIER (ELECTROMETER) NO 6 SEE SHEET 2
PREAMPLIFIER (ELECTROMETER) NO 5 SEE SHEET 2
PREAMPLIFIER (ELECTROMETER) NO 4 SEE SHEET 2
PREAMPLIFIER (ELECTROMETER) NO 3 SEE SHEET 2
PREAMPLIFIER (ELECTROMETER) NO 2 SEE SHEET 2
PREAMPLIFIER (ELECTROMETER) NO 1 SEE SHEET 2
8 7 6 5 4 3 2 1
PREAMPLIFIER CONNECTIONS:
1. +15V
2. ±0V
3 FEEDBACK, SHIELDED, YELLOW BAND, (VIOLET)
4 TESTPOINT ENERGIZER
5 28 V FOR HEATER
6 THERMISTOR OUT (NOT IN PR A # 5)
7 TESTPOINT VOLTAGE
8 PREAMP OUT, SHIELDED, RED BAND, (BROWN)
DENOTES COAXIAL CABLE
MC 75M -RM
WIRE-COLORS
HEATING BLANKET 1
HEATING BLANKET 2
HEATING BLANKET 3
HEATING BLANKET 4
±0
-28V
+28V
RINGS
01 06
12,13,15
11,14,15
WIRE COLOR 2
PLUG P2F
6 PREAMPLIFIERS

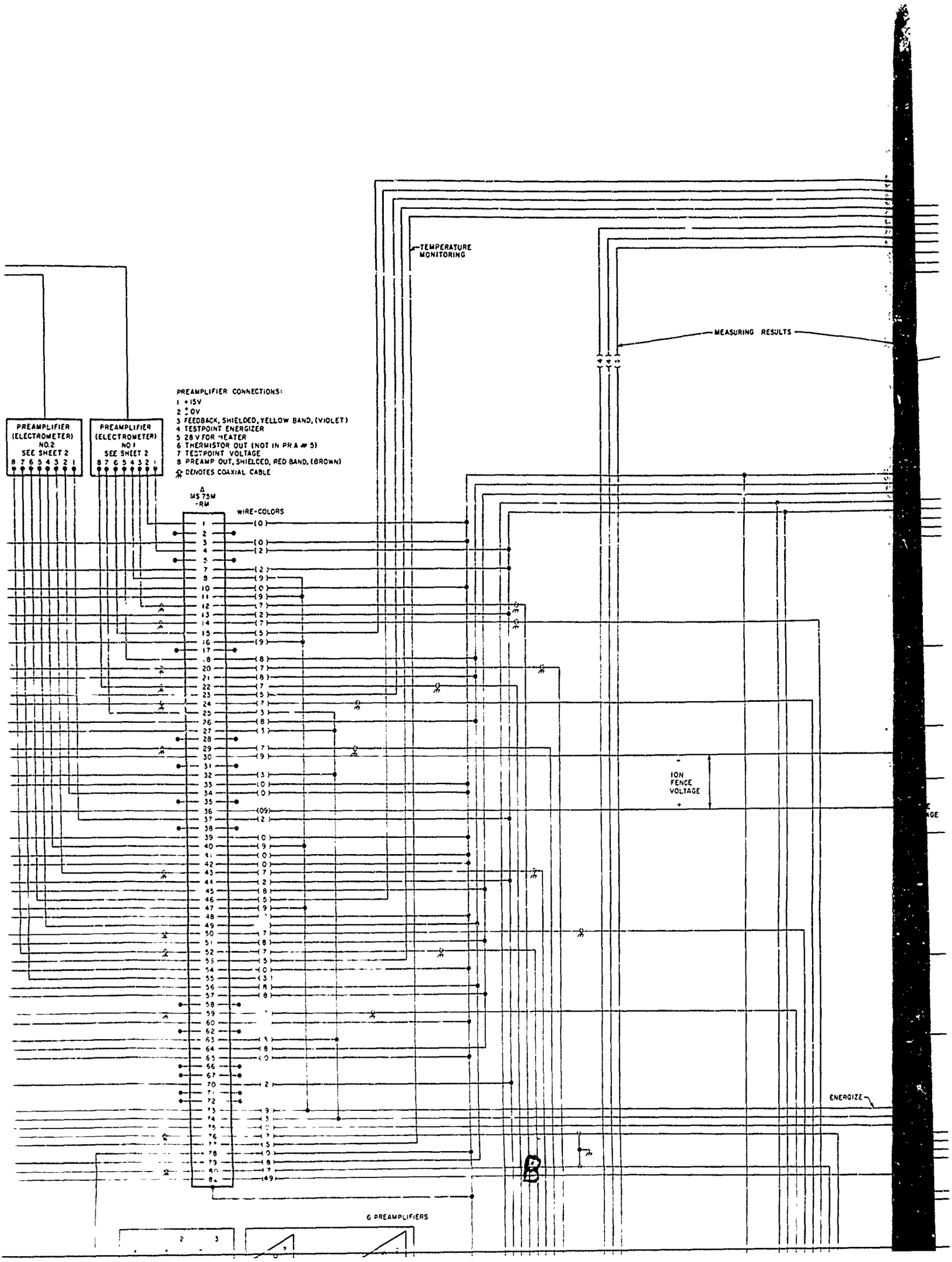
TEMPERATURE MONITORING
MEASURING RESULTS
PREAMPLIFIER (ELECTROMETER) NO.2 SEE SHEET 2
PREAMPLIFIER (ELECTROMETER) NO.1 SEE SHEET 2
PREAMPLIFIER CONNECTIONS:
1 +15V
2 ±0V
3 FEEDBACK, SHIELDED, YELLOW BAND, (VIOLET)
4 TESTPOINT ENERGIZER
5 28 V FOR HEATER
6 THERMISTOR OUT (NOT IN PR A # 5)
7 TESTPOINT VOLTAGE
8 PREAMP OUT, SHIELDED, RED BAND, (BROWN)
DENOTES COAXIAL CABLE
MS 75M -RM
WIRE-COLORS
ION FENCE VOLTAGE
ENERGIZE
6 PREAMPLIFIERS

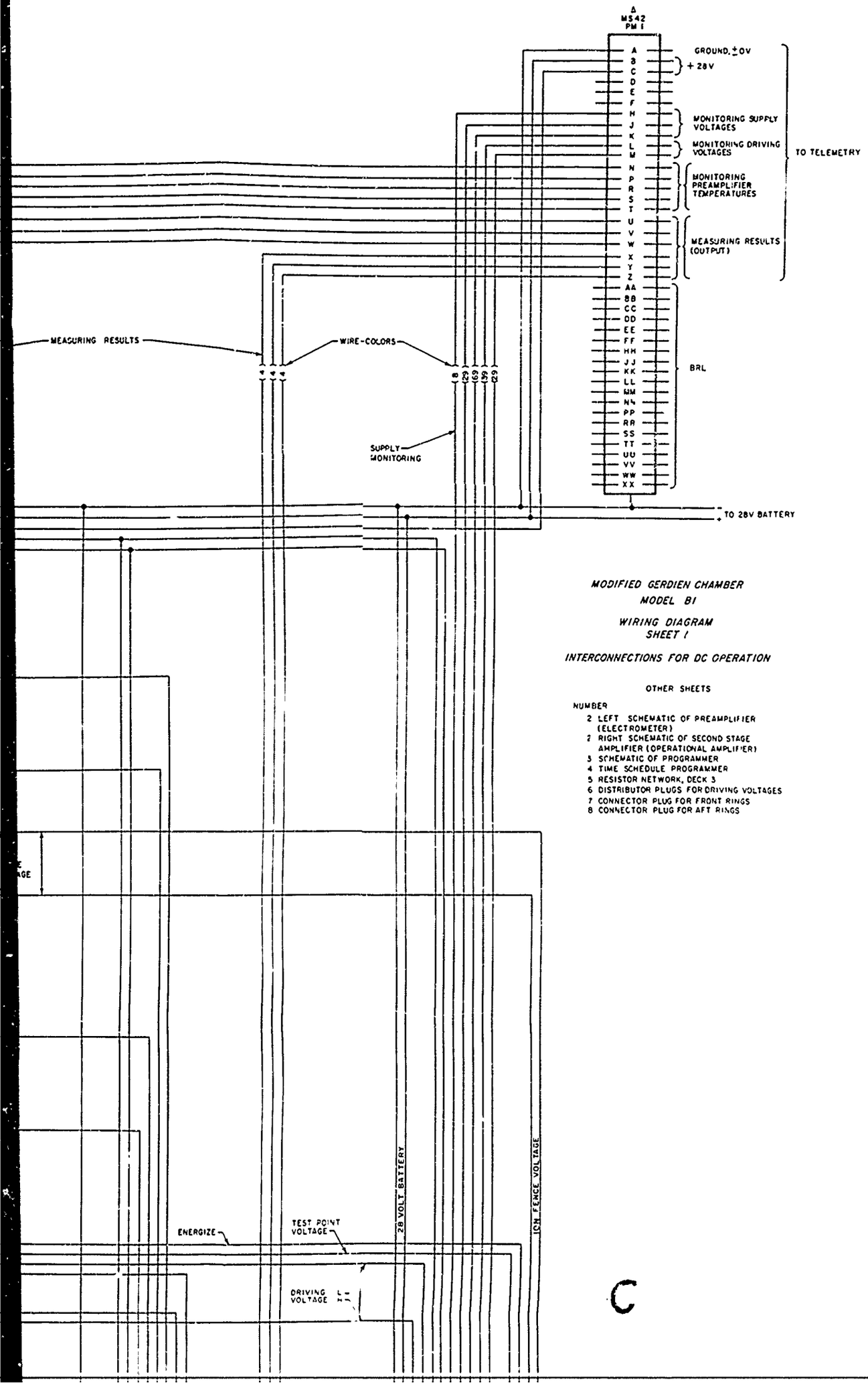

MODIFIED GERDIEN CHAMBER
MODEL BI

WIRING DIAGRAM
SHEET I

INTERCONNECTIONS FOR DC OPERATION

OTHER SHEETS

NUMBER

2 LEFT SCHEMATIC OF PREAMPLIFIER (ELECTROMETER)
2 RIGHT SCHEMATIC OF SECOND STAGE AMPLIFIER (OPERATIONAL AMPLIFIER)
3 SCHEMATIC OF PROGRAMMER
4 TIME SCHEDULE PROGRAMMER
5 RESISTOR NETWORK, DECK 3
6 DISTRIBUTOR PLUGS FOR DRIVING VOLTAGES
7 CONNECTOR PLUG FOR FRONT RINGS
8 CONNECTOR PLUG FOR AFT RINGS

C

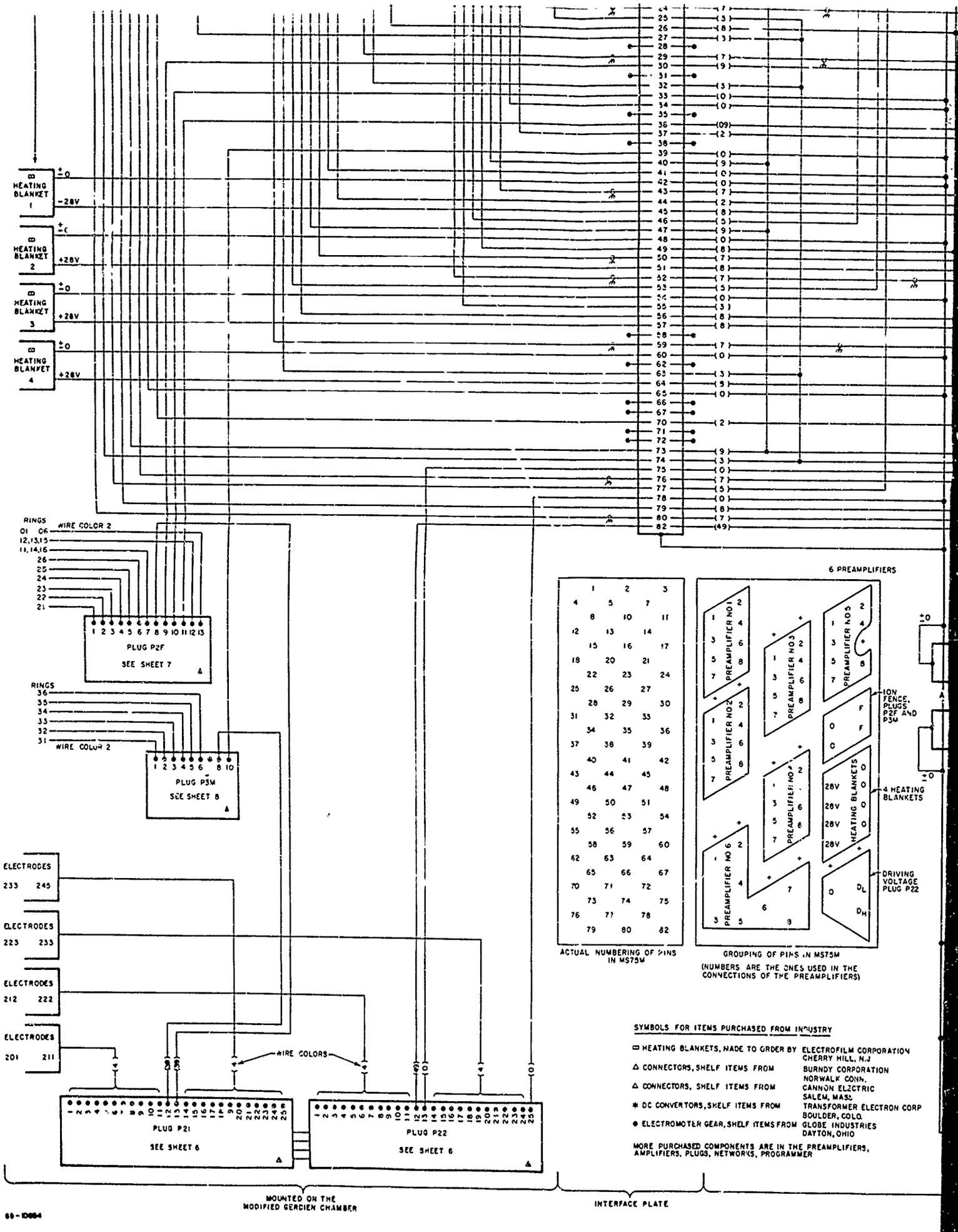

SYMBOLS FOR ITEMS PURCHASED FROM INDUSTRY

- ⊡ HEATING BLANKETS, MADE TO ORDER BY ELECTROFILM CORPORATION CHERRY HILL, N.J
- △ CONNECTORS, SHELF ITEMS FROM BURNDY CORPORATION NORWALK CONN.
- △ CONNECTORS, SHELF ITEMS FROM CANNON ELZCTRIC SALEM, MASS
- * DC CONVERTORS, SHELF ITEMS FROM TRANSFORMER ELECTRON CORP BOULDER, COLO.
- ● ELECTROMOTER GEAR, SHELF ITEMS FROM GLOBE INDUSTRIES DAYTON, OHIO

MORE PURCHASED COMPONENTS ARE IN THE PREAMPLIFIERS, AMPLIFIERS, PLUGS, NETWORKS, PROGRAMMER

D

Figure 55 ELECTRIC CONNECTIONS FOR T

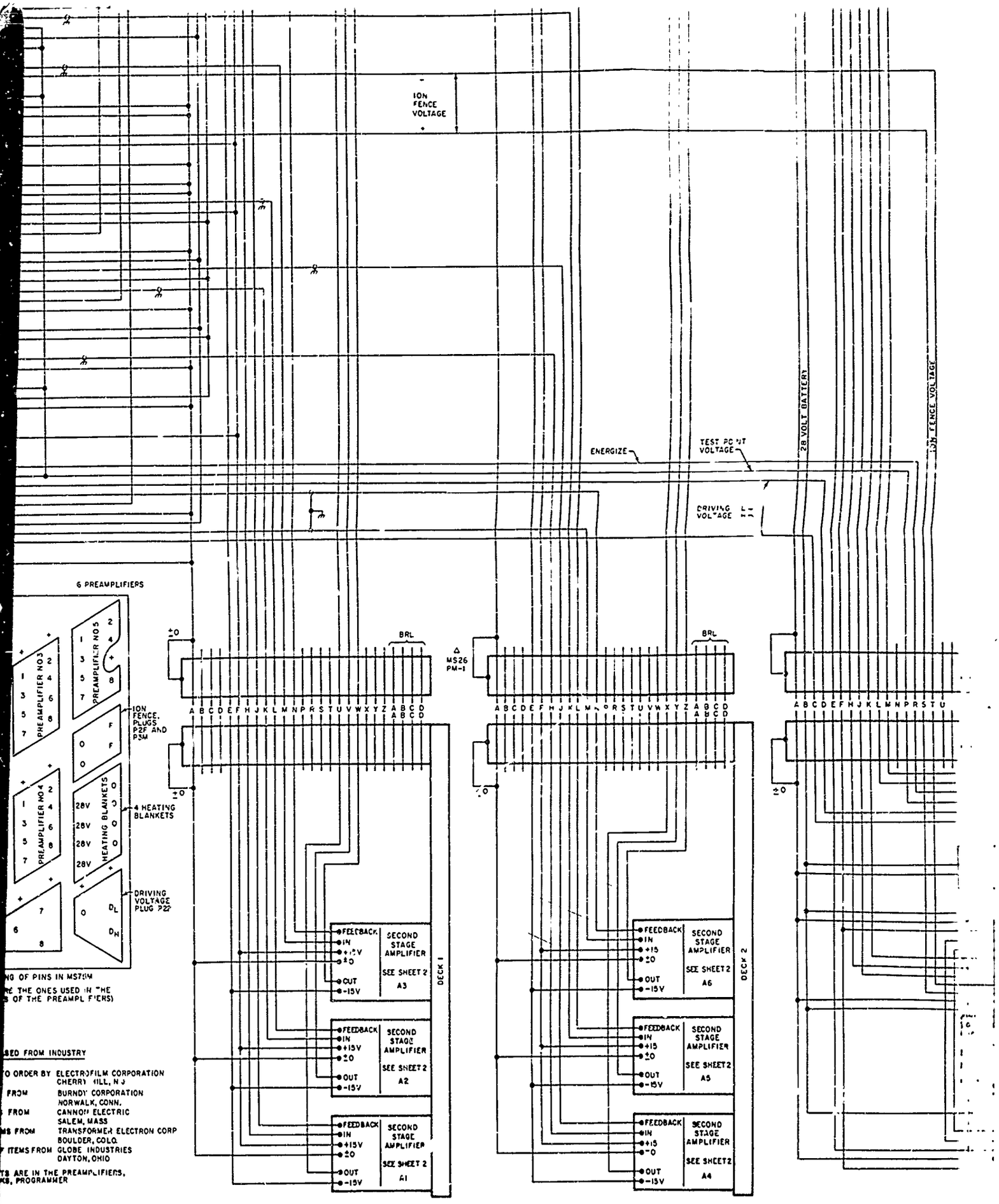

NG OF PINS IN MS75M
RE THE ONES USED IN THE
S OF THE PREAMPL FIERS)

SED FROM INDUSTRY

O ORDER BY ELECTROFILM CORPORATION CHERRY HILL, N J
FROM BURNDY CORPORATION NORWALK, CONN.
FROM CANNON ELECTRIC SALEM, MASS
MS FROM TRANSFORMER ELECTRON CORP BOULDER, COLO.
ITEMS FROM GLOBE INDUSTRIES DAYTON, OHIO

TS ARE IN THE PREAMPLIFIERS, KS, PROGRAMMER

ELECTRIC CONNECTIONS FOR THE MODIFIED GERDIEN CHAMBER -- MODEL B1

E

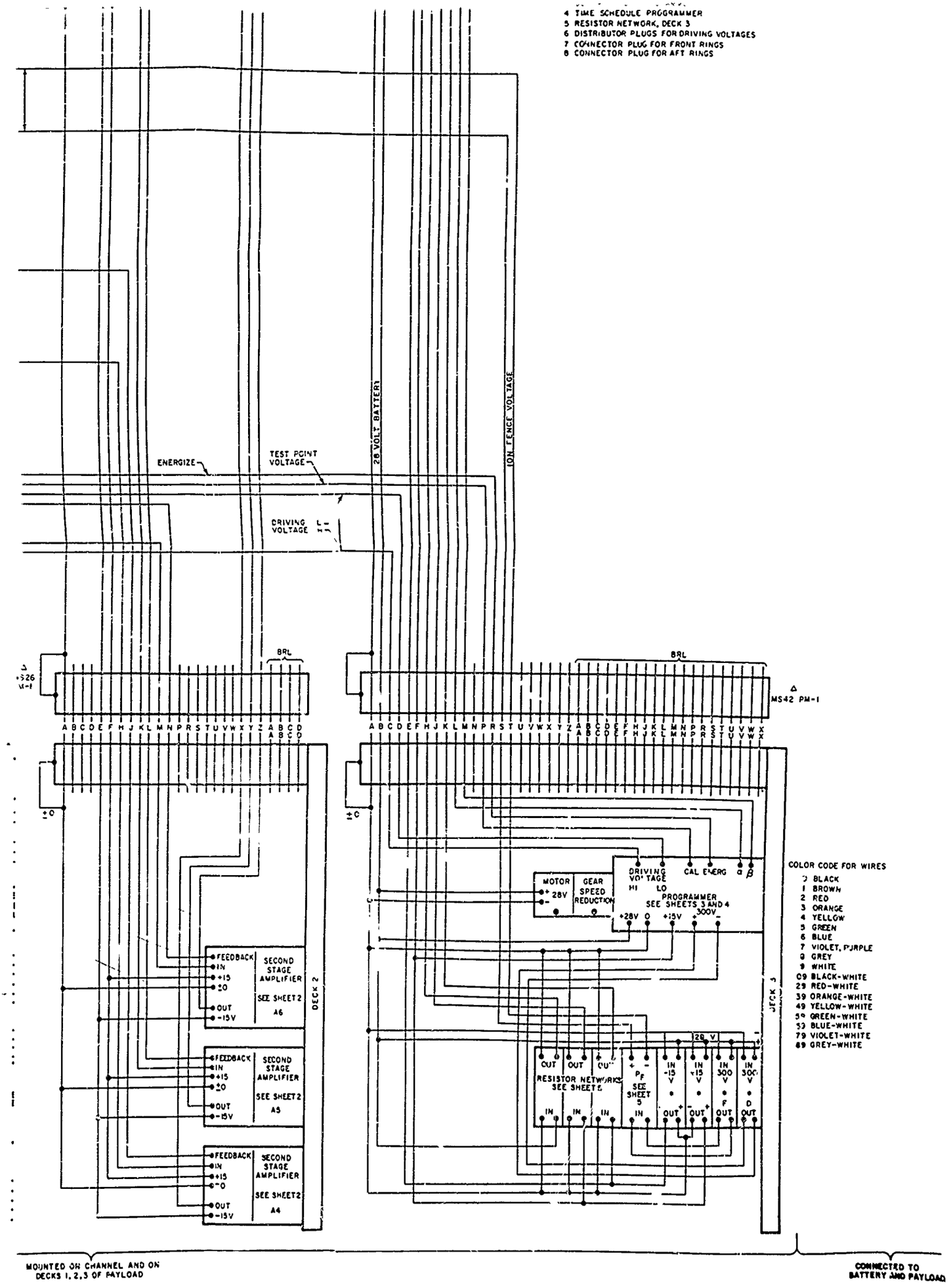
4 TIME SCHEDULE PROGRAMMER
5 RESISTOR NETWORK, DECK 3
6 DISTRIBUTOR PLUGS FOR DRIVING VOLTAGES
7 CONNECTOR PLUG FOR FRONT RINGS
8 CONNECTOR PLUG FOR AFT RINGS
ENERGIZE
TEST POINT VOLTAGE
28 VOLT BATTERY
ION FENCE VOLTAGE
DRIVING VOLTAGE
BRL
MS42 PM-1
MOTOR
+ 28V
GEAR SPEED REDUCTION
DRIVING VOLTAGE
HI LO
CAL ENERG
PROGRAMMER SEE SHEETS 3 AND 4
+28V 0 +15V 300V
FEEDBACK IN +15 ±0 OUT -15V
SECOND STAGE AMPLIFIER
SEE SHEET 2
A6
A5
A4
DECK 2
DECK 3
28 V
RESISTOR NETWORKS SEE SHEET 5
SEE SHEET 5
IN -15 V
IN +15 V
IN 300 V
COLOR CODE FOR WIRES
0 BLACK
1 BROWN
2 RED
3 ORANGE
4 YELLOW
5 GREEN
6 BLUE
7 VIOLET, PURPLE
8 GREY
9 WHITE
09 BLACK-WHITE
29 RED-WHITE
39 ORANGE-WHITE
49 YELLOW-WHITE
59 GREEN-WHITE
69 BLUE-WHITE
79 VIOLET-WHITE
89 GREY-WHITE
MOUNTED ON CHANNEL AND ON DECKS 1, 2, 3 OF PAYLOAD
CONNECTED TO BATTERY AND PAYLOAD

ODEL B1

F

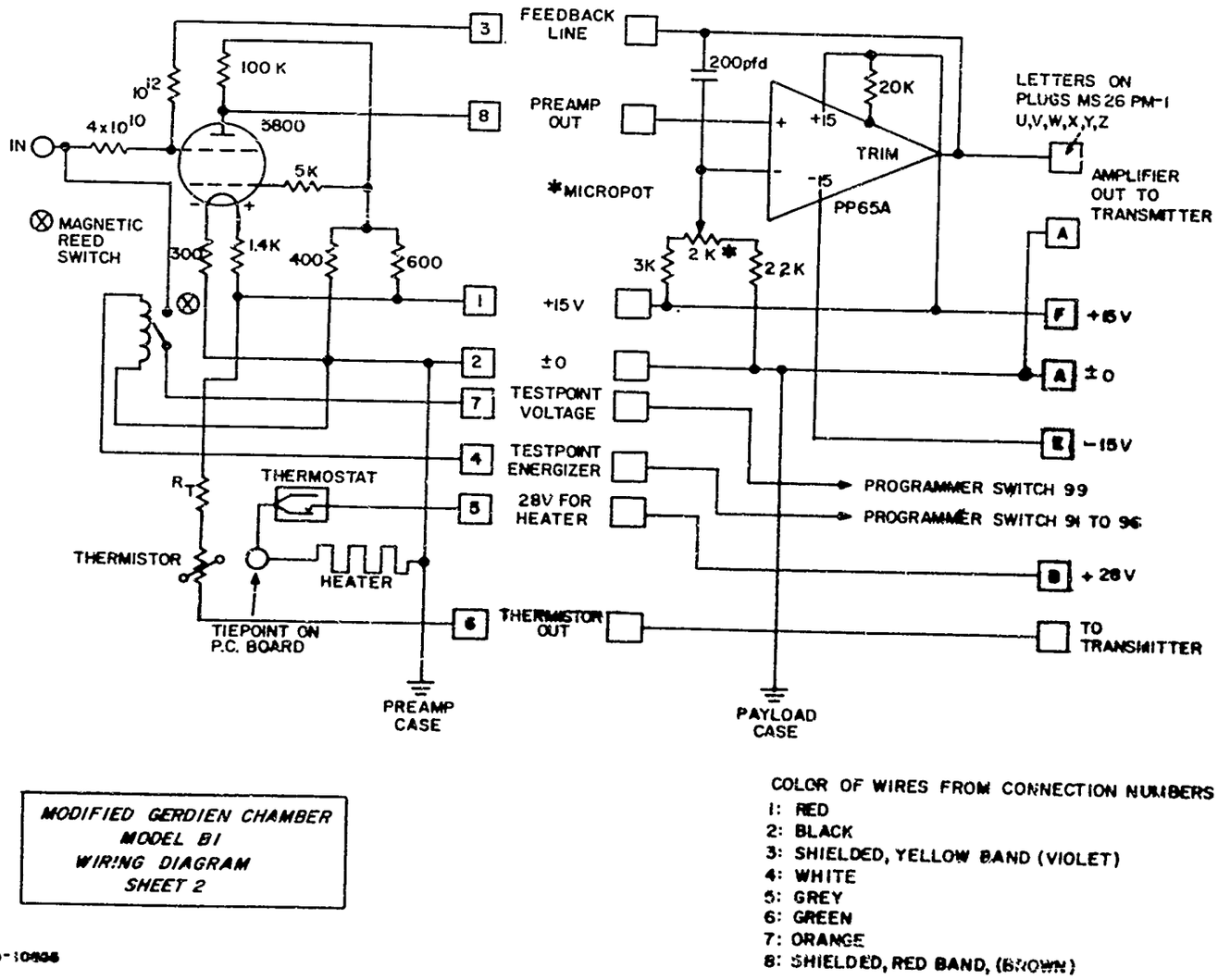

Figure 55 ELECTRICAL CONNECTIONS FOR MODIFIED GERDIEN CHAMBER MODEL B-1

Sheet 2: Left: Schematic of Preamplifier (Electrometer)
Right: Schematic of Second-Stage Amplifier (Operational Amplifier)

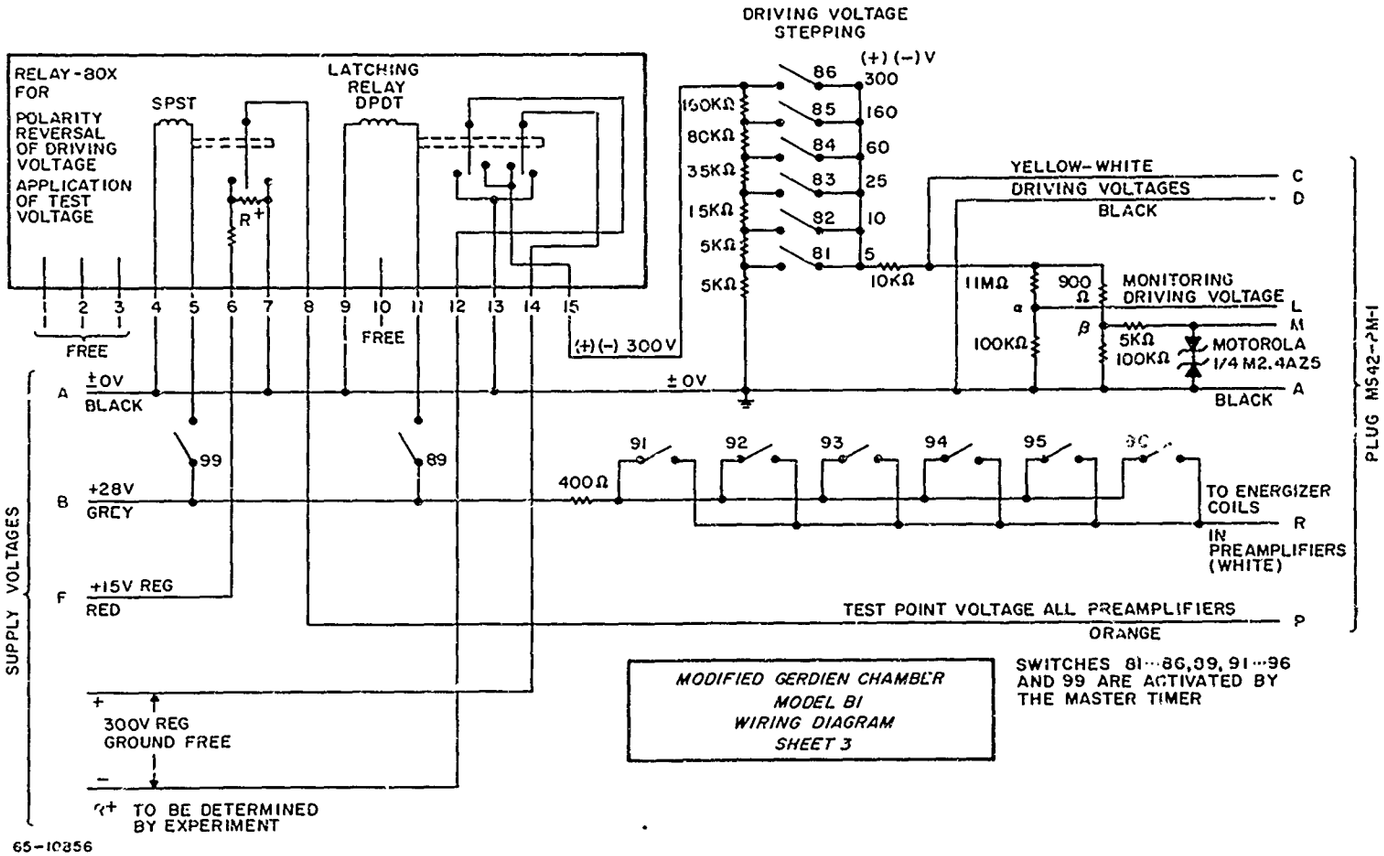

Figure 55 ELECTRICAL CONNECTIONS FOR MODIFIED GERDIEN CHAMBER
MODEL B-1
Sheet 3: Schematic of Programmer

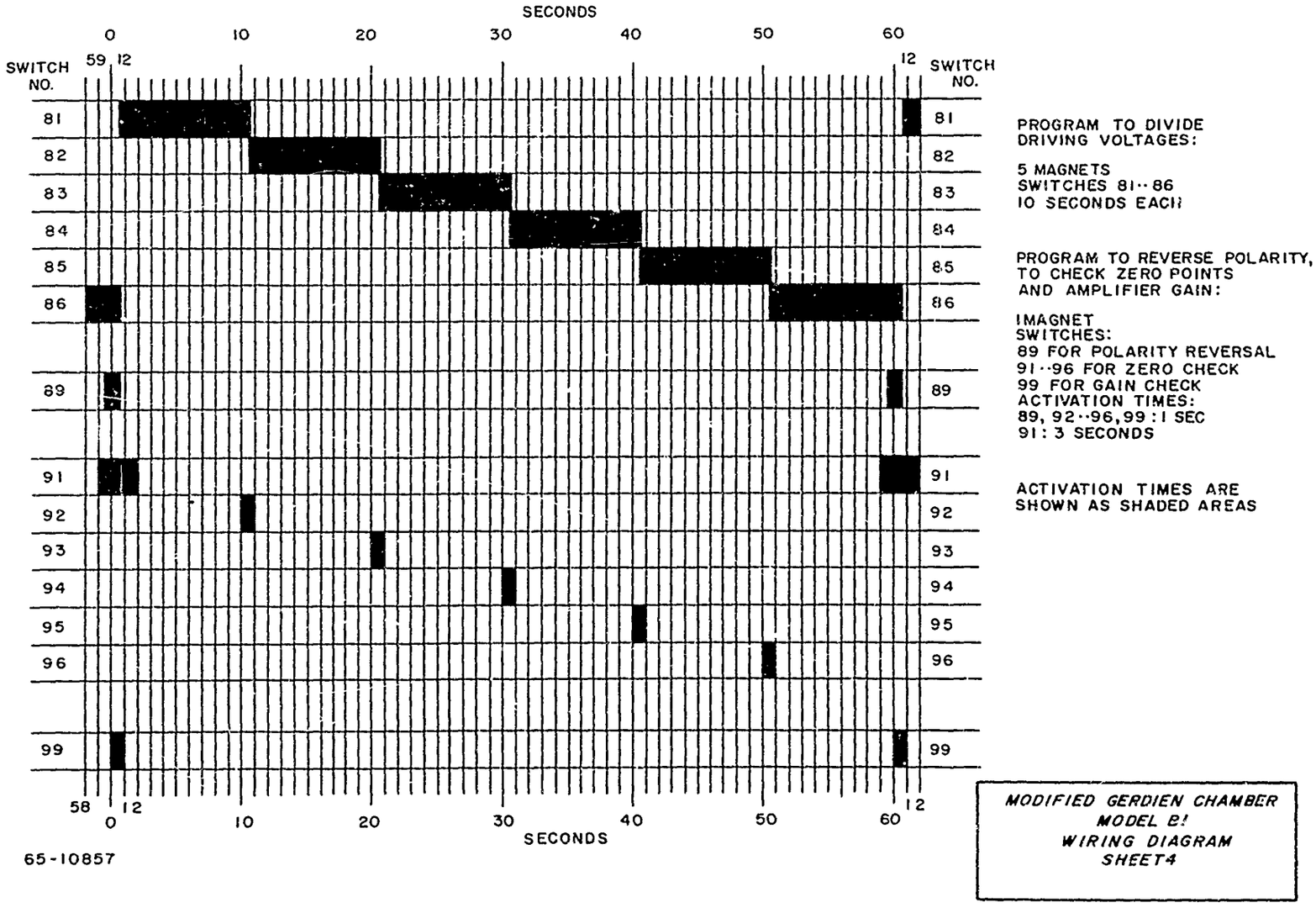

Figure 55 ELECTRICAL CONNECTIONS FOR MODIFIED GERDIEN CHAMBER MODEL B-1
Sheet 4: Time Schedule of Programmer

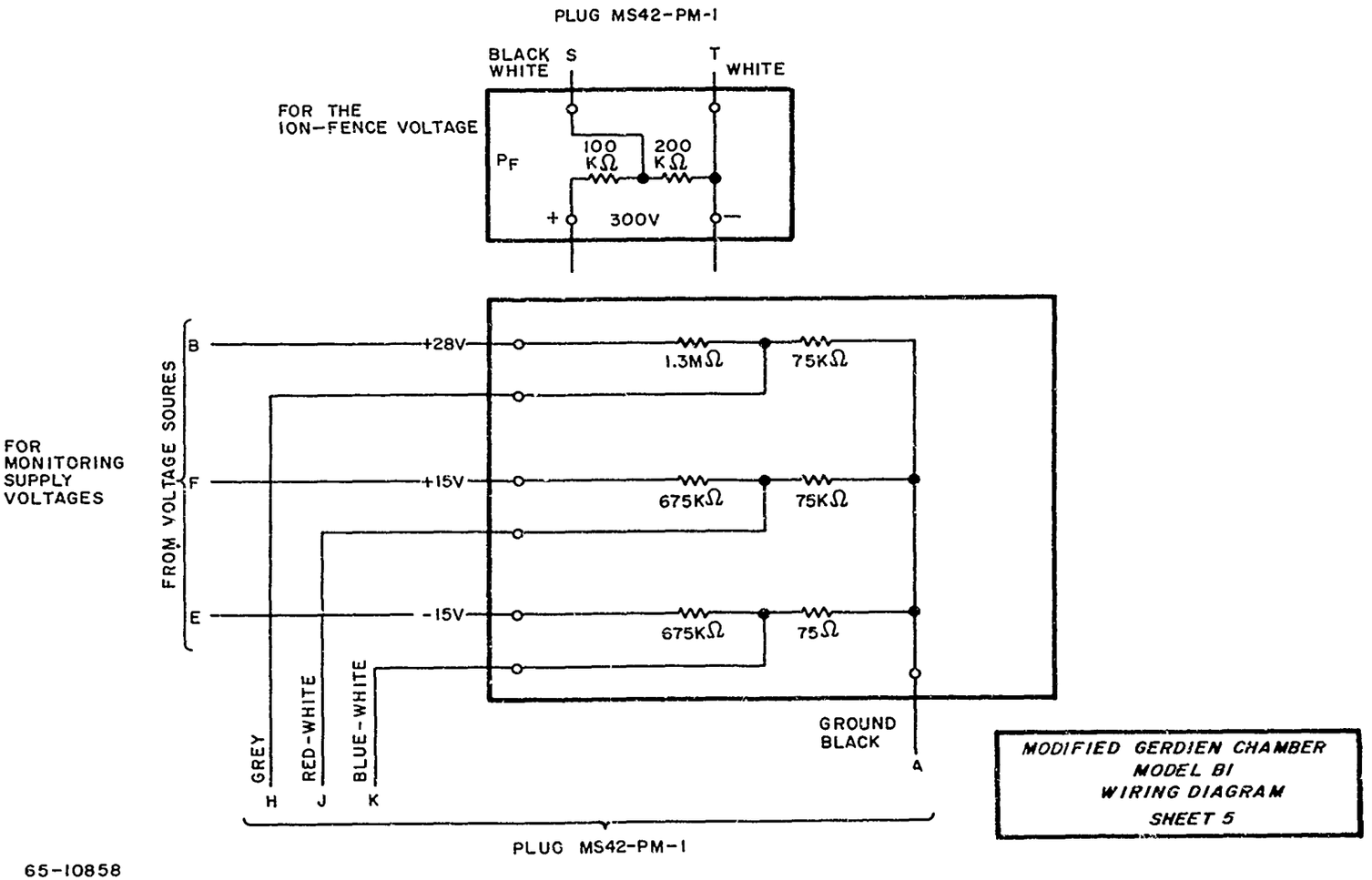

Figure 55 ELECTRICAL CONNECTIONS FOR MODIFIED GERDIEN CHAMBER MODEL B-1
Sheet 5: Additional Resistor Network on "Deck 3" of Payload

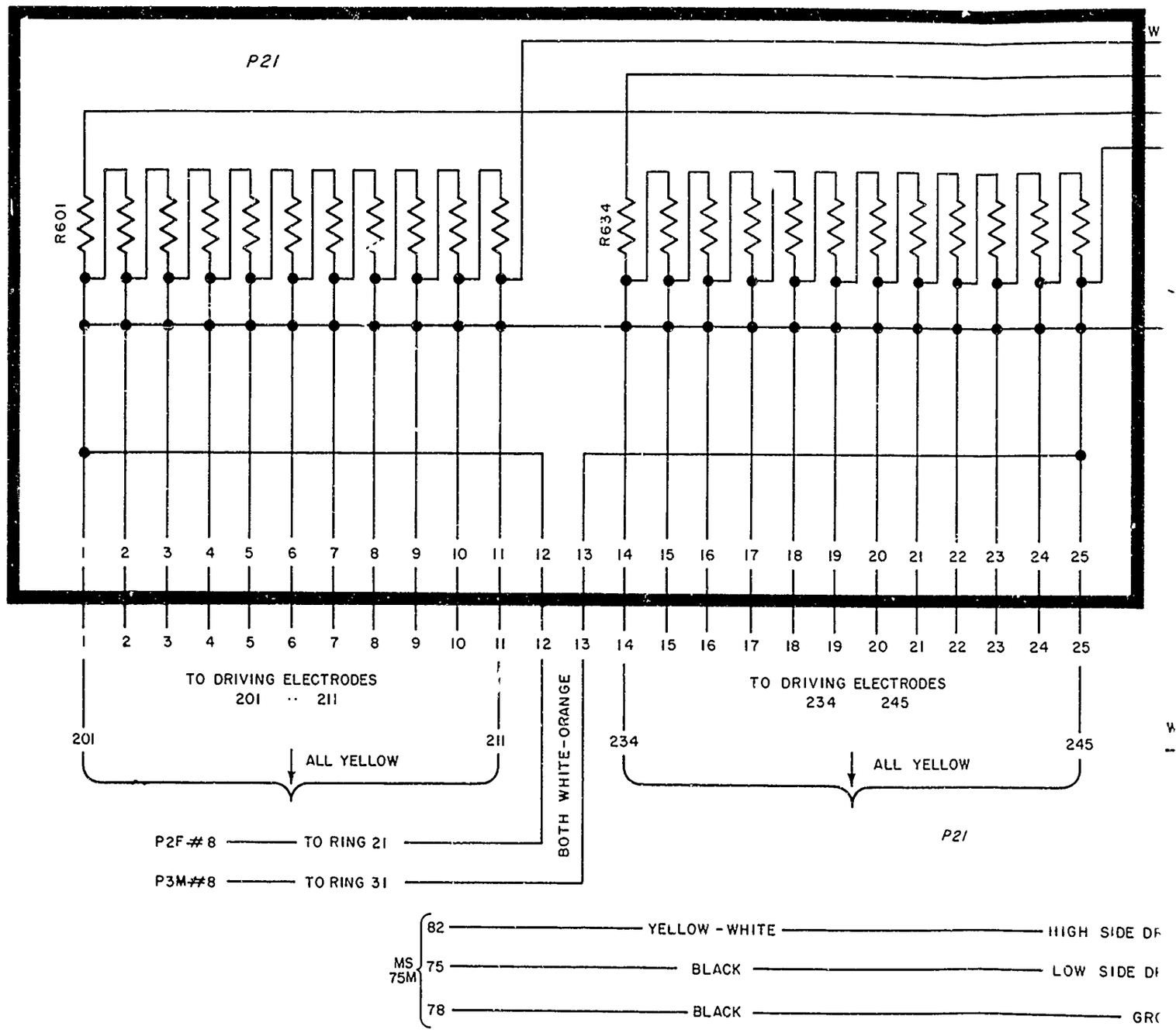

Figure 55 ELECTRICAL CONNECTIONS
MODEL
Sheet 6: Wiring of Distributor P

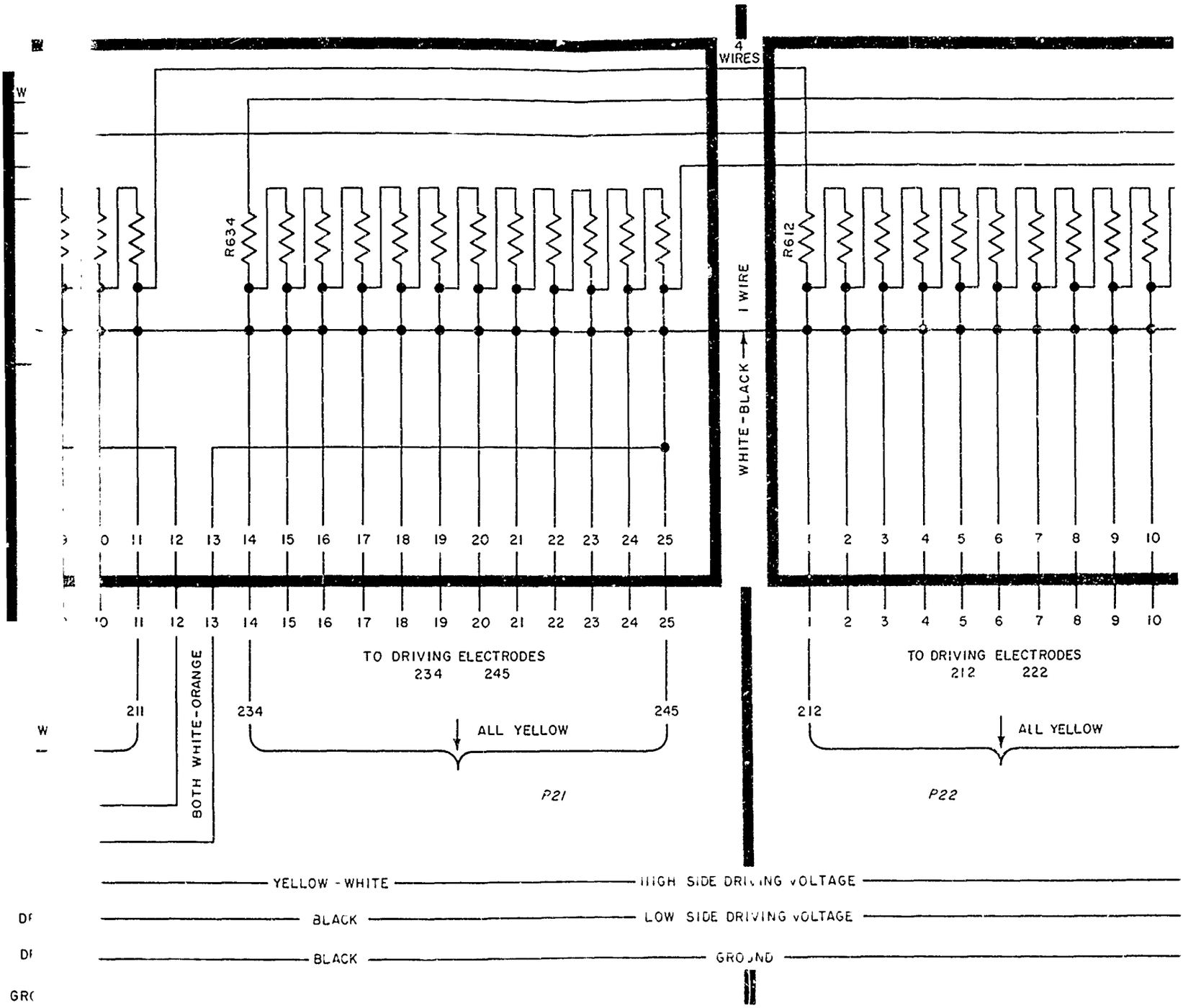

Figure 55 ELECTRICAL CONNECTIONS FOR MODIFIED GERDIEN CHAMBER
MODEL B-1
Sheet 6 Wiring of Distributor Plug for Driving Voltages

B

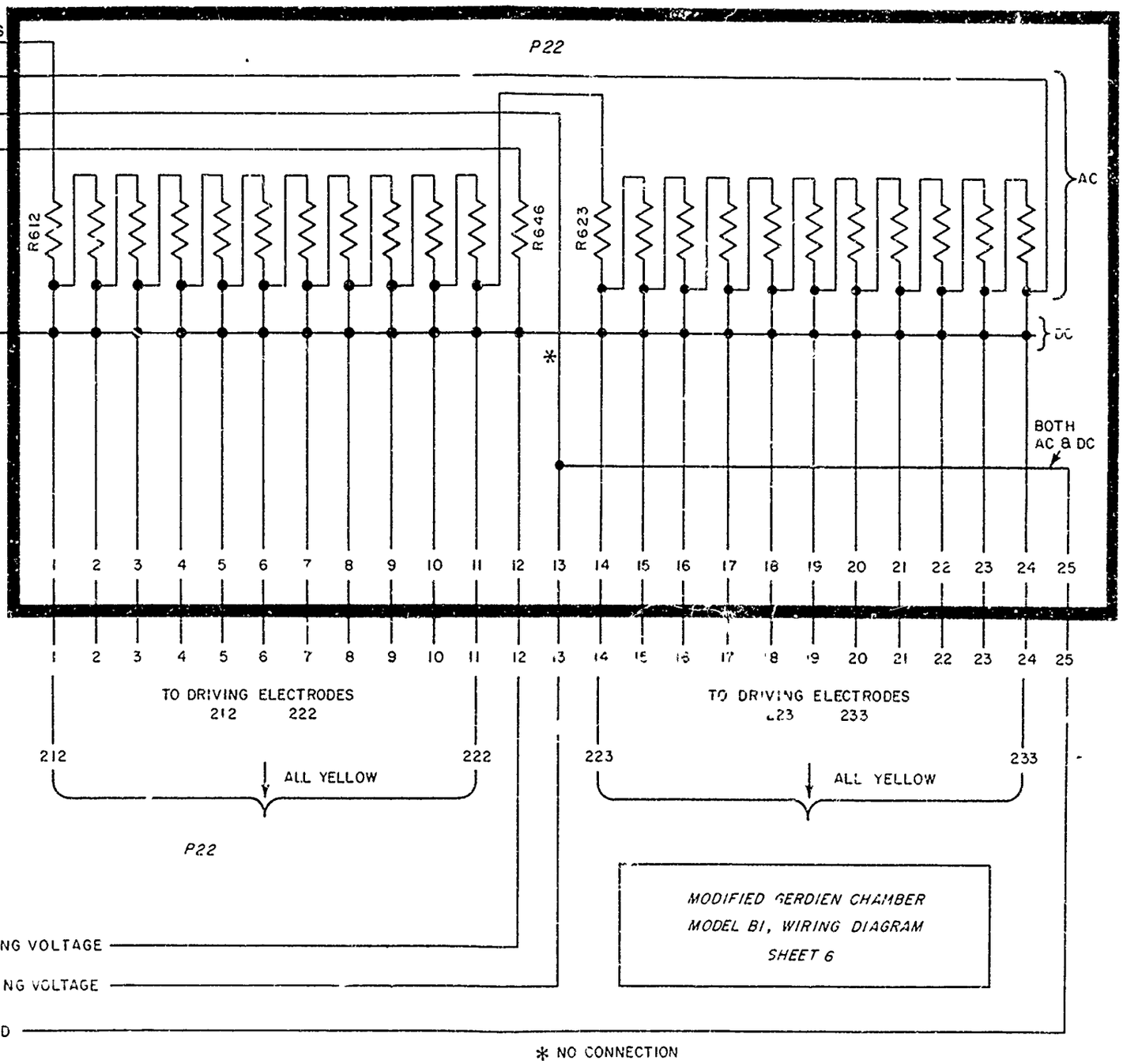

OR MODIFIED GERDIEN CHAMBER
-1
gs for Driving Voltages

C

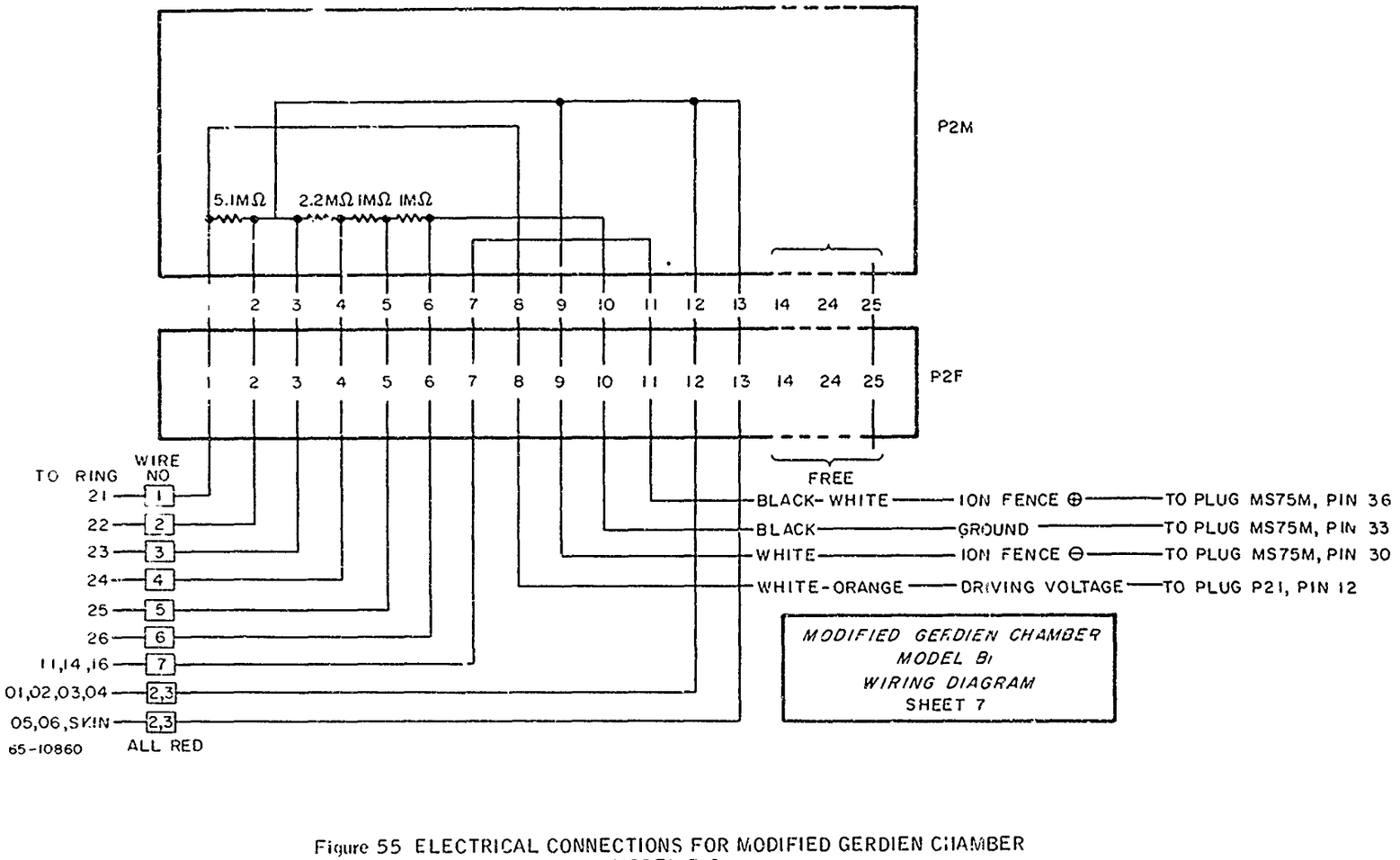

Figure 55 ELECTRICAL CONNECTIONS FOR MODIFIED GERDIEN CHAMBER
MODEL B-1
Sheet 7: Wiring of Connector Plug for Front Rings

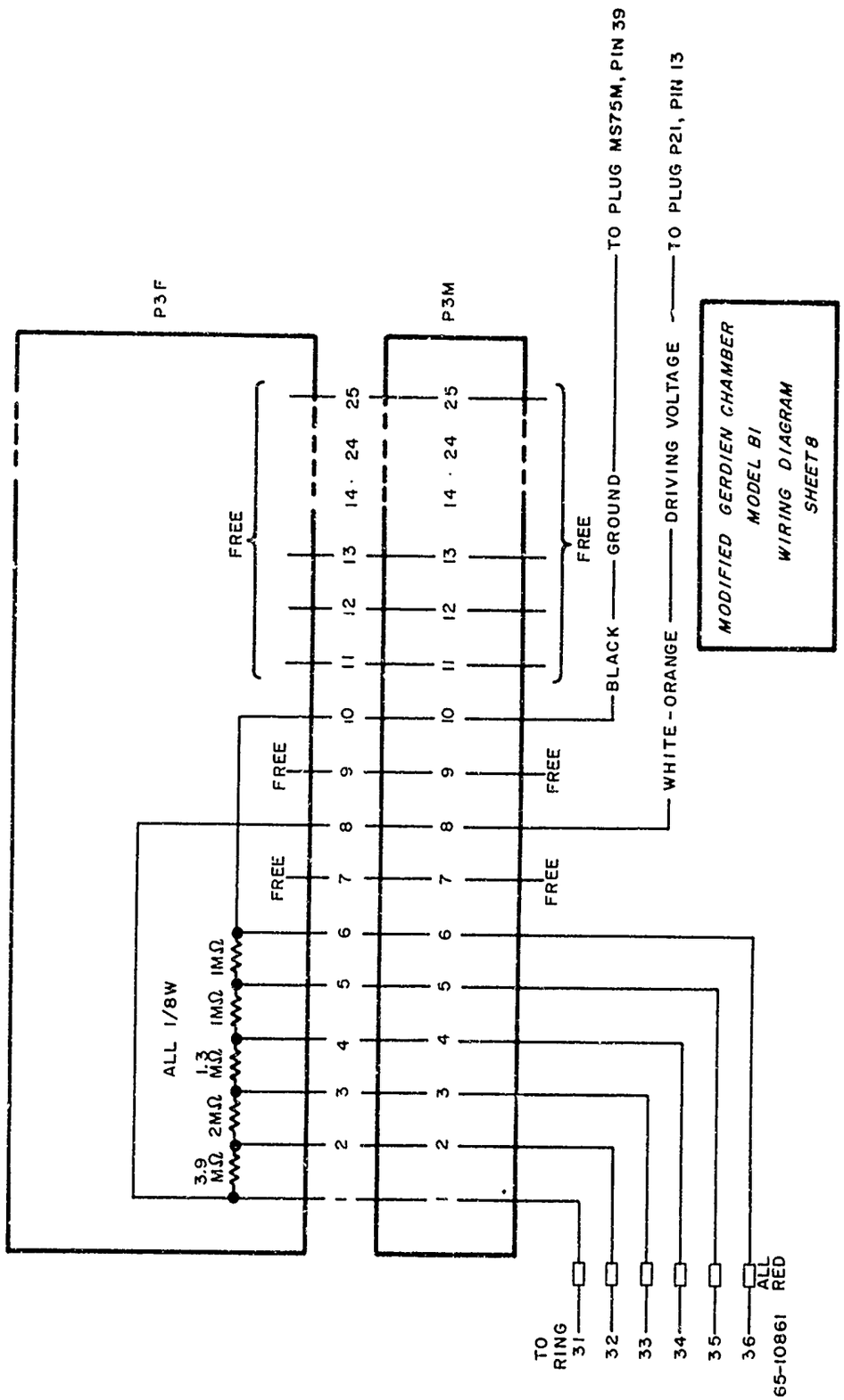

Figure 55 ELECTRICAL CONNECTIONS FOR MODIFIED GERDIEN CHAMBER MODEL B-1
Sheet 8: Wiring of Connector Plug for Aft Rings

3.3 TESTING OF MODEL B1

After the chamber had been built and the electronics have been completed, the wind tunnel was enlarged to suit the new instrument. At first, the new chamber was checked under atmospheric pressure; it turned out to be extremely sensitive to the slightest amounts of ionization or pollution in the laboratory air.

Then, the chamber was put into the wind tunnel. A dummy model for the programmer was built and connected. While the preamplifier operated under the low pressure in the wind tunnel, the second-stage amplifiers, the supply, and the programmer were installed outside the tunnel, the connections made by the way of feedthroughs. A pressure of a few torr was applied, with a wind speed corresponding to the data presented in section 3.1.3. Instead of a transmitter, a sensitive Sanborn eight-channel recorder was connected. By varying the driving voltage, it could be shown immediately that the new chamber was sensitive and delivered the data for the mobility spectra in the required amount.

During the time for the preparation for the planned experiments in the free atmosphere, the chamber will be used in the laboratory for a variety of experiments.

REFERENCES and AUTHOR INDEX

The numbers in brackets under the names of the authors refer to the section of this report in which the paper is quoted.

AMES RESEARCH STAFF, 1953: (2. 1) Equations, Tables and Charts for Compressible Flow. NACA Report 1153, Moffat Field, California

AUFM KAMPE, H. J., M. E. SMITH and R. M. BROWN, 1962 : (1. 6. 3) Winds between 60 and 110 Kilometer, Journ. Geophys. Res. 67 (1962) 4243... 4257

BERNSTEIN, M. R., 1965: (1. 5) Personal Communication

BIONDI, M. A., 1963: (1. 1. 2) Atomic Collisions Involving Low Energy Electrons and Ions. Advances in Electronics and Electron Physics, vol. 18 (1963) 57... 165 Academ. Press, New York

BLACKWOOD, O. 1920 : (1. 3. 5) The existence of homogeneous groups of large ions. Phys. Rev. 16 (1920) 85... 101

BOURDEAU, R., E. WHIPPLE, Jr., and J. F. CLARK, 1959: (1. 6. 4) Analytic and Experimental Conductivity between the Stratosphere and the Ionosphere. Journ. Geophys. Res. 64 (1959) 1363... 1370

BRICARD, J., 1949 : (1. 1. 2) L'équilibre ionique de la basse atmosphère. Journ. Geophys. Res. 54 (1949) 39... 52

BRICARD, J., 1964 : (1. 2. 4) Expression du coefficient de recombinaison en volume de petits ions dans l'air. Beiträge z. Physik d. Atmosphäre 37 (1964) 1... 9

CHANIN, L. M. A. V. PHELPS, and M. A. BIONDI, 1959 : (1. 1. 2) Measurement of the Attachment of Slow Electrons in Oxygen. Phys. Rev. Letters 2 (1959) 344... 346

CHAPMAN, Sydney, and T. G. COWLING, 1960 : (1. 2. 1) The Mathematical Theory of Non-Uniform Gases. Cambridge University Press. Second edition 1952, reprinted 1960, XIII/431 pp.

CHAPMAN, Seville, 1937 : (1. 3. 5) Carrier Mobility Spectra of Spray Electrified Liquids. Rev. Phys. 52 (1937) 184...190

COLE, R.K., Jr., and E. T. PIERCE, 1965 : (1. 1. 3, 1. 6. 1) Electrification in the Earth's Atmosphere for Altitudes between 0 and 100 Kilometers. Journ. Geophys. Res. 70 (1965) 2735...2749

CORONITI, S. C., A. NAZAREK, C. G. STERGIS, D. E. KOTAS, D. W. SEYMOUR, and J. V. WERME, 1954: (1. 6. 4) Balloon Borne Conductivity Meter. Instrumentation for Geophysical Research No. 3, AFCRC-TR54-206, December 1954.

CRAIN, C. M., 1961 : (1. 1. 2) Ionization Loss Rates Below 90 km. Journ. Geophys. Res. 66 (1961) 1117...1126

CUNNINGHAM, E. 1910 : (1. 2. 3) On the velocity of steady fall of spherical particles through fluid medium. Proc. Roy. Soc. 83,357-364

DALGARNO, A., 1958 : (1. 2. 3) The Mobilities of Ions in their Parent Gases. Phil. Trans. Roy. Soc. London A250 (1958) 426...439

DALGARNO, A., M. R. C. McDOWELL, and A. WILLIAMS 1958 : (1. 2. 2, 1. 2. 3) The Mobility of Ions in Unlike Gases. Phil. Trans. Roy. Soc. London London A 250 (1958) 411...425

DOLEZALEK, H., 1956 : (1. 4. 6) The Electrometer-Tube Amplifier in the Atmospheric Electric Measuring Technique. AF 19(514)-640, Techn. Note No. 2. Aachen 1956, 41 pp.

DOLEZALEK, H. 1956 : (1. 2. 2) On Antennas for Atmospheric Electric Measurements. Contract AFL9(514)-640, Technical Note No. 4, Aachen. 93 pp.

DOLEZALEK, H., 1960 : (1. 2. 2) Zur Berechnung des luftelektrischen Stromkreises, II: Über die Gültigkeit des Ohmschen Gesetzes in der Atmosphäre. Geofisica pura e applicata 45 (1960) 273...297

DOLEZALEK, H., 1961: (1. 4. 6) Elektrometerröhren. Archiv f. Techn. Messen ATM, J 833-3/-4/-5, 1961

DOLEZALEK, H. 1962: (1. 4. 1) On the Measurement of Mobility and Conductivity in the Mesosphere. Zeitschrift für Geophysik 28 239-243

DOLEZALEK, H. 1963: (1. 4. 1; 1. 4. 3) Ion Spectrometer for the Mesospheric Atmosphere. (Contribution to the Meeting of Instrumentation and Ionosphere Measurements Working Groups-DASA; held at University Park, Pennsylvania, 20 and 21 June 1963. 19 pp plus 7 figs.)

DOLEZALEK, H. and A. L. OSTER 1963: (2. 4. 1) Ion Spectrometer for the Upper Stratosphere and the Mesosphere. Conference on Direct Aeronomic Measurements in the Lower Ionosphere. Urbana, Illinois, 21 to 23 October 1963, 18 pp.

DOLEZALEK, H., and A. L. OSTER, 1964 : (1. 4. 1; 1. 4. 4; 1. 4. 6; 2. 3. 2; 2. 4. 2) Measuring Ionic Mobilities in the Mesosphere; Interim Technical Report No. 1, Contract DA-19-020-AMC-0058(R); Avco Corporation RAD-TR-64-14, 4 May 1964, Wilmington, Mass., 108 pp

DOLEZALEK, H., and A. L. OSTER 1965 : (1. 4. 1) Ion Spectrometer for High Mobilities. Amer. Geophys. Union, Southwestern Regional Meeting Socorro, N. M., 28-30 Jan 1965. - Trans. Amer. Geoph. Union 46 (1965) 433

EIBER, H., 1965 : (1. 2. 3) personal communication

ENKENHUS, K. R., 1957 : (2. 1. 5) Pressure Probes at Very Low Density. Utica Report H 43, Institute of Aerophysics, University of Toronto, 66 p.

ENKENHUS, K. R., 1957 : (2. 1. 6) The Design, Instrumentation, and Operation of the Utica Low Density Wind Tunnel. Utica Report No. 44, Institute of Aerophysics, University of Toronto, 36 p.

ERIKSON, H. A., 1921 : (1. 3. 5) Size and Aging of Ions Produced in Air. Phys. Rev. 17 (1921) 400.

ERIKSON, H. A., 1921 : The Change of Mobility of the Positive Ion in Air With Age. Phys. Rev. 18 (1921) 100...101
(1. 3. 5)

ERIKSON, H. A., 1922 : On the Nature of the Negative and Positive Ions in Air, Oxygen and Nitrogen Phys. Rev. 20 (1922) 117...126
(1. 3. 5)

ERIKSON, H. A., 1922 : The Change of Mobility of the Positive Ions with Age in Oxygen and Nitrogen Phys. Rev. 19 (1922) 275...276
(1. 3. 5)

ERIKSON, H. A., 1924 : On the Isolation of the Initial and Final Positive Ions Phys. Rev. 23 (1924) 110...111
(1. 3. 5)

ERIKSON, H. A., 1924 : On the Nature of the Ions in Air and in Carbon Oxide. Phys. Rev. 24 (1924) 502...509
(1. 3. 5)

ERIKSON, H. A., 1929 : Factor, Affecting the Nature of Ions in the Air Phys. Rev. 34 (1929) 635...643
(1. 3. 5)

FLEMING, J. A., 1940 : Research in Terrestrial Magnetism and Electricity at Dept. of Terr-Magn. Carnegie Inst. of Wash., for Year April 1939 to March 1940. Trans. Amer. Geophys. Union 21 (1940) 322...325
(1. 1. 2)

GANGNES, A. V., J. F. JENKINS, and J. A. VAN ALLEN, 1949 : The Cosmic-Ray Intensity above the Atmosphere. Phys. Rev. 75 (1949) 57...69
(1. 6. 4)

GERDIEN, H. 1905 : Demonstration eines Apparates zur absoluten Messung der elektrischen Leitfähigkeit der Luft. Physikalische Zeitschrift 6 (1905) 800...801. Terr. Magn. 10 65...79.
(1. 3. 1; 1. 3. 3)

GISH, O. H., and K. L. SHERMAN, 1940 : Ionic equilibrium in the troposphere and lower stratosphere. Trans. Washington Meeting UGGI, Assoc. Terr. Magn. Electr., Bull. No. 11 (1940) 474...491
(1. 1. 2)

GUNN, R., 1964 : The Secular Increase of the World-Wide Fine Particle Pollution. Journ. Atm. Sci. 21 (1964) 168...181
(1. 7. 2)

GUNTON, R. C., and E. C. Y. INN, 1961 : Rates of Electron Removal by Recombinations, Attachment and Ambipolar Diffusion in Nitric Oxide Plasmas. Journ. Chem. Phys. 35 (1961) 1896.

HASSE, H. R., and W. R. COOK, 1931 : The Calculation of the Mobility of Monomolecular Ions, Phil. Mag. 12 (1931) 554...566
(1. 2. 3)

HESS, V. F., 1927 : Die Ionenerzeugung und Ionenvernichtung in der Atmosphäre über dem Meere und im Gebirge. Akad. Wiss. Wien (IIa) 136 (1927) 603...643
(1. 1. 2)

HESS, V. F., 1927/8 : Die mittlere Lebensdauer der leichten Ionen und die Ionisierungsbilanz über dem Meere und im Gebirge. Physikal. Zs. 28 (1927) 882...894; 29(1928)849...851
(1. 1. 2)

HOEGL, A., 1962 : Zur integralen und differentiellen Konzentrationsbestimmung atmosphärischer Ionen. Dissertation, Technische Hochschule München, 1962
(1. 3. 6)

HOGG, A. R., 1934 : Some observations of the average life of small ions and atmospheric ionization equilibria. Gerlands Beitr. Geophysik 41 (1934) 32...54
(1. 1. 2)

HOGG, A. R., 1934 : Atmospheric electric observations. Gerlands Beitr. Geophysik 41 (1934) 1...31
(1. 1. 2)

HOLT, O., B. LANDMARK, and F. LIED 1961 : A Study of Polar Blackouts, Experimental Studies. Norwegian Defense Research Establishment, NDRE-REPORT 35, parts I, II, III. Technical Final Report Contract AF-61(052)-08, 1961
(1. 1, 2)

HOPPEL, W. A., 1963 : The Measurement of the Mobility Distribution of Small Ions in the Troposphere. Thesis, Dept. Phys. U. Maryland, 67 pp.
(1. 3. 6)

HOPPEL, W. A., and KRAAKEVIK, J. H., 1964 : The Mobility of Tropospheric Ions Above the Exchange Layer, Manuscript, 18 pp plus figures, U. S. Naval Research Laboratory, Washington, D. C., July 1964
(1. 3. 6)

ISRAËL, H., 1931: Zur Theorie und Methodik der Grössenbestimmung von Luftionen. Gerlands Beiträge z. Geophys. 31 (1931) 173... 216. English translation by J. Gough, Contract AF 19 (604)-203, Amer. Met. Soc.
(1. 3. 3)

ISRAËL, H., und H. W. KASEMIR, 1949 : In welcher Höhe geht der luftelektrische Ausgleich vor sich? Ann. de Géophysique 5 (1949) 313... 324
(1/6/4)

ISRAËL, H. 1957 : Atmosphärische Elektrizität, Teil I: Grundlagen, Leitfähigkeit, Ionen. Leipzig. Akademische Verlagsgesellschaft Geest & Portig K. G. X, 370 pp.
(1. 1. 1; 1. 1. 2; 1. 2. 3; 1. 3. 2; 1. 6. 4)

ISRAËL, H., und H. DOLEZALEK, 1957 : Zur Methodik luftelektrischer Messungen, IV: Störspannungen in luftelektrischen Messfühlern und ihre Verhütung. Gerlands Beiträge z. Geophys. 66 (1957) 129... 142
(1. 3. 6)

JOHNSON, F. S., 1961 : Satellite Environment Handbook. Stanford Calif. 1961, Stanford University Press
(1. 6. 3)

KADANOFF, L. P., 1964: personal communication
(1. 4. 3)

KÄHLER, K., 1903 : Über die durch Wasserfalle erzeugte Leitfühigheit der Luft. Ann. d. Physik (4) 12 (1903)1119... 1141
(1. 3. 1)

KENNEDY, H., 1916 : The large ions and condensation-nuclei from flames. Proc. Roy. Irish Acad. 33 (1916) 58... 74
(1. 1. 2)

KNEWSTUBB, P. F. and A. W. TICKNER, 1963 : Mass Spectrometry of Ions (1. 1. 3) in Glow Discharges, IV, Water Vapor. Journ, Chem. Phys. 38 (1963) 464...469

KNOLL, M., EICHMEIER, J., and SCHÖN, R. W., 1964 : Properties, Measurement, (1. 3. 6) and Bioclimatic Action of "Small" Multimolecular Atmospheric Ions. In: Advances in Electronics and Electron Physics, Aacademic Press Inc. New York, Vol. 19 (1964) 177...254

KOMAROV, N. N., 1960 a : Problems of Calculating the Unsteady (1. 3. 6) Currents in Measuring Capacitors of Ion Counters and Ion Spectrometers. Izv. Geophys. Ser. 1960, 309...317

KOMAROV, N. N., 1960 b : Some Results of a Study of Unstable Currents (1. 3. 6) in Ion Counters. Izv. Geophys. Ser. 1960, 459...466

LANGEVIN, P. 1902 : Recherches sur les gaz ionisés. Sur la (1. 2. 3) mobilité des ions dans les gaz. Comtes Rendues 134 414-417, 646-649

LANGEVIN, P., 1905 : Sur les ions de l'atmosphère. Comtes (1. 2. 3) Rend. 140 232-234,

LANGEVIN, P., et M. MOULIN, 1905 : Sur un enregistreur des ions de (1. 2. 3) l'atmosphère. Comptes Rend. 140 (1905) 305...310

LANGMUIR, I., and K. T. COMPTON, 1931 : Electrical Discharges in Gases, (1. 1. 2) Part II: Fundamental Phenomena in Electrical Discharges. Rev. Mod. Phys. 3 (1931) 191...257

LENARD, P., 1900 : Über die Elektricitätszerstreuung in ultra- (1. 3. 1) viclett durchstrahlter Luft. Ann. der Physik (4) 3 (1900) 298...319

LENARD, P. 1913 : Über Elektrizitätsleitung durch freie Elektronen (1. 2. 3) und Träger. Annalen der Physik 40 393-437

LENARD, P., 1919 : Über Elektrizitätsleitung durch freie Elek- (1. 2. 3) tronen und Träger, II: Wanderungsgeschwindigkeit kraftgetriebener Partikel in reibenden Medien. Annalen der Physik 60 329-380

LENARD, P., 1920 : Über Elektrizitätsleitung durch freie Elektronen und Träger, III: Wanderungsgeschwindigkeit kraftgetriebener Partikel in reibenden Medien. Annalen der Physik 61 665-741
(1. 2. 3)

LOEB, L. B., 1939 : Fundamental Processes of Electrical Discharges in Gases. New York 1939, J. Wiley & Sons, Inc., XVIII, 717 pp.
(1. 3. 6)

LOEB, L. B. 1955 : Basic Processes of Gaseous Electronics. University of California Press, Berkeley and Los Angeles, XVII, 1012 pages
(1. 3. 6; 1. 7. 2; 1. 7. 3)

MAHONEY, J. J., 1929 : Ion Mobilities using the ERIKSON method on gases of controlled purity. Phys. Rev. 33 (1929) 217... 228
(1. 3. 5)

MASON, E. A., and H. W. SCHAMP, Jr., 1958 : Mobility of Gaseos Ions in Weak Electric Fields. Annals of Physics 4 (1958) 233... 270
(1. 2. 2; 1. 2. 3)

MILLIKAN, R. A. 1913 : Brownian Movements in Gases at Low Pressures. Physical Review 1 218-221
(1. 2. 3)

MISAKI, M., 1950 : A method of measuring the ion spectrum. Pap. Met. Geophys. (Tokyo) 1 (1950) 313... 318
(1. 3. 6)

MISAKI, M., 1961 : Studies on the Atmospheric Ion Spectrum. Papers in Meteor. Geophys. (Tokyo) 12 (1961) 247... 276
(1. 3. 6)

MISAKI, M., 1964: Mobility Spectrums of Large Ions in the New Mexico Semidesert. Journ. Geophys. Res. 69 (1964) 3309... 3318
(1. 3. 6)

MOTT-SMITH, H. M., and I. LANGMUIR 1926 : The Theory of Collectors in Gaseous Discharges. Phys. Rev. 28 (1926) 727... 763
(1. 1. 2)

NARCISI, R. S., and A. D. BAILEY, 1965 : Mass Spectrometric Measurements of Positive Ions at Altitudes from 64 to 112 Kilometer. Journ. Geophys. Res. 70 (1965) 3687... 3700
(1. 1. 3)

NAWROCKI, P.J., and PAPA, R., 1961 : Atmospheric Processes. AFCRL-595, Contract AF 19(604)-7405, August 1961, Geophys. Corp. America, Bedford, Mass.
(1.1.3; 1.7.4)

NEHER, H.V., 1953 : An automatic ionization chamber. Rev. Sci. Instrum. 24 (1953) 99...102
(1.7.7)

NEHER, H.V., and H.R. ANDERSON, 1964 : Cosmic Ray Intensity at Thule, Greenland, during 1962 and 1963, and a Comparison with Data from Mariner 2. Journ. Geophys. Res. 69 (1964) 807...814
(1.7.7)

NOLAN, J.J., R.K. BOYLAN, and G.P. de SACHY, 1925 : The equilibrium of ionization in the atmosphere. Proc. Roy. Irish Acad. 37 (1925) 1...12
(1.1.2)

NOLAN, J.J., and G.P. de SACHY, 1927 : Atmospheric Ionization. Proc. Roy. Irish Acad. 37 (1927) 71...94
(1.1.2)

NOLAN, J.J., and C. O'BROLCHAIN, 1929 : Recombination of ions in atmospheric air I: Investigation of the decay coefficient by Schweidler's method. Proc. Roy Irish Acad. 38 (1929) 40...48
(1.1.2)

NOLAN, J.J., and R.I. GALT, 1944/45 : The equilibrium of small ions and nuclei. Proc. Roy. Irish Acad. 50 (1944/45) 51...68
(1.1.2)

PARKINSON, W.D., 1943 : Review of the literature on the ion balance of the lower atmosphere since 1939. UGGI Assoc. Terr. Mag. Electr. (IATME) Bull. No. 13 (1943) 307...313
(1.1.2)

PEDERSEN, A., 1964 : Measurements of Ion Concentrations in the D/Region of the Ionosphere with a GERDIEN Condenser Rocket Probe. Försvarets Forskningsanstalt, Stockholm, Sweden, FOA 3 Report A 607, Meddelande 13, July 1964, Uppsala Jonosfärobservatorium. 104 pp.
(1.1.2; 1.1.3; 1.4.7)

PENNDORF, R., 1941 : Die Konstitution der Stratosphäre. Meteor. Zs. 58 (1941) 103...105
(1.6.3)

PHELPS, A.V., and J.L. PACK, 1961 : Collisional Detachment in Molecular Oxygen. Phys. Rev. Letters 6 (1961) 111...113
(1.1.2)

PRANDTL, L., 1944 : Führer durch die Strömungslehre. Friedrich Vieweg & Sohn, Braunschweig 1944, 384 p.
(2. 1)

RAWER, K., 1953 : Die Ionosphäre. P. Noordhoff N. V., Groningen, Netherlands 1953, 189 pp
(1. 2. 3)

ROHSENOW, W. M., and H. Y. CHOI, 1961 : Heat, Mass, and Momentum Transfer, Prentice-Hall, Inc., Englewood Cliffs, New Jersey 1961. 537 p.
(2. 1. 3)

RUTHERFORD, E., 1897 : The Velocity and Rate of Recombination of the Ions of Gases Exposed to Röntgen Radiation. Phil. Mag. 44 (1897) 422...440
(1. 1. 2)

RUTHERFORD, E. 1899 : Uranium Radiation and the Electrical Conduction Produced by it. Phil. Mag. 47 109-163
(1. 3. 1)

SAPPUPO, S. A., 1964 : personal communication
(1. 4. 6)

v. SCHWEIDLER, E., 1918 : Über das Gleichgewicht zwischen ionenerzeugenden und ionenvernichtenden Vorgängen. Akad. Wiss. Wien (IIa) 127 (1918) 953...967
(1. 1. 2)

v. SCHWEIDLER, E., 1919 : Über das Gleichgewicht zwischen ionenerzeugenden und ionenvernichtenden Vorgängen. Akad. Wiss. Wien (IIa) 128 (1919) 947...955
(1. 1. 2)

v. SCHWEIDLER E., 1924 : Über die Charakteristik des Stromes in schwach ionisierten Gasen. Akad. Wiss. Wien (IIa) 133 (1924) 23...27
(1. 1. 2)

v. SCHWEIDLER, E., 1941 : Zur Berechnung des Ionisationsgleichgewichtes in kernhaltiger Luft. Gerlands Beitr. Geophysik 57 (1941) 283...288
(1. 1. 2)

SCRASE, F. J., 1935 : The charged and uncharged nuclei in the atmosphere and their part in atmospheric ionization. Geophys. Memoirs London VII (1935) No. 64
(1. 1. 2)

SEARS, F. W., 1959 : An Introduction to Thermodynamics, the (1. 2. 3) Kinetic Theory of Gases, and Statistical Mechanics, 2nd edition. Reading, Mass., and London, England, 1959. Addison-Wesley Publishing Comp., Inc. X, 374 pp.

SIKSNA, R., 1964 : The mean free path in the recombination of (1. 2. 4) air ions. Arkiv för Geofysik, 4 (1964) 473... 501

SMITH, S. J., D. S. BURCH and L. M. BRANSCOMB, 1958 : Experimental (1. 1. 2) Photodetachment Cross Sections and the Ionospheric Detachment Rate for O_2^-. Ann. de Géophysique 14 (1958) 225... 231

TALBOT, L., 1954 : Viscosity Corrections to Cone Probes in (2. 1. 5) Rarefied Supersonic Flow at a Nominal Mach Number of 4. NACA-Report, Technical Note 3219, University of California, 1954, 39 p.

TAMMET, H. F. 1960 : The Theory of the Aeroion Aspiration (1. 3. 5; 1. 3. 6) Counters. Akad. Nauk SSSR. Izv., Geofiz. Ser. 1960, 1263-1270. Bull. Acad. Sci. USSR, Geophys. Series, English Edition, 1960, 839-843.

TAMMET, H. F., 1962 : Distorting Effects in Aero-Ion Aspiration (1. 3. 6) Counters. Izc. Geophys. Ser. 1962, 845... 853

THELLIER, O., 1941 : Sur l'ionisation de l'air das une atmosphère (1. 1. 2) pure (campagne et polluée grandeville). Thèses, Paris 1941. Ann. Inst. Physique du Globe 19 (1941) 107... 179

THOMSON, F. F. and E. RUTHERFORD, 1896: On the Passage of Electricity (1. 1. 2) through Gases Exposed to Röntgen Rays. Phil. Mag. 42 (1896) 392... 407

TSVANG, L. R., 1956 : Impulse Method of Measuring the Spectrum (1. 3. 6) of Light Ions in the Atmosphere. Izv., Geophys. Ser. 1956, 202... 209

VOLKERS, W. K., 1963 : National Electric Conference, Chicago, (1. 4. 6) 30 October 1963

VOLKERS, W.K., 1964 : Electr. Equ. Eng., Jan. 1964, pp. 70...75
(1.4.6)

WAIT, G.R., 1934 : Ions in the Air. Carnegic Inst. of Wash.; News Service Bull. III, No. 12 (1934) 87...91
(1.1.1)

WAIT, G.R., 1935 : The intermediate ion of the atmosphere. Phys. Rev. 48 (1935) 383
(1.1.2)

WAIT, G.R., 1946 : Some experiments relating to the electrical conductivity in the lower atmosphere. Journ. Wash. Acad. Sci. 36 (1946) 321...343
(1.1.2)

WANNIER, G.H. 1953 : Motion of Gaseous Ions in Strong Electric Fields. The Bell System Technical Journal, 32 170-254.
(1.7.3)

WARFIELD, C.N., 1947 : Tentative Tables for the Properties of the Upper Atmosphere. NACA Technical Note 1200 (1947).
(1.6.3)

WHIPPLE, E., Jr., 1960 : An Improved Technique for Obtaining Atmospheric Ion Mobility Distributions. Journ. Geophys. Res. 65 (1960) 3679...3684
(1.3.6)

WHIPPLE, F.J.W., 1933 : Relations between the combination coefficients of atmospheric ions. Proc. Phys. Soc. 45 (1933) 367...380
(1.1.2)

WRIGHT, H.L., 1933 : Influence of atmospheric suspensions upon the earth's electric field as indicated by observations at Kew Observatory. Proc. Phys. Soc. 45 (1933) 152...170
(1.1.2)

WRIGHT, H.L., 1936 : The size of atmospheric nuclei : Some deductions from measurements of the number of charged and uncharged nuclei at Kew Observatory. Proc. Phys. Soc. 48 (1936) 675...689
(1.1.2)

YUNKER, A.E., 1940 : The Mobility Spectrum of Atmospheric Ions. Terr. Magn. Atm. Electr. 45 (1940) 127..132
(1.3.6)

ZELENY, J., 1900 : The Velocity of Ions produced in Gases by Röntgen Rays. Phil. Trans. Roy. Soc. London A 195 (1900) 193...234
(1.3.1)

UNCLASSIFIED

Security Classification

DOCUMENT CONTROL DATA - R&D

(Security classification of title, body of abstract and indexing annotation must be entered when the overall report is classified)

1 ORIGINATING ACTIVITY *(Corporate author)*
Avco-Corporation
Research and Advanced Development Division
Wilmington, Mass., 01887

2a. REPORT SECURITY CLASSIFICATION
Unclassified

2b GROUP
—

3. REPORT TITLE
Spectrometer for atmospheric ions in their uppermost range of mobility (Project: Measuring ionic Mobilities in the Terrestrial upper stratosphere and mesosphere; Phase I)

4. DESCRIPTIVE NOTES *(Type of report and inclusive dates)*
Scientific Report. Final.

5. AUTHOR(S) *(Last name, first name, initial)*
Dolezalek, Hans, and Oster, August L.

6. REPORT DATE	7a. TOTAL NO. OF PAGES	7b. NO. OF REFS
3 September 1965	196	124

8a. CONTRACT OR GRANT NO.	9a. ORIGINATOR'S REPORT NUMBER(S)
DA-19-020-AMC-0058(X)	RAD-TR-65-25
b. PROJECT NO.	
c.	9b. OTHER REPORT NO(S) *(Any other numbers that may be assigned this report)*
d.	

10 AVAILABILITY/LIMITATION NOTICES

11. SUPPLEMENTARY NOTES	12. SPONSORING MILITARY ACTIVITY
	Hq. Aberdeen Proving Ground, Maryland U.S. Army Ballistic Research Laboratories

13. ABSTRACT

In the past, the mobility of atmospheric ions, and the number density in different mobility ranges (Ion Spectrum) have been measured in the terrestrial atmosphere in the heights from ground to about 5 km. Electric conductivities of the atmosphere have been measured up to about 30 km, and ion number densities to about 75 km. To extend the possibility of ion spectrum measurements up to the same height, a new method has been developed and tested in the laboratory. Its application in the free atmosphere is being prepared. The instrument may be used in planetarian atmosphere.

The method consists of a GERDIEN-type "differential ion counter of the second order," providing a predetermined location of ion intake and a number of separate receiving electrodes for the ion impact. The driving voltage is a.c., its amplitude is increasing downstream the chamber.

A low pressure wind tunnel for continuous operation, mostly in the subsonic range, has been developed and constructed for the laboratory experiments. This tunnel and its possible applications for other purposes are discussed.

An outline of the theory of the different GERDIEN type ion counte s is communicated. The laboratory experiments are described, and ion spectrums obtained in the low pressure wind tunnel are presented.

DD FORM 1 JAN 64 1473

UNCLASSIFIED

Security Classification

14. KEY WORDS	LINK A		LINK B		LINK C	
	ROLE	WT	ROLE	WT	ROLE	WT
Mobility; Ions; Atmospheric Electricity; Stratosphere; Mesosphere; Lower Ionosphere; Ion Spectrum; Ion Counter; GERDIEN chambers; Conductivity; Wind tunnel.						

INSTRUCTIONS

1. ORIGINATING ACTIVITY: Enter the name and address of the contractor, subcontractor, grantee, Department of Defense activity or other organization *(corporate author)* issuing the report.

2a. REPORT SECURITY CLASSIFICATION: Enter the overall security classification of the report. Indicate whether "Restricted Data" is included. Marking is to be in accordance with appropriate security regulations.

2b. GROUP: Automatic downgrading is specified in DoD Directive 5200.10 and Armed Forces Industrial Manual. Enter the group number. Also, when applicable, show that optional markings have been used for Group 3 and Group 4 as authorized.

3. REPORT TITLE: Enter the complete report title in all capital letters. Titles in all cases should be unclassified. If a meaningful title cannot be selected without classification, show title classification in all capitals in parenthesis immediately following the title.

4. DESCRIPTIVE NOTES: If appropriate, enter the type of report, e.g., interim, progress, summary, annual, or final. Give the inclusive dates when a specific reporting period is covered.

5. AUTHOR(S): Enter the name(s) of author(s) as shown on or in the report. Enter last name, first name, middle initial. If military, show rank and branch of service. The name of the principal author is an absolute minimum requirement.

6. REPORT DATE: Enter the date of the report as day, month, year, or month, year. If more than one date appears on the report, use date of publication.

7a. TOTAL NUMBER OF PAGES: The total page count should follow normal pagination procedures, i.e., enter the number of pages containing information.

7b. NUMBER OF REFERENCES: Enter the total number of references cited in the report.

8a. CONTRACT OR GRANT NUMBER: If appropriate, enter the applicable number of the contract or grant under which the report was written.

8b, 8c, & 8d. PROJECT NUMBER: Enter the appropriate military department identification, such as project number, subproject number, system numbers, task number, etc.

9a. ORIGINATOR'S REPORT NUMBER(S): Enter the official report number by which the document will be identified and controlled by the originating activity. This number must be unique to this report.

9b. OTHER REPORT NUMBER(S): If the report has been assigned any other report numbers *(either by the originator or by the sponsor)*, also enter this number(s).

10. AVAILABILITY/LIMITATION NOTICES: Enter any limitations on further dissemination of the report, other than those imposed by security classification, using standard statements such as:

(1) "Qualified requesters may obtain copies of this report from DDC."

(2) "Foreign announcement and dissemination of this report by DDC is not authorized."

(3) "U. S. Government agencies may obtain copies of this report directly from DDC. Other qualified DDC users shall request through _____."

(4) "U. S. military agencies may obtain copies of this report directly from DDC. Other qualified users shall request through _____."

(5) "All distribution of this report is controlled. Qualified DDC users shall request through _____."

If the report has been furnished to the Office of Technical Services, Department of Commerce, for sale to the public, indicate this fact and enter the price, if known.

11. SUPPLEMENTARY NOTES: Use for additional explanatory notes.

12. SPONSORING MILITARY ACTIVITY: Enter the name of the departmental project office or laboratory sponsoring *(paying for)* the research and development. Include address.

13. ABSTRACT: Enter an abstract giving a brief and factual summary of the document indicative of the report, even though it may also appear elsewhere in the body of the technical report. If additional space is required, a continuation sheet shall be attached.

It is highly desirable that the abstract of classified reports be unclassified. Each paragraph of the abstract shall end with an indication of the military security classification of the information in the paragraph, represented as *(TS), (S), (C), or (U)*.

There is no limitation on the length of the abstract. However, the suggested length is from 150 to 225 words.

14. KEY WORDS: Key words are technically meaningful terms or short phrases that characterize a report and may be used as index entries for cataloging the report. Key words must be selected so that no security classification is required. Identifiers, such as equipment model designation, trade name, military project code name, geographic location, may be used as key words but will be followed by an indication of technical context. The assignment of links, rules, and weights is optional.